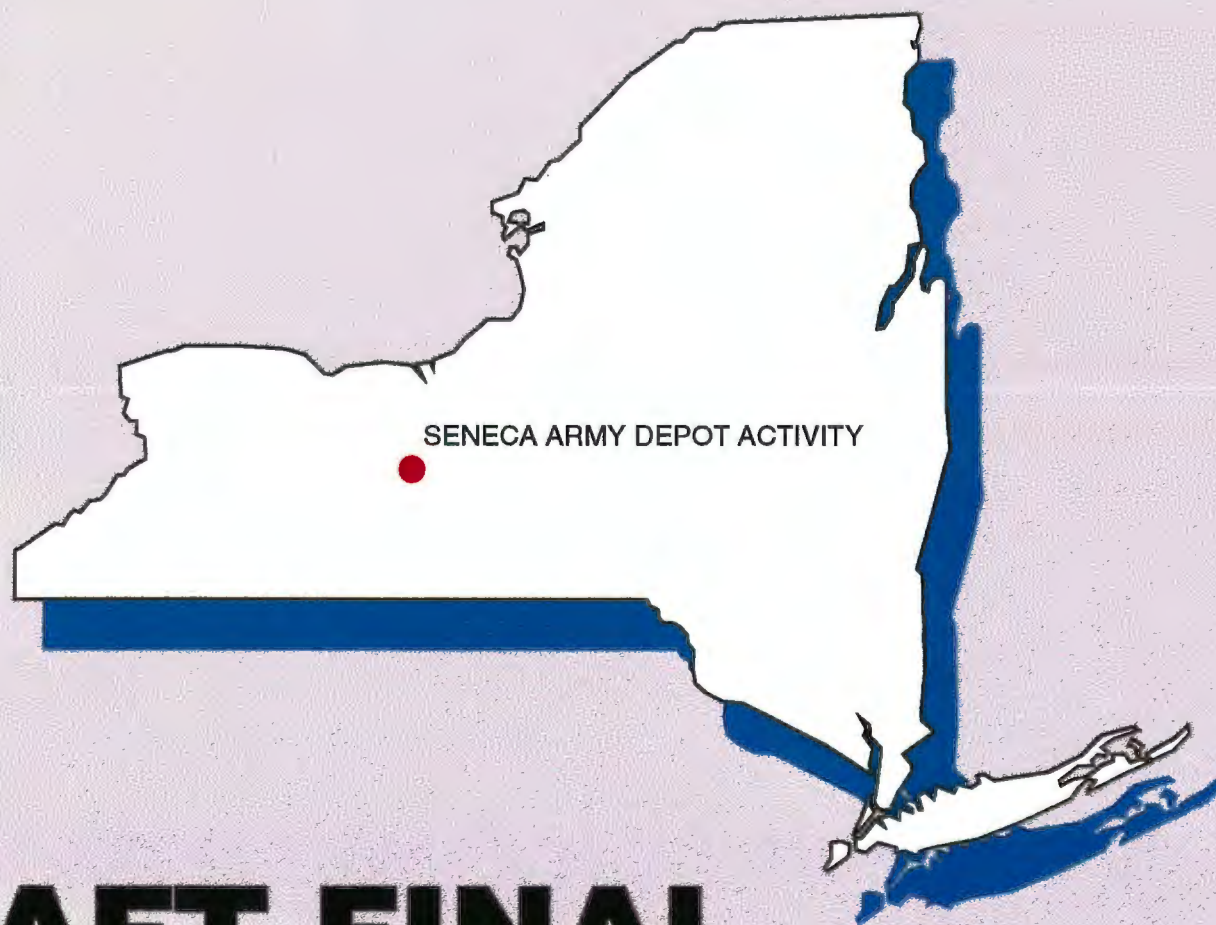


**U.S. ARMY ENGINEER DIVISION
HUNTSVILLE, ALABAMA**

01198



DRAFT FINAL

**GROUNDWATER MODELING REPORT
AT THE ASH LANDFILL SITE**

JANUARY 1996

**SIMULATION OF GROUNDWATER FLOW AND VOC PLUME MIGRATION AT
THE ASH LANDFILL,
SENECA ARMY DEPOT ACTIVITY,
ROMULUS, NEW YORK**

Prepared for :

**Seneca Army Depot Activity
Romulus, New York**

Prepared by:

**Parsons Engineering Science, Inc.
Prudential Center
Boston, MA**

TABLE OF CONTENTS

		<u>PAGE</u>
1.0	INTRODUCTION	1-1
1.1	Purpose	1-2
1.2	Previous Modeling Results	1-2
1.3	Technical Approach to Groundwater Flow and Transport Modeling	1-15
2.0	DESCRIPTION OF ASH LANDFILL AND SURROUNDING AREAS	2-1
2.1	Ash Landfill	2-1
2.2	Surrounding Area	2-3
3.0	HYDROGEOLOGIC SETTING	3-1
3.1	Topography	3-1
3.2	Climate	3-1
3.3	Surface Water	3-2
3.4	Site Geology	3-4
	3.4.1 Introduction	3-4
	3.4.2 Till/weathered shale	3-5
	3.4.3 Competent Shale	3-5
	3.4.4 Site Stratigraphy	3-7
3.5	Hydrogeologic Setting	3-11
	3.5.1 Introduction	3-11
	3.5.2 Groundwater Flow Directions	3-11
	3.5.3 Hydraulic Conductivities	3-13
	3.5.4 Velocity of Groundwater	3-14
	3.5.5 Vertical Hydraulic Heads and Gradients	3-14
	3.5.6 Vertical Connection Between Till/Weathered Shale and Competent Shale Aquifers	3-14
	3.5.7 Summary of Aquifer Characteristics and Behavior	3-15
	3.5.7.1 Introduction	3-15
	3.5.7.2 Till/Weathered Shale Aquifer	3-15
	3.5.7.3 Competent Shale Aquifer	3-22

4.0	CONCEPTUAL MODEL	4-1
4.1	Definition of Hydrostratigraphic Units	4-2
4.2	Water Balance from Precipitation	4-4
4.3	Preliminary Water Budget (Q_{in} vs Q_{out})	4-12
4.4	Definition of Flow System and Boundary Conditions	4-15
4.5	Contaminant Fate and Transport	4-18
5.0	GROUNDWATER FLOW MODEL DESIGN AND RESULTS	5-1
5.1	Selection of Model Code	5-1
5.2	Relationship Between Conceptual Model and MODFLOW Numerical Model	5-1
5.2.1	Boundary Conditions and Grid Layout	5-1
5.2.2	Assignment of Input Parameter Values	5-7
5.2.2.1	Basic Package	5-8
5.2.2.2	Block Centered Flow Package	5-10
5.2.2.3	Recharge Package	5-13
5.2.2.4	Preconditioned Conjugate Gradient Solution Package	5-13
5.3	Model Calibration	5-13
5.3.1	Hydraulic Heads and Gradients	5-13
5.3.2	Water Balance	5-24
5.3.3	Groundwater Velocity and Advective Travel Time	5-26
5.4	Sensitivity Analysis	5-30
5.5	Groundwater Flow Model Results	5-32
6.0	TRANSPORT MODEL DESIGN AND RESULTS	6-1
6.1	Selection of Model Code	6-1
6.2	Relationship Between Conceptual Model and MT3D Numerical Model	6-1
6.3	Assignment of Input Parameter Values for the Contaminant Transport Model	6-1
6.3.1	Basic Transport Package Parameters	6-2
6.3.2	Advection Package Parameters	6-5
6.3.3	Dispersion Package Parameters	6-6
6.3.4	Sink & Source Mixing Package Parameters	6-6
6.3.5	Chemical Reaction Package Parameters	6-6
6.4	Model Calibration	6-14
6.4.1	Scenario 1 (Simulation of plume from origin with TCE source)	6-14

6.5	Transport Model Predictions	6-16
6.5.1	Scenario 2 (Future plume migration with TCE source)	6-16
6.5.2	Scenario 3 (Future plume migration without TCE source)	6-24
6.6	Sensitivity Analysis	6-29
7.0	SUMMARY AND CONCLUSIONS	7-1
8.0	REFERENCES	8-1

LIST OF TABLES

	<u>Page</u>	
1-1	Summary of TCE Modeling Results at a Groundwater Velocity of 0.05 ft/day	1-7
1-2	Summary of 1,2-DCE Modeling Results at a Groundwater Velocity of 0.05 ft/day	1-8
1-3	Summary of TCE Modeling Results at a Groundwater Velocity of 0.213 ft/day	1-9
1-4	Summary of 1,2-DCE Modeling Results at a Groundwater Velocity of 0.213 ft/day	1-10
1-5	Summary of TCE Modeling Results Using ODAST at a Groundwater Velocity of 0.05ft/day (MW-44 Source Location)	1-13
1-6	Summary of 1,2-DCE Modeling Results Using ODAST at a Groundwater Velocity of 0.05ft/day (MW-44 Source Location)	1-14
3-1	Monthly Water Balance for 1990, 1991, and 1992	3-23
4-1	Statistical Parameters of Hydraulic Conductivity	4-3
4-2	Monthly Water Balance	4-6
4-3	Monthly Evapotranspiration from Grass	4-11
4-4	Data Used in Preliminary Water Budget Calculation	4-13
4-5	Chemical Parameters related to Biotic Degradation	4-20
4-6	Biodegradation Indicator Parameter Results	4-21
5-1	Reasonable Range, Best Estimate and Uncertainty for MODFLOW Input Parameters	5-9
5-2	Water Table Elevations and Development of Seasonally Averaged Groundwater Table	5-16
5-3	Comparison of Measured and Simulated Heads	5-22
6-1	Reasonable Range, Best Estimate and Uncertainty for MT3D Input Parameters	6-3
6-2	VOC and Sodium Concentrations Measured in Selected Monitoring Wells at the Ash Landfill	6-6
6-3	Sodium-Corrected VOC Concentrations at the Ash Landfill	6-11

LIST OF FIGURES

	<u>Page</u>
1-1 Ash Landfill Site Map with Volatile Organics Plume	1-2
2-1 Ash Landfill and Surrounding Area	2-2
3-1 Average Monthly Precipitation in Proximity to the Ash Landfill (1958-1991)	3-3
3-2 Location of Geologic Cross-section A-A'	3-8
3-3 Geologic Cross-section A-A'	3-9
3-4 Groundwater Flow Directions at the Ash Landfill and SEAD-64D	3-12
3-5 Historical Saturated Thicknesses in the Till/Weathered Shale Aquifer	3-12
4-1 Hydraulic Conductivity versus Depth at the Ash Landfill	4-5
5-1 Groundwater Flow Model Boundary Conditions and Groundwater Flow Directions	5-2
5-2 Plan View of Groundwater Flow Model Grid	5-4
5-3 Cross-Section of Groundwater Flow Model Grid at Column 42	5-5
5-4 Groundwater Flow Model Grid Near the Ash Landfill	5-6
5-5 Comparison of Measured and Simulated Potentiometric Surfaces	5-20
5-6 Plot of Simulated versus Measured Heads	5-21
5-7 Plot Showing the Effect of Net Recharge on MA, MAE, and RMS	5-25
5-8 Pathline Trace for a Single Particle Released in Layer 1 at the Ash Landfill	5-27
5-9 Cross-Section Pathline Trace for a Single Particle Released in Layer 1 at the Ash Landfill	5-28
5-10 Sodium Concentrations in Groundwater (maximum, minimum, and average)	5-29
5-11 Plot Showing the Sensivity of the Flow Model to Recharge, Kh, and Kv	5-31
6-1 MT3D Model Grid and Boundary Conditions	6-4
6-2 Na-Corrected VOC Concentrations vs Travel Time	6-12
6-3 Na-Corrected C/C ₀ for VOCs vs Travel Time	6-13
6-4 Simulation of VOC Plume in Layer 1 from Origin (t=0) to 30, 35, and 40 Years with a Constant Source (Scenario 1)	6-15
6-5 Simulation of VOC Plume in Layer 2 from Origin (t=0) to 30, 35, and 40 Years with a Constant Source (Scenario 1)	6-17

6-6	Simulation of VOC Plume in Layer 3 from Origin (t=0) to 30, 35, and 40 Years with a Constant Source (Scenario 1)	6-18
6-7	Mass Balance Discrepancy to 30 Years (Scenario 1)	6-19
6-8	Mass Balance Discrepancy to 50 Years (Scenario 1)	6-20
6-9	Simulation of Existing VOC Plume in Layer 1 with Constant Source at 30, 50, and 100 Years from the Present (Scenario 2)	6-21
6-10	Simulation of Existing VOC Plume in Layer 2 with Constant Source at 30, 50, and 100 Years from the Present (Scenario 2)	6-22
6-11	Simulation of Existing VOC Plume in Layer 3 with Constant Source at 30, 50, and 100 Years from the Present (Scenario 2)	6-23
6-12	Mass Balance Discrepancy to 100 Years (Scenario 2)	6-25
6-13	Simulation of Existing VOC Plume in Layer 1 after Source Removal at 30, 50, and 100 Years from the Present (Scenario 3)	6-26
6-14	Simulation of Existing VOC Plume in Layer 2 after Source Removal at 30, 50, and 100 Years from the Present (Scenario 3)	6-27
6-15	Simulation of Existing VOC Plume in Layer 3 after Source Removal at 30, 50, and 100 Years from the Present (Scenario 3)	6-28
6-16	VOC Concentrations Observed at the Farmhouse (Scenario 3)	6-30
6-17	Mass Balance Discrepancy to 100 Years (Scenario 3)	6-31
6-18	Plots showing the sensitivity of the Transport Model to the Degradation Constant, K.	6-33

APPENDICES

- A Northeast Regional Climate Center, Daily Evapotranspiration and Soil Moisture Estimates for the Northeastern United States - MORECS model.

- B Preliminary Water Budget Calculations (Q_{in} vs Q_{out})

- C MODFLOW Output files

- D MODFLOW Model Sensitivity Analysis Results
 - Sensitivity of Heads to Net Recharge
 - Sensitivity of Heads to K_h
 - Sensitivity of Heads to K_v

- E MODPATH Output file

- F MT3D Output file
 - Scenario 3

LIST OF ACRONYMS AND TERMS

AET	Actual Evapotranspiration
cis 1,2,-DCE	cis 1,2-Dichloroethylene
ASTM	American Society for Testing and Materials
bls	below land surface
B	Boring
BCF2	Block Centered Flow 2
BDL	Below Detection Limit
BRAC	Base Realignment and Closure
CERCLA	Comprehensive Environmental Response, Compensation and Liability Act
cm	Centimeters
cm/sec	Centimeters per second
COC	Constituents of Concern
DCE	Dichloroethylene
EPA	Environmental Protection Agency
FS	Feasibility Study
ft	Feet
ft/day	Feet per day
ft ² /day	Square feet per day
ft ³ /day	Cubic feet per day
ft ² /yr	Square feet per year
ft ³ /yr	Cubic feet per year
ft/ft	Feet per foot
ft/sec	Feet per second
ft/yr	Feet per year
HMOC	Hybrid Method of Characteristics
K	Hydraulic conductivity
K _h	Horizontal hydraulic conductivity
K _v	Vertical hydraulic conductivity
LTTD	Low Temperature Thermal Desorption
m	meter
ME	Mean error
MAE	Mean absolute error
mg/kg	Milligrams per kilogram
mg/L	Micrograms per liter
mi	Mile
mL	Milliliter
MMOC	Modified Method of Characteristics
MOC	Method of Characteristics
MODFLOW	Three dimensional finite difference groundwater flow model
MODPATH/	Particle tracking post-processing package to compute three dimensional flow paths
MODPATH-PLOT	Computer package to display the results of the MODPATH

**LIST OF ACRONYMS AND TERMS
(CONT.)**

MORECS	Meteorological Office Rainfall and Evapotranspiration Calculation System
m/s	meter per second
MSL	Mean sea level
MT3D	Three dimensional contaminant transport model
MW	Monitor Well
Parsons ES	Parsons Engineering Science, Inc.
PCG2	Preconditioned Conjugate Gradient 2
P_e	Peclet
PERC	Percolation
PET	Potential Evapotranspiration
ppm	parts per million
PT	Monitoring Well
QA	Quality Assurance
QA/QC	Quality Assurance/Quality Control
QC	Quality Control
Q_{in}	Flow in
Q_{out}	Flow out
RCRA	Resource Conservation and Recovery Act
RI	Remedial Investigation
RMS	Root Mean Square
RQD	Rock Quality Designation
SCS	Soil Conservation Service
SEAD	Seneca Army Depot (old name)
SEDA	Seneca Army Depot Activity (new name)
Sec	Seconds
SOP	Standard Operating Procedures
ST	Soil Moisture
SWMU	Solid Waste Management Unit
trans 1,2-DCE	trans 1,2-Dichloroethylene
TCE	Trichloroethylene
USACE	United States Army Corps of Engineers
USAEHA	United States Army Environmental Hygiene Agency
USCS	Unified Soil Classification System
USGS	United States Geological Survey
VC	Vinyl Chloride
V_{cont}	Vertical Conductance
VOA	Volatile organic analyte
VOC	Volatile Organic Compound
ypb	years before present

1.0 INTRODUCTION

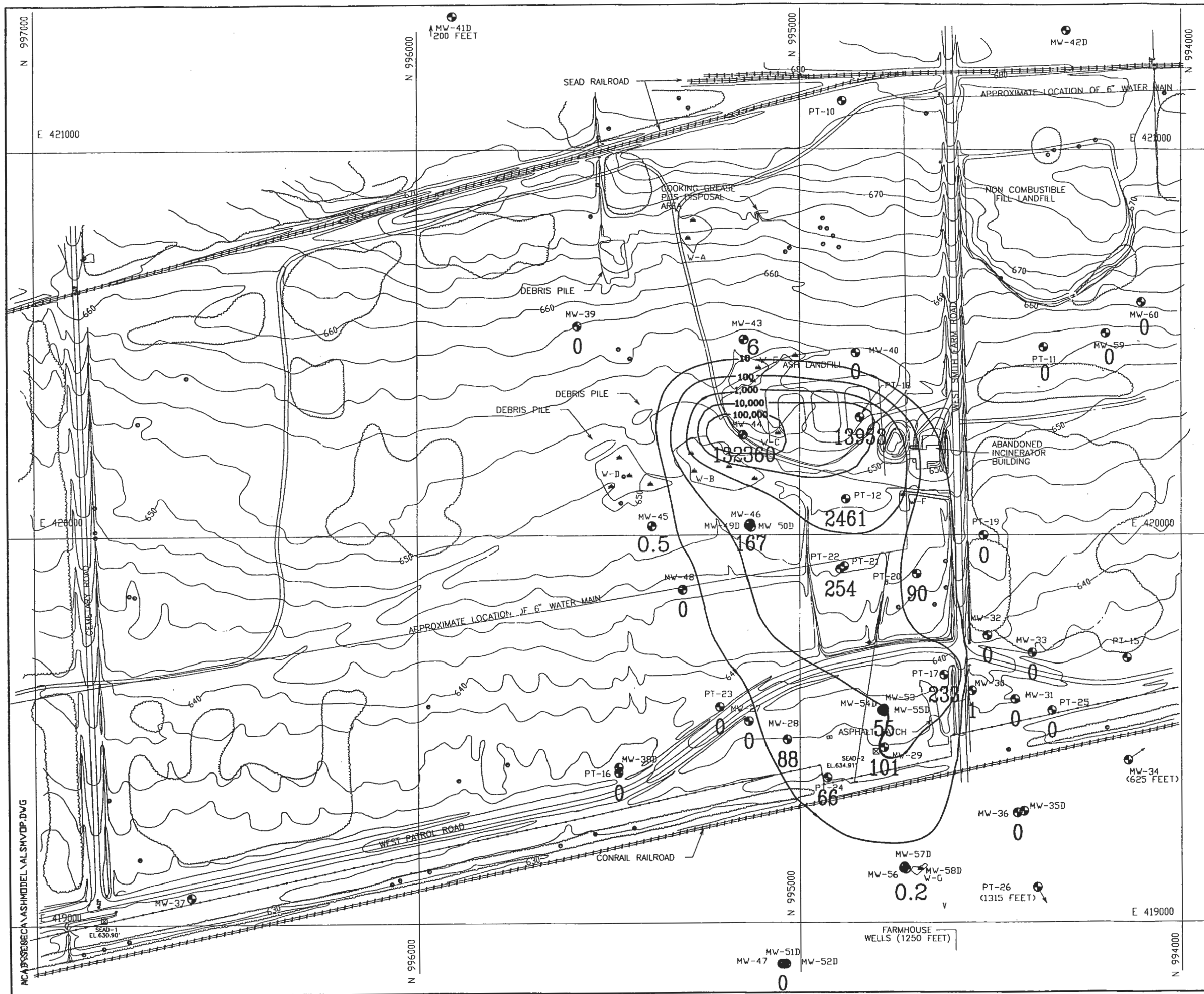
The groundwater at the Ash Landfill has been impacted by volatile organic compounds, predominantly trichloroethene (TCE) and the breakdown products, including 1,2-dichloroethene (1,2-DCE) and vinyl chloride (VC). The plume, as it existed in 1994, is shown in Figure 1-1.

The presence of volatile organics was first detected in 1987 during an initial installation assessment performed by the Army Environmental Hygiene Agency (AEHA). Since that time the plume has been monitored by SEDA quarterly as part of a groundwater sampling program. Generally, the monitoring results suggest that there has been no significant increase in the concentration of volatile organics at the wells sampled during the period of 1989 to 1995.

As part of the remedial investigation (RI) the full extent of the plume was delineated (Parsons ES, 1994a). The westernmost tip of the plume was shown to exist slightly beyond the SEDA boundary. Although the plume has not impacted any source of drinking water, a private drinking water well does exist at a nearby farmhouse residence (Figure 1-1). Cursory modeling of TCE plume migration at the site using a one-dimensional analytical model suggested that degradation was a possible explanation as to why the plume did not appear to be migrating. It was hypothesized that the plume had reached a steady-state condition. In other words, the natural degradation mechanisms in the groundwater/soil matrix were able to remove the mass of volatile organics that was added to the system annually due to leaching from the source area.

In the fall of 1994, the source area was decontaminated using Low Temperature Thermal Desorption (LTTD) and in the process several thousand gallons of groundwater from this area was extracted and treated from the till/weathered shale aquifer.

The remedial strategy was to eliminate the continued mass input to the groundwater system which would be followed by an in-depth evaluation of the ability of the natural system to degrade the remaining plume. If the results from this evaluation suggested that the existing conditions were favorable for the degradation process, then institutional controls in combination with continued groundwater monitoring would be selected as the preferred remedial alternative. For this study, numerical groundwater flow and transport models were selected as the preferred approach to evaluate this alternative. The USGS ground water flow model (MODFLOW) and a three dimensional transport model (MT3D) were selected as the mechanism to predict the future migration of the plume relative to its current configuration. The transport model was also used to



- LEGEND:**
- PAVED ROAD
 - DIRT ROAD
 - GROUND CONTOUR AND ELEVATION
 - TREE
 - WETLAND & DESIGNATION
 - APPROXIMATE EXTENT OF FILL
 - OUTLINE OF FORMER TRASH PITS (IDENTIFIED FROM AERIAL PHOTO)
 - APPROXIMATE EXTENT OF DEBRIS PILE
 - BRUSH
 - CHAIN LINK FENCE
 - UTILITY POLE
 - APPROXIMATE LOCATION OF FIRE HYDRANT
 - FUEL OR UNDERGROUND STORAGE TANK
 - SURVEY MONUMENT
 - SEAD-1 EL. 630.90'
 - PT-22
 - MW-37
 - MONITORING WELL AND DESIGNATION
 - 10,000 - GROUNDWATER ISOCONTOUR (ug/L)

PARSONS
PARSONS ENGINEERING SCIENCE, INC.

CLIENT/PROJECT TITLE
**SENECA ARMY DEPOT ACTIVITY
 ASH LANDFILL GROUNDWATER MODEL**

DEPT. ENVIRONMENTAL ENGINEERING Dwg. No. 720209-01002

**FIGURE 1-1
 ASH LANDFILL SITE MAP
 WITH VOLATILE ORGANICS PLUME**

SCALE 1" = 250' DATE october 1996 REV A

NCA\B02RECA\ASHMODEL\ALSHVDP.DWG

simulate the effect that eliminating the source material would have on the future migration of the plume.

1.1 Purpose

The purpose of this study is to predict the future migration of the plume of volatile organic compounds (VOC) and to evaluate the effect that eliminating the source of VOCs will have on the future migration of the plume. The results of the modeling will provide information on the potential for impacts to groundwater at off-site locations, including the farmhouse located on Old Smith Farm Road. Results from the groundwater flow and transport modeling will be used in the decision making process regarding the need for implementation of groundwater recovery system.

1.2 Previous Modeling Results

As part of the RI, a one dimensional analytical model was used to evaluate the future migration of the plume of TCE. Specifically, the model was used to determine when, and if the plume of VOCs would reach private wells at a downgradient farmhouse property.

The transport of dissolved materials (i.e., TCE) in the groundwater was initially evaluated using a groundwater transport model obtained from the document *Groundwater Transport: Handbook of Mathematical Models*, (1984). The model called ODAST considers convection, dispersion, decay, and adsorption in a porous media and utilizes an analytical solution, presented by *Van Genuchten and Alves (1982)*, for the one-dimensional groundwater transport of constituents from the source. The model is an analytical solution to the partial differential equation describing solute transport in saturated porous media given various simplifying assumption and boundary conditions. The model assumes an infinitely long homogeneous, isotropic porous medium in a steady uniform flow. It includes two function type subroutines, one calculates the product of the exponential, $\exp(A)$ and the other the complementary error function, $\text{erfc}(B)$. The modeling focused on both TCE and 1,2-DCE. The ODAST model provided a reasonable analysis of contaminant transport at the site during the RI. The discussion below is a summary of this modeling. The details of the ODAST modelling are provided in the Ash Landfill RI report (Parsons ES, 1994a).

This ODAST model calculates the ratio C/C_0 for any given point downstream from the source of contamination (x) at any given time (t) as a function of average pore water velocity (v), the dispersion coefficient (D), the retardation factor (R), the decay factor of the solute (λ), and the

decay factor of the source (α). For this initial analysis, the source was assumed not to change relative to the groundwater system and therefore, α was assumed to equal zero. The ODAST one dimensional analytical solution used to model this system is:

$$\begin{aligned} \frac{C}{C_o}(x,t) &= \frac{v}{v+U} \exp\left[\frac{x(v-U)}{2D}\right] \operatorname{erfc}\left[\frac{Rx-Ut}{2(DRt)^{1/2}}\right] \\ &+ \frac{v}{v-U} \exp\left[\frac{x(v+U)}{2D}\right] \operatorname{erfc}\left[\frac{Rx+Ut}{2(DRt)^{1/2}}\right] \\ &+ \frac{v^2}{2DRX} \exp\left[\frac{vx}{D} - Xt\right] \operatorname{erfc}\left[\frac{Rx+vt}{2(DRt)^{1/2}}\right] \end{aligned}$$

where:

$$U = [v^2 + 4DR(\lambda - \alpha)]^{1/2}$$

The input parameters to the model was as follows:

C = concentration at x,t

C_o = concentration at source

v = pore water velocity (m/day)

D = coefficient of dispersion (m²/day)

R = Retardation factor

T_o = total period of waste recharge (years)

λ = decay factor of the solute (day⁻¹)

α = decay factor of the source (day⁻¹)

x = distances from the source (m)

t = time elapsed since the beginning of the operation (year)

The potential migration of both TCE and 1,2-DCE onsite was evaluated using the above-mentioned analytical groundwater flow model. The evaluation incorporated a sensitivity analysis for TCE and 1,2-DCE by varying the pore water velocity at the Ash Landfill site, thereby evaluating their behavior under two sets of conditions. In the first condition a low velocity was used and in the second condition a high velocity was used.

For the low velocity condition a pore water velocity of 18.1 ft/yr or 0.05 ft/day (0.015 m/day) was used. The velocity calculation incorporated an effective porosity of 0.15 and a hydraulic conductivity of 0.35 ft/day as it is suspected that the lower hydraulic conductivities will be the rate-limiting factor.

A longitudinal dispersivity of 30 feet was used. This value was obtained from a recent article entitled *Extraction of TCE-Contaminated Ground Water by Subsurface Drains and a Pumping Well, Groundwater, Vol. 28, No.1, January-February 1990*. The geologic conditions of the site described in this article are similar to the conditions at the Ash Landfill. This value is consistent with values used in other transport simulations (Anderson, 1979). A retardation factor of 1.5 was used for TCE (which was obtained from the same article), and is consistent with literature values for the soil type at SEDA. For 1,2-DCE a lower retardation factor of 1.21 was used.

The product of the dispersivity (30 ft) and the groundwater velocity (18.1 ft/yr) is the coefficient of dispersion, 543 ft²/year (0.138 m²/day). A time period of up to 200 years was used to determine if TCE and/or 1,2-DCE would ever get to the farmhouse wells and also to determine when the concentration ratios would cease to change, or reach steady-state.

To evaluate plume conditions that may prevail using a higher pore water velocity a conservative velocity was calculated for the second condition. This velocity calculation included the use of a hydraulic conductivity of 1.5 ft/day while the other parameters in the velocity equation remained the same as in the first condition. The input parameters for the groundwater model under both conditions are included in the notes below the tables that summarize the results of the modeling (Tables 1-1 through 1-4). For the second condition a new coefficient of dispersion was calculated using a dispersivity of 30 feet and a groundwater velocity of 77.8 ft/yr.

For the purpose of this initial modeling scenario the locations of the TCE and 1,2-DCE source areas are different. The TCE concentration at PT-18 was assumed to be the source concentration term, (C_0) for TCE. PT-18 was chosen as the source instead of MW-44 for several reasons. First, historical monitoring data has shown that the concentration of TCE in PT-18 has remained relatively constant. Second, the four wells downgradient of the source that were part of the modelling array; PT-12, which is 200 ft. (61 m) from PT-18, PT-22, which is 390 ft. (119 m) from PT-18, MW-29, which is 850 ft. (259 m) from PT-18, and MW-56, which is 1,165 ft. (355 m) from PT-18, are essentially along the centerline of the groundwater plume, which meets a boundary condition of the modelling. Also, a downgradient location 2,510 ft. (766 m) from PT-18 was examined, since it is approximately the distance of the farmhouse wells from PT-18. For 1,2-DCE,

the concentration at PT-12 was assumed to be 1,2-DCE source concentration term, (C_o). PT-12 was chosen because this well is near the source area and contained the highest concentration of 1,2-DCE of the wells chosen for the model. Three downgradient monitoring wells (PT-22, MW-29, and MW-56) and the farmhouse well (FH-S) were included in the model for reasons cited above for TCE. Their respective distances from the 1,2-DCE source at PT-12, are 190 ft. (58m), 650 ft. (198m), 965 ft. (294m), and 2,310 ft. (705m). Various times from 5 to 200 years were examined for each of the compounds.

For the two pore water velocity conditions, the model was calibrated by comparing the model output to actual data from one well (PT-12) followed by adjusting one variable, the decay factor of the solute (λ), until the output, the TCE concentration ratio (C/C_o) for PT-12, matched the actual field well data. The final delay factors used to calibrate the model for TCE under low and high pore water velocity conditions were compared to literature data to determine if the decay factors used in this model were similar to that found at other sites.

In order to determine the validity of the value of λ , values were obtained from the article *In Situ Biodegradation of TCE Contaminated Groundwater*, *Environmental Progress*, Vol. 9, No. 3, August 1990, which presented a graphical description of time vs. TCE concentration before and after in-situ treatment. The slope of the line before treatment was determined to be -0.241 ppb degraded/day. Using the initial concentration, the rate was used to calculate a concentration after 250 days. Assuming a first order rate equation, a rate constant was calculated to be 0.0006 day⁻¹ which compared well with the value of 0.000622 day⁻¹ used in the modelling of TCE under the low velocity condition. The λ used to calibrate the model for the high velocity condition 0.002 did not correlate well with the value calculated from data presented in the literature.

Once the final calibration was performed for the low velocity condition by matching the (C/C_o) for PT-12, the output was also compared to the actual C/C_o values for other wells and found to be reasonably close. The actual TCE concentrations were 12,000 ug/l at PT-18, 575 ug/l at PT-12, 89 ug/l at PT-22, 2 ug/l at MW-29, and 0 ug/l at MW-56. From these values actual concentration ratios were determined to be 0.048 for PT-12/PT-18, 0.0074 for PT-22/PT-18, 0.00017 for MW-29/PT-18 and 2.06×10^{-7} for MW-56/PT-18. The decay factor of the source was assumed to be zero, suggesting that the source sink of TCE is large enough so that it is not being depleted rapidly enough that the input source strength relative to downgradient wells changed significantly. The calibrated value for the solute degradation term λ of 0.000622 day⁻¹ yielded the best results (Tables 1-1 through 1-4).

TABLE 1 - 1
 SUMMARY OF TCE MODELING RESULTS USING ODAST
 AT A GROUNDWATER VELOCITY OF 0.05 FT/DAY (PT-18 Source Location)

SENECA ARMY DEPOT
 ASH LANDFILL GROUNDWATER MODEL

TIME (years)	Predicted Concentration Ratio (C/Co), Predicted Conc. and Actual Measured Conc. for TCE														
	PT-12 200 feet (2)			PT-22 390 feet			MW-29 850 feet			MW-56 1165 feet			FARMHOUSE 2510 feet		
	Predicted Conc. Ratio	Predicted Conc. (ug/L)	Actual Conc. (ug/L)	Predicted Conc. Ratio	Predicted Conc. (ug/L)	Actual Conc. (ug/L)	Predicted Conc. Ratio	Predicted Conc. (ug/L)	Actual Conc. (ug/L)	Predicted Conc. Ratio	Predicted Conc. (ug/L)	Actual Conc. (ug/L)	Predicted Conc. Ratio	Predicted Conc. (ug/L)	Actual Conc. (ug/L)
5	0.02436	292.32		3.03E-09	0.00		0	0.00		0.00E+00	0.00		0	0	
10	0.02668	320.16		0.00006	0.77		0	0.00		0.00E+00	0.00		0	0	
15	0.04230	507.60		0.00093	11.12		1.28E-12	0.00		0.00E+00	0.00		0	0	
20	0.04676	561.12		0.00233	27.97		1.67E-09	0.00		0.00E+00	0.00		0	0	
25	0.04775	573.00		0.00321	38.56		7.44E-08	0.00		1.58E-13	0.00		0	0	
30	0.04795	575.40		0.00356	42.72		6.23E-07	0.01		2.25E-11	0.00		0	0	
35	0.04799	575.88		0.00367	44.00		2.07E-06	0.02		5.29E-10	0.00		0	0	
40	0.04800	576.00	575 (3)	0.00370	44.34		4.01E-06	0.05		4.09E-09	0.00		0	0	
60	0.04800	576.00		0.00370	44.45	89 (3)	7.41E-06	0.09		7.99E-08	0.00		0	0	
100	0.04800	576.00		0.00370	44.45		7.53E-06	0.09	2 (3)	1.08E-07	0.00	<0.5 (3)	0	0	<0.5 (3)
150	0.04800	576.00		0.00370	44.45		7.53E-06	0.09		1.08E-07	0.00		0	0	
200	0.04800	576.00		0.00370	44.45		7.53E-06	0.09		1.08E-07	0.00		0	0	

Notes:

1) Input parameters:

Velocity = 0.05 feet/day (Calculated using a gradient of 0.0213 ft/ft, an effective porosity of 0.15, and a K of 0.35 ft/day)

Dispersion coefficient = 1.5 ft²/day (based on a dispersivity of 30 ft)

Retardation factor = 1.5 (dimensionless)

Lambda (plume degradation rate constant) = 0.000622/day

Alpha (source degradation rate constant) = 0.000/day

2) Indicates distance from PT-18. The PT-18 TCE concentration is 12,000 ug/L, which is Co

3) Boldface indicates steady-state achieved

TABLE 1 - 2

SUMMARY OF 1,2-DCE MODELING RESULTS USING ODAST
AT A GROUNDWATER VELOCITY OF 0.05 FT/DAY (PT-18 Source Location)

SENECA ARMY DEPOT
ASH LANDFILL GROUNDWATER MODEL

TIME (years)	Predicted Concentration Ratio (C/Co), Predicted Conc. and Actual Measured Conc. for 1,2-DCE											
	PT-22 190 feet			MW-29 650 feet			MW-56 965 feet			FARMHOUSE 2310 feet		
	Predicted Conc. Ratio	Predicted Conc. (ug/L)	Actual Conc. (ug/L)	Predicted Conc. Ratio	Predicted Conc. (ug/L)	Actual Conc. (ug/L)	Predicted Conc. Ratio	Predicted Conc. (ug/L)	Actual Conc. (ug/L)	Predicted Conc. Ratio	Predicted Conc. (ug/L)	Actual Conc. (ug/L)
5	0.01602	12.82		0.00E+00	0.00		0.00E+00	0.00		0.00E+00	0	
10	0.09799	78.39		7.54E-09	0.00		0.00E+00	0.00		0.00E+00	0	
15	0.14020	112.16		8.95E-06	0.01		4.55E-12	0.00		0.00E+00	0	
20	0.15230	121.84		0.0001889	0.15		1.00E-08	0.00		0.00E+00	0	
25	0.15530	124.24		0.0008192	0.66		6.51E-07	0.00		0.00E+00	0	
30	0.15600	124.80		0.001683	1.35		7.36E-06	0.01		0.00E+00	0	
35	0.15610	124.88		0.00237	1.90		3.13E-05	0.03		0.00E+00	0	
40	0.15620	124.96	125 (3)	0.002761	2.21		7.37E-05	0.06		0.00E+00	0	
60	0.15620	124.96		0.003044	2.44		1.96E-04	0.16		3.29E-14	0	
100	0.15620	124.96		0.003048	2.44	84 (3)	2.06E-04	0.16	0.2 (3)	8.65E-10	0	
150	0.15620	124.96		0.003048	2.44		2.06E-04	0.16		2.06E-09	0	
200	0.15620	124.96		0.003048	2.44		2.06E-04	0.16		2.07E-09	0	<0.5 (3)

Notes:

1) Input parameters:

Velocity = 0.05 feet/day (Calculated using a gradient of 0.0213 ft/ft, an effective porosity of 0.15, and a K of 0.35 ft/day)

Dispersion coefficient = 1.5 ft²/day (based on a dispersivity of 30 ft)

Retardation factor = 1.21 (dimensionless)

Lambda (plume degradation rate constant) = 0.000699/day

Alpha (source degradation rate constant) = 0.000/day

2) Indicates distance from PT-12. The PT-12 total 1,2-DCE concentration is 800 ug/L, which is Co

3) Boldface indicates steady-state achieved

TABLE 1 - 3
 SUMMARY OF TCE MODELING RESULTS USING ODAST
 AT A GROUNDWATER VELOCITY OF 0.213 FT/DAY (PT-18 Source Location)

SENECA ARMY DEPOT
 ASH LANDFILL GROUNDWATER MODEL

TIME (years)	Predicted Concentration Ratio (C/Co), Predicted Conc. and Actual Measured Conc. for TCE														
	PT-12 200 feet (2)			PT-22 390 feet			MW-29 850 feet			MW-56 1165 feet			FARMHOUSE 2510 feet		
	Predicted Conc. Ratio	Predicted Conc. (ug/L)	Actual Conc. (ug/L)	Predicted Conc. Ratio	Predicted Conc. (ug/L)	Actual Conc. (ug/L)	Predicted Conc. Ratio	Predicted Conc. (ug/L)	Actual Conc. (ug/L)	Predicted Conc. Ratio	Predicted Conc. (ug/L)	Actual Conc. (ug/L)	Predicted Conc. Ratio	Predicted Conc. (ug/L)	Actual Conc. (ug/L)
5	0.34080	4089.60		0.05337	640.44		2.69E-07	0.00		4.04E-14	0.00		0	0.00	
10	0.40690	4882.80		0.1796	2155.20		0.003613	43.36		1.24E-05	0.15		0	0.00	
15	0.40890	4906.80		0.1936	2323.20		0.0223	267.60		1.58E-03	18.90		0	0.00	
20	0.40900	4908.00	575 (3)	0.1943	2331.60	89 (3)	0.03078	369.36		6.35E-03	76.15		1.86E-11	0.00	
25	0.40900	4908.00		0.1943	2331.60		0.03199	383.88		8.81E-03	105.74		2.61E-08	0.00	
30	0.40900	4908.00		0.1943	2331.60		0.03209	385.08		9.29E-03	111.53		1.29E-06	0.02	
35	0.40900	4908.00		0.1943	2331.60		0.0321	385.20	2 (3)	9.35E-03	112.19		1.01E-05	0.12	
40	0.40900	4908.00		0.1943	2331.60		0.0321	385.20		9.35E-03	112.24		2.71E-05	0.32	
60	0.40900	4908.00		0.1943	2331.60		0.0321	385.20		9.35E-03	112.25	<0.5 (3)	4.83E-05	0.58	
100	0.40900	4908.00		0.1943	2331.60		0.0321	385.20		9.35E-03	112.25		4.84E-05	0.58	<0.5 (3)
150	0.40900	4908.00		0.1943	2331.60		0.0321	385.20		9.35E-03	112.25		4.84E-05	0.58	
200	0.40900	4908.00		0.1943	2331.60		0.0321	385.20		9.35E-03	112.25		4.84E-05	0.58	

Notes:

1) Input parameters:

Velocity = 0.213 feet/day (Calculated using a gradient of 0.0213 ft/ft, an effective porosity of 0.15, and a K of 1.5 ft/day)

Dispersion coefficient = 6.39 ft²/day (based on a dispersivity of 30 ft)

Retardation factor = 1.5 (dimensionless)

Lambda (plume degradation rate constant) = 0.000622/day

Alpha (source degradation rate constant) = 0.000/day

2) Indicates distance from PT-18. The PT-18 TCE concentration is 12,000 ug/L, which is Co

3) Boldface indicates steady-state achieved

TABLE 1 - 4

SUMMARY OF 1,2-DCE MODELING RESULTS USING ODAST
AT A GROUNDWATER VELOCITY OF 0.213 FT/DAY (PT-18 Source Location)

SENECA ARMY DEPOT
ASH LANDFILL GROUNDWATER MODEL

TIME (years)	Predicted Concentration Ratio (C/Co), Predicted Conc. and Actual Measured Conc. for total 1,2-DCE											
	PT-22 190 feet			MW-29 650 feet			MW-56 965 feet			FARMHOUSE 2310 feet		
	Predicted Conc. Ratio	Predicted Conc. (ug/L)	Actual Conc. (ug/L)	Predicted Conc. Ratio	Predicted Conc. (ug/L)	Actual Conc. (ug/L)	Predicted Conc. Ratio	Predicted Conc. (ug/L)	Actual Conc. (ug/L)	Predicted Conc. Ratio	Predicted Conc. (ug/L)	Actual Conc. (ug/L)
5	0.5428	434.24		0.003793	3.03		6.39E-07	0.00		0	0.00	
10	0.5598	447.84		0.1367	109.36		1.14E-02	9.10		0	0.00	
15	0.601	480.80		0.2004	160.32		7.07E-02	56.56		9.45E-09	0.00	
20	0.6011	480.88	125 (3)	0.2062	164.96		9.59E-02	76.72		4.95E-06	0.00	
25	0.6011	480.88		0.2065	165.20	84 (3)	9.91E-02	79.27		2.67E-04	0.21	
30	0.6011	480.88		0.2065	165.20		9.93E-02	79.46	0.2 (3)	1.62E-03	1.30	
35	0.6011	480.88		0.2065	165.20		9.93E-02	79.46		3.31E-03	2.65	
40	0.6011	480.88		0.2065	165.20		9.93E-02	79.46		4.12E-03	3.30	
60	0.6011	480.88		0.2065	165.20		9.93E-02	79.46		4.37E-03	3.49	<0.5 (3)
100	0.6011	480.88		0.2065	165.20		9.93E-02	79.46		4.37E-03	3.49	
150	0.6011	480.88		0.2065	165.20		9.93E-02	79.46		4.37E-03	3.49	
200	0.6011	480.88		0.2065	165.20		9.93E-02	79.46		4.37E-03	3.49	

Notes:

1) Input parameters:

Velocity = 0.213 feet/day (Calculated using a gradient of 0.0213 ft/ft, an effective porosity of 0.15, and a K of 1.5 ft/day)

Dispersion coefficient = 6.39 ft²/day (based on a dispersivity of 30 ft)

Retardation factor = 0.75 (dimensionless)

Lambda (plume degradation rate constant) = 0.000699/day

Alpha (source degradation rate constant) = 0.000/day

2) Indicates distance from PT-12, The PT-12 total 1,2-DCE concentration is 800 ug/L, which is Co

3) Boldface indicates steady-state achieved

Therefore, for TCE the decay factor of 0.000622 was chosen to best represent conditions at the site because it is supported by the decay factor calculated using data represented in the literature, and it correlates well with the field data. For this reason a λ of 0.000622 was used to model both low and high velocity conditions for TCE.

A similar procedure was used to calibrate the model for 1,2-DCE. Because the low velocity condition was determined to best represent the site for TCE, this condition was used to calibrate the model for 1,2-DCE. Again, calibration was performed in a similar manner to that used for TCE. The decay factor for 1,2-DCE was determined to be 0.000699, which is consistent with that used for TCE.

Using these input parameters, the model was performed until the groundwater system reached steady-state for the first well downgradient of PT-18, which is PT-12. Since the source term was assumed to be constant, the maximum concentration predicted by the model occurs when steady state is achieved. Consequently, this situation is of interest in understanding if the TCE and 1,2-DCE will be expected to reach beyond the limits of the site boundary.

The results of the low and high velocity modelling are shown in Tables 1-1 through 1-4. The results of the analytical modelling for the lower pore water velocity condition (0.05 ft./day) closely match the field data for the monitoring wells chosen for the model. The results indicate that steady-state conditions are achieved in the wells. For TCE in PT-12 this condition occurs 40 years for the time the solvent spill impacted the groundwater and the concentration produced by the model (576 mg/L) agrees well with the actual concentration measured in this well (575 mg/L). Historical quarterly groundwater monitoring indicates that the concentration of TCE in PT-12 has been variable, however, the average concentration since January 1990 is 846 mg/L which is close to the concentration produced by the model under the low velocity condition. Monitoring well PT-22 reaches steady state in approximately 60 years, MW-29 in 100 years and MW-56 also reaches steady state in 100 years.

The exact timeframe for the release of solvents at the Ash Landfill is not known, however, it is likely that the releases occurred over a period of years beginning approximately 40 years ago. According to the model's prediction the spill would have occurred a minimum of 40 years ago. This is consistent with the suspected early operating dates of the Ash Landfill area.

The results of the modeling using the high pore water velocity (0.213 ft/day) are not likely to be representative of current or future site conditions. Instead, the model predicts conditions that are not consistent with the data from the wells used in the model, considering plausible time frames under which the release of solvents may have occurred. For example, the model indicates that steady-state conditions in PT-12 are met 20 years after the release, when TCE stabilized at 4,908 mg/L. This concentration is much greater than the concentration currently measured in the well (575 mg/L) and well above the average TCE concentration for this well since January 1990 (846 ug/L). More significantly, the model predicts that 5 years after the release, the concentration of TCE on PT-12 was 4,089 mg/L. This concentration is not consistent with the historical data from this well given the plausible time frame for the release of the solvents; the release is suspected to have occurred as long as 40 years ago. Similar inconsistencies hold true for PT-22 under these high velocity aquifer conditions.

Previously, in the initial modeling scenario, the model predicted concentrations for an array of wells using PT-18 for the source concentration term (C_o) for TCE, and PT-12 for the C_o for 1,2-DCE. MW-44, the well with the highest concentrations of TCE and 1,2-DCE was not used. To evaluate a second plausible scenario, the model was run using MW-44 as the C_o for TCE and 1,2-DCE. Using this scenario, the centerline of the plume is not a straight line, which is one of the boundary conditions of the model. However, because this source area (MW-44) contains the highest concentrations of TCE and 1,2-DCE on the site, modeling of this scenario is warranted.

This modeling was performed using the concentrations of TCE and 1,2-DCE at MW-44 as the source concentration terms (C_o), while maintaining the same parameters and assumptions used for the initial modeling scenario. However, new distances from the source area (MW-44) for the wells in the modelling array were calculated. Under this scenario, distances between the source concentration term (C_o) and the downgradient wells increased.

Results of the model runs for TCE and 1,2-DCE in MW-44 are shown on Tables 1-5 and 1-6, respectively. For TCE, the model results indicate that steady-state concentrations in the downgradient wells are generally similar to the actual concentrations determined by the laboratory. For 1,2-DCE, the results are also generally similar to actual concentrations, however, 1,2-DCE concentrations predicted by the model are higher in wells closer to the source area (MW-44) and are lower in the further downgradient wells; the shift occurs between wells PT-22 and MW-29.

TABLE 1 - 5

SUMMARY OF TCE MODELING RESULTS USING ODAST
AT A GROUNDWATER VELOCITY OF 0.05 FT/DAY (MW-44 Source Location)

SENECA ARMY DEPOT
ASH LANDFILL GROUNDWATER MODEL

TIME (years)	Predicted Concentration Ratio (C/Co), Predicted Conc. and Actual Measured Conc. for TCE														
	PT-12 310 feet (2)			PT-22 500 feet			MW-29 960 feet			MW-56 1275 feet			FARMHOUSE 2590 feet		
	Predicted Conc. Ratio	Predicted Conc. (ug/L)	Actual Conc. (ug/L)	Predicted Conc. Ratio	Predicted Conc. (ug/L)	Actual Conc. (ug/L)	Predicted Conc. Ratio	Predicted Conc. (ug/L)	Actual Conc. (ug/L)	Predicted Conc. Ratio	Predicted Conc. (ug/L)	Actual Conc. (ug/L)	Predicted Conc. Ratio	Predicted Conc. (ug/L)	Actual Conc. (ug/L)
5	0.00000	0.12		1.51E-14	0.00		0	0.00		0.00E+00	0.00		0	0	
10	0.00131	57.82		0.00000	0.01		0	0.00		0.00E+00	0.00		0	0	
15	0.00587	258.41		0.00003	1.52		0	0.00		0.00E+00	0.00		0	0	
20	0.00916	403.00		0.00023	10.19		8.07E-12	0.00		0.00E+00	0.00		0	0	
25	0.01041	458.04		0.00051	22.58		1.38E-09	0.00		0.00E+00	0.00		0	0	
30	0.01076	473.44		0.00071	31.09		2.78E-08	0.00		2.30E-13	0.00		0	0	
35	0.01085	477.40		0.00079	34.96		1.67E-07	0.01		1.28E-11	0.00		0	0	
40	0.01086	477.84		0.00083	36.34		4.86E-07	0.02		1.87E-10	0.00		0	0	
60	0.01087	478.28	575 (3)	0.00084	36.90		0.0000162	0.71		1.33E-08	0.00		0	0	
100	0.01087	478.28		0.00084	36.91	89 (3)	1.70E-06	0.07	2 (3)	2.44E-08	0.00	<0.5 (3)	0	0	<0.5 (3)
150	0.01087	478.28		0.00084	36.91		1.70E-06	0.07		2.44E-08	0.00		0	0	
200	0.01087	478.28		0.00084	36.91		1.70E-06	0.07		2.44E-08	0.00		0	0	

Notes:

1) Input parameters:

Velocity = 0.05 feet/day (Calculated using a gradient of 0.0213 ft/ft, an effective porosity of 0.15, and a K of 0.35 ft/day)

Dispersion coefficient = 1.5 ft²/day (based on a dispersivity of 30 ft)

Retardation factor = 1.5 (dimensionless)

Lambda (plume degradation rate constant) = 0.000622/day

Alpha (source degradation rate constant) = 0.000/day

2) Indicates distance from MW-44, The MW-44 TCE concentration is 44,000 ug/L, which is Co

3) Boldface indicates steady-state achieved

TABLE 1-6

SUMMARY OF 1,2-DCE MODELING RESULTS USING ODAST
AT A GROUNDWATER VELOCITY OF 0.05 FT/DAY (MW-44 Source Location)

SENECA ARMY DEPOT
ASH LANDFILL GROUNDWATER MODEL

TIME (years)	Predicted Concentration Ratio (C/Co), Predicted Conc. and Actual Measured Conc. for 1,2-DCE														
	PT-12 310 feet			PT-22 500 feet			MW-29 960 feet			MW-56 1275 feet			FARMHOUSE 2590 feet		
	Predicted Conc. Ratio	Predicted Conc. (ug/L)	Actual Conc. (ug/L)	Predicted Conc. Ratio	Predicted Conc. (ug/L)	Actual Conc. (ug/L)	Predicted Conc. Ratio	Predicted Conc. (ug/L)	Actual Conc. (ug/L)	Predicted Conc. Ratio	Predicted Conc. (ug/L)	Actual Conc. (ug/L)	Predicted Conc. Ratio	Predicted Conc. (ug/L)	Actual Conc. (ug/L)
5	0.0000489	4.96		1.85E-11	0.00		0.00E+00	0.00		0.00E+00	0.00		0.00E+00	0	
10	0.00556	564.75		9.38E-06	0.95		0.00E+00	0.00		0.00E+00	0.00		0.00E+00	0	
15	0.01581	1604.72		0.0003509	35.62		2.97E-12	0.00		0.00E+00	0.00		0.00E+00	0	
20	0.02063	2093.95		0.001292	131.14		4.09E-09	0.00		0.00E+00	0.00		0.00E+00	0	
25	0.02191	2223.87		0.002082	211.32		1.80E-07	0.02		2.92E-12	0.00		0.00E+00	0	
30	0.02227	2260.41		0.002443	247.96		1.45E-06	0.15		2.86E-10	0.00		0.00E+00	0	
35	0.02233	2266.50		0.002562	260.04		4.58E-06	0.47		5.03E-09	0.00		0.00E+00	0	
40	0.02234	2267.51	1400 (3)	0.002594	263.29		8.47E-06	0.86		3.08E-08	0.00		0.00E+00	0	
60	0.02234	2267.51		0.002604	264.31	150 (3)	1.42E-05	1.44		3.43E-07	0.03		0.00E+00	0	
100	0.02234	2267.51		0.002604	264.31		1.44E-05	1.46	97 (3)	4.07E-07	0.04	0.2 (3)	3.69E-14	0	
150	0.02234	2267.51		0.002604	264.31		1.44E-05	1.46		4.07E-07	0.04		1.01E-13	0	<0.5 (3)
200	0.02234	2267.51		0.002604	264.31		1.44E-05	1.46		4.07E-07	0.04		1.01E-13	0	<0.5 (3)

Notes:

1) Input parameters:

Velocity = 0.05 feet/day (Calculated using a gradient of 0.0213 ft/ft, an effective porosity of 0.15, and a K of 0.35 ft/day)

Dispersion coefficient = 1.5 ft²/day (based on a dispersivity of 30 ft)

Retardation factor = 1.21 (dimensionless)

Lambda (plume degradation rate constant) = 0.000699/day

Alpha (source degradation rate constant) = 0.000/day

2) Indicates distance from MW-44. The MW-44 total 1,2-DCE concentration is 101,500 ug/L, which is Co

3) Boldface indicates steady-state achieved

Thus, the results of modeling two contaminant transport scenarios showed that degradation is a significant factor affecting the fate and transport of the TCE/1,2-DCE plume and suggested that the plume may have reached a steady-state condition.

The ODAST one dimensional analytical model was able to provide some early insight into the suspected behavior of the plume, however, it is a relatively simplistic model with many assumptions. The more sophisticated MODFLOW and MT3D models used for this study are believed to more accurately represent the flow and transport systems at the Ash Landfill and the surrounding area and, therefore, better simulate the plume migration.

1.3 Technical Approach to Groundwater Flow and Transport Modeling

The technical approach used to accomplish the goals of the study incorporated the use of MODFLOW, a three-dimensional groundwater flow model and MT3D a three-dimensional transport model.

The modeling objectives are as follows:

- To use existing geologic and hydrogeologic data gathered for the RI at the Ash Landfill to develop a conceptual model that represent the groundwater flow system.
- To design a groundwater flow model that simulates steady-state flow at the Ash Landfill
- To perform contaminant transport modeling under three scenarios:

Scenario 1: Simulate the migration of the plume from time $t=0$ to the present day.

Scenario 2: Simulate the future migration of the existing VOC plume.

Scenario 3: Simulate the effect of source removal on the future migration of the VOC plume.

Initially, geologic and hydrogeologic data for the site was assembled from previous studies performed at the site. These data were used to define hydrostratigraphic units and to define the flow system for the site. The conceptual model was developed based on the geologic setting, hydrogeologic parameters, and the three-dimensional flow system. A water balance was prepared to determine the infiltration and evapotranspiration amounts for the site. The competent shale was represented as equivalent porous medium (EPM) for the model because the degree of secondary

porosity (i.e., cracks, microcracks and fracturing) in the shale is believed to form a continuous network of flow. A preliminary water budget was prepared to help define the vertical extent of the flow system to be modeled in the competent shale.

A profile groundwater flow model was initially prepared to provide a cursory check that the conceptual model and initial parameters values were accurate. Once the profile model was calibrated to the observed heads along the section, a three dimensional areal model was prepared and calibrated. Subsequently, sensitivity analyses of the flow model was performed.

Next, transport parameter values were assembled from literature and derived from chemical data collected at the site. The transport model was run using the transport parameter values and the flow data from the calibrated three-dimensional flow model. The transport model was calibrated based on the estimated time of the release of volatile organics to the groundwater (Scenario 1) and a sensitivity analyses was performed. Lastly, the transport model was used to simulate the effect of no removal of the TCE source area (Scenario 2) and then with the removal of the source area (Scenario 3) on the future migration of the plume.

The groundwater flow and transport models and pre-and post-processing software used for this modeling study are discussed below.

MODFLOW/EM (version 3.1), the United States Geological Survey three dimensional finite-difference groundwater flow model was used to simulate steady-state groundwater flow conditions at the Ash Landfill site and surrounding area. The pre-processor MFI/EM was used in conjunction with a spreadsheet program to develop the data files necessary to run MODFLOW. Post-processing of MODFLOW results was performed using MODPATH/MODPATH-PLOT (version 3) and HEDSRFEM. MODPATH/MODPATH-PLOT were used for the pathline analysis in the flow model. HEDSRFEM was used to convert unformatted head files to xyz data files for use in Geosoft, a mapping and processing program.

MT3D (version 1.85), a three dimensional transport model for simulation of the affects of advection, dispersion, and chemical reactions of contaminants in groundwater systems, was used to simulate the movement of the VOC plume. POSTMTED was used to generate plot data files from the unformatted concentration files and the model grid configuration files both of which are saved by MT3D. Geosoft was also used to process the plot data files generated by POSTMT3D.

2.0 DESCRIPTION OF THE ASH LANDFILL AND SURROUNDING AREAS

2.1 ASH LANDFILL

The Ash Landfill site area is located in the southwestern section of SEDA. It encompasses approximately 130-acres and is composed mostly of undeveloped land with a few areas that contain man-made features or structures related to past site activities. The site is bounded on the north by Cemetery Road, on the east by the Seneca Army Depot Railroad line, on the south by open grassland and brush, and on the west by the boundary of the depot (Figure 1-1). Undeveloped areas are present mostly in the northern and extreme southwestern portions of the site. The area to the north of the ash landfill and debris piles is comprised mostly of low grasses with areas of dense brush and a few trees. South of West Smith Farm Road dense brush with some small open grassy areas dominate.

From 1941 to 1974, uncontaminated trash was burned in a series of burn pits near the incinerator building. Between 1974 and 1979 rubbish and garbage was burned in the incinerator. Ashes from the incinerator were temporarily stored in an unlined cooling pond. When the pond filled the ashes were buried in the adjacent Ash Landfill. Large items that could not be burned were disposed of in the Non-Combustible Fill Landfill.

Major features on the site are the abandoned incinerator building (Building 2207), a cooling pond, the Ash Landfill, and the Non-Combustible Fill Landfill. The abandoned and somewhat dilapidated incinerator building is situated on a small artificially constructed mound and is accessed via a paved driveway off of West Smith Farm Road. An approximately 70-foot diameter abandoned cooling pond is located 10 feet from the northeastern corner of the incinerator building. The Ash Landfill is located slightly north of this point. The approximately 500 x 300 foot kidney-shaped Ash Landfill is defined by a 3 to 4 foot rise in topography (Figure 2-1). It is mostly vegetated with low grass, however, there are areas void of any vegetative cover near the bend in the road. The Non-Combustible Fill Landfill is located across West Smith Farm Road from the incinerator. This roughly rectangular, wedge-shaped fill area thickens to the west where it reaches a maximum total relief of approximately 14 feet.

2.2 SURROUNDING AREAS

This modeling study incorporated significant areas of land outside the Ash Landfill. Immediately west of the Ash Landfill is farmland as well as undeveloped land that extends to Route 96A (Figure 2-1). Beyond Route 96A lies Sampson State Park and Seneca Lake. The SEDA airstrip is approximately 3,000 feet southwest of the Ash Landfill. Reeder Creek is located approximately 3,800 feet north of the Ash Landfill and flows west toward Seneca Lake.

East of the Ash Landfill are rows of quonset huts that are in otherwise undeveloped land. Beyond this area is developed land near Route 96. Farmland lies east of Route 96. In addition to the Ash Landfill, six other sites at SEDA provided important information for the modeling study (Figure 2-1). These are: SEAD-64D, which is immediately adjacent to the Ash Landfill, and SEAD-16, -17, -25, -26, -50, and 64A, all located near Route 96.

3.0 HYDROGEOLOGIC SETTING

The hydrogeologic setting described in this section is based on information contained in the Ash Landfill RI (Parsons ES, 1994a) and in the Expanded Site Inspection (ESI) reports for the Seven Low Priority Areas of Concern (AOC)s, the Eight Moderately Low Priority AOCs and the Seven High Priority AOCs (Parsons ES, 1995a, 1995b, 1995c). The description below summarizes only the pertinent information provided in the these reports.

3.1 TOPOGRAPHY

SEDA lies on the western side of a series of north to south trending rock terraces that separate Cayuga Lake on the east and Seneca Lake on the west. The rock terraces range in elevation from 490 feet above MSL in northern Seneca County to as much as 1,600 feet above MSL at the southern end of the lakes. Elevations on SEDA range from 450 feet above MSL on the western boundary to 760 feet above MSL in the southeast corner. The Depot's land surface generally slopes to the west and north.

The Ash Landfill site is located on gently sloping terrain along the western boundary of SEDA, immediately west of the magazine area. The majority of the site, which slopes downward to the west-southwest, is vegetated with grasses and occasional brush thickets (Figure 1-1). Elevations range from 680 feet above MSL near the intersection of the railroad tracks and West Smith Farm Road to 630 to 635 feet along the fenced boundary line.

3.2 CLIMATE

The nearest source of climatological data is the Aurora Research Farm in Aurora, New York which is approximately ten miles east of SEDA on the east side of Cayuga Lake. This research farm is administered by the Northeast Regional Climate Center located at Cornell University in Ithaca, New York. Only precipitation and temperature measurements were available from this location.

A cool climate exists at SEDA with temperatures ranging from an average of 23°F in January to 69°F in July. Marked temperature differences are found between daytime highs and nighttime lows during the summer and portions of spring and autumn. Precipitation is unusually well-distributed, averaging approximately 3 inches per month. This precipitation is derived principally from cyclonic storms which pass from the interior of the country through the St. Lawrence Valley. Lakes

Seneca, Cayuga, and Ontario provide a significant amount of the winter precipitation and moderate the local climate. The annual average snowfall is approximately 100 inches. Wind velocities are moderate, but during the winter months, there are numerous days with sufficient winds to cause blowing and drifting snow. The most frequently occurring wind directions are westerly and west-southwesterly.

Daily precipitation data measured at the Aurora Research Farm in Aurora, New York for the period (1958-1991) were obtained from the Northeast Regional Climate Center at Cornell University. This station is located approximately 10 miles east of the depot. The average monthly precipitation during this 35-year period of record is summarized in Figure 3-1. The maximum 24-hour precipitation measured at this station during this period was 3.9 inches on September 26, 1975. Values of 35 inches mean annual pan evaporation and 28 inches for annual lake evaporation are cited in the Climate Atlas of United States (U.S. Dept. of Commerce, 1983). An independent value of 27 inches for mean annual evaporation from open water surfaces was estimated from an isopleth figure in "Water Atlas of the United States" (Water Information Center, 1973).

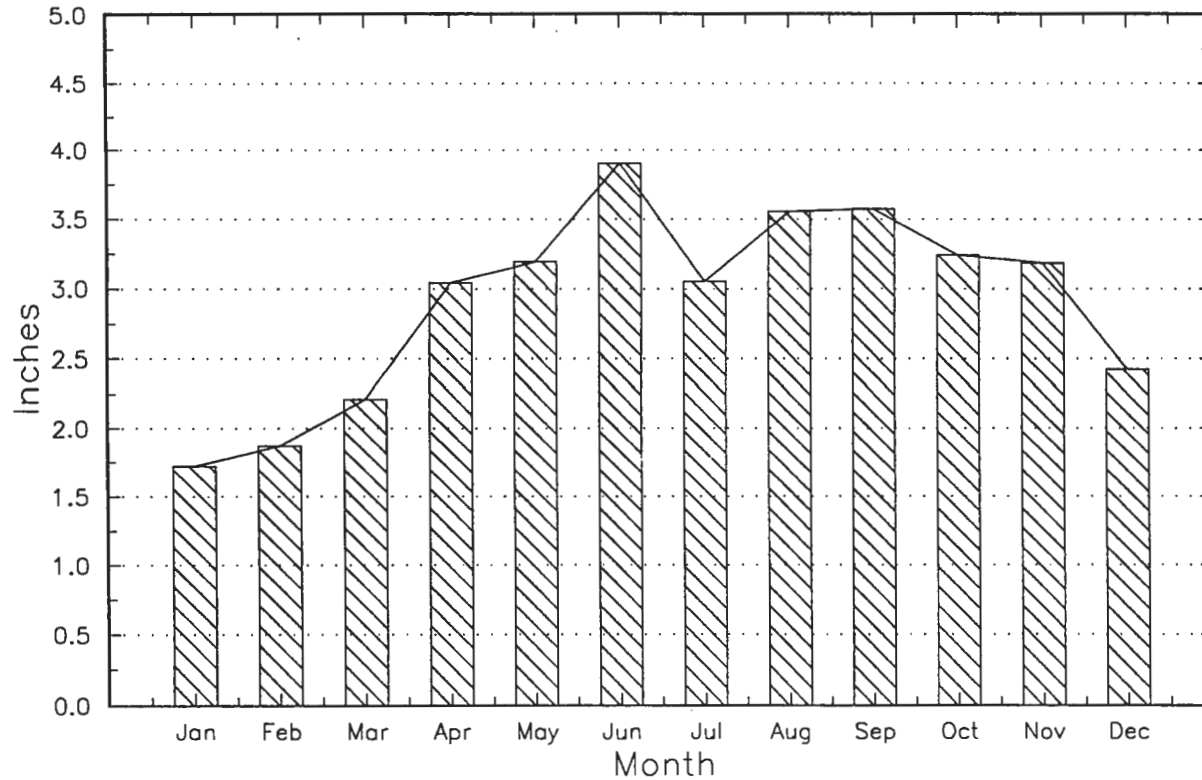
3.3 SURFACE WATER

Regionally, surface water flow at SEDA is controlled by the network of small drainage ditches that parallel the access roads on the Depot. These ditches are believed to receive overland flow during heavy rain events and meltwater during the late winter and spring months. However, they are dry for most of the year based on observations made during the investigations at SEDA. West of SEDA there are no such controls on surface water flow.

Intermittent stream drainage patterns and topography shown on United States Geological Survey (U.S.G.S) 7 1/2 minute topographic maps of the Ovid and Dresden quadrangles indicate that surface water flow directions are generally to the west on the Depot. However, east of Route 96 they indicate that flow is to the east, suggesting that there is a regional surface water divide located near Route 96.

All of the surface water at the Ash Landfill is suspected to drain into several small wetland areas on-site (Figure 1-1). Based on topographic expression, several of these wetland areas (W-B, W-D, W-E, and W-F) drain primarily into two small, but well developed, drainage swales south of the Ash Landfill and incinerator building (Figure 1-1). Farther north, less well developed swales drain areas in an near wetlands W-B and W-E. These ditches direct surface water flow westward into a

Average Monthly Precipitation in Proximity to the Ash Landfill (1958–1991)



drainage ditch along West Patrol Road. Surface water, when present, drains to the north on both sides of West Patrol Road. Wetland W-F also drains west along West Smith Farm Road to the ditch along West Patrol Road. Drainage along West Patrol Road (between West Smith Farm Road and Cemetery Road) is to the northwest based on topography. Drainage on both sides of West Smith Farm Road and Cemetery Road is to the west. North and east of the Ash Landfill site is Kendaia Creek which drains upland areas east of the Ash Landfill site. Kendaia Creek passes approximately 3,800 feet north of the Ash Landfill and eventually drains into Seneca Lake.

Precipitation data from the nearest monitoring station (Aurora Research Farm), was reviewed to gain a perspective on the seasonal variations in rainfall that would directly impact surface water flow. This data indicates that, historically, June has the greatest amount of rainfall, 3.9 inches, and the winter months (January and February) generally have had the least amount of rainfall (Figure 3-1).

Suspected spring locations within a one mile radius of the Ash Landfill were examined in the field as part of the Ash Landfill RI. Field observations made at potential seeps within wetlands in proximity to and downgradient of the Ash Landfill site found no evidence of springs within these wetlands. It appeared that low spots with poorly drained soils enabled surface run-off to collect and form hydric conditions that are conducive to wetland formation. No evidence of springs was observed within a one mile radius of the Ash Landfill during the Phase I and II field work.

3.4 SITE GEOLOGY

3.4.1 Introduction

The site geology is characterized by gray Devonian shale with a thin weathered zone where it contacts the overlying mantle of Pleistocene till. This stratigraphy is consistent over the entire Ash Landfill site and the six other sites (SEAD-16, -17, -25, -26, -50, and -64D) at SEDA. Because a significant amount of the geologic and hydrogeologic information was gathered at the Ash Landfill, much of the discussion below focuses on data from the Ash Landfill. And, because the geology of the region is consistent, this geologic and hydrogeologic information is directly applicable to areas outside the immediate vicinity of the Ash Landfill (i.e., the modeled area).

3.4.2 Till/Weathered Shale

The predominant surficial geologic unit present at the site is dense glacial till. The till is distributed across the entire region and ranges from in thickness from less than 4 to approximately 18 feet although it is generally only a few feet thick. The till is generally characterized by brown to gray-brown silt, clay and fine sand with few fine to coarse gravel-sized inclusions of weathered shale. Larger diameter weathered shale clasts (as large as 6-inches in diameter) are more prevalent in basal portions of the till and are probably ripped-up clasts removed from the shale by the active glacier. The general Unified Soil Classification System description of the till on-site is as follows: Clay-silt, brown; slightly plastic, small percentage of fine to medium sand, small percentage of fine to coarse gravel-sized gray shale clasts, dense and mostly dry in place, till, (ML). Grain size analyses performed by Metcalf & Eddy (1989) on glacial till samples collected during the installation of monitoring wells on another portion of SEDA show a wide distribution of sediment sizes. These tills have a high percentage of silt and clay with trace amounts of fine gravel. The porosities of five gray-brown silty clay (i.e., till) samples ranged from 34.0 percent to 44.2 percent with an average of 37.3 percent (USAEHA Hazardous Waste Study No. 37-26-0479-85).

At the Ash Landfill site and surrounding area, Darian silt-loam soils, 0 to 18 inches thick, are developed over the till on-site, however, in some locations, till is exposed at the surface. The surficial soils are somewhat poorly drained and have a silt clay loam and clay subsoil.

The zone of gray weathered shale has a variable thickness and was encountered below the till in almost all locations drilled at SEDA. The thickness of the weathered shale varies at the Depot, however, it is generally only a few feet thick. Differential weathering through geologic time is likely responsible for the variable thicknesses.

3.4.3 Competent Shale

The bedrock underlying the Ash Landfill and the surrounding region is composed of the Ludlowville Formation of the Devonian age Hamilton Group. The Ludlowville Formation is a gray-black, calcareous shale that is fissile and exhibits parting (or separation) along bedding planes; it is approximately 140 feet thick in Seneca County (Mozola, 1951). Three predominant joint directions, N60°E, N30°W, and N20°E are present within this unit (Mozola, 1951). These joints are primarily vertical. Merin (1992) also cites three prominent vertical joint directions of northeast,

north-northwest, and east-northeast in outcrops of the Genesee Formation 30 miles southeast of the Ash Landfill site near Ithaca, New York.

Data from boring logs indicates that the surface of the competent shale slopes consistently to the west. The bedrock topographic gradient (as well as the land surface topography) is steeper in the eastern portion of the Ash Landfill site than in the southwestern portion of the site. Based upon the available data, the competent shale surface flattens out under a cultivated field west of the Conrail railroad tracks.

The characteristics of the competent shale were observed in a total of 236 feet of core collected during packer testing and monitoring well installation performed at the Ash Landfill. Major characteristics of the bedrock cores include bedding plane fractures, breccia zones, tectonic joints, fossil beds, and minor deposits of iron sulfides. Bedding plane fractures were present throughout the competent shale although they were more well developed and more closely spaced near the top of the competent shale where they were observed to have a spacing of approximately 0.5 inches in the rock cores. Bedding plane fractures also tended to be filled with silt and clay near the top of the shale. Well defined bedding plane fractures were also noted by Merin (1992) in cores from well cemented, gray, thin-bedded siltstones of the Genesee Formation near Ithaca, New York. Generally, the fracture frequency decreased with depth as evidenced by the increase in RQDs. RQDs are the total length of recovered core sections over 4" in length expressed as a percentage of the interval cored. The core recoveries are influenced by the number of bedding plane fractures and tectonic fractures in the shale. Merin (1992) also noted that bedding plane fracture frequency decreased with depth in Devonian siltstones near Ithaca, New York.

Breccia zones are present in several of the cores at varying depths. These zones range from 3 to 12 inches thick and are composed of angular shale fragments in a fine silt and clay matrix. The upper and low contacts of these zones are generally sharp. The breccia is believed to have been formed during small tectonic movements along preexisting bedding plane fractures. No breccia zones were observed along any other type of fracture (e.g., vertical fracture or low angle fracture) except for bedding plane fractures. Brecciated zones were identified in cores for monitoring wells MW-49D (4"-thick zone at 24 feet), MW-50D (12"-thick zone at 41 feet), MW-52D (3"-thick zone at 40 feet), MW-54D (8" thick zone at 30 feet), MW-55D (3"-thick zone at 50 feet), and MW-55D (3" thick zone at 20 feet).

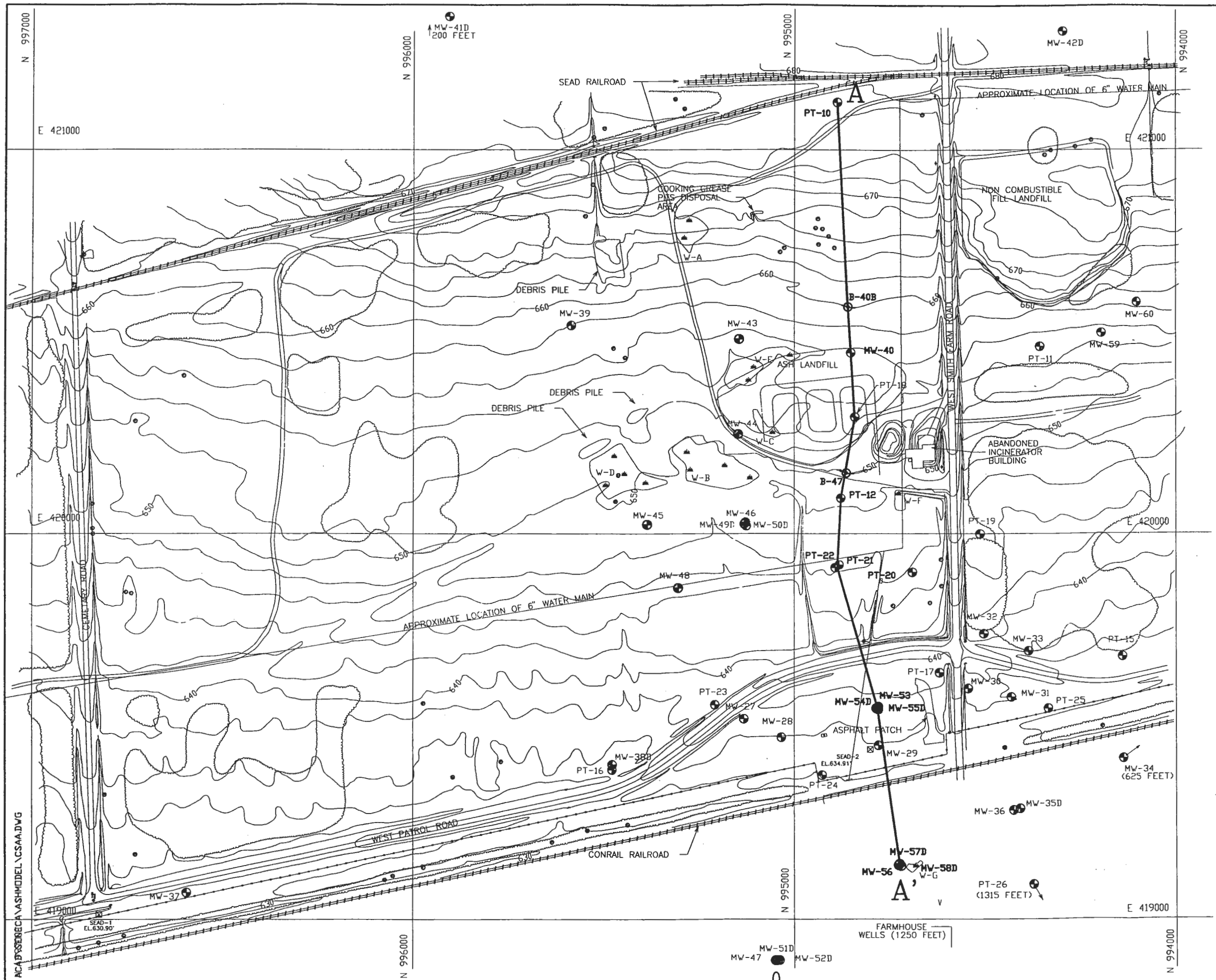
Joint fractures were very common in the competent shale. They were observed in most cores at a variety of angles (between 5° and 90°) although most tended to be between 30° and 60°. Below the top of the competent shale fractures were less than a millimeter thick. They were generally free of silt or clay except in the upper few feet of the shale where they were filled with silt and clay. In some instances, the fractures were filled with a secondary calcium carbonate mineral. The spacing between the joints was usually 4-5 inches in the 0 to 20-foot upper zone of the competent shale; joints spacings below 20 feet were variable but were generally greater than 4-5 inches. The orientation of the joints in space could not be determined because the drilling program did not require the collection of oriented cores.

Thin fossil beds were present at many locations in the shale. The beds ranged in thickness from less than 1 inch to 3 inches. Occasionally only a single fossil was seen in the shale and not associated with an accumulation bed. The fossil beds provide planes of weakness in the shale and were almost always associated with bedding plane fractures.

Iron sulfides were present throughout the cores; however, they were more abundant below 80 feet. Evidence for this is available only from the core for MW-52 which penetrated to 100 feet below the land surface.

3.4.4 Site Stratigraphy

A geologic cross-section was constructed for the Ash Landfill site. The location of the section is shown in Figure 3-2. The east-west cross-section A-A' shows the consistent till, weathered shale, competent shale stratigraphy beneath the site based on data from borings and monitoring wells (Figure 3-3). The Ash Landfill, which is up to 4 feet-thick, is also shown on the section A-A'. The section was drawn to provide a somewhat detailed view of the subsurface stratigraphy by intersecting as many data points (i.e., soil borings or monitoring wells) as possible while maintaining a uniform direction for the cross-section. The scale of the sections did not permit identification of a soil horizon.



- LEGEND:**
- PAVED ROAD
 - DIRT ROAD
 - GROUND CONTOUR AND ELEVATION
 - TREE
 - WETLAND & DESIGNATION
 - APPROXIMATE EXTENT OF FILL
 - OUTLINE OF FORMER TRASH PITS (IDENTIFIED FROM AERIAL PHOTO)
 - APPROXIMATE EXTENT OF DEBRIS PILE
 - BRUSH
 - CHAIN LINK FENCE
 - UTILITY POLE
 - APPROXIMATE LOCATION OF FIRE HYDRANT
 - FUEL OR UNDERGROUND STORAGE TANK
 - SURVEY MONUMENT
 - SEAD-1 EL. 630.90'
 - PT-22 MONITORING WELL AND DESIGNATION
 - MW-37
 - B-40B SOIL BORING AND DESIGNATION
 - LOCATION OF CROSS SECTION

ACA\SENeca\ASHMODEL\CSAA.DWG

PARSONS
PARSONS ENGINEERING SCIENCE, INC.

CLIENT/PROJECT TITLE
**SENECA ARMY DEPOT ACTIVITY
 ASH LANDFILL GROUNDWATER MODEL**

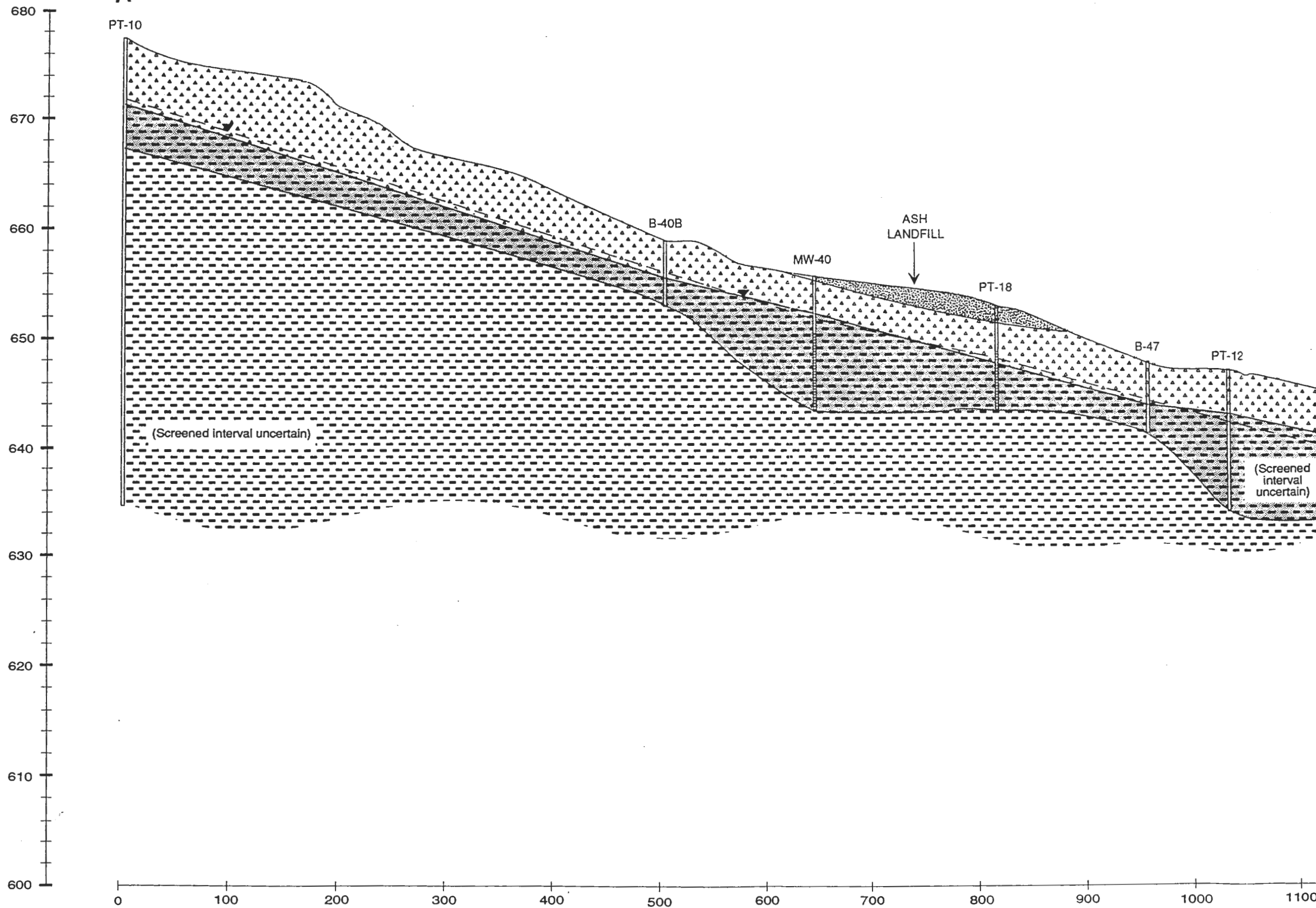
DEPT. ENVIRONMENTAL ENGINEERING Dwg. No. 720209-01002

**FIGURE 3-2
 LOCATION OF GEOLOGIC
 CROSS-SECTION A-A'**

SCALE 1" = 250' DATE OCTOBER 1995 REV. A

CROSS SECTION A - A'

ELEVATION (FEET)



NOTES:

1. Lithologic units are based on descriptions supplied by Engineering-Science, Inc. Interpretations are based on extrapolations between widely spaced boreholes, actual conditions may vary.
2. Groundwater table based on depth to water measurements made in June 1993.

MW-44



LEGEND:

- FILL
- TILL
- WEATHERED SHALE
- COMPETENT SHALE
- GROUNDWATER TABLE

PARSONS
PARSONS ENGINEERING SCIENCE, INC.

CLIENT/PROJECT TITLE
**SENECA ARMY DEPOT ACTIVITY
ASH LANDFILL GROUNDWATER MODEL**

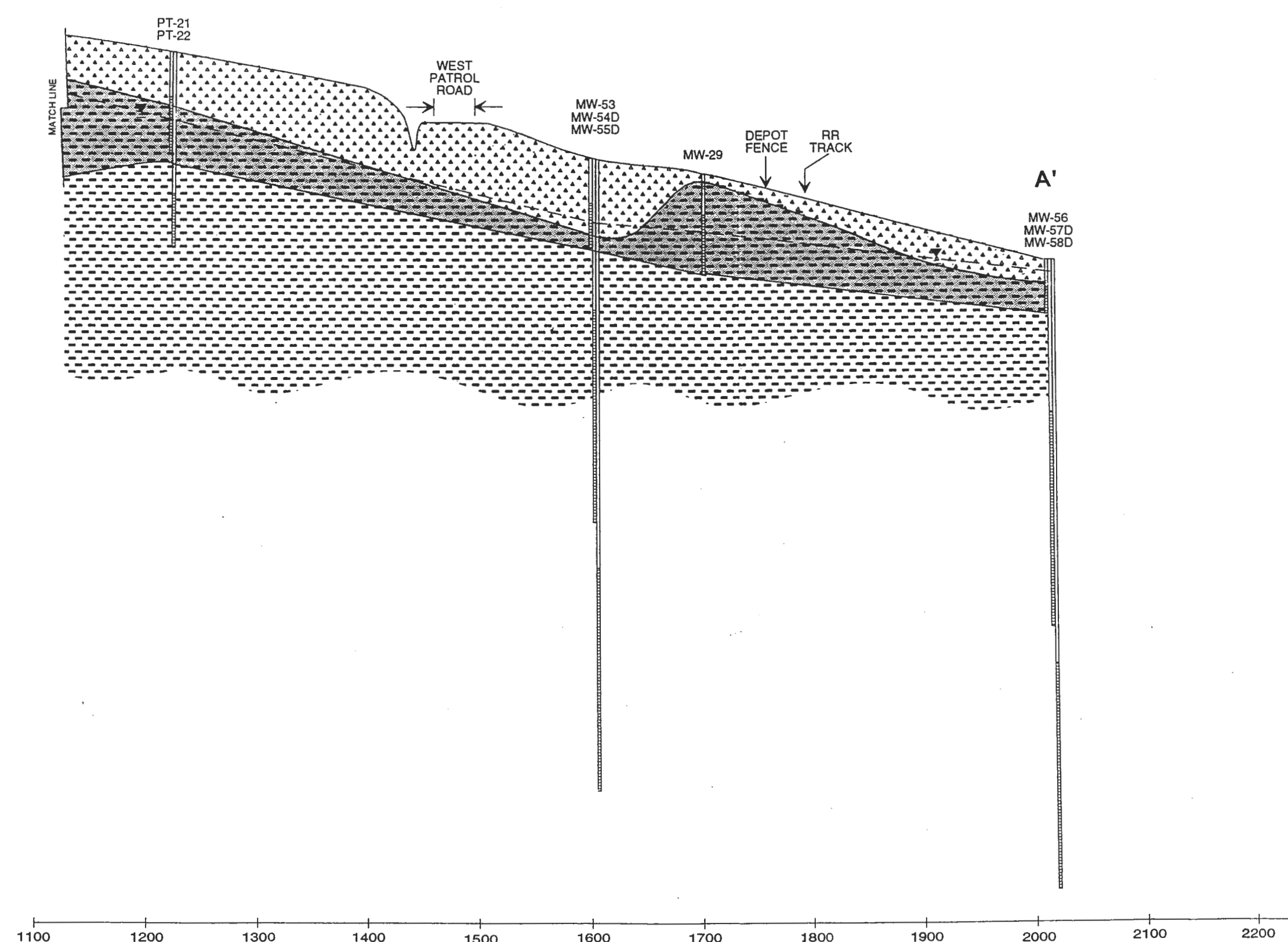
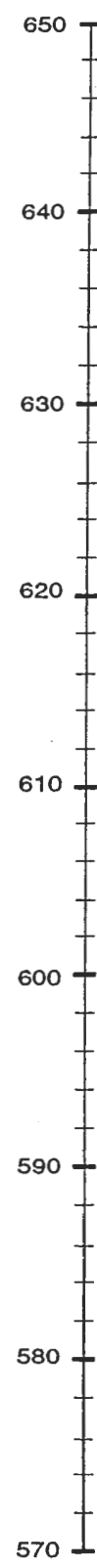
DEPT. ENVIRONMENTAL ENGINEERING DWG NO. 726209-01002

**FIGURE 3-3
CROSS SECTION A - A'**

SCALE: NA DATE: OCTOBER 1995

CROSS SECTION A - A' (CONTINUED)

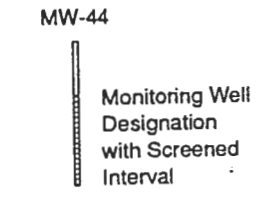
ELEVATION (FEET)



HORIZONTAL DISTANCE (FEET)

NOTES:

1. Lithologic units are based on descriptions supplied by Engineering-Science, Inc. Interpretations are based on extrapolations between widely spaced boreholes, actual conditions may vary.
2. Groundwater table based on depth to water measurements made in June 1993.



LEGEND:

- FILL
- TILL
- WEATHERED SHALE
- COMPETENT SHALE
- GROUNDWATER TABLE



CLIENT/PROJECT TITLE
**SENECA ARMY DEPOT ACTIVITY
 ASH LANDFILL GROUNDWATER MODEL**

DEPT. ENVIRONMENTAL ENGINEERING DWG NO. 726209-01002

**FIGURE 3-3
 CROSS SECTION A - A' (CONTINUED)**

SCALE: NA DATE: OCTOBER 1995

3.5 HYDROGEOLOGIC SETTING

3.5.1 Introduction

The hydrogeologic properties of the till/weathered shale and competent shale aquifers were derived from investigations performed at the Ash Landfill. Specifically, this section addresses topics such as groundwater flow directions, hydraulic conductivities, velocity of groundwater, vertical gradients, and vertical connection tests between the shallow and deep aquifers. A conceptual model that describes the aquifer characteristics and behavior is presented at the end of the section.

3.5.2 Groundwater Flow Directions

A groundwater contour map was constructed for the Ash Landfill and SEAD-64D using depth to groundwater measurements in the till/weathered shale aquifer. The groundwater contour map was constructed based on depth to water measurements made on June 14, 1993 (Figure 3-4). The map indicates that the general direction of groundwater flow in the shallow aquifer was to the west toward Seneca Lake, similar to the surface topography. The aquifer surface elevations were approximately 655 feet above MSL in the eastern portion of the site and 630 feet above MSL in the western portion of the site. Generally groundwater flow contours indicate that there is a consistent gradient over the entire area. The groundwater gradient between wells PT-18 and PT-17 was calculated to be 2.13×10^{-2} feet per foot. The site wide hydraulic gradient (between wells MW-40 and MW-56) was calculated to be 1.95×10^{-2} feet per foot.

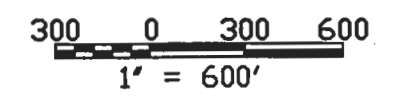
The groundwater flow direction in the competent shale aquifer based on data collected from 5 wells at the Ash Landfill is to the west-southwest. While the control on the flow direction is not as good as for the till/weathered shale aquifer due to a greater spacing between competent shale wells, it does provide useful information regarding general flow directions within the competent shale. The gradient between wells PT-10 and MW-36 was calculated to be 2.5×10^{-2} feet per foot.

The physical characteristics of the competent shale aquifer that affect the flow of groundwater were investigated by reviewing a report prepared by Mozola (1951) and reviewing the core data collected during the monitoring well installation. Mozola (1951) described two distinct sets of joints in the area. The main set, termed dip joints, appear to be in the form of two conjugate shear planes that intersect to form acute angles ranging from 10° to 30° . The mean direction of the dip joints ranges from North 15° to 30° East to North 30° to 45° West. Strike joints at right angles to the dip joints



LEGEND

- ⊕ MONITORING WELL
- SURVEY MONUMENT
- ↘ GROUNDWATER CONTOUR WITH FLOW DIRECTION



C:\ACAD\SENECA\ASHMODEL\GF.DWG

P PARSONS
PARSONS ENGINEERING SCIENCE, INC.

CLIENT/PROJECT TITLE
**SENECA ARMY DEPOT ACTIVITY
 ASH LANDFILL GROUNDWATER MODEL**

DEPT. ENVIRONMENTAL ENGINEERING Dwg. No.

**FIGURE 3-4
 GROUNDWATER FLOW DIRECTIONS AT
 THE ASH LANDFILL AND SEAD-64D**

SCALE 1" = 600' DATE OCTOBER 1995 REV A

trend from North 50° East to North 70° East and are spaced from 1 inch to 4 feet apart. The dip of the joint planes ranges from 46° to nearly vertical. In addition Mozola (1951) found that, most of the joints in the beds of the shale are filled with clay or fine silt which may inhibit groundwater flow.

The flow of groundwater in the competent shale is believed to be influenced primarily by the joints and bedding plane fractures that were observed in the cores. No other flow pathways were observed in the core samples. This view was put forth by Mozola (1951) for rocks of the Hamilton Group and more recently by Merin (1992) for Devonian siltstones near Ithaca, New York. Brecciated zones in the shale may have once transported significantly greater amounts of water than the unbrecciated shale, however, today they are not believed to be major transport pathways because they are filled tightly with a fine silt and clay matrix. In Merin's (1992) conceptual model of groundwater flow in a siltstone aquifer near Ithaca, New York, a network of horizontal and vertical bedding plane fractures and joints exists in the subsurface. Groundwater moves through vertical and horizontal planes of porosity (i.e., fractures) each of which is a fraction of a millimeter thick and extends several inches to tens of feet in length. Based on the physical characteristics of the competent shale observed in this investigation, this model is believed to apply to the shale at the Ash Landfill site.

3.5.3 Hydraulic Conductivities

Hydraulic conductivities were determined for 23 wells at the Ash Landfill site 8 of which are till/weathered shale wells and 14 are competent shale wells. Hydraulic conductivities on the site ranged from 7.8×10^{-4} to 1.9×10^{-7} cm/sec with one anomalous value of 5.8×10^{-11} cm/sec. Hydraulic conductivity values for the shallow till/weathered shale aquifer ranged from 3.9×10^{-5} cm/sec to 1.8×10^{-4} cm/sec. Hydraulic conductivity values for the competent shale aquifer as determined by slug testing ranged from 1.9×10^{-7} to 1.2×10^{-4} cm/sec. In most instances the conductivity values for the till/weathered shale aquifer are greater than for the competent shale aquifer. Within the competent shale aquifer, conductivity values generally decrease with depth, a phenomenon which can be attributed to an increase in mechanical stresses causing fractures to close (deMarsily, 1986). Merin (1992) noted a similar trend in fractured Devonian siltstones near Ithaca, New York and attributed it to the fact that shallower wells intercepted more highly fractured rock in contrast to the deeper wells.

3.5.4 Velocity of Groundwater

The average linear velocity of groundwater in the till/weathered shale was calculated using the method described by Darcy's Law based on: 1) an average hydraulic conductivity of 4.5×10^{-4} cm/sec (0.77 ft/day), 2) an estimated effective porosity of 15% (0.15) to 20% (0.20), and 3) a groundwater gradient of 1.95×10^{-2} ft/ft (Parsons ES, 1994a). The average linear velocity was calculated to be 7.5×10^{-2} feet/day or 27.4 feet/year at 20% effective porosity and 1.0×10^{-1} feet/day or 36.5 feet/year at 15% effective porosity. The actual velocity on-site may be locally influenced by more permeable zones possibly associated with differences in the actual porosity of the till/weathered shale.

The average linear velocity of groundwater in the competent shale was also calculated using the method described by Darcy's Law based on: 1) an average hydraulic conductivity of 3.73×10^{-5} cm/sec (0.06 ft/day), 2) an estimated effective porosity of 6.75% (0.0675), and 3) a groundwater gradient of 2.5×10^{-2} ft/ft. An average linear velocity of 2×10^{-2} ft/day or 7.3 ft/year was calculated for the shale.

3.5.5 Vertical Hydraulic Heads and Gradients

Vertical hydraulic head profiles for the two well pairs (PT-16/MW-38D and MW36/MW-35D) and four well clusters (MW-46/MW-49D/MW-50D, MW-47/MW-51D/MW-52D, MW-53/MW-54D/MW-55D, and MW-56/MW-57D/MW-58D) show variable fluctuations in water levels with depth (Parsons ES, 1994a). Generally, there is no consistent trend in any of the vertical hydraulic head profiles at the Ash Landfill site and there are no areas of the site where there is a consistent distribution of head. Each well pair/cluster location tends to have individual flow characteristics.

3.5.6 Vertical Connection Between Till/Weathered Shale and Competent Shale Aquifers

Vertical connection test data are available for two paired wells (PT-16 and MW-38D, MW-36 and MW-35D), and four well clusters [(MW-46, MW-49D, and MW-50D), (MW-47, MW-51D, and MW-52D), (MW-53, MW-54D, and MW-55D), and (MW-56, MW-57D, and MW-58D)] (Parsons ES, 1994a). These tests were performed to determine the degree of connection between the till/weathered shale and competent shale aquifers. Specifically, the tests were performed to determine whether the contact between the till/weathered shale and competent shale could be

considered a lower impermeable boundary for the shallow groundwater flow systems at the Ash Landfill. Such an impermeable boundary would prove to be an important influence on the possible spread of volatiles and other constituents.

In all of the vertical connection tests at the well clusters, the degree of displacement in the till/weathered shale wells (up to 0.3 feet) was greater during purging of the shallow shale wells than the deep shale wells. These greater displacements can be attributed to the close proximity of the shallow shale wells to the till/weathered shale wells. The degree of vertical connection within the competent shale aquifer is comparatively greater than the connection observed between the till/weathered shale and competent shale aquifers. The results indicate that the till/weathered shale aquifer is connected although not significantly to the competent shale aquifer below it. This could be due to refilling of bedding plane fractures and joints (noted earlier) by silt and clay in the upper portions of the shale aquifer. Flow into the competent shale is likely controlled by vertical gradients. Vertical connections for wells screened within the competent shale aquifer are significantly greater due to clean vertical sub-millimeter scale joints which exist in the shale aquifer. However, the vertical connection between competent shale wells MW-51D and MW-52D is comparatively poor.

3.5.7 Summary of Aquifer Characteristics and Behavior

3.5.7.1 Introduction

An analysis of the tests performed for this investigation and 3 years of historical data collected at the Ash Landfill site provide information for a conceptual model of the overall behavior of the till/weathered shale and competent shale aquifers. The historical depth to ground water data was collected for the years 1990 through 1993 during quarterly sampling events at the Ash Landfill site. No significant historical data was available from the wells installed during the Ash Landfill RI (Parsons ES, 1994a) and the ESI investigations (Parsons ES, 1995a, 1995b, 1995c) so the data discussed below represents wells installed prior to 1992.

3.5.7.2 Till/Weathered Shale Aquifer

For the relatively thin till/weathered shale aquifer, historical plots of water table elevations indicate that they fluctuate as much as 8.72 feet in well PT-26, which is located off-site near the SEDA airfield. The maximum fluctuation on the Ash Landfill site is seen in the plot for well PT-25 which

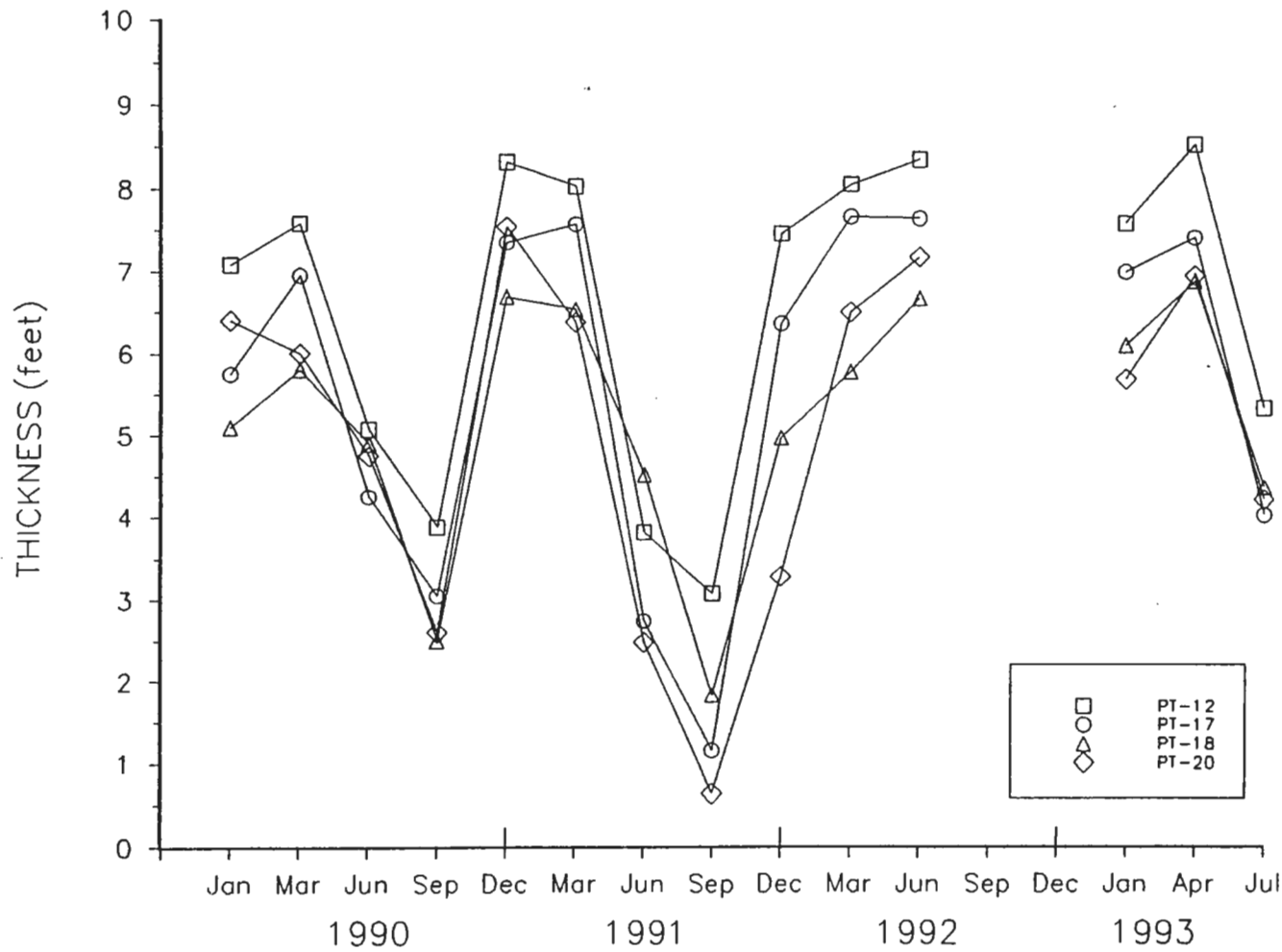
fluctuates up to 8.21 feet (Figure 3-5). The maximum thickness of the till/weathered shale aquifer is 11.6 feet, again in PT-26. On-site, the maximum thickness occurs in PT-25 at 8.59 feet. It is noteworthy that at certain times of the year, the aquifer becomes quite thin, approximately 1 to 3 feet thick, and even dries up in some locations (PT-29 and PT-30).

Based on the historical data, the 21 wells on the Ash Landfill site exhibit rhythmic, seasonal water table and saturated thickness fluctuations (Figure 3-5). The aquifer is at its thinnest (generally between 1 and 3 feet thick) in the month of September and its thickest (generally between 6 and 8.5 feet thick) between the months of December and March. It is likely that for the portions of the graphs where data is not available (September and December 1992), the water table behaves in a similar way as in the past, exhibiting a seasonal low.

Mozola (1951) states that groundwater in Seneca County (including the Ash Landfill site) is derived almost entirely from precipitation within the County. To investigate historical precipitation events and the likely relationship between fluctuations in the water table of the till/weathered shale aquifer and these precipitation events, monthly precipitation data for the years 1990 through most of 1993 were obtained from the Aurora Research Farm located 10 miles east of the site. Although no definitive trend is depicted by the data, they generally show higher amounts of precipitation in the spring (March and April) and fall (September) and relatively lower amounts in the summer (with the exception of the month of July 1992) and winter (January and February). These data alone do not explain the fluctuations observed on the saturated thickness plots (Figure 3-5).

The rhythmic behavior of the aquifer is not solely controlled by precipitation events, rather it is more likely affected by a combination of precipitation amounts and evapotranspiration rates. The later phenomenon is affected by temperature, exposure to the intensity of the sun, velocity of the wind, and the amount of vegetation. Horizontal flow is not believed to play a major role in discharging water from the till/weathered shale unit which has a relatively low conductivity (an average of 3.65×10^{-4} cm/sec). While vertical connection tests indicate that low degrees of downward movement are possible from the till/weathered shale aquifer to the competent shale aquifer, no strong downward vertical gradients are believed to occur on-site and, therefore, downward flow is also believed to be minimal compared to evaporative losses.

Therefore, based on the hydrographs for the wells, a conceptual model is that the high water table in the winter months is sustained by generally high precipitation amounts that last into the spring (March and April) and low evapotranspiration rates. Decreasing precipitation amounts



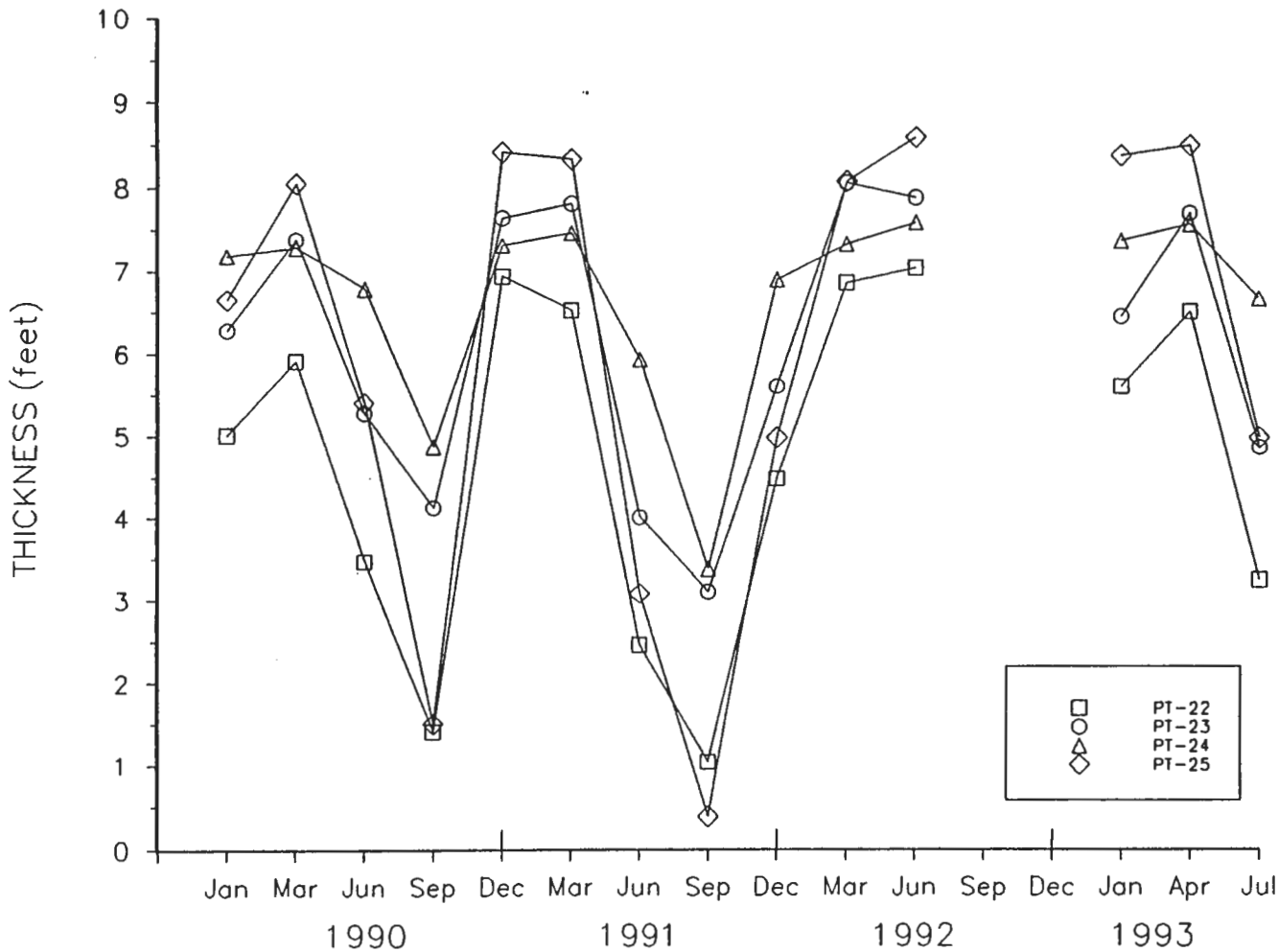
PARSONS
PARSONS ENGINEERING SCIENCE, INC.

CLIENT/PROJECT TITLE
**SENECA ARMY DEPOT ACTIVITY
 ASH LANDFILL GROUNDWATER MODEL**

DEPT. ENVIRONMENTAL ENGINEERING DWG NO. 726209-01002

**FIGURE 3-5
 HISTORICAL SATURATED THICKNESS
 IN THE
 TILL/WEATHERED SHALE AQUIFER**

SCALE NA DATE OCTOBER 1995



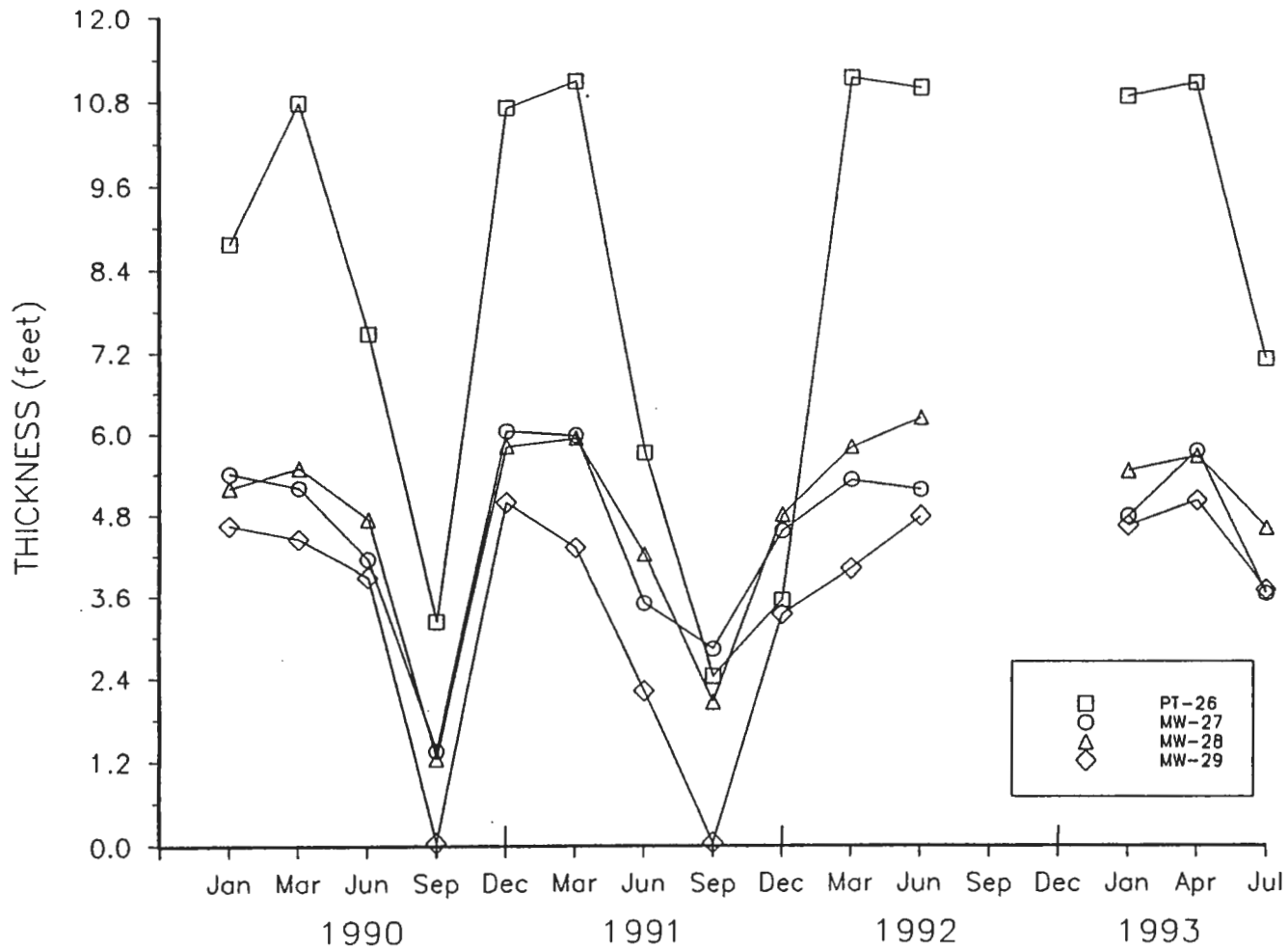
PARSONS
PARSONS ENGINEERING SCIENCE, INC.

CLIENT/PROJECT TITLE
**SENECA ARMY DEPOT ACTIVITY
 ASH LANDFILL GROUNDWATER MODEL**

DEPT. ENVIRONMENTAL ENGINEERING DWG NO. 726209-01002

**FIGURE 3-5 (CONTINUED)
 HISTORICAL SATURATED THICKNESS
 IN THE
 TILL/WEATHERED SHALE AQUIFER**

SCALE: NA DATE: OCTOBER 1995



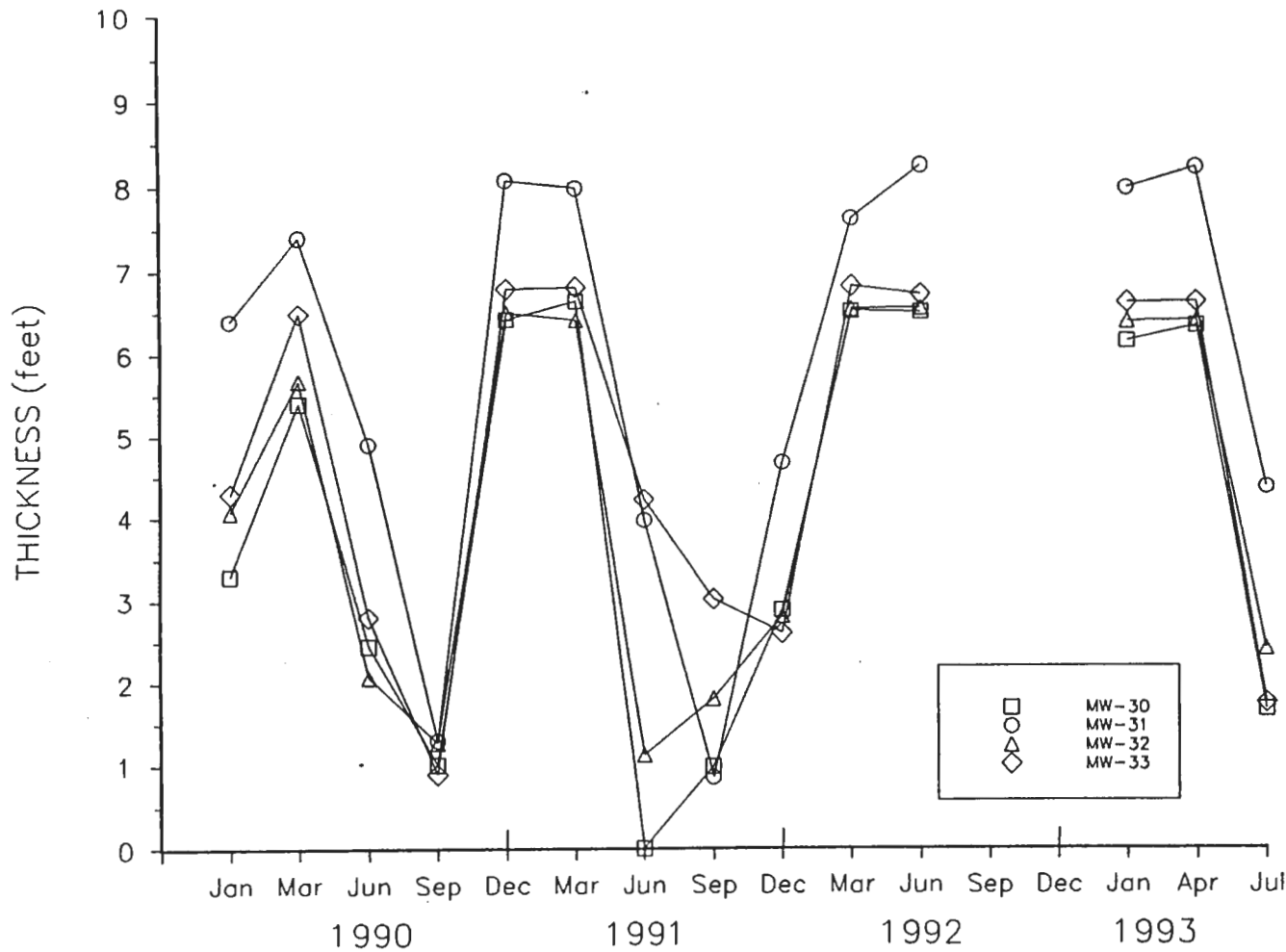
PARSONS
PARSONS ENGINEERING SCIENCE, INC.

CLIENT/PROJECT TITLE
**SENECA ARMY DEPOT ACTIVITY
ASH LANDFILL GROUNDWATER MODEL**

DEPT. ENVIRONMENTAL ENGINEERING DAG NO. 726209-01002

**FIGURE 3-5 (CONTINUED)
HISTORICAL SATURATED THICKNESS
IN THE
TILL/WEATHERED SHALE AQUIFER**

SCALE NA DATE OCTOBER 1995



PARSONS
PARSONS ENGINEERING SCIENCE, INC.

CLIENT/PROJECT TITLE
**SENECA ARMY DEPOT ACTIVITY
 ASH LANDFILL GROUNDWATER MODEL**

DEPT. ENVIRONMENTAL ENGINEERING DWG NO. 726209-01002

**FIGURE 3-5 (CONTINUED)
 HISTORICAL SATURATED THICKNESS
 IN THE
 TILL/WEATHERED SHALE AQUIFER**

SCALE NA DATE OCTOBER 1995

accompanied by an increase in evapotranspiration (due to an increase in temperature and more vegetation) in the summer results in little recharge to the aquifer and thus a fall in the water table. In the summer, when there is generally less rainfall and increased temperatures, evapotranspiration at the surface causes water to move up from the water table to the surface by capillary action, a phenomenon noted by deMarsily (1986). In the fall (September and October) there is generally an increase in precipitation and a decrease in evapotranspiration accounting for the increasing water table elevations observed into the winter months.

Support for the concept describing the behavior of the till/weathered shale aquifer can be found in the literature. Jones et al. (1992) discusses a shallow ground water flow system in a Wisconsin-age weathered till in Iowa and cites vertical upward movement and evapotranspiration as a primary source of discharge from the till. Cravens and Ruedisili (1987) and Hendry (1988) performed earlier studies at the Iowa site that showed that the recharge from surface percolation was predominantly discharged through capillary rise and evapotranspiration, and that lateral flow within the weathered till and vertical downward flow were minor. Cravens and Ruedisili (1987) also documented that the water table depth ranged from an average minimum of 2.4 feet in the Summer to an average maximum of 8.5 feet in the Fall; a similar seasonal trend is evident on the Ash Landfill site. Specifically, they attributed the rise and fall of the water table to "seasonal changes in precipitation, plant water use, and evaporation through micropores and fractures." According to Fetter (1980) water can rise by capillary action about 4.9 feet in silts and 9.8 feet in some clays and allows for large losses of water from the weathered till zone without the required movement of water downward through the unweathered till (Cravens and Ruedisili, 1987). Davis and Dewiest (1966) assert that use of water by plants is generally much more important as a means of ground water discharge than is direct soil evaporation. However, evaporation, aided by soil cracks and capillary transfer, is effective in the upper 3 feet of sandy soil and the upper 10 feet of clayey soil.

In another instance, hydrographs for peizometers screened in the upper portions of a Saskatchewan till showed seasonal fluctuations of up to 8 feet over an approximately 4 month period (Keller, et al., 1988). However, at this particular site, the seasonal ground water high occurs in September-October and the low in May-June. Based on hydrographs from nested peizometers the loss of groundwater at this site was shown not to be from downward flow, but was attributed to a combination of lateral flow and upward losses due to evapotranspiration, freezing in the unsaturated zone, and/or other causes.

DeMarsily (1986) describes the higher moisture content of the soil and generally a higher water table in the winter compared to the summer. A comparison of general moisture profiles in soil for these seasons indicates that precipitation events in the winter months are more likely to have a direct impact on the water table. This is due to the higher moisture content of the soil in the winter which allows for greater infiltration (recharge) of water during and after precipitation events. The moisture profiles indicate that in the summer, when evaporation is high, the atmosphere generally takes back all the moisture received during a storm, resulting in little recharge to the aquifer.

The various losses and gains in the till/weathered shale aquifer at the Ash Landfill site, as depicted on the water table elevation and saturated thickness plots and in the conceptual water balance described above, are supported by a monthly water balance model that was run for the same four years of historical data. The monthly water balance is presented in Table 3-1. This water balance was developed using the rational method described in "Use of the Water Balance Method for Predicting Leachate Generation From Solid Waste Disposal Sites" (EPA, 1975). The model takes into account evapotranspiration, precipitation, precipitation runoff, and infiltration. A more complete discussion of the water balance model can be found in Section 4.2. As shown in Table 3-1, much of the runoff and almost all of the percolation (groundwater recharge) occurs during March, April, and May, during the snow melt period. There is continued runoff throughout the time period when the temperature stays above freezing. This is consistent with observations made at the site regarding runoff and groundwater. There is always runoff at the site during a major rainfall since the clay soils on-site prevent rapid infiltration. Groundwater levels measured in the spring have been highest with levels dropping over the summer. Water levels in the winter have been lower than those in spring, indicating little or no recharge in summer and fall.

The large fluctuations in the saturated thickness of the till/weathered shale aquifer would likely have a direct impact on the ground water flow regime and thus the transport of volatile organics or other constituents. This would be especially true when the aquifer is at its thinnest (1 to 3 feet) in the summer and early fall, becoming dry at some locations.

3.5.7.3 Competent Shale Aquifer

The historical data base for the competent shale aquifer is very limited. Historical water table elevations are available for only one well (PT-10) which is believed to be screened in the competent shale. Unfortunately, the screened interval for this well is not known. Seasonally this well shows the same magnitude of fluctuations in water table elevation as the till/weathered shale wells.

TABLE 3 - 1
MONTHLY WATER BALANCE
1990
SENECA ARMY DEPOT
ASH LANDFILL GROUNDWATER MODEL

	Jan	Feb	Mar	Apr	May	Jun	Jul	Aug	Sep	Oct	Nov	Dec	Annual
Mean Temp. (°F)	22.5	23.4	32.0	44.8	54.5	64.6	69.1	66.9	60.6	50.4	39.4	27.9	46.3
Heat Index	0	0	0	1.7	4.0	7.0	8.5	7.8	5.8	2.9	0.7	0.0	38.4
Unadj. PET (in)	0.000	0.000	0.000	0.039	0.079	0.118	0.134	0.126	0.102	0.063	0.024	0.000	
Corr. Factor	24.6	24.6	30.9	33.6	37.8	38.1	38.4	35.7	31.2	28.5	24.6	23.7	
Adj. PET (in)	0.0	0.0	0.0	1.3	3.0	4.5	5.1	4.5	3.2	1.8	0.6	0.0	24.0
P (in)	2.16	3.71	2.23	4.58	6.24	2.82	3.14	1.89	4.36	5.86	3.02	4.92	44.9
Corr. P (in)	0	0	6.3	6.3	6.2	2.8	3.1	1.9	4.4	5.9	3.0	4.9	44.9
C R/O	0.22	0.22	0.22	0.22	0.20	0.18	0.18	0.18	0.18	0.18	0.20	0.22	
R/O (in)	0.0	0.0	1.4	1.4	1.2	0.5	0.6	0.3	0.8	1.1	0.6	1.1	9.0
I (in)	0.0	0.0	4.9	4.9	5.0	2.3	2.6	1.5	3.6	4.8	2.4	3.8	36.0
I-PET(in)	0.0	0.0	4.9	3.6	2.0	-2.2	-2.6	-2.9	0.4	3.0	1.8	3.8	11.9
neg (I-PET)						-2.2	-4.8	-7.7					
ST (in)	3.9	3.9	3.9	3.9	3.9	2.2	1.1	0.5	0.9	3.9	3.9	3.9	
delta ST (in)	0.0	0.0	0.0	0.0	-0.0	-1.7	-1.1	-0.6	0.4	3.0	0.0	0.0	
AET (in)	0.0	0.0	0.0	1.3	3.0	4.0	3.7	2.1	3.2	1.8	0.6	0.0	19.7
PERC (in)	0.0	0.0	4.9	3.6	2.1	0.0	0.0	0.0	0.0	0.0	1.8	3.8	16.2
delta W.T. (feet)	0.0	0.0	1.4	0.6	-0.3	-1.6	-1.3	-0.8	-0.8	0.3	0.3	1.1	

NOTES:

PET = Potential Evapotranspiration

P = Precipitation

Corr. P = Corrected precipitation (rain + melting snow)

C R/O = Surface Runoff Coefficient

R/O = Surface Runoff

I = Infiltration

I-PET = Infiltration minus Potential Evapotranspiration

neg (I-PET) = Accumulated Potential Water Loss

ST = Soil Moisture Storage (for negative accumulated water loss values, soil storage values were obtained from table 9 of "A Current Report on Solid Waste Management.")

delta ST = Change in Storage

AET = Actual evapotranspiration

PERC = Percolation

delta W.T. = PERC + delta ST - AET

TABLE 3 - 1
MONTHLY WATER BALANCE
1991
SENECA ARMY DEPOT
ASH LANDFILL GROUNDWATER MODEL

	Jan	Feb	Mar	Apr	May	Jun	Jul	Aug	Sep	Oct	Nov	Dec	Annual
Mean Temp. (°F)	22.5	23.4	32.0	44.8	54.5	64.6	69.1	66.9	60.6	50.4	39.4	27.9	46.3
Heat Index	0	0	0	1.7	4.0	7.0	8.5	7.8	5.8	2.9	0.7	0.0	38.4
Unadj. PET (in)	0.000	0.000	0.000	0.039	0.079	0.118	0.134	0.126	0.102	0.063	0.024	0.000	
Corr. Factor	24.6	24.6	30.9	33.6	37.8	38.1	38.4	35.7	31.2	28.5	24.6	23.7	
Adj. PET (in)	0.0	0.0	0.0	1.3	3.0	4.5	5.1	4.5	3.2	1.8	0.6	0.0	24.0
P (in)	1.54	1.13	2.59	4.60	1.87	0.89	3.38	3.29	2.62	2.68	3.63	2.10	30.3
Corr. P (in)	0	0	4.5	5.4	1.9	0.9	3.4	3.3	2.6	2.7	3.6	2.1	30.3
C R/O	0.22	0.22	0.22	0.22	0.20	0.18	0.18	0.18	0.18	0.18	0.20	0.22	
R/O (in)	0.0	0.0	1.0	1.2	0.4	0.2	0.6	0.6	0.5	0.5	0.7	0.5	6.0
I (in)	0.0	0.0	3.5	4.2	1.5	0.7	2.8	2.7	2.1	2.2	2.9	1.6	24.3
I-PET(in)	0.0	0.0	3.5	2.9	-1.5	-3.8	-2.4	-1.8	-1.0	0.4	2.3	1.6	0.3
neg (I-PET)					-1.5	-5.3	-7.6	-9.4	-10.5				
ST (in)	3.9	3.9	3.9	3.9	2.7	1.0	0.6	0.4	0.2	0.6	3.0	3.9	
delta ST (in)	0.0	0.0	0.0	0.0	-1.2	-1.7	-0.5	-0.2	-0.1	0.4	2.3	0.9	
AET (in)	0.0	0.0	0.0	1.3	2.7	2.4	3.2	2.9	2.3	1.8	0.6	0.0	17.2
PERC (in)	0.0	0.0	3.4	2.9	-0.0	0.0	-0.0	-0.0	-0.0	0.0	0.0	0.7	7.0
delta W.T. (feet)	0.0	0.0	1.0	0.4	-1.1	-1.1	-1.0	-0.9	-0.7	-0.4	0.5	0.5	

TABLE 3 - 1
MONTHLY WATER BALANCE
1992
SENECA ARMY DEPOT
ASH LANDFILL GROUNDWATER MODEL

	Jan	Feb	Mar	Apr	May	Jun	Jul	Aug	Sep	Oct	Nov	Dec	Annual
Mean Temp. (°F)	22.5	23.4	32.0	44.8	54.5	64.6	69.1	66.9	60.6	50.4	39.4	27.9	46.3
Heat Index	0	0	0	1.7	4.0	7.0	8.5	7.8	5.8	2.9	0.7	0.0	38.4
Unadj. PET (in)	0.000	0.000	0.000	0.039	0.079	0.118	0.134	0.126	0.102	0.063	0.024	0.000	
Corr. Factor	24.6	24.6	30.9	33.6	37.8	38.1	38.4	35.7	31.2	28.5	24.6	23.7	
Adj. PET (in)	0.0	0.0	0.0	1.3	3.0	4.5	5.1	4.5	3.2	1.8	0.6	0.0	24.0
P (in)	1.54	1.56	3.22	2.90	3.27	2.93	8.81	3.20	5.25	3.04	3.22	2.90	41.8
Corr. P (in)	0	0	5.4	3.8	3.3	2.9	8.8	3.2	5.3	3.0	3.2	2.9	41.8
C R/O	0.22	0.22	0.22	0.22	0.20	0.18	0.18	0.18	0.18	0.18	0.20	0.22	
R/O (in)	0.0	0.0	1.2	0.8	0.7	0.5	1.6	0.6	0.9	0.5	0.6	0.6	8.1
I (in)	0.0	0.0	4.2	3.0	2.6	2.4	7.2	2.6	4.3	2.5	2.6	2.3	33.7
I-PET(in)	0.0	0.0	4.2	1.7	-0.4	-2.1	2.1	-1.9	1.1	0.7	2.0	2.3	9.7
neg (I-PET)					-0.4	-2.5		-1.9					
ST (in)	3.9	3.9	3.9	3.9	3.5	2.0	3.9	2.4	3.5	3.9	3.9	3.9	
delta ST (in)	0.0	0.0	0.0	0.0	-0.4	-1.5	1.9	-1.5	1.1	0.4	0.0	0.0	
AET (in)	0.0	0.0	0.0	1.3	3.1	3.9	5.1	4.1	3.2	1.8	0.6	0.0	23.1
PERC (in)	0.0	0.0	4.2	1.7	0.0	0.0	0.2	0.0	0.0	0.3	2.0	2.3	10.6
delta W.T. (feet)	0.0	0.0	1.2	0.1	-1.0	-1.5	-0.8	-1.6	-0.6	-0.3	0.4	0.6	

4.0 CONCEPTUAL MODEL

This section will describe the conceptual model that was developed prior to the initiation of modeling activities. The conceptual model for the Ash Landfill has two main components associated with it. The first component includes aspects of the model associated with flow conditions and the hydrogeological setting. The second component includes aspects associated with the fate and transport of the chlorinated organic compounds present in the groundwater. The complete conceptual model will present a proficient understanding of these two aspects so that the modeling will be consistent with and represent, as much as possible, the actual physical condition of the Ash Landfill.

The first sections of the conceptual model focuses on the hydrogeological facets of the model. The final section of the conceptual model describes information pertinent to the fate and transport of chlorinated organics. The intent of the conceptual model is to integrate the physical hydrogeological setting at the site into a simplified, yet representative, depiction of the various hydrological units to be modeled. The conceptual model will also define the vertical and horizontal boundaries of the modeling effort. The significance of the conceptual model cannot be underscored as the numerical model grid is a mathematical representation of the system described by the conceptual model.

The conceptual model was developed following an evaluation of soil and groundwater stratigraphy data collected from the Ash Landfill RI. The Ash Landfill site is located approximately halfway between the topographic high of 760 feet msl and Seneca Lake, which has an elevation of approximately 455 msl. The land surface slopes from the topographic high to Seneca Lake. There are no other high points between these two points. Groundwater flow in the overlying glacial till is known to follow the slope of the land surface and therefore groundwater is expected to flow from the topographic high area, past the Ash Landfill site, eventually discharging into Seneca Lake. The direction of flow would be from east to west.

Based upon this information, the area to be modeled includes an area, beyond the Ash Landfill site, encompassing the western flank of the highlands separating Seneca and Cayuga Lakes. The eastern highland area is considered to be a groundwater divide between the two finger lakes; this area is also believed to be a recharge zone for both the shallow till/weathered shale and deeper competent shale aquifers. Seneca Lake is the discharge area for the two aquifer systems. The eastern to western extent of the conceptual model corresponds to a distance of approximately 24,000 feet, and it extends from the groundwater divide to the surface of Seneca Lake. The groundwater divide was

established to represent a no flow boundary condition whereas, Seneca Lake was established as a constant head boundary condition. The boundary conditions along the northern and southern edges of the modeling grid are defined as no flow conditions represented by groundwater streamlines. This is consistent with the conceptual model since groundwater at the site is known to flow down the hill in an east to west direction. Since flow contours are east to west, streamlines have been established that are sufficiently wide to encompass the area to be modeled. These streamlines provide the northern and southern boundaries of the conceptual model grid covering an area 6,800 feet wide. The total area to be modeled is approximately 3,750 acres.

4.1 DEFINITION OF HYDROSTRATIGRAPHIC UNITS

The vertical description of the conceptual model will be described in the following section. Geologic information including geologic maps, soil boring and rock coring logs were combined with information describing hydrogeologic properties of the stratigraphic units identified at this site. Anderson and Woessner (1992) define hydrostratigraphic units as geologic units that comprise similar hydrogeologic properties.

Two hydrostratigraphic units were identified for this model. The first unit is the till/weathered shale unit and the second unit competent shale unit. These two geologic units have different depositional environments. The shale was deposited in an inland sea during the Devonian Period (approximately 400,000 million ybp) and the till was deposited directly by a continental glacier that advanced over the Finger Lakes region approximately 10,000 ybp. As a result, these two units have separate and distinct compositional and hydrologic properties.

The first hydrostratigraphic unit is till. The till is a dense, poorly sorted mixture of predominantly silt and clay with lesser amount of sand and gravel. Upper portion of the till are generally less dense than the lower portions, probably a result of a greater effect from weathering processes. The base of the till contains clasts of shale that are likely rip-up clasts incorporated into the till by the glacier. No vertical fracturing was observed in the till. The till gives way to a weathered shale that contains variable amounts of silt and clay in centimeter-scale bedding plane fractures. The weathered shale is generally only a few feet thick on the site. From previous drilling efforts conducted at the Ash Landfill site and other sites at SEDA, it is known that the till/weathered shale unit has an average thickness of approximately 12 feet. The till/weathered shale unit has an average horizontal hydraulic conductivity (K_h) of 3.65×10^{-4} cm/sec (Table 4-1).

TABLE 4 - 1

STATISTICAL PARAMETERS OF HYDRAULIC CONDUCTIVITY

SENECA ARMY DEPOT
ASH LANDFILL GROUNDWATER MODEL

	Kh (cm/sec)	Kh (ft/day)	Kv (cm/sec)	Kv (ft/day)
Layer 1				
Till/W. Shale				
	3.090E-05	0.09	3.433E-06	0.01
	7.800E-04	2.21	8.667E-05	0.25
	1.847E-04	0.52	2.052E-05	0.06
	5.258E-04	1.49	5.842E-05	0.17
	7.066E-04	2.00	7.851E-05	0.22
	3.871E-05	0.11	4.301E-06	0.01
	7.031E-04	1.99	7.812E-05	0.22
Minumum	3.090E-05	0.09	3.433E-06	0.01
Maxiumum	7.800E-04	2.21	8.667E-05	0.25
Arith. Mean	3.650E-04	1.03	4.055E-05	0.11
Stand. Dev.	3.430E-04	0.97	3.811E-05	0.11
Layer 2				
C. Shale				
	4.719E-05	0.13	4.719E-06	0.01
	1.222E-04	0.35	1.222E-05	0.03
	1.595E-04	0.45	1.595E-05	0.05
	5.044E-05	0.14	5.044E-06	0.01
	3.786E-05	0.11	3.786E-06	0.01
Minumum	3.786E-05	0.11	3.786E-06	0.01
Maxiumum	1.595E-04	0.45	1.595E-05	0.05
Arith. Mean	7.142E-05	0.20	7.142E-06	0.02
Stand. Dev.	5.902E-05	0.17	5.902E-06	0.02
Layer 3				
C. Shale				
	6.934E-06	0.02	6.934E-07	0.002
	5.639E-06	0.02	5.639E-07	0.002
	3.505E-06	0.01	3.505E-07	0.001
	1.671E-05	0.05	1.671E-06	0.005
	3.004E-05	0.09	3.004E-06	0.009
Minumum	3.505E-06	0.01	3.505E-07	0.001
Maxiumum	3.004E-05	0.09	3.004E-06	0.009
Arith. Mean	1.344E-05	0.04	1.344E-06	0.004
Stand. Dev.	1.271E-05	0.04	1.271E-06	0.004
Layer 4				
C. Shale (NO MEASUREMENTS FROM THIS LAYER)				

The second hydrostratigraphic unit is the competent shale. This shale is a gray calcareous shale of the Ludlowville Formation, characterized by thin limestone units, fossil beds, and minor deposits of iron sulfides. Bedding plane fractures, joints and breccia zones all contribute to secondary porosity in the shale. Generally, fracture frequency decreases with depth. The competent shale unit has an average K_h of 4.24×10^{-5} cm/sec (Table 4-1).

The data indicates that hydraulic conductivity values in the till/weathered shale are greater than those measured in the competent shale, and hydraulic conductivity values continue to decrease within the competent shale unit with depth (Figure 4-1). Since the hydraulic conductivity of these two units are over an order of magnitude different, it was decided that these two units would be modeled separately.

Further evidence for differentiating these two hydrostratigraphic units is supported by the vertical connection testing performed on paired wells and well clusters at the Ash Landfill site. A comparison of drawdowns in the wells indicated that the degree of vertical connection within the competent shale aquifer is better than the connection observed between the till/weathered shale and competent shale aquifers. Thus, the results indicate that the till/weathered shale aquifer is connected, although not significantly, to the competent shale aquifer below it.

4.2 WATER BALANCE FROM PRECIPITATION

The fate and transport of the constituents of concern is influenced by the interaction with precipitation, the recharge to groundwater and the migration with groundwater. Moisture content in the vadose zone of soil can also influence the rate of biological decomposition and the rate of volatilization. Accordingly, understanding the water balance of the site is helpful in evaluating the contaminant fate and transport at the Ash Landfill. A water balance was developed for this site using the rational method described in *Use of the Water Balance Method for Predicting Leachate Generation from Solid Waste Disposal Sites* (EPA, 1975). This procedure calculates the percolation of pore water to groundwater as recharge. Recharge is the difference between the amount of water that infiltrates into the ground minus the actual evapotranspiration and any changes in soil moisture. Infiltration is the difference between precipitation and runoff. The results of these calculations are summarized in Table 4-2.

TABLE 4-2
MONTHLY WATER BALANCE
SENECA ARMY DEPOT ACTIVITY
ASH LANDFILL GROUNDWATER MODEL

<i>Line #</i>	<i>Parameter</i>	<i>Jan</i>	<i>Feb</i>	<i>Mar</i>	<i>Apr</i>	<i>May</i>	<i>Jun</i>	<i>Jul</i>	<i>Aug</i>	<i>Sep</i>	<i>Oct</i>	<i>Nov</i>	<i>Dec</i>	<i>Annual</i>
1	Mean Temp. (°F)	22.5	23.4	32.0	44.8	54.5	64.6	69.1	66.9	60.6	50.4	39.4	27.9	46.3
2	Heat Index	0	0	0	1.7	4.0	7.0	8.5	7.8	5.8	2.9	0.7	0.0	38.4
3	Unadj. PET (in)	0.000	0.000	0.000	0.039	0.079	0.118	0.134	0.126	0.102	0.063	0.024	0.000	
4	Corr. Factor	24.6	24.6	30.9	33.6	37.8	38.1	38.4	35.7	31.2	28.5	24.6	23.7	
5	Adj. PET (in)	0.0	0.0	0.0	1.3	3.0	4.5	5.1	4.5	3.2	1.8	0.6	0.0	24.0
6	P (in)	1.88	2.16	2.45	2.86	3.17	3.70	3.46	3.18	2.95	2.80	3.15	2.57	34.3
7	Corr. P (in)	0	0	7.1	4.8	3.2	3.7	3.5	3.2	3.0	2.8	3.2	0	34.3
8	C R/O	0.22	0.22	0.22	0.22	0.20	0.18	0.18	0.18	0.18	0.18	0.20	0.22	
9	R/O (in)	0.0	0.0	1.6	1.1	0.6	0.7	0.6	0.6	0.5	0.5	0.6	0.0	6.8
10	I (in)	0.0	0.0	5.5	3.8	2.5	3.0	2.8	2.6	2.4	2.3	2.5	0.0	27.5
11	I-PET(in)	0.0	0.0	5.5	2.5	-0.4	-1.5	-2.3	-1.9	-0.8	0.5	1.9	0.0	3.5
12	neg (I-PET)					-0.4	-1.9	-4.2	-6.1	-6.9				
13	ST (in)	3.1	3.1	3.9	3.9	3.5	2.4	1.3	0.8	0.7	1.2	3.1	3.1	
14	delta ST (in)	0.0	0.0	0.8	0.0	-0.4	-1.1	-1.1	-0.5	-0.1	0.5	1.9	0.0	
15	AET (in)	0.0	0.0	0.0	1.3	3.0	4.1	3.9	3.1	2.5	1.8	0.6	0.0	20.4
16	PERC (in)	0.0	0.0	4.7	2.5	0.0	0.0	0.0	0.0	-0.0	0.0	0.0	0.0	7.1

References:

1. Thornthwaite and Mather, 1957. Instructions and Tables for Computing Potential Evapotranspiration and the Water Balance.
2. EPA, 1975. Use of the Water Balance Method for Predicting Leachate Generation from Solid Waste Disposal Sites.

Notes:

1. Mean temperatures (from Table 3.1, Section 3, of this report)
2. Heat index values (from Tables 1 and 2 of Thornthwaite and Mather, 1957)
3. PET = Potential Evapotranspiration (from Tables 3 and 4 of Thornthwaite and Mather, 1957)
4. Correction factors (from Table 6 of Thornthwaite and Mather, 1957)
5. Adj. PET = Unadj. PET times Correction Factor
6. P = Precipitation (from Table 3.1, Section 3, of this report)
7. Corr. P = Corrected precipitation (rain + melting snow)
8. C R/O = Surface Runoff Coefficient (from EPA, 1975)
9. R/O = Surface Runoff
10. I = Infiltration
11. I-PET = Infiltration minus Potential Evapotranspiration
12. neg (I-PET) = Accumulated Potential Water Loss
13. ST = Soil Moisture Storage (Maximum value of 3.9" obtained from Table 10 of Thornthwaite and Mather, 1957., Other values obtained from Table 9 of EPA, 1975.)
14. delta ST = Change in Storage
15. AET = Actual evapotranspiration
16. PERC = Percolation

The potential evapotranspiration (PET), was estimated using the procedure described by C.W. Thornthwaite and J.R. Mather in *Publications In Climatology, Volume X, Number 3; Instructions and Tables for Computing Potential Evapotranspiration and the Water Balance, (1957)*. Evapotranspiration is an estimate of the amount of water which is released from the site through both evaporation and plant uptake (transpiration). The methodology begins by determining the Heat Index, which is obtained from either Table 1 or 2 of the Thornthwaite and Mather document. Mean monthly temperature data was obtained from the nearby meteorological station, the Aurora Research Farm, which is operated by Cornell University. The data is shown on Line 1 on Table 4-2. The monthly Heat Indexes are shown on Line 2 of Table 4-2. Heat Indexes are zero when the mean monthly temperature is less than 32°F. From the sum of the monthly Heat Indexes, the unadjusted potential evapotranspiration is obtained from either Table 3 or 4 of the Thornthwaite and Mather document. The unadjusted potential evapotranspiration values are presented on Line 3 of Table 4-2. To change the unadjusted values of potential evapotranspiration into the adjusted monthly potential evapotranspiration, the unadjusted values were multiplied by a correction factor. The correction factor is expressed in terms of a 12-hour day, which provides an indication of the duration of sunlight for a particular month. Correction factors for the unadjusted potential evapotranspiration are obtained from Table 6 of the same document and depend upon the latitude of the site. This value is presented on Line 4 of Table 4-2. The adjusted Potential Evapotranspiration (PET) is then calculated as the product of Lines 3 and 4 of Table 4-2.

Although site specific precipitation data was not available, monthly precipitation values from the Aurora Research Farm was used. A comprehensive discussion of the weather data is presented in Table 3-1, and discussed in Section 3 of this report.

When the mean monthly temperatures are below 32° F the monthly precipitation values were then corrected to account for precipitation as snowfall in the months of December through March. It was assumed that all of the snowfall remained on the ground as snow, with no evaporation, infiltration, or runoff until March when the snow began to melt. It was also assumed that 60% of the snow (the total precipitation for December, January, and February) melted in March, and therefore entered the water balance as precipitation in addition to the normal monthly precipitation for March. The remaining 40% of the accumulated snowfall was assumed to melt in April.

The total monthly precipitation was then adjusted to account for the percent of water which runs off as overland flow. Line 8, in Table 4-2, contains the Runoff Coefficient, C_{RO} . This coefficient is a measure of the amount of precipitation that will runoff from any given area, and will depend on the

soils, vegetation, and slopes found at a site. Generally, C_{RO} values range from 0.05 to 0.35 (EPA, 1975). At the Ash Landfill, the surface soils are primarily silty clay loams, as described in Section 1. Much of the area is covered with native grasses, though some of the road areas have no vegetative cover. The site slopes generally range from 1 to 3%. For these conditions, the C_{RO} values range from 0.13 (less than 2% slope) to 0.22 (2-7% slopes). Following EPA guidance (1975), a higher C_{RO} (0.22) was used for the cooler months, and a lower value (0.18) was used for the warmer months. For the transitional months, (May and November), a value of 0.20 was used.

Infiltration (I), Line 10, is calculated as the difference between the monthly corrected precipitation values, Line 7, and the calculated runoff values, Line 9. Infiltration (Line 10) minus the adjusted potential evapotranspiration values, Line 5, yields I-PET, Line 11. This value was used to assess periods of time when the soil moisture is decreasing. A positive value of I-PET indicates the amount which is available to increase soil moisture or percolate to groundwater. Negative values indicates that potential evapotranspiration exceeds infiltration and there is a net decrease in the soil moisture.

Soil moisture (ST) is a measurement of the available field moisture and is related to soil type. The available moisture is obtained as the difference between the field capacity, i.e. the point at which water will drain by gravity, and the wilting point, i.e. the point at which water is unavailable for plant uptake. For this site, the available soil maps, shown in Section 1 of this report, indicate the soil type to be a silty loam. From Table 10 of the Thornthwaite and Mather document. The field capacity for a silty loam is approximately 3.6 inches per foot of root zone. The wilting point for a silty loam is approximately 1.2 inches per foot of root zone. The available soil moisture (ST) is the difference of 3.6 and 1.2 inches per foot or 2.4 inches per foot of root zone. The *Soil Survey of Seneca County, New York*, (April 1972) indicates that the root zone for this area generally ranges from 18 to 24 inches. This analysis used 1.62 feet (19.4 inches) as the root zone, therefore, the ST value used in these calculations was 3.9 inches as shown on Line 13, which was the product of 2.4 inches per foot of root zone and 1.62 feet of root zone. This initial value is assigned to the last month having a positive value of I-PET, which is the month of April. In other words, the last month that the field capacity of the soil was achieved and drainage occurred was April and the value of 3.9 was set for this month. The water balance then proceeded to calculate the ST for the remaining months.

The Actual Evapotranspiration (AET), Line 15, is a calculated value only when the change in soil moisture is negative. The change in soil moisture is presented on Line 14. If the Heat Index, Line 2

is zero then the AET is also zero. In other words when the temperature is below freezing there is no AET. If the ST, Line 13, is equal to the field capacity, which is the maximum value ST can be, then the AET equals the Adjusted PET, Line 5. In other words, the AET is greatest when the soil moisture is maximum. When the change in soil moisture is negative, i.e. the soil moisture is decreasing, the AET is calculated as:

$$AET = PET + (I - PET - \Delta ST)$$

where: AET = Actual Evapotranspiration, Line 15,
PET = Adjusted Potential Evapotranspiration, Line 5,
I-PET = Infiltration minus Adjusted Potential Evapotranspiration, Line 11 and
 ΔST = Change in Soil Moisture, Line 14.

Percolation (PERC), Line 16, which is recharge to the groundwater, is calculated as the remainder when the change in soil moisture, Line 14, and the AET, Line 15, is subtracted from I, Line 10.

The results of the water balance analysis indicates that much of the runoff and almost all of the percolation (groundwater recharge) occur in March and April, during the snow melt period. There is continued runoff throughout the time period when the temperature stays above freezing, however, recharge is eliminated by the large amount of water that is released to the atmosphere through evapotranspiration; the average annual evapotranspiration at the site is 20.4 inches. These estimates are consistent with observations made at the site regarding runoff and groundwater. During field operations, runoff was observed following any major rainfall event. This observation is consistent with expectations since the dense clay rich till soils prevent rapid infiltration. With respect to the groundwater, water levels measured in the spring have historically been the highest, with the levels dropping substantially throughout the summer months. Changes in water levels of three to four feet have been observed. During the late summer and early fall, the groundwater table is the lowest, in some instances the water level appears close to the top of the competent bedrock. Water levels measured in the winter have also been lower than those in the spring, indicating little or no recharge in the summer and fall.

Using the values developed from the water balance for annual runoff, 6.8 inches, and the surface area of the Ash Landfill site, which is approximately 130 acres, the total annual amount of potential runoff is 74 acre-feet (24 million gallons) per year. Much of this flow is captured and diverted

away from the site by the surface drainage swales which line the edges of the roads surrounding the site, while some is retained on-site in the freshwater wetlands and low spots.

To provide a check of the average annual evapotranspiration (ET) rate calculated by the Thornthwaite and Mather (1957) method in the water balance, an evapotranspiration computer model, developed and executed by the Northeast Regional Climate Center at Cornell University, was run. This general ET model was developed based on the British Meteorological Office Rainfall and Evaporation Calculation System (MORECS).

According to DeGaetano et al. (1994), MORECS is used "operationally in Great Britain to obtain weekly and monthly estimates of average evaporation and soil moisture deficits over 40 km x 40 km grid squares. The system relies on routinely observed daily meteorological data as its input." Moreover, MORECS determines potential and actual ET over a variety of different surface types. The Northeast Regional Climate Center model has been modified and validated for use in the northeastern United States. Using MORECS, "historical and real-time estimates of potential ET from grass, evapotranspiration from bare soil and standard evaporation pans, as well as actual ET from grass- deciduous tree-covered surfaces are available" (DeGaetano et al., 1994).

For application to the Ash Landfill, actual ET rates from a grass-covered surface were chosen as the most appropriate for the site. Meteorological data from Ithaca, New York was used for the model because this was the closest location that could provide the necessary input data for the model; Ithaca is approximately 20 miles south of the Ash Landfill. The model evaluated meteorological data for the years 1984 through 1994 and derived the monthly total evapotranspiration from a grass-covered field (Table 4-3). The average yearly total evapotranspiration for the grass-covered field is 21.19 inches. This compares favorably with the total evapotranspiration value calculated using the Thornthwaite and Mather (1957) method of 20.40 inches. Details of the MORECS model are included in Appendix A.

While there is close agreement between both of these models, neither accounts for ET from groundwater after percolation has occurred. This importance of this effect is discussed in the Section 4.3, Preliminary Water Budget (Q_{in} vs Q_{out}).

TABLE 4-3
MONTHLY EVAPOTRANSPIRATION FROM GRASS
IN ITHACA, NY
SENECA ARMY DEPOT ACTIVITY
ASH LANDFILL GROUNDWATER MODEL

Year Month	1984 (inches)	1985 (inches)	1986 (inches)	1987 (inches)	1988 (inches)	1989 (inches)	1990 (inches)	1991 (inches)	1992 (inches)	1993 (inches)	1994 (inches)
January	0.24	0.22	0.28	0.24	0.27	0.37	0.33	0.30	0.27	0.24	0.17
February	0.53	0.39	0.31	0.55	0.48	0.35	0.53	0.47	0.22	0.43	0.54
March	0.80	1.28	1.20	1.65	1.26	1.19	1.27	1.00	0.67	0.93	0.87
April	1.80	2.00	2.17	1.96	1.73	1.91	1.99	2.08	1.64	1.57	1.93
May	2.12	3.48	3.71	3.46	3.20	2.51	2.52	4.03	2.84	3.43	2.64
June	4.30	3.15	3.38	3.51	4.39	3.02	3.60	3.65	3.51	3.42	4.20
July	4.26	4.10	3.49	4.19	3.43	4.51	3.81	3.38	2.35	4.09	4.05
August	3.39	2.77	3.34	3.08	3.33	3.27	3.10	2.03	2.91	3.00	2.97
September	2.37	2.38	2.00	1.52	2.57	2.04	2.03	1.04	2.21	1.53	2.05
October	1.30	1.27	0.93	1.09	0.94	1.41	1.10	1.44	1.14	1.11	1.45
November	0.52	0.32	0.40	0.51	0.53	0.33	0.69	0.53	0.43	0.42	0.61
December	0.32	0.21	0.27	0.28	0.34	0.25	0.31	0.30	0.28	0.40	0.41
TOTAL (inches):	21.95	21.57	21.48	22.04	22.47	21.16	21.28	20.25	18.47	20.57	21.89

ARITHMATIC MEAN: 21.19 inches

4.3 PRELIMINARY WATER BUDGET (Q_{in} vs Q_{out})

A preliminary field estimated water budget was prepared for the area to be modeled based on the expected sources of water to the system as well as the expected flow directions and discharge areas. This preliminary water budget was prepared to obtain information on the magnitudes of these flows prior to running the model. It was also used as a calibration criteria for the water budget computed by the model.

The field-estimated water budget encompassed an area equal in size to the area to be modeled. The eastern boundary was the groundwater divide (no flow boundary) between Seneca and Cayuga Lakes (near Route 96) and the western boundary was Seneca Lake (constant head boundary) (Figure 2-1). Because groundwater topographic maps for the site and surrounding area indicate a fairly consistent east to west flow direction the northern and southern boundaries were streamline no flow boundaries.

Based on the boundary conditions, recharge to the aquifer system is wholly from precipitation and groundwater flow is from east to west and eventually discharges into Seneca Lake. The total area of the region modeled was 150,413,697.2 ft². The annual recharge from precipitation derived from the water balance is 7.1 inches (0.592 ft). To calculate the total recharge to the aquifer systems (Q_{in}) the total area was multiplied by the annual amount of recharge from precipitation;

$$Q_{in} = \text{Area of model} \times \text{Amount of recharge from precipitation.}$$

This resulted in a Q_{in} value of 89,044,908.74 ft³/yr or 243,958.65 ft³/day.

The volume of water flowing into Seneca Lake (Q_{out}) was calculated based on flow through 4 proposed layers that are defined primarily by composition and by differences in hydraulic conductivity (Figure 4-1). The composition of the 4 layers, their thickness relative to the ground surface, and their hydraulic conductivity's, cross-sectional areas and ground water gradients are shown on Table 4-4.

Layer 1, the tili weathered shale unit, is approximately 12 feet thick and has an average saturated thickness of 6 feet. A layer thickness of 20 feet was used for the layer thicknesses of the three competent shale units because this is the interval for which the data was available from the monitoring wells at the Ash Landfill site; these units are fully saturated.

TABLE 4-4

DATA USED IN PRELIMINARY WATER BUDGET CALCULATION

**SENECA ARMY DEPOT ACTIVITY
ASH LANDFILL GROUNDWATER MODEL**

Proposed Layer	Composition	Stratigraphic Depth (feet bls)	Hydraulic Conductivity (feet/day)	Cross-Sectional Area (square feet)	Groundwater Gradient (feet/foot)	Qout (cu feet/day)	Percentage of Total Qout
1	Till/W. Shale	0 to 12	1.03	55,339.68	0.02	1,139.99	50.5%
2	Competent Shale	12 to 32	0.2	184,465.60	0.025	922.33	40.9%
3	Competent Shale	32 to 52	0.04	184,465.60	0.025	184.47	8.2%
4	Competent Shale	52 to 72	0.0023	184,465.60	0.025	10.61	0.5%
					Total Qout =	2,257.40	

The flow for each proposed layer was calculated using the flow equation:

$$Q_{\text{out}}=KAI$$

where: Q_{out} = flow out of the layer,
 K = horizontal hydraulic conductivity (K_h),
 A = cross-sectional area through which the flow occurs, and
 I = groundwater gradient.

The individual components of total Q_{out} are 1,139.99 ft³/day, 922.33 ft³/day, 184.47 ft³/day, and 10.61 ft³/day for layers 1, 2, 3 and 4, respectively (Table 4-4). The volume of water flowing into Seneca Lake was calculated to be 2,257.4 ft³/day. The flow calculations are included in Appendix B.

As a mechanism to reasonably define the bottom of the flow system to be modeled, the percentage of flow within the individual layers was compared to the overall aquifer flow into Seneca Lake. Based on these calculations, the contribution of flow from layer 4 (approximately 0.5%) was determined to not be significant when compared to the total flow through the system and ,therefore, a fourth layer was not considered in the numerical MODFLOW model. This method of determining a practical bottom of the flow system is not believed to compromise the accurate representation of the flow system from a modeling perspective.

Clearly, when Q_{in} (243,958.65 ft³/day) from precipitation is compared to Q_{out} (2,257.4 ft³/day) at Seneca Lake there is an obvious discrepancy. Conceptually, the model is believed to represent the flow system accurately and this is not believed to be responsible for the disagreement in the two flows. More likely, the discrepancy is believed to be caused by the lack of the water balance to account for evapotranspiration from groundwater after percolation has occurred, which would remove more water from the flow system. The Q_{in} from precipitation is reasonable and was calculated based on annual percolation of 0.59 feet from the water balance using the method of Thornthwaite and Mather (1957). Thus, based on a comparison of Q_{in} vs Q_{out} , significantly more water would have to be removed from the flow system via evapotranspiration from groundwater in order for the two flows to balance. The phenomenon of high evapotranspiration rates in unconfined, fine-grained aquifers where the water table is close to a vegetated land surface is not uncommon and has been documented by many researchers (Jones et al., 1992; Cravens and Ruedisili, 1987; Hendry, 1988; and Keller et al., 1988). Furthermore, the characteristics and

behavior of the aquifer flow system at the Ash Landfill suggest that this phenomenon is occurring at the Ash Landfill and in the surrounding area. Thus, it is reasonable to conclude that a significant amount of the water that percolates into the groundwater flow system at the Ash Landfill is later lost to evapotranspiration and is never discharged to Seneca Lake.

4.4 DEFINITION OF FLOW SYSTEM AND BOUNDARY CONDITIONS

The flow system at the Ash Landfill is defined by hydrostratigraphy, hydrologic information, and geochemical data.

The groundwater flow system is primarily recharged by precipitation within Seneca County (Mozola, 1955). Approximately 34.3 inches of rain falls in the region. Approximately 6.8 inches is lost to runoff, 20.4 is lost to evapotranspiration, and 7.1 percolates into the groundwater (Table 4-2). However, this model does not account for the loss of groundwater from the system via evapotranspiration. It is clear from calculation of groundwater flow through the system that only a small percentage of the water that percolates to the groundwater is actually moved throughout the system. A large percentage is lost from the system though evapotranspiration directly from the water table. The shallowness of the water table, the fine-grained nature of the till, and the relatively large fluctuations in the water table indicate that it is likely that evapotranspiration plays a major role in removing water from the till/weathered shale aquifer system.

The flow of groundwater at the Ash Landfill occurs primarily through two hydrostratigraphic units; a till/weathered shale unit and a competent shale unit. Hydrologic data from these units provides a more complete definition of the flow system. Water level measurements from the till/weathered shale unit at five sites within the modeled area indicate that the general direction of groundwater flow is to the west toward Seneca Lake. At the Ash Landfill and at the Garbage Disposal Area (SEAD-64D) sites, the groundwater flow direction is consistently to the west over an area that encompasses approximately 3/4 of the width of the area to be modeled. The flow direction in the competent shale at the Ash Landfill site is also to the west. In the eastern portion of the modeled area at SEAD-16, -17, -25, and -64A, groundwater flow directions are to the west and southwest (Figure 2-1) (Parsons ES, 1995a, 1995b, 1995c).

In the far eastern portion of the modeled area the combination of an easterly groundwater flow direction at SEAD-50 and a topographic high along Route 96 provides support for a groundwater divide (Figure 2-1). In the south, the groundwater divide is defined by both the easterly

groundwater flow and the topography. To the north along Route 96, the topography and drainage pattern of small intermittent streams forms the basis for the divide.

Groundwater flow in the western portion of the modeled area is controlled by Seneca Lake, which is a large, stable water body whose surface elevation is approximately 455 feet above mean sea level.

The hydraulic conductivity of the layers helped to define the vertical extent of the flow system. Hydraulic conductivity data for the modeled area was obtained from slug tests that were performed in the till/weathered shale and in the competent shale at the Ash Landfill. Hydraulic conductivity values ranged from 7.8×10^{-4} cm/sec to 1.9×10^{-11} cm/sec. The data indicate that the conductivity values for the till/weathered shale are greater than those for the competent shale. The average hydraulic conductivity of the till/weathered shale unit is 3.65×10^{-4} cm/sec and for the competent shale it is 4.24×10^{-5} cm/sec. Also, within the competent shale aquifer conductivity values generally decrease with depth. Initially, three separate flow units were defined in the competent shale (Figure 4-1); a hydraulic conductivity value for the third flow unit in the shale was extrapolated from shallower data because no wells were screened at this depth. However, as part of the initial determination of the bottom of the flow system in the preliminary water budget calculations, the lowermost unit in the competent shale was eliminated from the model due to lack of significant volume of flow in this unit compared to the total flow through the system. Therefore, for the purposes of this model, flow was modeled to a depth of 52 feet below the land surface.

No significant vertical gradients exist in the well clusters at the Ash Landfill. Although small upward and downward gradients were observed in some of the well, there is no dominant trend in the flow directions (Parsons ES, 1994a).

An important distinction in the flow system is that the competent shale, and its network of bedding plane fractures and joints, was considered an equivalent porous medium (EPM) in the groundwater flow model. Fractured rock systems simulate EPM when the fracture apertures are constant, the fracture orientations are randomly distributed and the fracture spacing is small relative to the scale of the flow system (EPA, 1989). Generally, in the EPM approach the fractured rock is treated as if it were an unconsolidated porous media. The shale at the Ash Landfill is believed to approximate EPM because it is characterized by vertical and horizontal joints, and horizontal bedding plane fractures. The frequency and size of the bedding plane fractures decreases with depth based on an analysis of bedrock cores collected at the Ash Landfill and this is supported by a measured decrease in hydraulic conductivity with depth (Figure 4-1).

Merin (1992) characterized groundwater flow in fractured siltstone approximately 15 miles south of the site near Ithaca, New York based on a detailed analysis of rock cores, borehole geophysics and thin sections. The results of this analysis indicate that "groundwater flow is conceptualized as moving through vertical and horizontal planes of porosity, each of which is a fraction of a millimeter thick and extends for several inches to tens of meters in length." In addition, three zones of bedding plane fractures were delineated based on the vertical distribution of horizontal fractures, and the spacing between these horizontal fractures increases with depth. This supports the finding that hydraulic conductivities are higher in the upper portions of the bedrock. Furthermore, Merin (1992) argues that the vertical joints and horizontal bedding plane fractures are conduits in shallow bedrock and that groundwater flow might approximate EPM conditions. The data from the Ash Landfill site and nearby areas (e.g., Ithaca, NY) do not support a discrete fracture approach to modeling groundwater flow in the shale.

The validity of using the EPM approach to model contaminant transport is not well established. However, Pankow et al. (1986) evaluated EPM at two fractured rock sites and they concluded that "the EPM approach would work well in describing contaminant transport for the system with small interfracture spacing and high enough matrix porosity and diffusion coefficient to rapidly establish matrix/fracture equilibrium."

In summary, three flow units were defined in the analysis of the flow system at the Ash Landfill site (Section 4.4) and therefore, the model consisted of 3 layers: layer 1 - till/weathered shale from 0 to 12 feet bls; layer 2 - competent shale from 12 to 32 feet bls; and layer 3 - competent shale from 32 to 52 feet bls.

Several types of boundary conditions were used for the model. The eastern model boundary was represented by a groundwater divide no-flow boundary and is supported by the topography, stream drainage patterns, and groundwater flow directions established at nearby sites. Seneca Lake forms a constant head boundary at the western extent of the model. Between these two boundaries groundwater flow is essentially to the west as supported by flow directions established at the Ash Landfill and five other sites within the modeled area. Thus, streamline no-flow boundaries were used to represent the northern and southern boundaries of the model.

4.5 CONTAMINANT FATE AND TRANSPORT

The constituents of concern (COC) at this site include volatile chlorinated organic compounds that were within the boundaries of a well defined groundwater plume. These compounds include trichloroethene (TCE), cis and trans dichloroethene (DCE) and vinyl chloride (VC). These compounds have been detected in various monitoring wells at the site and have been monitored over time. From this database, various patterns are apparent which include:

- The total concentration of the COCs in the plume decreased with increasing distance from the source area.
- The direction of plume travel was consistent with the movement of groundwater.
- The ratio of TCE to the breakdown products changed as the distance from the source are increased.
- The concentration of individual COCs in various wells appeared to remain constant over the years of groundwater monitoring.
- The boundaries of the plume did not appear to be expanding.

From this information and the analytical modeling that was performed during the RI, a hypothesis was suggested that degradation of the COC within the plume was occurring such that the plume had reached steady state conditions. In other words, the extent has not changed because the rate of input of COC equalled the removal of COC by biotic degradation. If the site conditions are supportive of biotic degradation it may likely be that the indigenous microbial community are controlling the COC present in the plume rendering them non-toxic. As a result of the hypothesis the remedial strategy of interest that this modeling effort would be used to support is one that would incorporate institutional controls in association with continued long term monitoring of groundwater. This approach deemed appropriate as source control was accomplished in the spring of 1995 and was successful in eliminating continued leaching of COC to the groundwater system.

The COC at the Ash Landfill are known to be resistant to aerobic microbial degradation. However, these compounds have been shown to be susceptible to degradation through a batch process called reductive dechlorination. Reductive dechlorination occurs under anaerobic conditions and is capable of removing halogens, in this case chloride, to produce less toxic compounds. Reductive dechlorination is possible because unlike non-halogenated compounds, halogenated compounds are in an oxidized state due to the presence of the large electronegative chloride group. This makes the organochloride molecule susceptible to reduction rather than oxidation, thus, compounds with more

chloride are more susceptible to reduction than compounds with less chloride. This process sequentially dechlorinates chlorinated organic molecules with compounds containing large amounts of chloride, such as TCE, being easier to dechlorinate than the less chlorinated breakdown products.

The process of dechlorination involves a transfer of electrons. Compounds that gain electrons are reduced whereas the compounds that donated electrons are oxidized. Oxygen is typically the acceptor of electrons for environmental oxidation processes however, under anaerobic condition the acceptor of electrons can be either other organic compounds or inorganic anions such as oxidized forms of sulfur, nitrogen, iron or carbonate. For anaerobic (anoxic) bacteria to degrade chlorinated hydrocarbons, certain requirements for the environmental system must be present. These requirements include:

- availability of carbon sources (electron donors),
- presence of electron acceptors,
- essential nutrients,
- proper ranges of pH, temperature and salinity,
- absence of dissolved oxygen and
- proper redox potential

With this essential information, it will be possible to evaluate the likelihood the biotic anaerobic dechlorination is active in controlling the migration of the dissolved COCs at the Ash Landfill. This information will allow the completion of the conceptual model.

As part of the conceptual model development Parsons ES conducted an extensive field sampling program with the intention of obtaining data that will provide the understanding of the status of biotic processes that are on-going at the site.

Table 4-5 presents the parameters that were measured in the monitoring wells that were within the boundary of the groundwater plume. These parameters include alternative electron acceptors, general water quality parameters and final end products of biotic degradation.

Field activities for collection of this data was performed during June 1995. The results of this field efforts summarized in Table 4-6. The results presented in Table 4-6 suggest that several alternative electron acceptors are available to complete the transfer of electrons through an anaerobic dechlorinative process. The concentration of carbonates, sulfate and nitrate are high enough to

TABLE 4-5

CHEMICAL PARAMETERS RELATED TO BIOTIC DEGRADATION

SENECA ARMY DEPOT ACTIVITY
ASH LANDFILL GROUNDWATER MODEL

PARAMETER	METHOD OF ANALYSES	DATA USE OF SIGNIFICANCE
Ferrous (Fe^{+2})	Colorimetric HACH Kit	Presence of iron in the reduced, divalent state, may indicate anaerobic reduction as ferric Fe^{+3} , an electron acceptor is reduced to ferrous, Fe^{+2} .
Chloride (Cl)	EPA Method 300.0	General water quality parameter used as a marker of biological dechlorination. Presence of chloride in areas of anaerobic dechlorination supports dechlorination process since chloride is being sequentially removed from the organic molecule and being released to the groundwater.
Specific Conductivity	EPA Method 120.1	General water quality parameter, useful to identify areas where leaching from the landfill could be occurring.
Alkalinity	EPA Method 310.1	General water quality parameter, provides an indication of the presence of carbonates. Carbonates could be an electron acceptor under anaerobic conditions.
Nitrate (NO_3^-)	EPA Method 300.0	Potential source as an electron acceptor under anaerobic processes. Nitrate can be used as an electron acceptor by facultative anaerobic microorganisms via either denitrification or direct nitrate reduction.
Nitrite (NO_2^-)	EPA Method 300.0	Presence of nitrite is an indication that denitrification process is ongoing.
Sulfate ($SO_4^{=}$)	EPA Method 300.0	Possible electron acceptor in the anaerobic microbial degradation process.
Dissolved Sulfide ($S^{=}$)	Standard Method 4500E	Product of sulfate based anaerobic microbial respiration.
Redox Potential (E_h)	Standard Method 2580A	Redox potential influences the nature of the biologically produced degradation process. Indicator of the tendency of a solution to accept or transfer electrons. Anaerobic conditions exist at E_h values less than +750mV.
Methane	Robert S. Kerr Standard Operating Procedure (RSKSOP) - 175	Indicator of reducing conditions, product of anaerobic reduction of carbon dioxide.
Carbon Dioxide	RSKSOP-175	Possible source of electron acceptors during methanogenesis.
Ethane, Ethene	RSKSOP - 175	Products of biotransformation of chlorinated hydrocarbons, the presence of these compounds indicate that anaerobic degradation is occurring.
pH	EPA Method 150.1	General water quality parameter, for microbial dechlorination to occur, pH must be within acceptable range.
Dissolved Organic Carbon	EPA Method 415.1	Maybe the source of electrons, acts as an electron donor during anaerobic dechlorination processes.

TABLE 4-3

BIODEGRADATION INDICATOR PARAMETER RESULTS

SENECA ARMY DEPOT ACTIVITY
ASH LANDFILL GROUNDWATER MODEL

Monitoring Well	Ethene (mg/L)	Ethane (mg/L)	Methane (mg/L)	Chloride (mg/L)	CO2 (mg/L)	Spec. Cond. (umho/cm)	Ferrous (mg/L)	Sulfide (mg/L)
PT-10	<0.11	<0.08	<0.004	59.7	327	794	<0.01	<0.10
PT-17	<0.11	<0.08	<0.004	59.3	349	906	0.01	0.32
PT-18	<0.11	<0.08	0.424	57.7	629	1450	0.01	<0.10
PT-20	<0.11	<0.08	<0.004	67.1	331	954	0.01	<0.10
PT-22	<0.11	<0.08	<0.004	148	352	1230	<0.01	<0.1
PT-22 (Dup)	NA	NA	NA	NA	349	NA	NA	NA
MW-24	<0.11	<0.08	<0.004	40.3	275	763	0.12	<0.10
MW-24 (Dup)	NA	NA	NA	NA	276	NA	NA	NA
MW-27	<0.11	<0.08	0.184	37.8	268	633	0.21	<0.10
MW-28	<0.11	<0.08	<0.004	25.3	293	656	0.04	<0.10
MW-29	<0.11	<0.08	<0.004	58.2	316	944	0.24	0.16
MW-32	<0.11	<0.08	<0.004	67.7	284	800	0.27	<0.10
MW-36	<0.11	<0.08	<0.004	48.8	270	706	<0.01	<0.10
MW-39	<0.11	<0.08	<0.004	22	145	617	<0.01	<0.10
MW-40	<0.11	<0.08	<0.004	12.5	221	486	<0.01	<0.10
MW-41D	<0.11	<0.08	<0.004	12.7	279	652	0.03	<0.10
MW-42D	<0.11	<0.08	<0.004	4.6	266	533	<0.01	<0.10
MW-43	<0.11	<0.08	<0.004	26.5	369	766	0.12	<0.10
MW-43 (Dup)	NA	NA	NA	NA	366	NA	NA	NA
MW-45	<0.11	<0.08	<0.004	24.4	285	567	0.07	<0.10
MW-46	<0.11	<0.08	<0.004	25.7	298	675	0.01	<0.10
MW-48	<0.11	<0.08	<0.004	27.5	271	578	0.11	<0.10
MW-49D	<0.11	<0.08	0.009	25.1	259	646	0.06	<0.10
MW-149(Dup of 49D)	<0.11	<0.08	0.011	24.8	264	640	NA	<0.10
MW-49 (Rinsate)	<0.11	<0.08	<0.004	1.9	<5	1.83	NA	<0.10
MW-50D	<0.11	<0.08	<0.004	15.2	220	486	0.13	<0.10
MW-53	<0.11	<0.08	<0.004	74.7	308	904	0.15	0.32
MW-54D	<0.11	<0.08	<0.004	53.4	222	629	<0.01	<0.10
MW-55D	<0.11	<0.08	<0.004	4.6	218	534	0.46	<0.10
MW-56	<0.11	<0.08	<0.004	42.4	302	700	0.02	<0.10
MW-56 (Dup)	NA	NA	NA	NA	294	NA	NA	NA

Notes:

NA - Not Available

* - Nitrate-N and Nitrite-N combined due to late holding times

TABLE 4-6

BIODEGRADATION INDICATOR PARAMETER RESULTS

SENECA ARMY DEPOT ACTIVITY
ASH LANDFILL GROUNDWATER MODEL

Monitoring Well	DOC (mgC/L)	Sulfate (mg/L)	Nitrate-N (mg/L)	Nitrite-N (mg/L)	Redox Pot. (mV)	pH	Tot. Alk. (mgCaCO ₃ /L)
PT-10	<1.0	22.6	<0.056	<0.076	367.9	7.35	333
PT-17	148	78	0.61	<0.076	361.8	7.03	331
PT-18	6.1	231	<0.056	<0.076	NA	6.87	548
PT-20	1.9	22.6	0.15	<0.076	NA	7.05	310
PT-22	3.1	218	0.18	<0.76	352.4	7.02	316
PT-22 (Dup)	NA	NA	NA	NA	NA	NA	NA
MW-24	4.6	79	0.15	<0.076	372.4	7.09	288
MW-24 (Dup)	NA	NA	NA	NA	NA	NA	NA
MW-27	2.3	50.7	0.098	<0.076	394.7	7.73	292
MW-28	2.8	49.5	0.089	<0.076	362.5	7.09	282
MW-29	3.2	126	0.21	<0.076	365.6	7.06	313
MW-32	1.6	56.4	0.79	<0.076	415.3	7.16	294
MW-36	1.8	62.6	1.7	<0.076	379.3	7.25	273
MW-39	3.5	26.7	0.091	<0.076	398.2	7.2	264
MW-40	1.4	56.7	0.13*	NA	362.3	7.41	217
MW-41D	1.2	41.1	0.077	<0.076	371.4	7.62	300
MW-42D	3.2	24.6	0.088	<0.076	390.8	7.48	279
MW-43	4.4	43.4	<0.056	<0.076	365.5	7.09	362
MW-43 (Dup)	NA	NA	NA	NA	NA	NA	NA
MW-45	1.7	39.1	0.064	<0.076	351.2	7.22	281
MW-46	42	46.7	<0.056	<0.076	347.9	7.13	297
MW-48	2.5	41.4	0.081	<0.076	382.3	7.25	276
MW-49D	5.3	57.6	0.11	<0.076	379.5	7.32	264
MW-149(Dup of 49D)	3.7	58.5	0.084	<0.076	NA	7.36	264
MW-49 (Rinsate)	2.3	1.1	<0.056	<0.076	NA	6.64	<5
MW-50D	3.3	32.8	0.11	<0.076	NA	7.59	231
MW-53	3.5	103	0.15	<0.076	359.6	7.08	289
MW-54D	4.1	40.6	0.27	<0.076	373.9	7.48	223
MW-55D	<1.0	31.3	0.23	<0.076	340.6	8.88	253
MW-56	2.5	81.7	0.23	<0.076	360.6	7.11	289
MW-56 (Dup)	NA	NA	NA	NA	NA	NA	NA

Notes:

NA - Not Available

* - Nitrate-N and Nitrite-N combined due to late holding times

suggest that either compound could act as electron acceptors. Further, the concentration of COC throughout the site suggest that COC could be a reasonable source of electrons acting as electron donors in the transfer of electrons. The concentration of general water quality parameter such as pH, specific conductance and chloride all are within the range of what would be acceptable for biological growth. Finally, the redox potential values are within the range of what would be considered anaerobic, suggesting that anaerobic dichlorination could be occurring. Although the redox potential measured at SEDA does not suggest strongly anaerobic conditions at the time of measurement, it is nonetheless within the anaerobic range and was measured during seasonally low groundwater conditions. Low groundwater conditions would be more indicative of aerobic conditions as air with 20% oxygen replace the pore space previously saturated with groundwater.

5.0 GROUNDWATER FLOW MODEL DESIGN AND RESULTS

5.1 Selection of Model Code

This modeling study required a computer code that could simulate three dimensional groundwater flow, the results of which could be used directly by a three dimensional transport model. The MODFLOW computer code was selected to simulate groundwater flow for this project because of the following:

- MODFLOW simulates three dimensional groundwater flow;
- The head and flow data saved by MODFLOW can be used with particle tracking models (e.g., MODPATH and MODPATH-PLOT) and three dimensional transport models (e.g., MT3D);
- The accuracy of the code has been checked against one or more analytical solutions;
- The code includes a water balance computation; and
- The code has been used to simulate groundwater flow in numerous studies.

5.2 Relationship Between Conceptual Model and MODFLOW Numerical Model

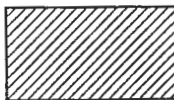


This section describes how the conceptual model was translated to the grid of the numerical model. First, the boundary conditions and grid layout will be discussed followed by the method of assignment of input parameter values.

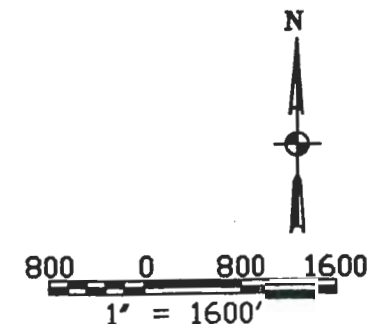
5.2.1 Boundary Conditions and Grid Layout

The area modeled extends considerably beyond the Ash Landfill and its immediate surrounding area to take advantage of meaningful physical and hydraulic boundaries (Figure 5-1). Seneca Lake, a physical boundary, formed a constant head boundary at the western edge of the model. The eastern model boundary was represented by a groundwater divide no-flow (i.e., hydraulic) boundary and this supported by the land surface topography, stream drainage patterns, and groundwater flow directions established at nearby sites (SEAD-50, SEAD-64A, SEAD-25, SEAD-16 and SEAD-17). Between these two boundaries, groundwater flow is essentially to the west as supported by flow directions established at the Ash Landfill and other sites within the modeled area. Thus, streamline no-flow (i.e., hydraulic) boundaries were used to represent the northern and southern boundaries of the model. Finally, the bottom of the model was represented by an "impermeable", no-flow boundary in the competent shale.



C:\ACAD\SENECA\ASHMODEL\GVF\FIB.DWG

-  AREA OF INACTIVE CELLS
-  GROUNDWATER FLOW DIRECTION IN TILL/WEATHERED SHALE AQUIFER
-  ACTIVE MODEL BOUNDARY



P PARSONS	
PARSONS ENGINEERING SCIENCE, INC.	
CLIENT/PROJECT TITLE	
SENECA ARMY DEPOT ACTIVITY ASH LANDFILL GROUNDWATER MODEL	
DEPT.	Dwg. No.
ENVIRONMENTAL ENGINEERING	
FIGURE 5-1	
GROUNDWATER FLOW MODEL BOUNDARY CONDITIONS AND GROUNDWATER FLOW DIRECTIONS	
SCALE	DATE
1" = 1600'	01/19/96
REV	A

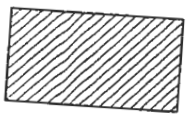
The model grid was constructed for the purposes of simulating ground water flow and contaminant transport at the Ash Landfill and the surrounding area. Because the MODFLOW and MT3D numerical models were used for the modeling, the "continuous problem domain" was replaced by a "discretized domain" consisting of nodes and associated finite difference blocks or cells representing a block-centered grid; also the grid met the Peclet criterion required for the transport model. Model boundaries were defined based on physical and hydraulic considerations in order to most accurately represent the flow system beneath the Ash Landfill.

The block-centered finite difference grid was overlaid on the map of the area to be modeled such that the horizontal plane of the aquifer was colinear with the principal directions of hydraulic conductivity tensors K_x and K_y (Figure 5-2). In addition, three flow units were modeled: layer 1 - till/weathered shale from 0 to 12 feet bls; layer 2 - competent shale from 12 to 32 feet bls; and layer 3 - competent shale from 32 to 52 feet bls (Section 4.3). The thicknesses of the layers remains constant throughout the horizontal extent of the model grid. However, the array of cells that comprises each layer dips gently to the west generally mimicking the land surface topography, resulting in a stratigraphic three-dimensional (or non-horizontal model-layer) grid (Figure 5-3). By applying a non-horizontal model layer vertical discretization scheme to simulate flow at the Ash Landfill site, discrete units could be assigned to discrete model layers, and the flow system could be simulated with fewer layers that would be necessary to represent them with a three-dimensional rectangular grid. Thus, the vertical axes of the model are not strictly parallel to the bedding planes using the non-horizontal model layer grid. However, it was assumed that the angle between the dip of the beds and the horizontal axis was so small that K_z was assumed to be nearly colinear with the vertical axis, a viewpoint argued by Anderson and Woessner (1992). Furthermore, Harte (1994) showed that for sites with model layer slopes of 0.17 feet/foot and under, the benefits of applying a non-horizontal model layer vertical discretization scheme to simulate flow, especially considering the improved ability to represent discrete hydrogeologic units, exceeded the numerical errors due to the misalignment of the model axes with the hydraulic conductivity tensor (K_z).

The flow model used a variable grid with three layers that totalled 54,120 cells; each layer consisted of 18,040 cells (Figure 5-2). A variable grid was used for this model to achieve increased resolution (for hydraulic heads and plume concentrations) at the Ash Landfill and provide less defined data for the surrounding areas where no plume migration was expected to occur. The grid consists of a central area of regularly-spaced, 25-foot cells that encompasses the Ash Landfill and its immediate surrounding area (Figure 5-4). Beyond this area of regularly-spaced cells, the grid expands in increments of 1.5 times (37.50, 56.25, 84.37, 126.56, 189.84) until a cell size of 284.76 is reached. Then, this cell size extends to the model boundaries in all directions. The



C:\ACAD\SENECA\ASHMODEL\FIG5-2.DWG



AREA OF INAC



ACTIVE MODEL

1600



PARSONS ENGINEERING SCIENCE, INC.

CLIENT/PROJECT TITLE
**SENECA ARMY DEPOT ACTIVITY
 ASH LANDFILL GROUNDWATER MODEL**

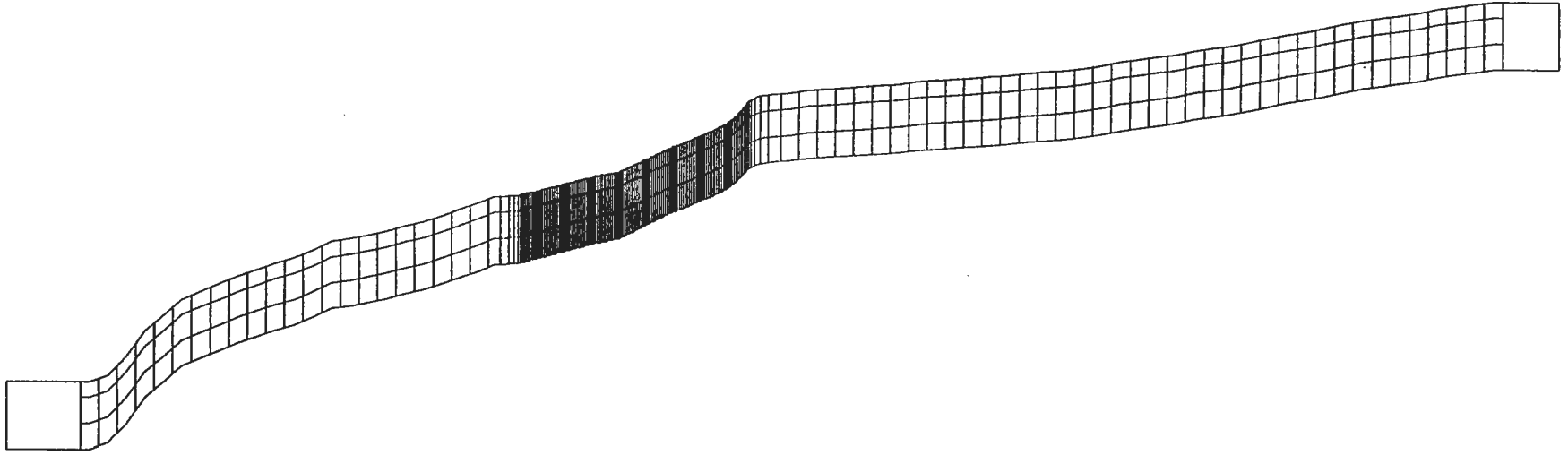
DEPT. ENVIRONMENTAL ENGINEERING Dwg. No.

**FIGURE 5-2
 PLAN VIEW OF GROUNDWATER
 FLOW MODEL GRID**

SCALE 1" = 1600'

DATE OCTOBER 1985

REV



0 1000 4000 FEET

VERTICAL EXAGGERATION IS 20.0

Cross-section of Model Grid

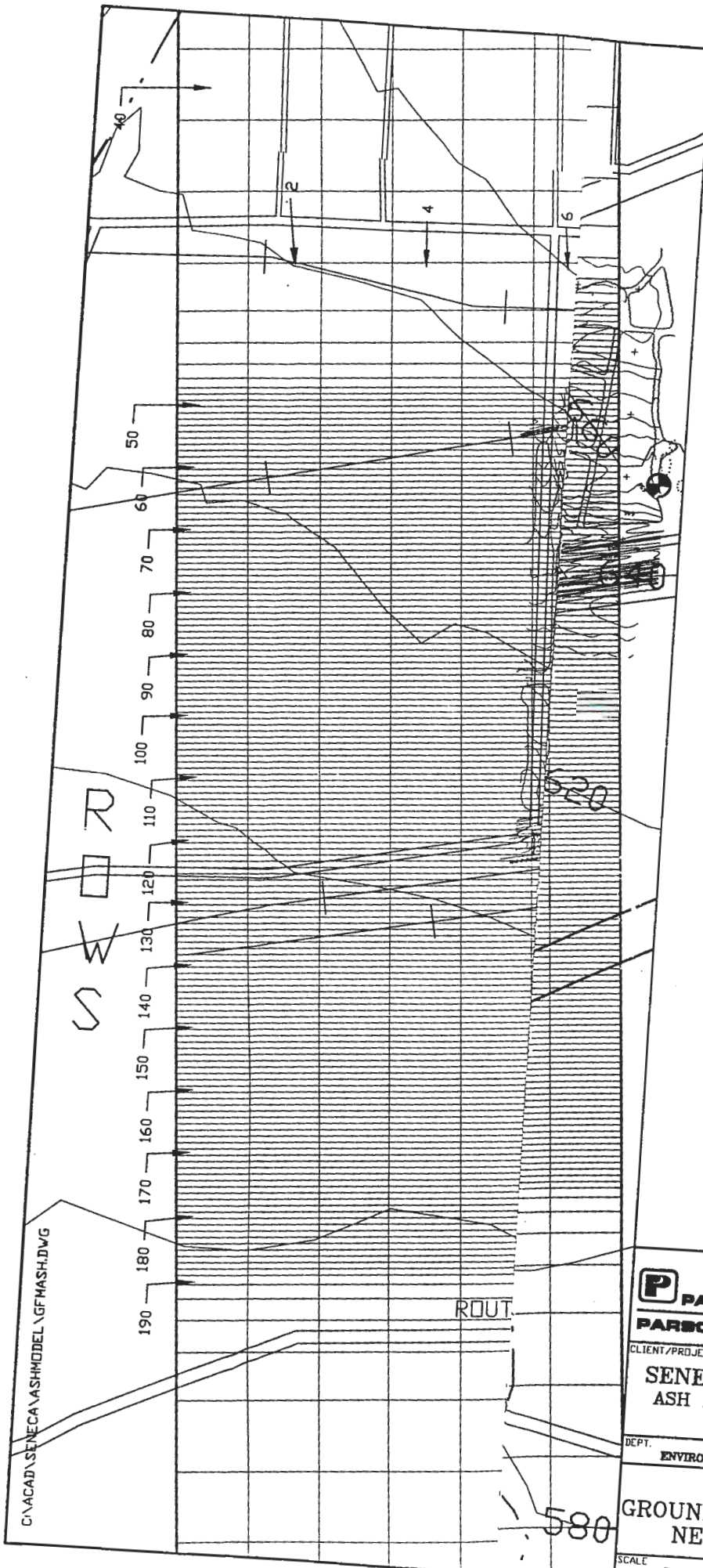
PARSONS
 PARSONS ENGINEERING SCIENCE, INC.

CLIENT/PROJECT TITLE
**SENECA ARMY DEPOT ACTIVITY
 ASH LANDFILL GROUNDWATER MODEL**

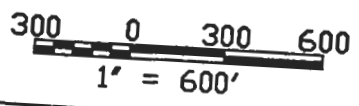
DEPT. ENVIRONMENTAL ENGINEERING DWG NO. 726209-01002

**FIGURE 5-3
 CROSS SECTION OF
 GROUNDWATER FLOW MODEL
 GRID AT COLUMN 42**

SCALE NA DATE OCTOBER 1995



C:\ACAD\SENECA\ASHMODEL\GF\MASH.DWG



P PARSONS
PARSONS ENGINEERING SCIENCE, INC.

CLIENT/PROJECT TITLE
SENECA ARMY DEPOT ACTIVITY
ASH LANDFILL GROUNDWATER MODEL

DEPT. ENVIRONMENTAL ENGINEERING Dwg. No.

FIGURE 5-4
GROUNDWATER FLOW MODEL GRID
NEAR THE ASH LANDFILL

SCALE 1" = 800' DATE OCTOBER 1996 REV A

approximately 284-foot grid size provided enough detail so that simulated heads outside the area of interest could be calibrated to observed heads with some degree of spatial accuracy, yet it reduced data preparation and computing time for the model. Additionally, there were 562 inactive cells in the model; inactive cells are those cells west of the constant head cells at Seneca Lake and east of the groundwater divide cells along Route 96 (Figure 5-2).

The 25-foot, regular grid in the area of the Ash Landfill was designed to meet the Peclet criteria for the solute transport model, thereby minimizing effect of numerical dispersion in the finite difference solution. Anderson and Woessner (1992) state that the grid should be designed so that the Peclet number (P_e) be less than or equal to 1, although acceptable solutions can be obtained with P_e as high as 10. However, in general they recommend that the grid be designed so that P_e is less than 4. The equation used to calculate the Peclet number is:

$$P_e = \Delta L / \alpha$$

where: P_e = Peclet number
L = characteristic nodal spacing, and
 α = characteristic dispersivity.

Using a dispersivity of 10 feet for the till/weathered shale, P_e for the 25-foot grid spacing is 2.5. A dispersivity of 20 feet for the competent shale results in a P_e of 1.25. Thus, within the 25-foot grid spacing P_e numbers for both the till/weathered shale and the competent shale meet the Peclet criteria recommended in literature for solute transport modeling.

5.2.2 Assignment of Input Parameter Values For MODFLOW

The MODFLOW model uses packages to represent basic categories of the model. Input parameter values are entered into the various packages for use in the model. Groundwater flow was simulated using four MODFLOW packages. They are as follows:

1. Basic Package
2. Block Centered Flow Package
3. Recharge Package
4. Preconditioned Conjugate Gradient (PCG-2) Solution Package

Input parameter values for the MODFLOW groundwater flow model were derived from both site investigation data and from the literature when site specific data were not available. Table 5-1 shows the selected input parameters for the flow model along with an acceptable range for each value; the best estimate for the parameters used in the model are also presented. The parameter values that describe the physical geometry of the flow system as well as those values that describe the aspects of groundwater flow are discussed below. This section is not intended to discuss input values related to setting up or executing the groundwater flow computer model, such as output control values.

5.2.2.1 Basic Package

Model Layers and Aquifer Types

Three model layers were simulated in the model. Model layer 1 simulated groundwater flow in the till/weathered shale unit, 0 to 12 feet below the land surface. Model layer two simulated flow the upper 20 feet of the competent shale unit and, model layer 3 simulated flow in the next lowest 20 foot interval in the competent shale. Therefore, in model space, the tops and bottoms of the layers relative the land surface are, respectively, 0 to 12 feet for layer 1, the till/weathered shale, 12 to 32 feet for layer 2, the competent shale, and 32 to 52 feet for layer 3, also in the competent shale.

The land surface elevations were established from 2-foot contour maps of selected sites at SEDA and from 1:24,000-scale (7.5 min) U.S.G.S. maps (the Dresden and Ovid, NY quadrangles) The 2-foot contour maps were available for only six areas within the model grid boundaries and outside of these areas the 1:24,000 scale maps were used.

All three model layers were assigned an aquifer type. Model layer 1, which is considered to be an unconfined water table aquifer, was assigned an confined aquifer type for the purposes of the flow model. The reason for this is that the solution scheme of the MODFLOW model was not stable enough to meet the closure criteria for the heads because model layer 1 is only 12 feet thick. Simulating model layer 1 as confined in a steady state model does not significantly effect the heads calculated by MODFLOW, although this does result in the use of a constant transmissivity throughout the simulation. Model layers 2 and 3 were simulated as confined because the water table in each layer was above the top of the model layers.

TABLE 5-1
REASONABLE RANGE, BEST ESTIMATE AND UNCERTAINTY FOR
MODFLOW INPUT PARAMETERS

SENECA ARMY DEPOT ACTIVITY
ASH LANDFILL GROUNDWATER MODEL

Input Parameter	Units	Reasonable Range			Best Estimate	Source	Uncertainty
		Low	nominal	High			
<u>Aquifer Types:</u>							
Layer 1 aquifer type	NA	NA	unconfined	NA	unconfined	field data	low
Layer 2 aquifer type	NA	NA	confined	NA	confined	field data	low
Layer 3 aquifer type	NA	NA	confined	NA	confined	field data	low
<u>Layer Thicknesses:</u>							
Layer 1 Thickness	(feet)	4.5	12	18	12	field data	low
Layer 2 Thickness	(feet)	20	20	20	20	field data	low
Layer 3 Thickness	(feet)	20	20	20	20	field data	low
<u>Conductivity:</u>							
Layer 1 Kh	(feet/day)	0.09	1.03	2.21	1.03	field data	low
Layer 1 Kv	(feet/day)	0.01	0.11	0.25	0.11	Literature	medium
Layer 1 Vcont		0.0007	0.0018	0.0041	0.0018	Calculation	med.- high
Layer 2 Kh	(feet/day)	0.11	0.20	0.45	0.20	field data	low
Layer 2 Kv	(feet/day)	0.01	0.02	0.05	0.02	Literature	high
Layer 2 Vcont		0.0001	0.0003	0.0008	0.0003	Calculation	high
Layer 3 Kh	(feet/day)	0.01	0.04	0.09	0.04	field data	low
<u>Transmissivity:</u>							
Layer 1 Transmissivity	(sq feet/day)	0.54	6.18	13.26	6.18	field data	low
Layer 2 Transmissivity	(sq feet/day)	2.20	4.05	9.00	4.05	field data	low
Layer 3 Transmissivity	(sq feet/day)	0.20	0.76	1.80	0.76	field data	low
<u>Heads:</u>							
Constant Head Seneca Lake	(feet, msl)	455	455	455	455	Literature	low
<u>Recharge:</u>							
Net Recharge	(feet/day)	0.000012	0.000013	0.000014	0.000013	field data	low
<u>Boundaries:</u>							
Northern Boundary	NA	NA	streamline	NA	streamline	field data	low
Southern Boundary	NA	NA	streamline	NA	streamline	field data	low
Eastern Boundary	NA	NA	gw divide	NA	gw divide	field data	low
Western Boundary	NA	NA	constant head	NA	constant head	Literature	low
Bottom Boundary	NA	NA	low conductivity	NA	low conductivity	field data	low

Boundaries for the Flow Field

The boundary array for the flow model consisted of constant head cells along the extent of Seneca Lake. The northern and southern extents of the model were designated as streamline no flow boundaries. A groundwater divide is present on the eastern boundary of the model. All of the cells west of the constant head cells and east of the groundwater divide were inactive for the model runs; all other cells in the model were active.

The bottom of the model, which was a no flow boundary, was defined at 52 feet below the land surface based on the preliminary water budget analysis.

Starting Heads

The starting head arrays for the three model layers were derived from observed groundwater elevations at groundwater monitoring wells. In other areas where there were no monitoring wells, they were extrapolated relative the land surface. The elevation of Seneca lake, 455 feet msl (Mozola, 1955), was the basis for the heads (455 feet) used at the constant head cells.

For layer 1, seasonally averaged groundwater elevations were assigned to their corresponding model cells as a basis for constructing the starting head array. The process of deriving these elevations is described in Section 5.4.1. Starting heads for layers 2 and 3 were 1.0 and 2.0 feet, respectively, below the starting heads for layer 1.

To construct this array in selected areas where no monitoring wells were present, groundwater elevations were derived by subtracting 5 feet from the land surface elevation. Thus, the measured and extrapolated water table elevations provided a close approximation to the actual groundwater table at these locations. The final array was derived by using the observed and approximated data, and a four-point moving average calculation on a spreadsheet program. Because the starting heads were close to the measured heads the number of iterations required by the MODFLOW model was reduced.

5.2.2.2 Block Centered Flow Package

Horizontal hydraulic conductivity (K_h) values for the three layers of the model were obtained from the Ash Landfill RI report (Parsons ES, 1994a). A horizontal hydraulic conductivity of 1.03 feet/day was used for layer 1, the till/weathered shale. Horizontal conductivities of 0.2 feet/day and

0.04 feet/day were used for layers 2 and 3 (in the competent shale), respectively. The conductivity values represent an average for the particular geologic unit represented in a model layer (Table 4-1).

Vertical hydraulic conductivities (K_v) were derived from literature values and from the physical make up of the aquifer material. For layer 1, the K_v was based on an anisotropy of K in a fine-grained till aquifer in western New York State where K_h/K_v is 9 (Prudic, 1992). For layers 2 and 3, the K_v values were derived based on an anisotropy of K in the aquifer where K_h/K_v is 10.

Vertical Conductance (Vcont)

Vertical conductances (Vcont)s were calculated for layers 1 and 2 using equation (51) provided in McDonald and Harbough (1988). The equation is as follows:

$$V_{cont_{ij,k}}^{+1/2} = \frac{1}{\frac{(\Delta v_k)/2}{K_{z_{ij,k}}} + \frac{(\Delta v_{k+1})/2}{K_{z_{ij,k+1}}}}$$

where:

Δv_k is the thickness of model layer k

Δv_{k+1} is the thickness of model layer $k+1$

$K_{z_{ij,k}}$ is the vertical hydraulic conductivity of the upper layer in cell ij,k

$K_{z_{ij,k+1}}$ is the vertical hydraulic conductivity of the lower layer in cell $ij,k+1$

The equation is meant to represent a case in which two adjacent model layers are used to represent two vertically adjacent hydrogeologic units. It incorporates both K_v and the thickness of the unit.

Using the above equation, a V_{cont} of 0.0018 was calculated for layer 1. For layer 2, V_{cont} of 0.0003 was calculated. A V_{cont} value was not need for layer 3 because the bottom of this layer is a no flow boundary.

Transmissivity

Transmissivity was calculated by multiplying the saturated thickness by the horizontal hydraulic conductivity (K_h). A transmissivity value of 6.18 ft²/day was used for layer 1; this value is based on a saturated thickness of 6 feet and an K_h of 1.03 ft/day. Transmissivities of 4.05 ft²/day and 0.76 ft²/day were used for layers 2 and 3; these values were based on a saturated thickness of 20 feet and K_h values of 0.20 ft/day and 0.04 ft/day, respectively.

Groundwater Gradients

A groundwater gradient of 0.020 feet/foot was used for the till/weathered shale (model layer 1). This was based on a gradient of 0.0213 feet/foot between wells PT-18 and PT-17 and a gradient of 0.0195 between wells MW-40 and MW-56. In the competent shale, a gradient of 2.5×10^{-2} ft/ft (0.025) was measured between wells PT-10 and MW-35D; a downgradient of 0.025 feet/foot was used for the competent shale (model layers 2 and 3).

Dispersivity

Dispersivity values for the till and the competent shale were obtained from literature.

Other Selected Parameters

Error Criterion for Heads: MODFLOW selects the largest absolute difference in heads as a measure of the residual error and compares it to the user-defined error criterion. Anderson and Woessner (1992) recommend as a "rule of thumb" that the error criterion should be one or two orders of magnitude smaller than the level of accuracy desired in the head results. Because the desired accuracy for head results in this model was 0.1 feet, an error criterion of 0.001 was used for the model

Error Criterion for Water Balance: MODFLOW also calculates an error in the water balance by comparing the total simulated inflows and outflows, which serves as another way of checking the amount of residual error in the solution. For the water balance, water entering storage is treated as outflow and water released from storage is treated as inflow. The difference between total inflow and total outflow is the percent error and it is calculated by MODFLOW using the equation that follows:

$$D = 100(\text{IN} - \text{OUT})/(\text{IN} + \text{OUT})/2$$

where: IN = total flow into the system
OUT = total flow out of the system
D = percent error term

According to Konikow (1978), the ideal error in the water balance should be less than 0.1 percent, however, an error of around 1 percent is usually considered acceptable (Anderson and Woessner, 1992).

Wetting Option: The wetting option (BCF2) was used for the model simulations because of the thin nature of the model layers used.

5.2.2.3 Recharge Package

Net areal recharge from precipitation was used in the model as the only source of water for the flow system. Based on the results of the preliminary water balance, the shallow till/weathered shale aquifer received 0.59 ft/year of recharge from precipitation however, a significant amount of this water is subsequently lost due to evapotranspiration. Instead of simulating both recharge from precipitation and evapotranspiration, a net recharge value was used in the model. A net recharge of 0.000013 ft/day was estimated based on the preliminary water budget and this was used to begin the calibration process for the model. Recharge was specified to enter the simulated flow system through the uppermost active layer in the model.

5.2.2.4 Preconditioned Conjugate Gradient Solution Package

The preconditioned conjugate gradient (PCG-2) solution scheme was used for the model because it works well with a wide variety of problems and usually very little adjustment of the solution parameters is necessary (NGWA, 1994).

5.3 Model Calibration

The groundwater flow model was calibrated using industry standard calibration criteria. A flow model is considered calibrated when it "is capable of producing field measured heads and flow which are the calibrated values" (Anderson and Woessner, 1992). Additionally, EPA (1992) states that a model can be considered calibrated when it reproduces historical data within some acceptable level of accuracy determined prior to the calibration process.

This groundwater flow model was calibrated for steady-state conditions. Prior to calibration, a range of uncertainty in each parameter value was quantified (Table 5-1) and target heads were established.

Based on the conceptual model for the site, a significant amount of water that percolates into the groundwater is subsequently lost through evapotranspiration. Thus, the value of the net recharge parameter was determined to have a significant effect on heads in the model. Additionally, many of the other parameters were reasonably well known based on site measurements and literature sources. Therefore, calibration of the model was performed by starting with the best estimates for all hydraulic parameters and then, through trial-and-error, the net recharge value for the flow system was adjusted until simulated heads reasonably matched measured heads.

Thus, the model calibration process began with the net recharge value of 0.000013 feet/day determined in the preliminary water budget. This is significantly less than the 0.0016 feet/day (or 0.59 feet/year) of percolation calculated in the water balance because evapotranspiration removes water from the groundwater system throughout the year. Ultimately, the model was calibrated using a net recharge of 0.00001332 feet/day. Output from the calibrated MODFLOW run is shown in Appendix C.

The results of the calibration of the groundwater flow model were evaluated both qualitatively and quantitatively. These calibration criteria are as follows:

1. Hydraulic Heads (ME, MAE, and RMS) and Gradients;
2. Water Balance and Volumetric Flow; and
3. Groundwater Velocity and Advective Travel Time.

5.3.1 Hydraulic Heads (ME, MAE, and RMS) and Gradients

The comparison of simulated heads with observed (or target) heads was one of the most important calibration criteria for the model. For this model, target heads were available from 60 monitoring wells within the modeled area. Additionally, estimated heads were established at 24 "ghost" well locations where no observed data were available due to the lack of monitoring wells.

The target heads for the model cells were derived using the seasonal arithmetic mean of the observed water table elevations in the monitoring wells from 1990 to 1995. Table 5-2 presents the

observed water table elevations as well as their seasonal arithmetic means. For wells that had a lot of water elevation data, the seasonal arithmetic mean was taken to be a reasonably acceptable target elevation for the model. Sample standard deviations for each well for the years 1990, 1991, 1993, and 1994 were also calculated as well as an average standard deviation for each year.

However, this process could not be applied to all of the wells because for some of the wells, the amount of data was limited (i.e., only one or two seasons were represented in the data). For these latter wells, the seasonal arithmetic mean was derived by making appropriate adjustments to the observed data based on the average standard deviation of elevations from the wells where adequate data were available. These adjustments were based on knowledge of the established seasonal behavior of heads in the aquifer. For example, for well MW-53 for which there is only elevation data from a period of high water (i.e., winter and spring), the December 1994 elevation was adjusted down by 1 average standard deviation for 1994 (Table 5-2).

After model calibration was completed, simulated heads were compared to measured (target) heads using both maps and X-Y scatter plots. A comparison between contour maps of simulated and measured heads is depicted in Figure 5-5. In general, breaks in the slope of the land surface are locations where the heads do not match well (e.g., immediately east of the ash landfill and near Seneca lake).

A scatter plot of measured heads versus simulated heads shows the calibration fit for the model (Figure 5-6). The plot shows that the simulated heads depart from the measured (or target) heads between the elevations of approximately 604 and 680 feet above msl, which corresponds to a steep break in land surface slope east of the Ash Landfill (Figures 5-6 and 5-3). A similar departure of simulated head from the target heads would likely occur in the western portion of the site at the break in land surface slope near Seneca Lake, however, no monitoring wells were available from this area.

A listing of measured and simulated heads together with their differences and three types of average of the differences is presented in Table 5-3. The average of the differences can be used to quantify the average error in the calibration with the final objective being to minimize this error. The three types of averages are as follows:

TABLE 5-2

WATER TABLE ELEVATIONS AND DEVELOPMENT OF A SEASONALLY AVERAGED
GROUNDWATER TABLE AT THE ASH LANDFILL

SENECA ARMY DEPOT ACTIVITY
ASH LANDFILL GROUNDWATER MODEL

WELL	ELEVATION TOP OF PVC	SEASONAL ARITHMETIC MEAN OF ELEVATIONS (MSL) - per Anderson and Woessner, 1992.				ARITHMETIC MEAN	SAMPLE STANDARD DEVIATION OF ELEVATIONS			
		1990	1991	1993	1994		1990	1991	1993	1994
1	PT-10	681.58	673.28	673.16	674.09	673.51	1.99	2.97	2.17	
2	PT-11	658.28	651.54	651.16	652.33	651.68	1.76	2.36	1.21	
3	PT-12	652.03	644.56	644.25	645.90	644.90	1.73	2.51	1.35	
4	PT-15	637.84	630.57	629.71	630.78	630.35	2.19	2.68	2.60	
5	PT-16	637.76	633.28	632.88	634.35	633.43	1.47	2.02	0.83	
6	PT-17	640.82	633.97	633.43	635.25	634.21	1.71	3.01	1.53	
7	PT-18	658.59	649.47	649.36	650.73	648.85	1.44	1.98	1.08	
8	PT-19	645.45				640.17				
9	PT-20	647.28	640.42	638.88	640.88	640.02	1.71	2.40	1.15	2.09
10	PT-21	647.51	640.87	640.09	642.34	641.03	1.91	2.01	3.86	
11	PT-22	648.82	640.78	640.44	641.85	640.95	1.97	2.40	1.50	
12	PT-23	641.54	635.23	634.59	635.33	635.05	1.39	2.08	1.50	
13	PT-24	636.35	631.00	630.39	631.87	631.02	1.12	1.81	0.39	
14	PT-25	637.02	630.47	629.27	631.84	630.56	2.82	3.34	1.64	
15	PT-26	614.84	608.23	608.37	610.24	608.28	3.19	3.85	1.88	
16	MW-27	639.42	633.05	633.25	634.08	633.45	1.87	1.38	1.08	
17	MW-28	637.41	631.19	631.29	632.28	631.58	1.97	1.83	0.48	
18	MW-29	637.33	630.04	629.28	631.25	630.19	2.17	1.84	0.58	
19	MW-30	640.23	632.77	632.38	634.28	633.19	1.94	2.93	2.18	
20	MW-31	636.86	631.36	630.73	632.84	631.84	2.87	2.93	1.81	
21	MW-32	641.85	634.55	634.32	636.47	635.11	1.89	2.35	1.90	
22	MW-33	639.52	632.75	633.29	634.20	633.41	2.37	1.89	2.30	
23	MW-34	632.89			628.38	628.38				
24	MW-35D	631.82			629.08	629.08				
25	MW-36	632.08			629.38	629.02				1.58
26	MW-37	632.88			629.14	628.14				
27	MW-38D	637.99			633.97	633.97				
28	MW-39	659.72			657.12	657.12				
29	MW-40	659.48			654.75	654.55				
30	MW-41D	694.02			686.82	686.82				1.87
31	MW-42D	683.04			678.34	678.34				
32	MW-43	657.8			652.89 NSA-2	652.89 NA				
33	MW-44	654.12			647.81 NSA-2	647.81 NA				
34	MW-45	651.13			645.78 NSA-2	648.88				1.73
35	MW-46	650.85			643.31 NSA-2	643.31 NA				
36	MW-47	628.53			622.38 NSA-2	623.98				2.05
37	MW-48	648.57			642.48 NSA-2	643.75				1.95
38	MW-49D	650.89			643.80 NSA-2	643.80 NA				
39	MW-50D	650.27			643.73 NSA-2	643.73 NA				
40	MW-51D	629.84			622.39 NSA-2	622.39 NA				
41	MW-52D	628.7			621.55 NSA-2	621.55 NA				
42	MW-53	639.83			630.81 NSA-2	630.81 NA				
43	MW-54D	639.34			630.84 NSA-2	630.84 NA				
44	MW-55D	639.43			630.37 NSA-2	630.37 NA				
45	MW-56	630.89			627.12 NSA-2	627.27				0.58
46	MW-57D	630.27			627.13 NSA-2	627.13 NA				
47	MW-58D	629.88			628.06 NSA-2	628.06 NA				
48	MW-59	656.83				653.78				1.57
49	MW-80	680.15				656.99				1.55
50	MW84D-1	667.79				664.70 NSA-2	664.70 NA			
51	MW84D-2	635.2				632.12 NSA-2	632.12 NA			
52	MW84D-3	648.88				648.40 NSA-2	648.40 NA			
53	MW84D-4	651.33				656.25 NSA-2	656.25 NA			
54	MW84D-5	652.49				648.98 NSA-1	648.98 NA			
55	MW84A-1	745.77				738.83 NSA-1	738.83 NA			
56	MW84A-2	740.98				734.53 NSA-1	734.53 NA			
57	MW84A-3	739.85				734.08 NSA-1	734.08 NA			
58	MW16-1	735.54				732.14 NSA-1	732.14 NA			
59	MW16-2	734.55				731.01 NSA-1	731.01 NA			
60	MW16-3	735.48				731.28 NSA-1	731.28 NA			
61	MW17-1	736.27				733.47 NSA-1	733.47 NA			
62	MW17-2	733.74				730.55 NSA-1	730.55 NA			
63	MW17-3	732.15				729.77 NSA-1	729.77 NA			
64	MW17-4	734.58				731.58 NSA-1	731.58 NA			
65	MW25-3	745.58				742.41 NSA-1	742.41 NA			
							1.98	2.37	1.58	1.86

Note:
NSA-1 = Not a seasonal average, represents only 1 water elevation for the given year
NSA-2 = Not a seasonal average, represents only 2 water elevations for the given year
NA = Needs Adjusting

TABLE 5-2

WATER TABLE ELEVATIONS AND DEVELOPMENT OF A SEASONALLY AVERAGED
GROUNDWATER TABLE AT THE ASH LANDFILL

SENECA ARMY DEPOT ACTIVITY
ASH LANDFILL GROUNDWATER MODEL

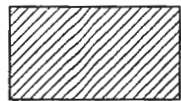
WELL	ELEVATION TOP OF PVC	ADJUSTED ARITHMETIC MEAN	COMMENTS	SEASONALLY AVERAGED GROUNDWATER ELEVATION FOR MODEL CALIBRATION (MSL)	
1	PT-10	681.58	673.51	no adjustment	673.51
2	PT-11	658.26	651.68	no adjustment	651.68
3	PT-12	652.03	644.90	no adjustment	644.90
4	PT-15	637.84	630.35	no adjustment	630.35
5	PT-16	637.78	633.43	no adjustment	633.43
6	PT-17	640.82	634.21	no adjustment	634.21
7	PT-18	656.59	649.85	no adjustment	649.85
8	PT-19	645.45	640.17	no adjustment	640.17
9	PT-20	647.28	640.02	no adjustment	640.02
10	PT-21	647.51	641.03	no adjustment	641.03
11	PT-22	648.82	640.95	no adjustment	640.95
12	PT-23	641.54	635.05	no adjustment	635.05
13	PT-24	638.35	631.02	no adjustment	631.02
14	PT-25	637.02	630.56	no adjustment	630.56
15	PT-26	614.84	608.28	no adjustment	608.28
16	MW-27	638.42	633.45	no adjustment	633.45
17	MW-28	637.41	631.58	no adjustment	631.58
18	MW-29	637.33	630.19	no adjustment	630.19
19	MW-30	640.23	633.13	no adjustment	633.13
20	MW-31	638.86	631.84	no adjustment	631.84
21	MW-32	641.85	635.11	no adjustment	635.11
22	MW-33	639.52	633.41	no adjustment	633.41
23	MW-34	632.89	628.38	no adjustment	628.38
24	MW-35D	631.62	629.08	no adjustment	629.08
25	MW-36	632.09	629.02	no adjustment	629.02
26	MW-37	632.86	629.14	no adjustment	629.14
27	MW-38D	637.98	633.97	no adjustment	633.97
28	MW-39	659.72	657.12	no adjustment	657.12
29	MW-40	659.46	654.55	no adjustment	654.55
30	MW-41D	694.02	688.82	no adjustment	688.82
31	MW-42D	683.04	678.34	no adjustment	678.34
32	MW-43	657.9	653.78	1 std dev subtracted from Dec '94 elev	653.78
33	MW-44	654.12	648.59	1/2 std dev added to arithmetic mean	648.59
34	MW-45	651.13	648.88	no adjustment	648.88
35	MW-46	650.85	645.82	1 std dev subtracted from Dec '94 elev	645.82
36	MW-47	628.53	623.96	no adjustment	623.96
37	MW-48	648.57	643.75	no adjustment	643.75
38	MW-49D	650.88	645.45	1 std dev subtracted from Dec '94 elev	645.45
39	MW-50D	650.27	644.73	1 std dev subtracted from Dec '94 elev	644.73
40	MW-51D	626.84	624.02	1 std dev subtracted from Dec '94 elev	624.02
41	MW-52D	628.7	622.54	1 std dev subtracted from Dec '94 elev	622.54
42	MW-53	639.63	631.17	1 std dev subtracted from Dec '94 elev	631.17
43	MW-54D	639.34	631.93	1 std dev subtracted from Dec '94 elev	631.93
44	MW-55D	639.43	631.71	1 std dev subtracted from Dec '94 elev	631.71
45	MW-56	630.89	627.27	no adjustment	627.27
46	MW-57D	630.27	626.94	1 std dev subtracted from Dec '94 elev	626.94
47	MW-58D	629.86	626.87	1 std dev subtracted from Dec '94 elev	626.87
48	MW-59	656.63	653.76	no adjustment	653.76
49	MW-60	660.15	656.99	no adjustment	656.99
50	MW64D-1	667.79	663.37	1 std dev subtracted from Dec '94 elev	663.37
51	MW64D-2	635.2	631.83	1 std dev subtracted from Dec '94 elev	631.83
52	MW64D-3	648.88	645.25	1 std dev subtracted from Dec '94 elev	645.25
53	MW64D-4	661.33	655.73	1 std dev subtracted from Dec '94 elev	655.73
54	MW64D-5	652.49	648.20	3/4 std dev added to Jul '94 elev	648.20
55	MW64A-1	745.77	737.87	3/4 std dev added to Jul '94 elev	737.87
56	MW64A-2	740.88	735.77	3/4 std dev added to Jul '94 elev	735.77
57	MW64A-3	739.85	735.32	3/4 std dev added to Jul '94 elev	735.32
58	MW16-1	735.54	730.87	3/4 std dev subtracted from Nov/Dec'93 elev	730.87
59	MW16-2	734.55	729.84	3/4 std dev subtracted from Nov/Dec'93 elev	729.84
60	MW16-3	735.48	730.09	3/4 std dev subtracted from Nov/Dec'93 elev	730.09
61	MW17-1	736.27	731.81	1 std dev subtracted from Dec '94 elev	731.81
62	MW17-2	733.74	728.89	1 std dev subtracted from Dec '94 elev	728.89
63	MW17-3	732.15	728.11	1 std dev subtracted from Dec '94 elev	728.11
64	MW17-4	734.56	729.92	1 std dev subtracted from Dec '94 elev	729.92
65	MW25-3	745.58	740.75	1 std dev subtracted from Dec '94 elev	740.75

Justification for adjustments to obtain seasonal average elevation:

- 1) Adjustments were based on seasonal data for selected wells for which standard deviations were calculated
- 2) December through March elevations represent maximum water table and were adjusted down by 1 standard deviation
- 3) July elevations represent near minimum water table and were adjusted up by 3/4 standard deviation.
- 4) Nov/Dec elevations represent near maximum water table and were adjusted down by 3/4 standard deviation.



C:\ACAD\SENECA\ASHMODEL\CHSPS.DWG



AREA OF INAC



GROUNDWATER
IN TILL/WEATI
AQUIFER



ACTIVE MODEL

N



1600



PARSONS

PARSONS ENGINEERING SCIENCE, INC.

CLIENT/PROJECT TITLE

SENECA ARMY DEPOT ACTIVITY
ASH LANDFILL GROUNDWATER MODEL

DEPT.

ENVIRONMENTAL ENGINEERING

Dwg No.

FIGURE 5-5
COMPARISON OF MEASURED AND SIMULATED
HEADS

SCALE

1" = 1600'

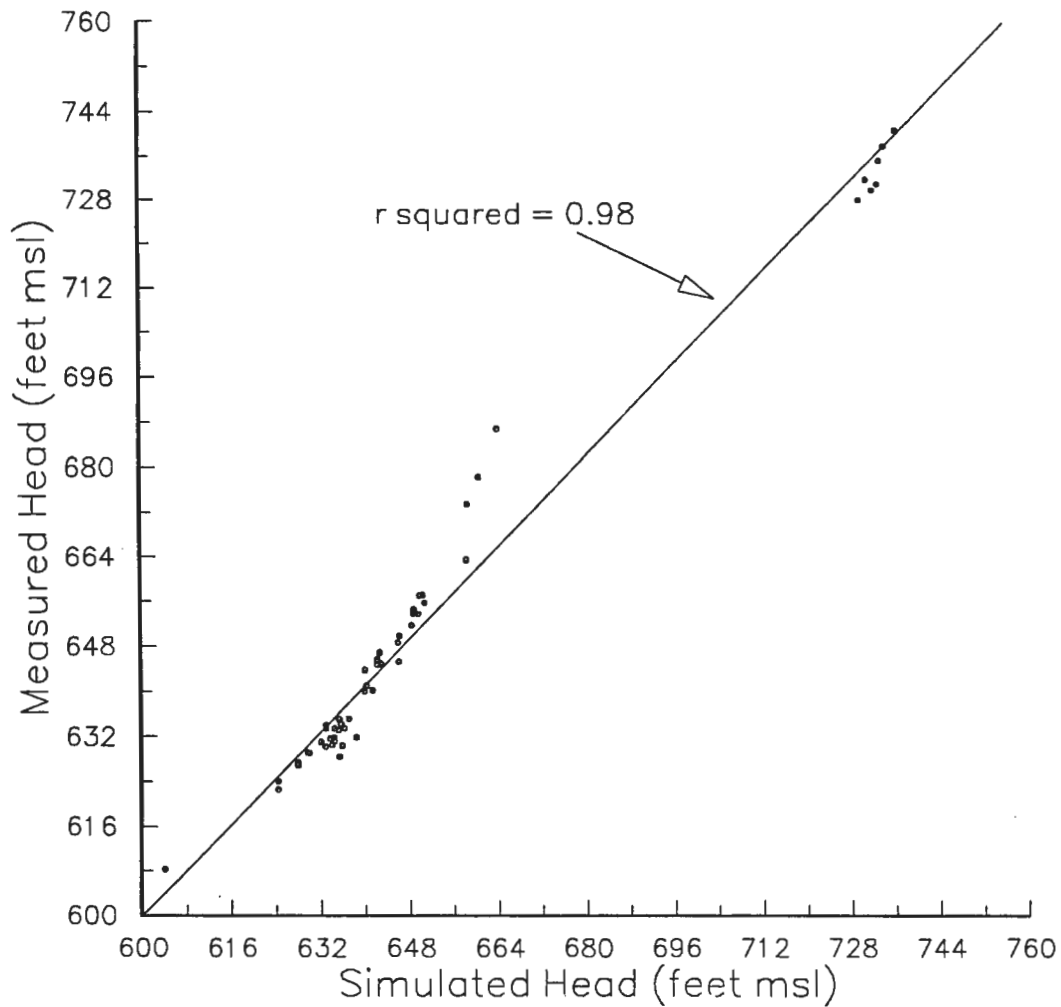
DATE

OCTOBER 1995

REV

A

Plot of Simulated versus Measured Heads Monitoring Wells




 PARSONS PARSONS ENGINEERING SCIENCE, INC.	
<small>CLIENT/PROJECT TITLE</small> SENECA ARMY DEPOT ACTIVITY ASH LANDFILL GROUNDWATER MODEL	
<small>DEPT.</small> ENVIRONMENTAL ENGINEERING	<small>DWG NO.</small> 726209-01002
FIGURE 5-6 PLOT OF SIMULATED VERSUS MEASURED HEADS	
<small>SCALE</small> NA	<small>DATE</small> OCTOBER 1995

TABLE 5-3

COMPARISON OF MEASURED AND SIMULATED HEADS

SENECA ARMY DEPOT ACTIVITY
ASH LANDFILL GROUNDWATER MODEL

WELL	MODEL COLUMN	MODEL ROW	MODEL LAYER	MEAS. HIGH	MEAS. LOW	TARGET MEAN	TARGET HIGH	TARGET LOW	MODEL HEAD	Difference (feet)	Absolute Difference	Squared Difference
MW25-3	4	9	1	742.41	742.41	740.75	743.75	737.75	736.1	-4.7	4.7	21.66
MW64A-1	82	11	1	736.63	736.63	737.87	740.87	734.87	734.0	-3.9	3.9	14.99
MW64A-3	82	12	1	734.08	734.08	735.32	738.32	732.32	733.2	-2.1	2.1	4.50
MW17-1	4	15	1	733.47	733.47	731.81	734.81	728.81	730.8	-1.0	1.0	1.03
MW16-1	2	13	1	732.14	732.14	730.97	733.97	727.97	732.9	1.9	1.9	3.74
MW16-2	2	14	1	731.01	731.01	729.84	732.84	726.84	731.9	2.1	2.1	4.25
MW17-3	4	16	1	729.77	729.77	728.11	731.11	725.11	729.5	1.4	1.4	1.92
GHOST19	42	18	1	NA	NA	715.00	718.00	712.00	726.7	11.7	11.7	136.89
GHOST20	42	18	2	NA	NA	714.00	717.00	711.00	726.7	12.7	12.7	161.29
GHOST21	42	18	3	NA	NA	713.00	716.00	710.00	726.7	13.7	13.7	187.69
GHOST1	77	28	1	NA	NA	695.00	698.00	692.00	707.3	12.3	12.3	151.29
GHOST4	9	27	1	NA	NA	695.00	698.00	692.00	709.8	14.8	14.8	219.04
GHOST5	9	27	2	NA	NA	694.00	697.00	691.00	709.8	15.8	15.8	249.64
GHOST2	77	28	2	NA	NA	694.00	697.00	691.00	707.3	13.3	13.3	176.89
GHOST3	77	28	3	NA	NA	693.00	696.00	690.00	707.3	14.3	14.3	204.49
GHOST6	9	27	3	NA	NA	693.00	696.00	690.00	709.8	16.8	16.8	282.24
MW-41D	11	42	2	687.96	685.74	686.82	687.32	686.32	663.9	-22.9	22.9	525.10
MW-42D	70	43	2	680.66	674.94	678.34	678.84	677.84	660.6	-17.7	17.7	314.53
PT-10	47	44	2	677.79	670.57	673.51	674.01	673.01	658.5	-15.0	15.0	225.28
MW64D-1	77	44	1	665.03	664.36	663.37	663.87	662.87	658.3	-5.1	5.1	25.75
MW-39	17	61	1	657.99	656.37	657.12	657.62	656.62	650.4	-6.7	6.7	45.19
MW-60	72	62	1	658.13	654.83	656.99	657.49	656.49	649.8	-7.2	7.2	51.73
MW64D-4	79	59	1	657.39	655.10	655.73	656.23	655.23	650.7	-5.0	5.0	25.34
MW-40	46	65	1	656.40	652.18	654.55	655.05	654.05	648.8	-5.8	5.8	33.09
MW-59	71	65	1	654.95	651.61	653.78	654.28	653.28	648.7	-5.1	5.1	25.81
MW-43	35	63	1	655.42	652.46	653.76	654.26	653.26	649.6	-4.2	4.2	17.34
PT-11	66	66	1	654.02	648.49	651.68	652.18	651.18	648.4	-3.3	3.3	10.73
PT-18	46	72	1	651.78	646.72	649.85	650.35	649.35	646.2	-3.7	3.7	13.32
MW-44	34	73	1	648.63	646.98	648.59	649.09	648.09	645.9	-2.7	2.7	7.22
MW-45	24	82	1	648.47	644.75	646.88	647.38	646.38	642.6	-4.3	4.3	18.28
MW-46	34	83	1	647.28	642.61	645.62	646.12	645.12	642.2	-3.4	3.4	11.73
MW-49D	34	83	2	647.11	642.74	645.45	645.95	644.95	642.2	-3.3	3.3	10.59
MW64D-3	77	72	1	646.91	645.89	645.25	645.75	644.75	646.0	0.7	0.7	0.56
PT-12	44	81	1	647.25	641.73	644.90	645.40	644.40	642.9	-2.0	2.0	4.00
MW-50D	34	83	3	646.39	642.90	644.73	645.23	644.23	642.2	-2.5	2.5	6.42
MW-48	26	89	1	645.47	641.57	643.75	644.25	643.25	639.9	-3.9	3.9	14.84
PT-21	43	88	2	647.51	635.37	641.03	641.53	640.53	640.2	-0.8	0.8	0.69
PT-22	43	88	1	645.45	637.85	640.95	641.45	640.45	640.2	-0.7	0.7	0.56
PT-19	58	85	1	642.35	637.81	640.17	640.67	639.67	641.3	1.1	1.1	1.28
PT-20	51	89	1	644.21	636.11	640.02	640.52	639.52	639.8	-0.2	0.2	0.05
MW-32	58	96	1	637.84	632.40	635.11	635.61	634.61	637.0	1.9	1.9	3.56
PT-23	30	101	1	638.71	632.56	635.05	635.55	634.55	635.2	0.1	0.1	0.02
PT-17	53	100	1	636.85	630.12	634.21	634.71	633.71	635.5	1.3	1.3	1.65
MW-38D	18	107	2	634.67	632.76	633.97	634.47	633.47	632.9	-1.1	1.1	1.14
MW-27	33	103	1	635.62	630.37	633.45	633.95	632.95	634.4	0.9	0.9	0.90
PT-16	18	107	1	635.06	630.17	633.43	633.93	632.93	632.9	-0.5	0.5	0.28
MW-33	63	98	1	635.95	630.02	633.41	633.91	632.91	636.2	2.8	2.8	7.77
MW-30	56	101	1	636.37	629.73	633.13	633.63	632.63	635.1	2.0	2.0	3.89
MW64D-2	75	92	1	633.49	630.75	631.83	632.33	631.33	638.4	6.6	6.6	43.11
MW-55D	47	103	3	633.37	630.23	631.71	632.21	631.21	634.3	2.6	2.6	6.69
MW-31	61	103	1	634.60	627.21	631.64	632.14	631.14	634.3	2.7	2.7	7.05
MW-54D	47	103	2	633.29	629.88	631.63	632.13	631.13	634.3	2.7	2.7	7.11
MW-28	36	105	1	633.28	628.26	631.58	632.08	631.08	633.6	2.0	2.0	4.07
MW-53	47	103	1	632.83	630.13	631.17	631.67	630.67	634.4	3.2	3.2	10.41
PT-24	40	109	1	633.19	627.85	631.02	631.52	630.52	632.0	1.0	1.0	0.97
PT-25	64	104	1	633.66	625.45	630.56	631.06	630.06	633.9	3.3	3.3	11.17
PT-15	71	99	1	634.09	627.40	630.35	630.85	629.85	635.8	5.5	5.5	29.71
MW-29	46	107	1	631.82	626.83	630.19	630.69	629.69	632.8	2.6	2.6	6.83
MW-37	7	116	1	630.91	626.65	629.14	629.64	628.64	629.6	0.5	0.5	0.22
MW-35D	61	114	2	629.66	628.01	629.08	629.58	628.58	629.9	0.8	0.8	0.67
MW-36	61	114	1	629.94	626.43	629.02	629.52	628.52	629.9	0.9	0.9	0.78
MW-34	75	100	1	630.28	626.39	628.38	628.88	627.88	635.3	6.9	6.9	47.85
MW-56	48	119	1	627.78	626.67	627.27	627.77	626.77	627.9	0.6	0.6	0.40
MW-57D	48	119	2	628.60	627.11	626.94	627.44	626.44	627.9	1.0	1.0	0.91
MW-58D	48	119	3	628.53	625.66	626.87	627.37	626.37	627.9	1.0	1.0	1.05

TABLE 5-3

COMPARISON OF MEASURED AND SIMULATED HEADS

**SENECA ARMY DEPOT ACTIVITY
ASH LANDFILL GROUNDWATER MODEL**

WELL	MODEL COLUMN	MODEL ROW	MODEL LAYER	MEAS. HIGH	MEAS. LOW	TARGET MEAN	TARGET HIGH	TARGET LOW	MODEL HEAD	Difference (feet)	Absolute Difference	Squared Difference
MW-51D	35	128	2	625.68	621.56	624.02	624.52	623.52	624.3	0.3	0.3	0.08
MW-47	35	128	1	625.69	621.47	623.96	624.46	623.46	624.3	0.3	0.3	0.12
MW-52D	35	128	3	624.20	620.04	622.54	623.04	622.04	624.3	1.8	1.8	3.08
PT-26	73	174	1	611.82	603.10	608.28	608.78	607.78	604.0	-4.3	4.3	18.30
GHOST22	42	174	1	NA	NA	601.00	604.00	598.00	604.5	3.5	3.5	12.25
GHOST23	42	174	2	NA	NA	600.00	603.00	597.00	604.5	4.5	4.5	20.25
GHOST24	42	174	3	NA	NA	599.00	602.00	596.00	604.5	5.5	5.5	30.25
GHOST10	7	199	1	NA	NA	575.00	578.00	572.00	560.6	-14.4	14.4	207.36
GHOST7	77	198	1	NA	NA	575.00	578.00	572.00	566.7	-8.3	8.3	68.89
GHOST8	77	198	2	NA	NA	574.00	577.00	571.00	566.7	-7.3	7.3	53.29
GHOST11	7	199	2	NA	NA	574.00	577.00	571.00	564.7	-9.3	9.3	86.49
GHOST9	77	198	3	NA	NA	573.00	576.00	570.00	566.7	-6.3	6.3	39.69
GHOST12	7	199	3	NA	NA	573.00	576.00	570.00	564.7	-8.3	8.3	68.89
GHOST16	6	213	1	NA	NA	515.00	518.00	512.00	483.2	-31.8	31.8	1011.24
GHOST17	6	213	2	NA	NA	514.00	517.00	511.00	483.2	-30.8	30.8	948.64
GHOST18	6	213	3	NA	NA	513.00	516.00	510.00	483.2	-29.8	29.8	888.04
GHOST13	74	211	1	NA	NA	495.00	498.00	492.00	481.8	-13.2	13.2	174.24
GHOST14	74	211	2	NA	NA	494.00	497.00	491.00	481.8	-12.2	12.2	148.84
GHOST15	74	211	3	NA	NA	493.00	496.00	490.00	481.8	-11.2	11.2	125.44

NOTE: Wells are sorted in order of decreasing Target Mean Values

Statistical Calculations:

Monitoring Wells Only	Monitoring and Ghost		
ME=	-1.58	ME=	-1.66
MAE=	4.03	MAE=	7.03
RMS=	5.71	RMS=	9.86
	32.57		97.24

1. Mean Error (ME), which is the mean difference between the measured heads and the simulated heads;
2. Mean Absolute Error (MAE), which is the mean of the absolute value of the differences in measured and simulated heads; and
3. Root Mean Squared (RMS), which is the average of the squared differences in measured and simulated heads.

To help in evaluating the calibration of the flow model ME, MAE, and RMS were plotted against net recharge, the most significant calibration criterion. The plots indicate that all three averages provide a well defined minimum (Figure 5-7). Specifically, the ME provided the lowest minimum when a net recharge rate of 0.00486 feet/year (or 0.00001332 feet/day) was used.

Hydraulic gradients for the simulated heads at the Ash Landfill are very similar to those for the observed heads. The simulated gradient between till/weathered shale wells PT-18 and PT-17 was 0.014 feet/foot compared to a measured gradient of 0.021 feet/foot. Between wells MW-40 and MW-56, which are also till/weathered shale wells, the simulated gradient was 0.016 feet/foot compared to a gradient of 0.019 feet/foot measured in the field. For the competent shale wells PT-10 and MW-36, a simulated gradient of 0.015 feet/foot was computed while a gradient of 0.025 was measured.

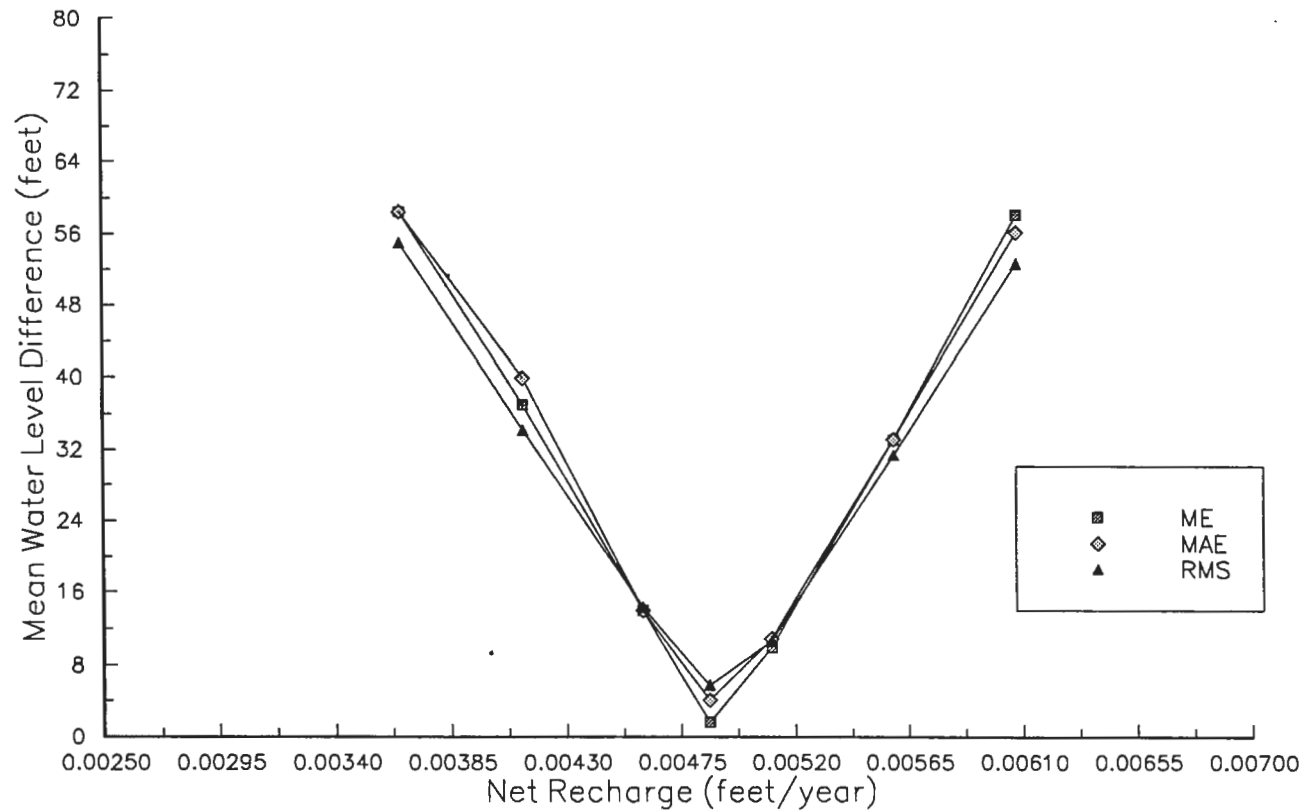
5.3.2 Water Balance

The water balance also served as a calibration criterion for the groundwater flow model. Two aspects of the water balance (or volumetric budget) were evaluated.

First, there was relatively good agreement between the flows out of the model as calculated in the preliminary water budget and in the MODFLOW model. In the preliminary water budget at total flow out (Q_{out}) of 2,257.4 ft³/day was calculated, compared to a total flow out of 2,004 ft³/day calculated by the model.

Second, the percent discrepancy in the volumetric budget as calculated by the MODFLOW model was 0.0 percent, with a total flow in (Q_{in}) of 2003.9 ft³/day solely from recharge and a total flow out (Q_{out}) of constant head cells at Seneca Lake of 2,004.0 ft³/day. The model calculated a difference between Q_{in} and Q_{out} of -0.077393 ft³/day.

ME, MAE, and RMS for MONITORING WELLS



PARSONS
PARSONS ENGINEERING SCIENCE, INC.

CLIENT/PROJECT TITLE
**SENECA ARMY DEPOT ACTIVITY
ASH LANDFILL GROUNDWATER MODEL**

DEPT ENVIRONMENTAL ENGINEERING DWG NO 726209-01002

FIGURE 5-7
PLOT SHOWING THE
EFFECT OF NET RECHARGE ON
ME, MAE, AND RMS

SCALE NA DATE OCTOBER 1995

5.3.3 Groundwater Velocity and Advective Travel Time

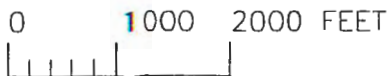
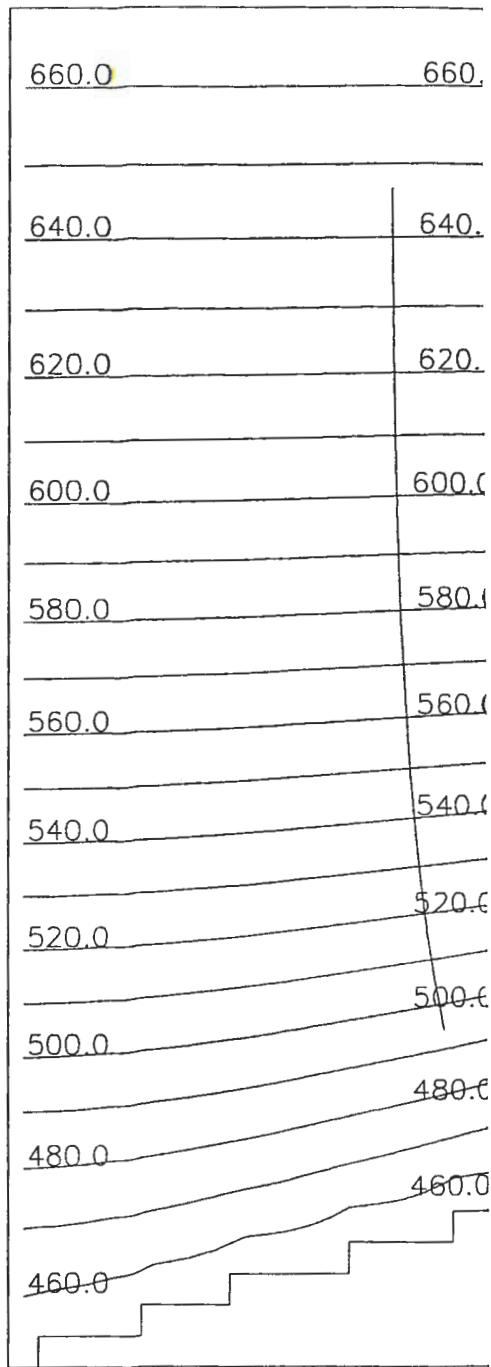
Model calibration was also supported by comparing groundwater velocities calculated using three different methods. The methods are as follows:

- Darcy equation
- MODPATH
- 50% plume concentration travel time

A range for the groundwater flow velocity of the till/weathered shale was calculated to be 27.4 feet/year to 36.5 feet/year (n_e of 20% and 15%, respectively) using the Darcy equation and hydraulic data for the Ash Landfill site (Parsons ES, 1994a). And, using this same method, the groundwater velocity of the competent shale was calculated to be 7.3 feet/year.

The computer model MODPATH was used to determine the time it would take groundwater to travel a fixed distance in layer 1 (Appendix E). Using this information the groundwater velocity in layer 1 was calculated. The model released one particle at the center of a cell ($70_{row}, 42_{col}, 1_{layer}$) within the Ash Landfill and then it used particle tracking methods to calculate an average travel time of $1.87590E+05$ days for the particle to discharge into layer 2 (Figures 5-8 and 5-9). The particle was stopped by the model when it entered a cell ($210_{row}, 62_{col}, 2_{layer}$) in layer 2. The particle was allowed to travel a total distance of approximately 8,000 feet in layer 1 before discharging into layer 2. Therefore, based on these results, the velocity of the particle was calculated to be 0.067 feet/day or approximately 25 feet/year. Note that in the plan view of the pathline trace for the particle that it bends to follow a course perpendicular to contours defining piezometric head (Figure 5-8). Figure 5-9 shows a cross-section of the same pathline trace using column 42 of the grid for the section. To construct the section MODPATH projected the particle's pathline back onto column 42 because it exited layer 1 in column 62, as noted above. Because a stratigraphic three-dimensional grid was used for the model, an artifact of this projection is the appearance that the particle was allowed to travel into layer 2.

In addition, the 50% concentration of a sodium plume that originated near well PT-18 and extended west along a series of other wells was used to provide further evidence of model calibration (Figure 5-10). The series included wells PT-18, PT-12, PT-22, MW-53, and MW-56 and whose maximum average sodium concentration was approximately 104 ppm at PT-18. The 50% concentration of the plume was thus determined to be 52 ppm and this corresponded with a distance of 520 feet from the source, PT-18. Assuming that the release of sodium corresponds with the suspected release of



PARSONS

PARSONS ENGINEERING SCIENCE, INC.

CLIENT/PROJECT TITLE

**SENECA ARMY DEPOT ACTIVITY
ASH LANDFILL GROUNDWATER MODEL**

DEPT

ENVIRONMENTAL ENGINEERING

DWG NO.

726209-01002

FIGURE 5-8

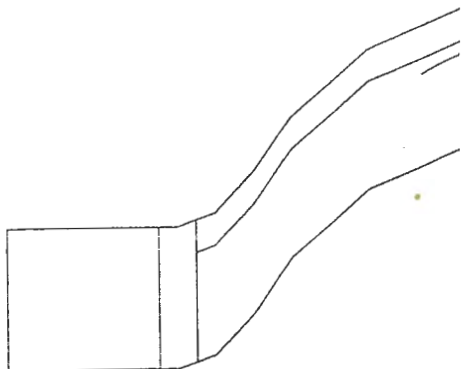
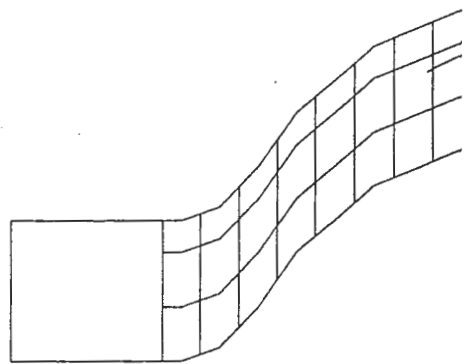
**PATHLINE TRACE FOR A
SINGLE PARTICLE RELEASED IN
LAYER 1 AT THE ASH LANDFILL**

SCALE

NA

DATE

OCTOBER 1995



0 1000 2000 FEET

VERTICAL EXAGGERATED

Pathline Trace



PARSONS

PARSONS ENGINEERING SCIENCE, INC.

CLIENT/PROJECT TITLE

SENECA ARMY DEPOT ACTIVITY
ASH LANDFILL GROUNDWATER MODEL

DEPT.

ENVIRONMENTAL ENGINEERING

DWG NO.

726209-01002

FIGURE 5-9

CROSS-SECTION PATHLINE TRACE
FOR A SINGLE PARTICLE RELEASED IN
LAYER 1 AT THE ASH LANDFILL

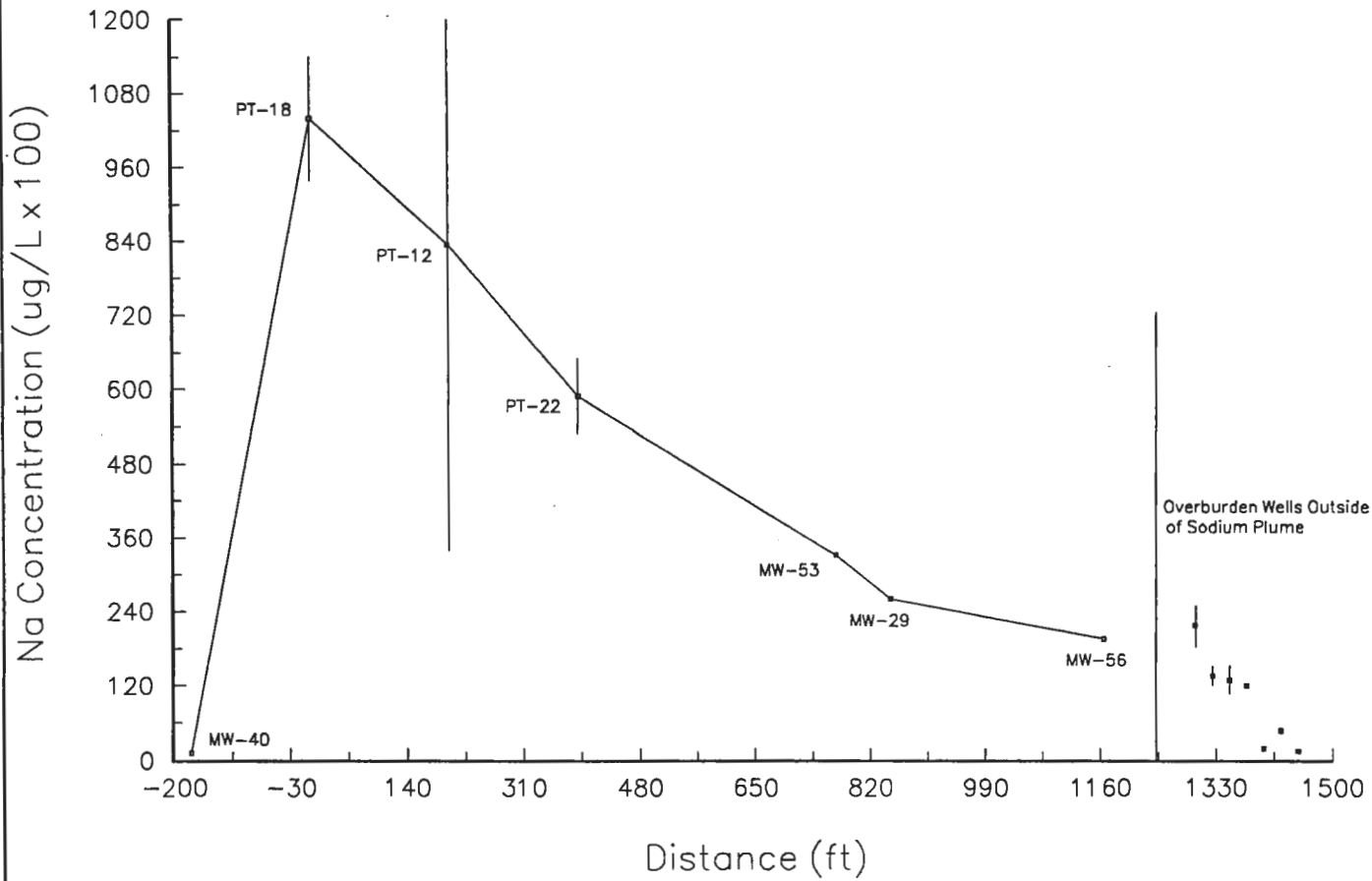
SCALE

NA

DATE

OCTOBER 1995

SODIUM CONCENTRATIONS IN GROUNDWATER (Maximum, Minimum, and Average)



CLIENT/PROJECT TITLE
**SENECA ARMY DEPOT ACTIVITY
 ASH LANDFILL GROUNDWATER MODEL**

DEPT. ENVIRONMENTAL ENGINEERING DWG. NO. 726209-01002

**FIGURE 5-10
 SODIUM CONCENTRATIONS
 IN GROUNDWATER
 (MAXIMUM, MINIMUM, AND AVERAGE)**

volatiles at the site, which is suspected to be approximately 20 to 40 years ago, the range of velocities for the sodium plume was calculated to be 26 feet/year to 13 feet/year. Clearly, there is some uncertainty in the velocities calculated using this method because the exact time of the release of sodium is unknown. The 13 feet/year velocity does not agree well with the velocity calculated using the Darcy equation and, therefore, it is not believed to represent groundwater flow on-site.

Generally, the velocities calculated using the Darcy equation, MODPATH and the 50% plume concentration travel time provide good evidence that the calibration of the groundwater flow model was achieved.

5.4 Sensitivity Analysis

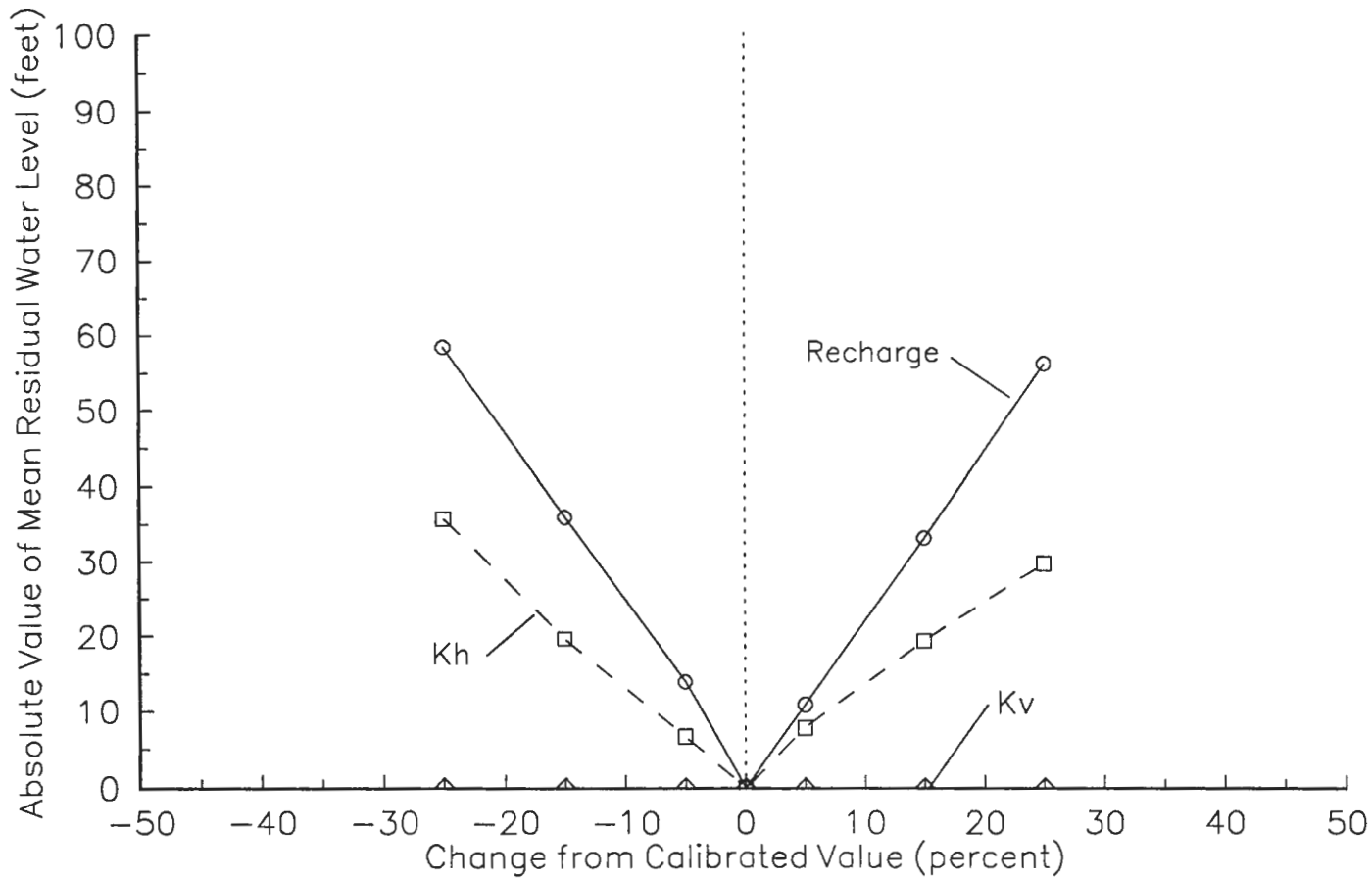
A sensitivity analysis was performed after the flow model was calibrated. The purpose of the sensitivity analysis was to determine how sensitive the calibrated model was to variations or uncertainty in the aquifer parameters, stresses, and boundary conditions. Thus, during the sensitivity analysis the calibrated values for hydraulic conductivity storage parameters recharge and boundary conditions are systematically changed within the previously established plausible range (Anderson and Woessner, 1992). For this model, boundary conditions were characterized using well defined physical and hydrologic boundaries and thus they were not part of the sensitivity analysis.

The sensitivity analysis was performed by changing one input parameter at a time and evaluating the effects on the distribution of the heads (the dependent variable) in the model. The input parameters evaluated for the sensitivity analysis of the model were as follows:

1. net recharge;
2. horizontal hydraulic conductivity (k_h); and
3. vertical hydraulic conductivity (k_v).

Each parameter was varied by 10, 20, and 50 percent from its original calibrated value and the resulting effects on the head were noted (Appendix D). The results of the analysis are graphically shown in Figure 5-11. Clearly, net recharge is the most sensitive parameter compared to K_h and K_v .

Changes of up to +/- 25% from the calibrated value of net recharge produced a mean residual of approximately 60 feet for the model. For K_h a change of +/- 25% from the calibrated value produced approximately 30 to 35 foot mean residual. Changes of up to +/- 25% in K_v produced no measurable changes in head from their calibrated values.



PARSONS
PARSONS ENGINEERING SCIENCE, INC.

CLIENT/PROJECT TITLE
**SENECA ARMY DEPOT ACTIVITY
 ASH LANDFILL GROUNDWATER MODEL**

DEPT. ENVIRONMENTAL ENGINEERING DWG. NO. 726209-01002

FIGURE 5-11
PLOT SHOWING THE SENSIVITY
OF THE FLOW MODEL TO
RECHARGE, Kh, AND Kv

SCALE NA DATE OCTOBER 1995

5.5 Groundwater Flow Model Results

The steady-state groundwater flow system at the Ash Landfill was simulated by MODFLOW using a stratigraphic three-dimension grid that extended to 52 feet below the land surface. The model successfully simulated heads over the at the Ash Landfill site and the surrounding area using well defined physical and hydraulic boundaries for the flow system. The heads calculated by the model indicate that groundwater flow is primarily to the west in the upper portions of the plateau that separates Seneca and Cayuga Lakes, but that the flow bends to the southwest at it approaches Seneca Lake (Figure 5-5).

It is noteworthy that the heads were consistently low in areas where the gradient of the land surface was steep (i.e., near Seneca Lake and east of the Ash Landfill). However, for this model simulation of the head at the Ash Landfill and in the area west to Route 96A was a primary goal as the head and flow data for this region was used in the transport model to simulate the migration of the plume of VOCs.

The volumetric budget output for the MODFLOW model indicates a total Q_{in} of 2003.9 ft³/day soley from recharge (i.e., precipitation) and a total Q_{out} of constant head cells at Seneca Lake of 2004.0 ft³/day.

6.0 TRANSPORT MODEL DESIGN AND RESULTS

6.1 Selection of Model Code

The transport modeling portion of this study required a computer code that could simulate important physical and chemical effects in three dimensional groundwater flow systems. The MT3D computer code was selected to simulate contaminant transport for this project because of the following:

- MT3D simulates advection, dispersion, and chemical reactions for contaminants in groundwater flow systems in three dimensions;
- MT3D uses unformatted head and flow files saved in MODFLOW for the transport calculations;
- The accuracy of the MT3D code has been checked against one or more analytical solutions;
- MT3D includes a mass balance computation;
- MT3D has been used to simulate contaminant transport in numerous studies; and
- MT3D allows the flow model to be constructed and calibrated independently.

6.2 Relationship Between Conceptual Model and MT3D Numerical Model

The MT3D transport model can be used in conjunction with the block-centered finite-difference MODFLOW model. Thus, the aspects of the conceptual model are preserved in the transport model because MT3D retrieves the hydraulic heads and the various flow and sink/source terms saved by the flow model, automatically incorporating the specified hydrologic boundary conditions.

6.3 Assignment of Input Parameter Values for MT3D

The MT3D model uses a modular structure similar to that implemented in MODFLOW. Like the MODFLOW model, the MT3D model uses a main program and complementary series of packages, and each of these packages deals with a single aspect of the transport simulation. Input parameter values are entered into the main program and the various packages for use in the model. The three model scenarios were simulated using five packages. The packages are as follows:

1. Basic Transport Package
2. Advection Package
3. Dispersion Package

4. Sink & Source Mixing Package
5. Chemical Reaction Package

Input parameter values for the MT3D contaminant transport model were derived from both site investigation data and from the literature when site specific data were not available. The parameter values that define and affect contaminant transport are discussed below relative to the package in which they are specified. Because three scenarios were simulated for this project, some of the input parameters were different depending on what scenario was simulated. Table 6-1 presents the selected input parameters for the transport model along with an acceptable range for each value; the best estimates for the parameters used in the model are also presented.

Because MT3D is a complimentary program to MODFLOW, it uses the same model boundary and grid conditions that were used for MODFLOW (Figure 6-1). Therefore, none of the physical aspects of the model grid or groundwater flow parameters will be discussed here.

6.3.1 Basic Transport Package Parameters

In the Basic Transport Package, which is the main program, general model characteristics are specified including: the number of model layers, aquifer layer types, grid dimensions and elevations, the major transport packages to be used, effective porosity values, concentration boundary conditions, the starting concentration field, and various aspects of the model output.

For this model, the number of model layers, the aquifer layer types and the grid was the same as that used in the MODFLOW model.

The effective porosity of the till/weathered shale aquifer was specified as 15 % (0.15) and 6% (0.06) for the competent shale aquifer. These are the same effective porosities used to calculate the likely range of groundwater velocities in the Ash Landfill RI report (Parsons ES, 1994a).

For Scenarios 1 and 2, two model cells were defined as constant unchanging source concentration terms (i.e., MW-44 and PT-18) and the rest were specified as active cells, subject to the boundary conditions established in the model. For Scenario 3, all of the model cells were active.

For the transport modeling, three initial concentration scenarios were generated for use with the three transport scenarios. For the Scenario 1, the initial concentration matrix consisted of defining concentrations at only two point sources. In other words, Scenario 1 was established to simulate

TABLE 6-1
REASONABLE RANGE, BEST ESTIMATE, AND UNCERTAINTY FOR
MT3D INPUT PARAMETERS

SENECA ARMY DEPOT ACTIVITY
ASH LANDFILL GROUNDWATER MODEL

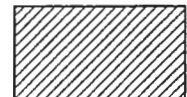


Input Parameter	Units	Reasonable Range			Best Estimate	Source	Uncertainty
		Low	Nominal	High			
Advection Terms:							
Effective Porosity Layer 1	percent	15	15	25	15 (or 0.15)	Literature	low
Effective Porosity Layer 2	percent	6	6	6	6 (or 0.06)	Literature	low
Effective Porosity Layer 3	percent	6	6	6	6 (or 0.06)	Literature	low
Dispersion Terms:							
Long. Dispersivity (L) Layer 1	feet	10	10	30	10	Literature	low
Long. Dispersivity (L) Layer 2	feet	15	20	40	20	Literature	low
Long. Dispersivity (L) Layer 3	feet	15	20	40	20	Literature	low
Ratio of TH / L		0.06	0.1	0.5	0.1	Literature	medium
Ratio of TV / L		0.006	0.01	0.05	0.01	Literature	medium
Coeff. of Molecular Diffusion		0	0	0	0		low
Chemical Reaction Terms:							
Sorption Constant (Kd)	ml/gram	0.006	0.013	0.013	0.013	Literature	low
Bulk Dry Density (Pb)	gram/cu. cm	1.51	1.69	1.78	1.65	field data	low
K (dissolved phase)	/day	5.0E-06	0.00005	0.0006	0.00005	Literature	low
K (sorbed phase)	/day	5.0E-06	0.00005	0.0006	0.00005	Literature	low

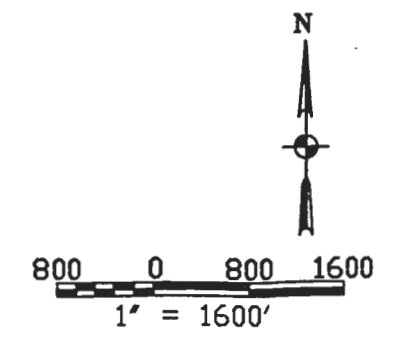
Notes:

- 1) TH = transverse horizontal dispersivity
- 2) TV = transverse vertical dispersivity
- 3) K = first order biodegradation rate constant



C:\ACAD\SENECA\ASHMODEL\MGB.C.DWG

-  AREA OF INACTIVE CELLS
-  GROUNDWATER FLOW DIRECTION IN TILL/WEATHERED SHALE AQUIFER
-  ACTIVE MODEL BOUNDARY



P PARSONS	
PARSONS ENGINEERING SCIENCE, INC.	
CLIENT/PROJECT TITLE	
SENECA ARMY DEPOT ACTIVITY ASH LANDFILL GROUNDWATER MODEL	
DEPT.	Dwg. No.
ENVIRONMENTAL ENGINEERING	
FIGURE 6-1 MT3D MODEL GRID AND BOUNDARY CONDITIONS	
SCALE	DATE
1" = 1600'	OCTOBER 1995
REV	A

the situation that would be analogous to releasing COC at time equal to the initial release. Under this scenario, the groundwater, other than in the source area, is initially free of impacts. This approach was used to simulate the migration of the plume from the origin, i.e., $t=0$, to the present day. This scenario was used as a calibration scenario, since the outcome of the modeling runs was a simulation that matched the plume size and concentrations, prior to the implementation of the source removal effort that was completed in June of 1995. Scenario 1 was used to calibrate the model input parameters such as dispersion coefficients and degradation rates in addition to simulating continual leaching of chlorinated organics to the groundwater. For Scenario 1, these two specified source concentrations were held constant over the timeframe of Scenario 1. For Scenario 2, the initial modeling concentrations were the concentration of the plume as described in the RI report, prior to the remediation of the source area. The goal of this scenario was to evaluate the existing plume of VOCs (TCE, cis- and trans-1,2-DCE, and VC) as depicted in the Ash Landfill RI report over an extended timeframe, had no source removal been performed. A four-point moving average method was used to generate the concentrations at model cells that did not correspond with existing monitoring well locations and concentrations where specific concentrations were available. The two point source concentrations used for Scenario 1 were also kept constant for Scenario 2. This would simulate continual leaching of chlorinated organics to the groundwater, similar to the conditions of Scenario 1. For Scenario 3, the initial concentration field was established to be equivalent to the plume of VOCs (TCE, cis- and trans-1,2-DCE, and VC) after the remediation of the source areas at the Ash Landfill had been completed. A complete round of groundwater quality data, performed in July, 1995, one month following completion of the source remediation program, was used as the input file for Scenario 3. Again, the four-point moving average method was used to generate the concentrations at model cells that did not correspond with monitoring well locations where specific concentrations were unavailable.

6.3.2 Advection Package Parameters

For this model the hybrid Method of Characteristics/Modified Method of Characteristics (MOC/MMOC) or HMOC advection solution scheme was used. This solution scheme was chosen because it combines the strengths of MOC and MMOC by using an automatic adaptive scheme that depends on the nature of the concentration field. Thus, the advection term is solved by the MOC technique when sharp concentration fronts are present. Away from sharp concentration fronts the advection term is solved by the MMOC technique. The critical relative concentration gradient for controlling the selective use of either MOC or MMOC in the HMOC solution scheme was 0.01.

The number of cells any particle was allowed to move in any one direction in one transport step (the courant number) was 1.0.

The Runge-Kutta particle tracking algorithm was used for this model.

6.3.3 Dispersion Package Parameters

In this package, the dispersion terms for both the till and the competent shale were specified. Because no site-specific dispersivity data were available for the geologic units at the Ash Landfill, the longitudinal dispersivity for the till and the shale were obtained from the literature. Anderson (1979) cites longitudinal dispersivities of 3 meters (9.8 feet) for till and 6.1 meters (20.0 feet) for a shale unit directly below the till that were used in a groundwater modeling study. Thus, for this model, the longitudinal dispersivity of 10 feet was specified for the till and a longitudinal dispersivity of 20 feet was specified for the competent shale. The ratio of horizontal transverse dispersivity to the longitudinal dispersivity was specified as 0.1. The ratio of vertical transverse dispersivity to the longitudinal dispersivity was specified as 0.01. Effective molecular diffusion coefficient was set at 0.0 as this process was not expected to play a major role in contaminant transport.

6.3.4 Sink & Source Mixing Package Parameters

Only the recharge option was activated for the Sink & Source Mixing Package but it was not used to simulate the constant source terms under Scenarios 1 and 2 for the transport model. Thus, no concentration of recharge flux was specified in this package because the constant source concentration terms for the cells that contain MW-44 and PT-18 were defined in the concentration boundary array contained in the Basic Transport Package.

6.3.5 Chemical Reaction Package Parameters

The Chemical Reaction Package was used to simulate the effects of sorption and biodegradation on the movement of VOCs (TCE, cis- and trans-1,2-DCE, and VC) in the aquifer flow system.

Sorption refers to the mass transfer process between the contaminants dissolved in groundwater (solution phase) and the contaminants sorbed on the porous medium (solid phase). Additionally, it is generally assumed that equilibrium conditions exist between the solution-phase and the solid-phase concentrations and that the sorption reaction is fast enough relative to groundwater velocity

so that it can be treated as instantaneous. MT3D incorporates the sorption isotherms into the transport model through the use of the retardation factor (S.S. Papadopulos & Associates, 1992).

The linear sorption isotherm was used in the transport model. The linear sorption isotherm assumes that the sorbed concentration (C_{sorb}) is directly proportional to the dissolve concentration (C_{diss}):

$$C_{\text{sorb}} = K_d C_{\text{diss}}$$

where: K_d = the distribution coefficient

For linear sorption, the first order sorption constant is the distribution coefficient (K_d). For this model, a K_d of 0.013 ml/g for TCE was used to calculate the sorption term (Looney et al., 1983). The retardation factor was calculated by the model using the equation that follows:

$$R = 1 + [P_b/P_{\text{or}}] * K_d$$

where: R = retardation factor

P_b = bulk density of the soil or rock

P_{or} = porosity of soil or rock

K_d = distribution coefficient

For this model, a bulk density of 1.69 g/cm³ was used for the till (USAEHA, 1984).

Also, a first order constant rate for biodegradation term was derived for the model. The biodegradation constant rate used for the dissolved and sorbed phase of VOCs (TCE, cis- and trans-1,2-DCE and VC) was 0.00005/day. The derivation of the biodegradation rate constant was calculated using a method developed by Wedemeier et al. (1995) that was modified for the Ash Landfill site constituents. A description of the method used to derive the biodegradation rate constant is given below.

Initially, the chemistry of the groundwater in and downgradient of the Ash Landfill was reviewed to identify any existing constituents within the area of VOC plume that could likely have been released coincidentally with the VOCs at the initial release event. Sodium was identified as a good candidate as the extent and concentrations of sodium paralleled the VOC plume downgradient of the Ash Landfill. For example, the sodium plume also originates at PT-18, which is near a source area for VOCs. Sodium is considered to be a good tracer because it is not adsorbed to soil particles, is not

biodegraded, and it is therefore mobile in aquifers. Thus, for this model, a single biodegradation rate was developed for three volatile organic compounds (TCE, cis- and trans-1,2 DCE, and VC) at the Ash Landfill using sodium as a conservative tracer.

The biodegradation rate constant was calculated using the method described in Wiedemeier et al. (1995) as modified for the site constituents at the Ash Landfill. Wiedemeier et al. (1995) suggests using a biologically recalcitrant compound found in a BTEX plume as the tracer. However, such a tracer was not present in the database of the Ash Landfill. Instead, using the same principles described in Wiedemeier et al. (1995), biodegradation rate constants were adapted for use at the Ash Landfill.

The first step in the method was to determine the portion of observed decreases in VOC concentrations that can be attributed to biodegradation, and to determine a biodegradation rate constant. To accomplish this, measured concentrations of VOCs were corrected for the effects of dispersion, dilution from recharge, and sorption. Sodium was used as a conservative tracer to do this because it is not easily adsorbed to soil particles, (i.e., it moves at the same velocity as groundwater), and is not biodegraded. Although sodium and the three volatile compounds of interest (i.e., TCE, cis- and trans-1,2-DCE and VC) do not have the same volatilization properties, this was not considered to be significant enough to exclude sodium from use as a tracer at the site. In fact, during the soil gas survey that was performed at the Ash Landfill, the concentration of the three volatile chlorinated compounds were undetected or very low in areas away from the source area.

According to Wiedemeier et al., "the corrected concentration of a compound is the concentration of the compound that would be expected at one point (B) located downgradient from another point (A) after correcting for the effects of dispersion, dilution from recharge, volatilization, and sorption between points A and B." For this study, the concentrations of the VOCs was corrected using the equation of Weidemeier et al. (1995) and Wilson et al. (1994) as follows:

$$C_{B,corr} = C_B (Na_A/Na_B)$$

where:

- $C_{B,corr}$ = corrected concentration of compound of interest at Point B
- C_B = measured concentration of compound of interest at Point B
- Na_A = measured concentration of sodium at Point A
- Na_B = measured concentration of sodium at Point B.

Six points along a single flow path parallel to the direction of groundwater flow were chosen for comparison of corrected and observed VOC concentrations to assess the effects of dispersion, dilution, and sorption and to determine the biodegradation rate constant. The raw VOC and sodium data for these wells is presented in Table 6-2. The Na-corrected concentrations are also shown in Table 6-3.

A first order biological decay rate can be calculated if it can be shown that the biodegradation is a first order process. A log-linear plot of Na-corrected VOC concentration versus downgradient travel time along the flow path is shown in Figure 6-2. Since the semi-log plot of the data produced a reasonably straight line, there is evidence to suggest that biodegradation along the flow path is approximated by first-order kinetics.

First order decay is described by the relationship:

$$C = C_0 e^{-\lambda t}$$

where: C = contaminant concentration at time t

C_0 = initial contaminant concentration

λ = first order decay constant

Travel time, t, was calculated using the following formula:

$$t = x / v$$

where: t = travel time between two points

x = distance between two points

v = advective groundwater velocity or retarded solute velocity (where applicable)

A first order exponential decay analysis was performed once the travel time between the points were determined and the total VOC concentrations were corrected for the effects of dilution. Exponential decay results were presented with C/C_0 as the ordinate and travel time in years as the abscissa (Figure 6-3). From the exponential decay analysis, the equation of the line of best fit for the data being regressed was obtained from a log-linear plot. It is possible to determine the biodegradation rate constant, since the equation of a straight line is:

TABLE 6-2

**VOC AND SODIUM CONCENTRATIONS MEASURED IN SELECTED
MONITORING WELLS AT THE ASH LANDFILL**

**SENECA ARMY DEPOT ACTIVITY
ASH LANDFILL GROUNDWATER MODEL**

Location	1992		1993		AVERAGE	
	VOCs (µg/L)	Sodium (µg/L)	VOCs (µg/L)	Sodium (µg/L)	VOCs (µg/L)	Sodium (µg/L)
PT-18	11,850	114,000.0	13,740	93,900	12,795	103,950
PT-12	384	33,800.0	2,458	133,000	1,421	83,400
PT-22	180	52,800.0	248	64,900	214	58,850
MW-53	NA	NA	55.0	33,000	55.0	33,000
MW-29	72.0	26,200.0	99.0	25,600	85.5	25,900
MW-56	NA	NA	0.2	19,500	0.2	19,500

Note:

- 1) VOCs = TCE, cis- and trans-1,2-DCE and VC
- 2) NA = not available

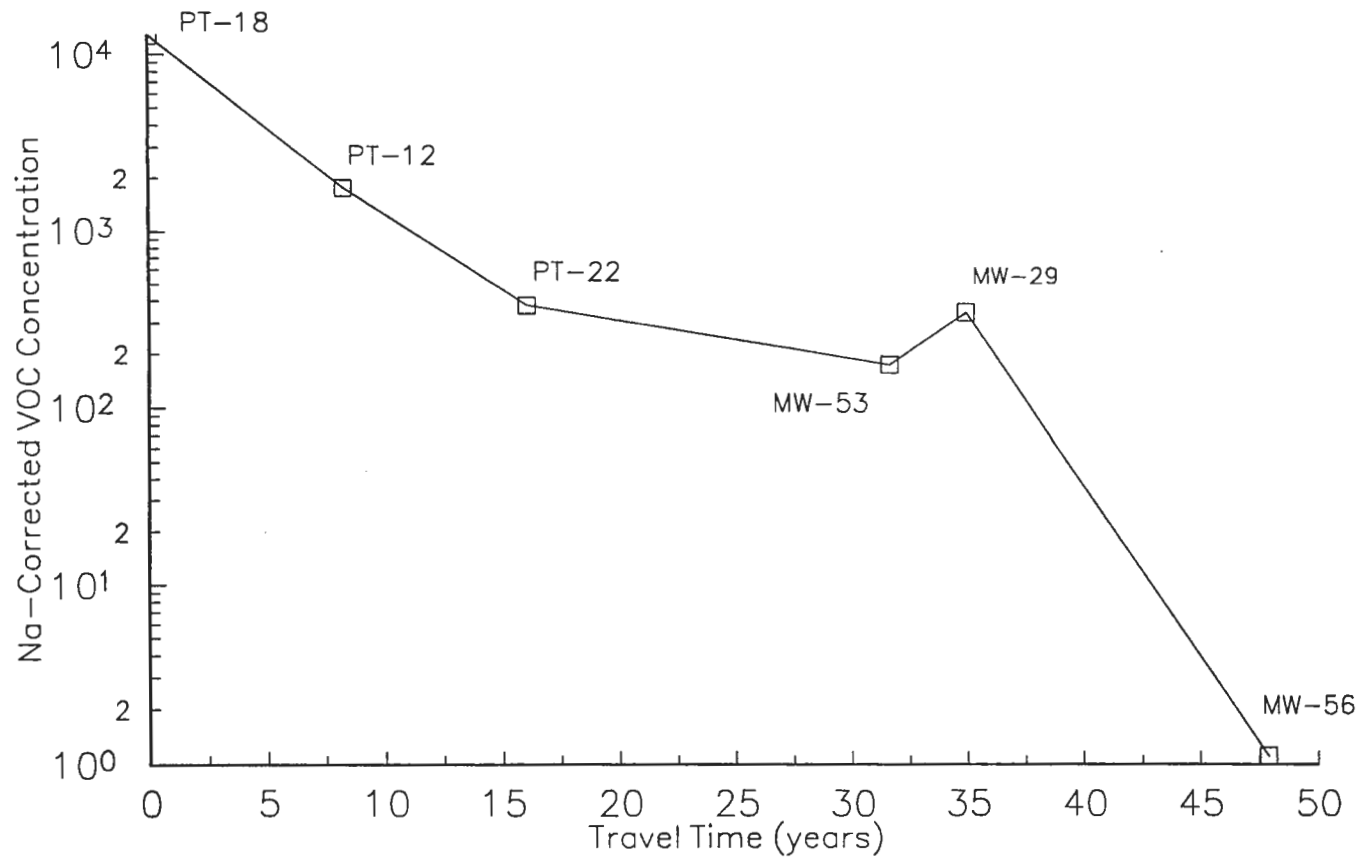
TABLE 6-3
SODIUM-CORRECTED VOC CONCENTRATIONS
AT THE ASH LANDFILL
SENECA ARMY DEPOT ACTIVITY
ASH LANDFILL GROUNDWATER MODEL

Location	Distance Down Gradient (ft)	Travel Time from PT-18 (years as VOCs)	Na-Corrected VOC Concentration (µg/L)	Concentration Ratio (C/Co)
PT-18	0	0	12,795.0	1
PT-12	200	8.22	1,771.1	0.138
PT-22	390	16.03	378.0	0.030
MW-53	770	31.64	173.3	0.014
MW-29	850	34.93	343.2	0.027
MW-56	1,165	47.88	1.1	0.000083

Note:

1. Travel time calculated in years as VOCs (TCE, cis- and trans-1,2-DCE, VC) with a retardation factor of 1.5

Na-Corrected VOC Concentration vs Travel Time



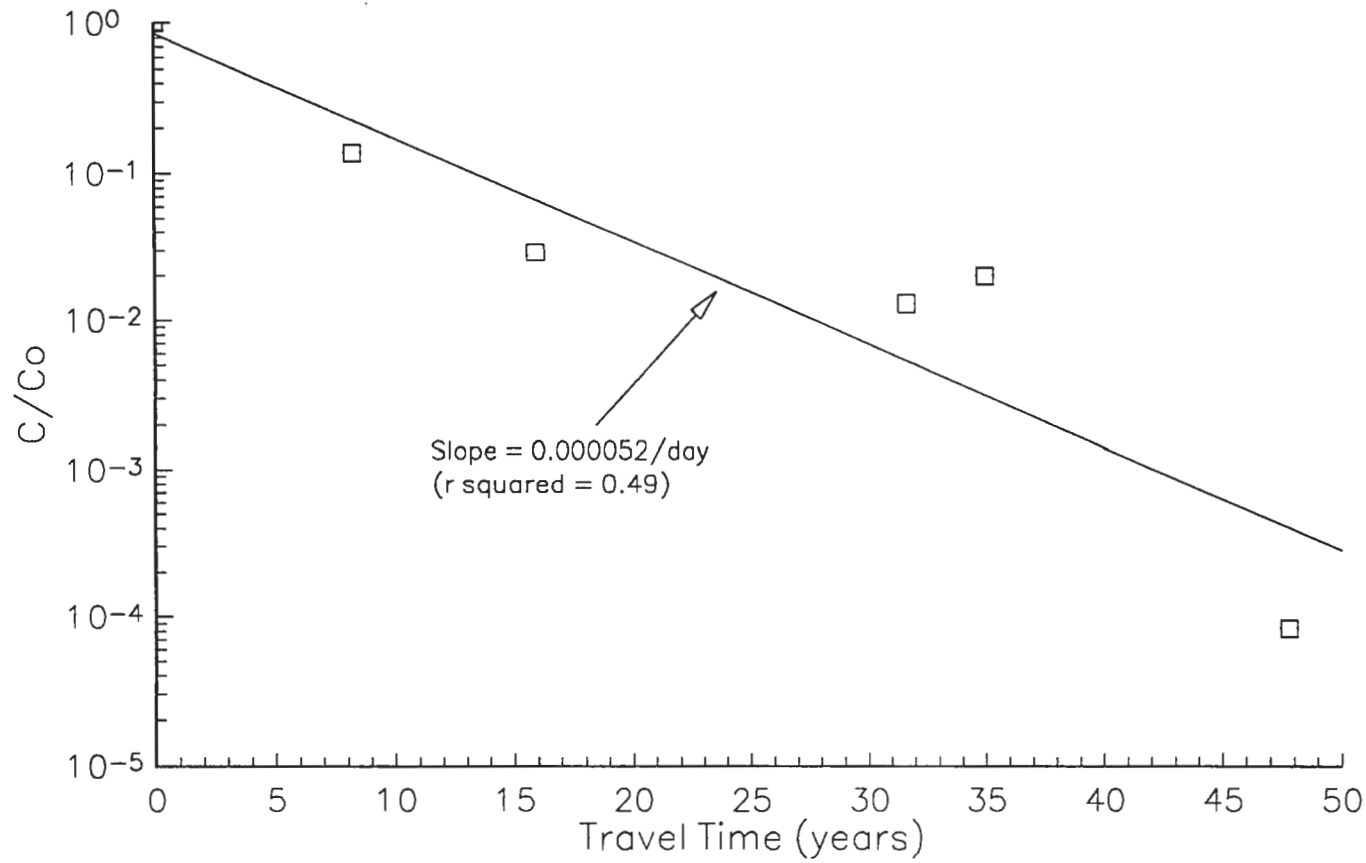
CLIENT/PROJECT TITLE
**SENECA ARMY DEPOT ACTIVITY
 ASH LANDFILL GROUNDWATER MODEL**

DEPT. ENVIRONMENTAL ENGINEERING DWG NO. 726209-01002

**FIGURE 6-2
 Na-CORRECTED
 VOC CONCENTRATIONS VS
 TRAVEL TIME**

SCALE NA DATE OCTOBER 1995

Na-Corrected C/C₀ for VOCs vs Travel Time



CLIENT/PROJECT TITLE
**SENECA ARMY DEPOT ACTIVITY
 ASH LANDFILL GROUNDWATER MODEL**

DEPT. ENVIRONMENTAL ENGINEERING DWG NO. 726209-01002

**FIGURE 6-3
 Na-CORRECTED
 C/C₀ CONCENTRATIONS VS
 TRAVEL TIME**

SCALE NA DATE OCTOBER 1995

$$y = mx + b$$

where: y = y axis value (C_0/C),

b = y intercept,

m = slope of regression line, (biodegradation decay constant) and

x = x axis value, (travel time).

Following the convention of Weidemeier et al. (1995), the first order biodegradation rate constant for the VOCs was calculated as 0.000052/day.

6.4 Model Calibration and Verification

6.4.1 Simulation of Plume from Origin with VOC Source - Scenario 1

The transport model was calibrated by simulating the plume migration from its origin at the two source areas, represented by the concentrations of MW-44 and PT-18, with the reasonable assumption that the release of VOCs occurred between 30 and 40 years ago. This simulation is Scenario 1.

For this simulation, the model used the constant source concentrations in the cells that contained wells MW-44 and PT-18; their respective concentrations as measured during the Ash Landfill RI were 132,000 ug/L and 13,950 ug/L. We have assumed that there has been no degradation of the VOC source material in the soils at these two areas since the time of the release. Two model runs, one to 30 years and one to 50 years, were used to generate the simulated plume data.

To determine the degree of model calibration, the simulated plumes (solid contours) were visually compared to the existing plume (dashed contours) as shown in Figure 6-4. The geometry of the simulated plumes between 30 and 40 years from the release of VOCs best fits the configuration of the existing plume in the till/weathered shale aquifer, layer 1 (Figure 6-4). This geometry was achieved using the best estimate values for the input parameters shown in Table 6-1. The 10 ug/L contour of the simulated plume at 35 and 40 years extends to the fenced SEDA boundary and lower concentrations extend beyond this boundary in a similar fashion to the existing plume.

The configuration of the eastern portion of the simulated plume reflects the two source areas of elevated VOCs in soil, which is supported by the results of the soil gas surveys in this area (Parsons ES, 1994a).

30 YEARS FROM T=0

35 YEARS FROM T=0

40 YEARS FROM T=0



C:\ACAD\SENECA\ASHMODEL\SLAY1.DWG

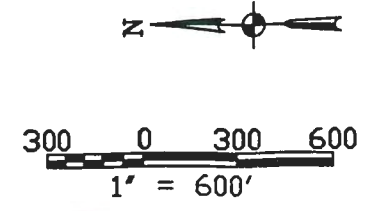
P PARSONS
PARSONS ENGINEERING SCIENCE, INC.

CLIENT/PROJECT TITLE
**SENECA ARMY DEPOT ACTIVITY
 ASH LANDFILL GROUNDWATER MODEL**

DEPT. ENVIRONMENTAL ENGINEERING Dwg. No.

FIGURE 6-4
 SIMULATION OF VOC PLUME IN LAYER 1 FROM ORIGIN
 (t=0) TO 30,35, AND 40 YEARS WITH CONSTANT
 SOURCE (SCENARIO 1)

SCALE 1" = 600' DATE october 1995 REV A



The model is believed to be conservative and predicts higher concentrations of VOCS in layers 2 and 3 than were observed in the few bedrock wells located near the source areas (MW-49D, MW-50D and PT-21) (Figures 6-5 and 6-6).

The mass balance discrepancies for the two model runs that were used for the Scenario 1 simulation are shown in Figures 6-7 and 6-8. For the model run to 30 years (Figure 6-7) early mass balance discrepancies of up to 60 % are quickly reduced to less than 6 % and as the simulation continued the discrepancy was held at approximately 6 %. For the model run to 50 years (Figure 6-8) the mass balance discrepancies are approximately the same as for the 30 year model run, however, beyond 30 years they increase slightly to approximately 8 %.

6.5 Transport Model Predictions

6.5.1 Future Plume Migration with VOC Source - Scenario 2

For Scenario 2, the future migration of the existing plume prior to the removal of the VOC source soils was evaluated.

For this simulation, as in Scenario 1, the model used the constant source concentrations in the cells that contained the monitoring wells MW-44 and PT-18. Again, the use of these concentrations assumes that there has been no degradation of the VOC source material in the soils at these two areas since the time of the release.

Snapshots of the simulated plume at 30, 50, and 100 years from the present are shown in Figures 6-9, 6-10 and 6-11. At 30 years the model predicts that the plume in layer 1 will have migrated off-site, with the 10 ug/L contour approximately 700 feet west of the SEDA boundary (Figure 6-9). At 50 years the 10 ug/L contour will reach to approximately 1000 feet beyond this boundary and the 100 and 1,000 ug/L contours will also extend beyond the boundary (Figure 6-9). By 100 years from the present the 10 ug/L contour will have reached the farmhouse and significant areas west of the SEDA boundary will have been impacted by concentrations of VOCs greater than 100 and 1,000 ug/L (Figure 6-9). By this time the model predicts that the plume will have more than doubled in length compared to its existing configuration.

Not unexpectedly, the concentrations predicted for layers 2 and 3 are smaller than those for the layer 1 (Figures 6-10 and 6-11). However, they are likely to reflect a worst-case impact because

30 YEARS FROM T=0

35 YEARS FROM T=0

40 YEARS FROM T=0



CAACAD\SENECA\ASHMODEL\SL1\AY2.DWG

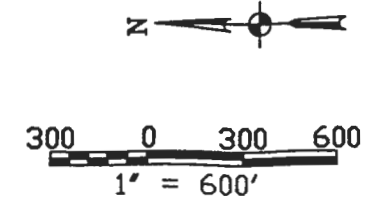
P PARSONS
PARSONS ENGINEERING SCIENCE, INC.

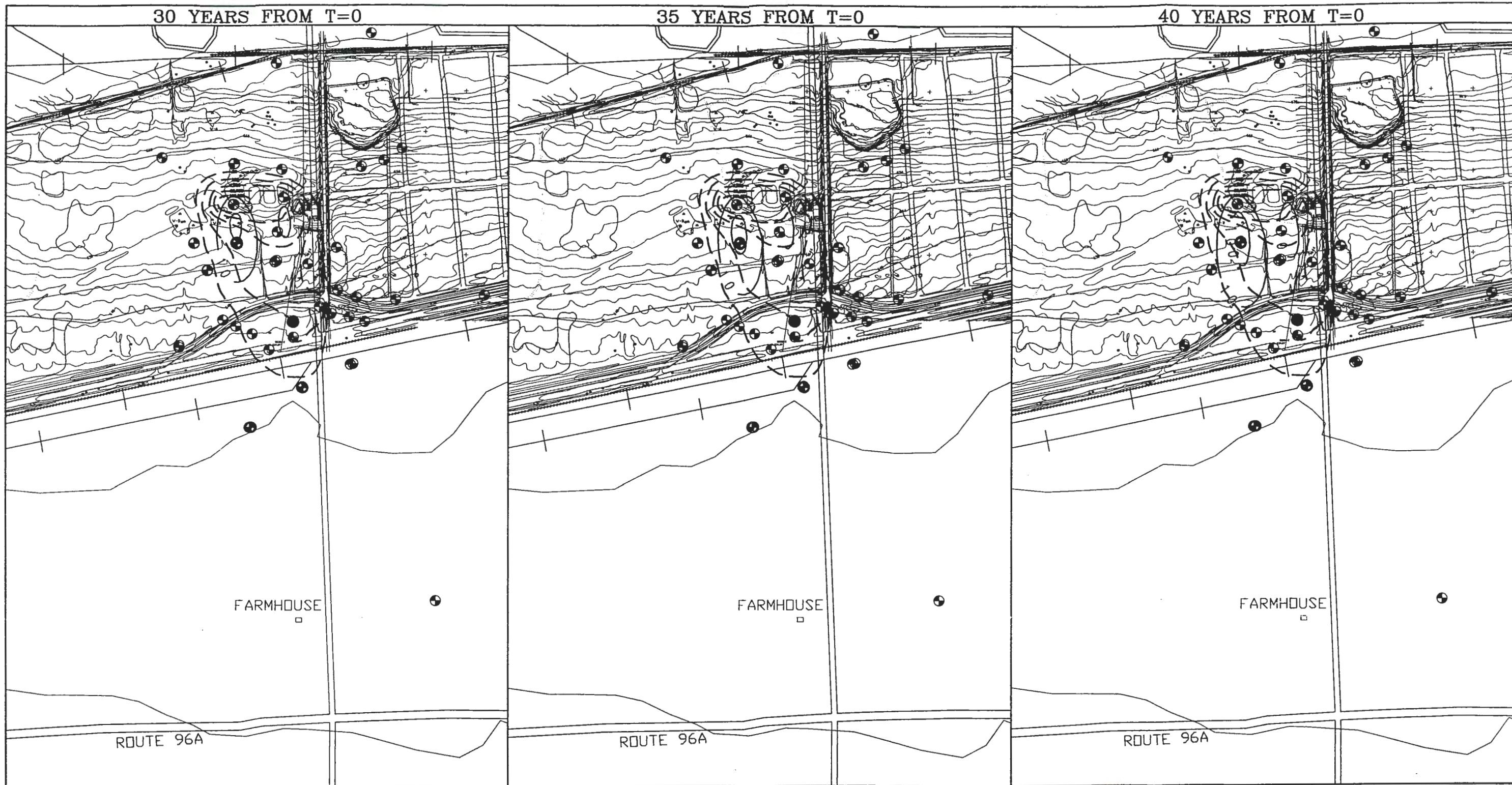
CLIENT/PROJECT TITLE
**SENECA ARMY DEPOT ACTIVITY
 ASH LANDFILL GROUNDWATER MODEL**

DEPT. ENVIRONMENTAL ENGINEERING Dwg. No.

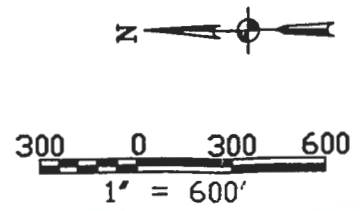
FIGURE 6-5
 SIMULATION OF VOC PLUME IN LAYER 2 FROM ORIGIN
 (t=0) TO 30,35, AND 40 YEARS WITH CONSTANT
 SOURCE (SCENARIO 1)

SCALE 1" = 800' DATE OCTOBER 1995 REV A



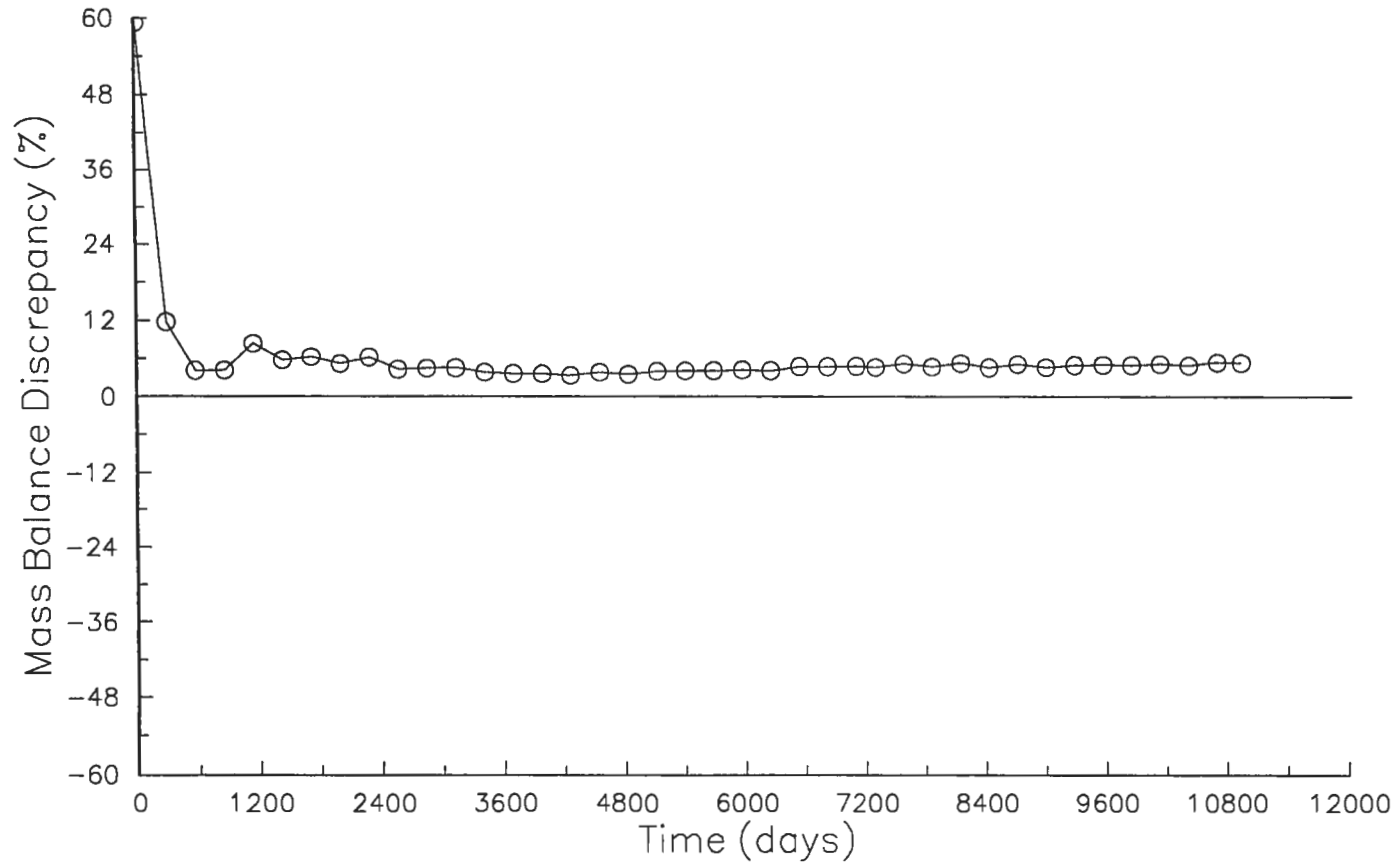


C:\ACAD\SENECA\ASHMODEL\SLAY3.DWG



PARSONS	
PARSONS ENGINEERING SCIENCE, INC.	
CLIENT/PROJECT TITLE	
SENECA ARMY DEPOT ACTIVITY ASH LANDFILL GROUNDWATER MODEL	
DEPT. ENVIRONMENTAL ENGINEERING	Dwg. No.
FIGURE 6-6	
SIMULATION OF VOC PLUME IN LAYER 3 FROM ORIGIN (t=0) TO 30, 35, AND 40 YEARS WITH CONSTANT SOURCE (SCENARIO 1)	
SCALE 1" = 600'	DATE OCTOBER 1995
	REV A

Scenario 1



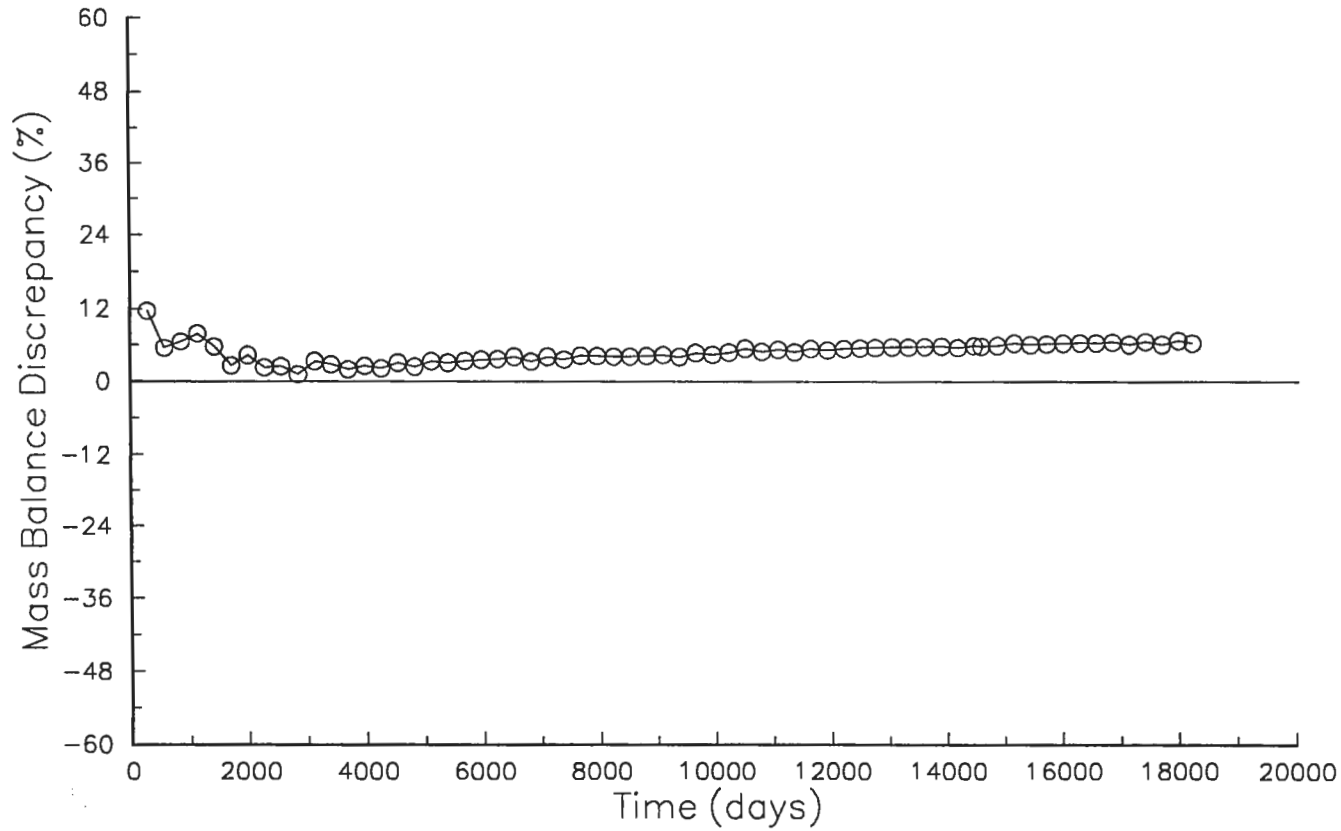
CLIENT/PROJECT TITLE
**SENECA ARMY DEPOT ACTIVITY
 ASH LANDFILL GROUNDWATER MODEL**

DEPT. ENVIRONMENTAL ENGINEERING DWG. NO. 726209-01002

**FIGURE 6-7
 MASS BALANCE
 DISCREPANCY TO
 30 YEARS (SCENARIO 1)**

SCALE NA DATE OCTOBER 1995

Scenario 1



CLIENT/PROJECT TITLE
**SENECA ARMY DEPOT ACTIVITY
ASH LANDFILL GROUNDWATER MODEL**

DEPT. ENVIRONMENTAL ENGINEERING DIAG NO. 726209-01002

**FIGURE 6-8
MASS BALANCE
DISCREPANCY TO
50 YEARS (SCENARIO 1)**

30 YEARS FROM PRESENT

50 YEARS FROM PRESENT

100 YEARS FROM PRESENT



C:\ACAD\SENECA\ASHMODEL\SLAY1.DWG



300 0 300 600
1" = 600'

P PARSONS	
PARSONS ENGINEERING SCIENCE, INC.	
CLIENT/PROJECT TITLE	
SENECA ARMY DEPOT ACTIVITY ASH LANDFILL GROUNDWATER MODEL	
DEPT.	DWG No.
ENVIRONMENTAL ENGINEERING	
FIGURE 6-9	
SIMULATION OF EXISTING VOC PLUME IN LAYER 1 WITH CONSTANT SOURCE AT 30.50. AND 100 YEARS FROM THE PRESENT (SCENARIO 2)	
SCALE	DATE
1" = 600'	OCTOBER 1995
REV	A

30 YEARS FROM PRESENT

50 YEARS FROM PRESENT

100 YEARS FROM PRESENT



C:\ACAD\SENECA\ASHMODEL\AS2LAY2.DWG

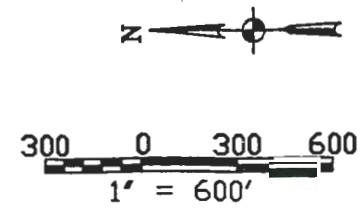
P PARSONS
PARSONS ENGINEERING SCIENCE, INC.

CLIENT/PROJECT TITLE
**SENECA ARMY DEPOT ACTIVITY
 ASH LANDFILL GROUNDWATER MODEL**

DEPT. ENVIRONMENTAL ENGINEERING Dwg. No.

FIGURE 6-10
 SIMULATION OF EXISTING VOC PLUME IN LAYER 2 WITH
 CONSTANT SOURCE AT 30.50. AND 100 YEARS FROM
 THE PRESENT (SCENARIO 2)

SCALE 1" = 600' DATE OCTOBER 1995 REV A



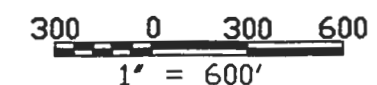
30 YEARS FROM PRESENT

50 YEARS FROM PRESENT

100 YEARS FROM PRESENT



C:\ACAD\SENECA\ASHMODEL\SLAY3.DWG



P PARSONS	
PARSONS ENGINEERING SCIENCE, INC.	
CLIENT/PROJECT TITLE	
SENECA ARMY DEPOT ACTIVITY ASH LANDFILL GROUNDWATER MODEL	
DEPT.	Dwg. No.
ENVIRONMENTAL ENGINEERING	
FIGURE 6-11	
SIMULATION OF EXISTING VOC PLUME IN LAYER 3 WITH CONSTANT SOURCE AT 30.50. AND 100 YEARS FROM THE PRESENT (SCENARIO 2)	
SCALE	DATE
1" = 600'	OCTOBER 1986
	REV
	A

the calibration run in Scenario 1 indicated that concentrations in layer 2 and 3 are higher than those observed in bedrock wells.

The mass balance discrepancy for the model run that was used for the Scenario 2 simulation is shown in Figure 6-12. The model run is for 100 years and initial instability of the mass balance is stabilized at approximately 8 % by the end of the model run.

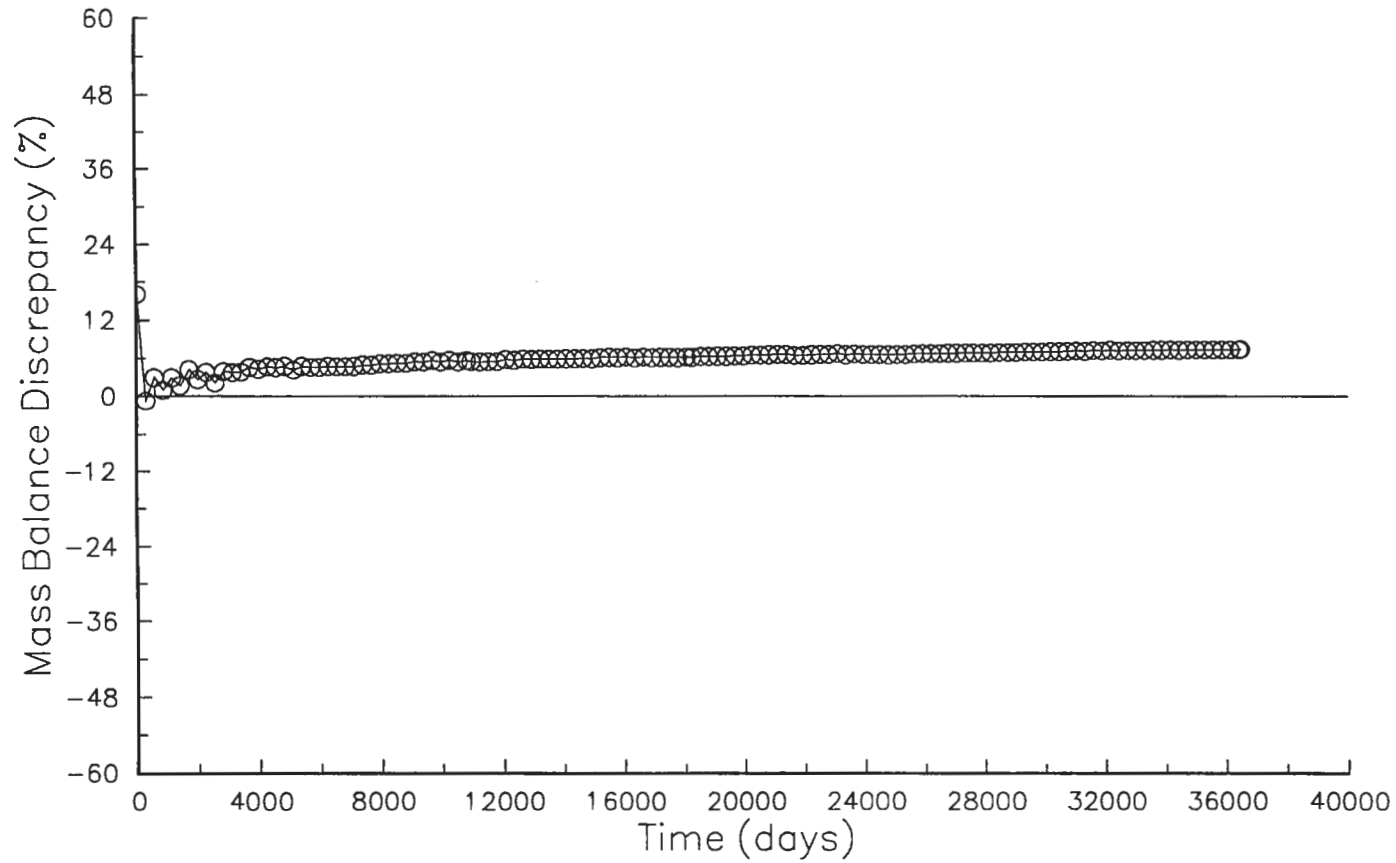
6.5.2 Future Plume Migration without VOC Source - Scenario 3

For Scenario 3, the future migration of the plume after the removal of the VOC source soils was evaluated. The source soils for VOCs were removed as part of a removal action at the Ash Landfill (Parsons ES, 1994b). Groundwater in the vicinity of the source soils was also removed during this remedial event.

For this simulation the model used starting concentrations in groundwater based on groundwater sampling performed after the removal action. The post-remediation starting concentrations were based on a maximum concentration of 23,000 µg/L measured at PT-18. In addition, there was no constant source for the VOCs in this scenario (Appendix F).

To allow a comparison to Scenario 2 results, snapshots of the simulated plume at 30, 50 and 100 years from the present for Scenario 3 are shown in Figures 6-13, 6-14, and 6-15. The most obvious difference between the plumes simulated in Scenarios 2 and 3 is that both the size (i.e., length) and the concentrations were greatly reduced in Scenario 3. At 30 years the plume in layer 1 for Scenario 3 does not look significantly different from the plume predicted in Scenario 2 (Figure 6-13 and 6-9). Both figures show the 10 ug/L contour hundreds of feet beyond the SEDA boundary, however, the maximum concentration within the plume is greatly reduced in Scenario 3; this maximum occurs approximately 500 feet west of the former source areas at the Ash Landfill. By 50 years the plume is significantly shortened compared to its pre-remediation configuration (Scenario 2) and the 10 ug/L contour is approximately 700 feet beyond the SEDA boundary compared to approximately 1,000 feet under Scenario 2. Additionally, the maximum concentration is less than 1,000 ug/L. Comparison of the plumes simulated under Scenarios 2 and 3 at 100 years provides the most contrast. With the source removed (Scenario 3), the plume is reduced to a relatively small oval shape with concentrations mostly less than 100 ug/L and in only a small area are concentrations predicted to exceed 100 ug/L. At this time the plume is roughly 1,200 feet long compared to a length of almost 3,000 feet under Scenario 2. Also, under Scenario 3 this 10 ug/L contour has not reached the farmhouse as it was predicted to do in Scenario 2.

Scenario 2



CLIENT/PROJECT TITLE
**SENECA ARMY DEPOT ACTIVITY
 ASH LANDFILL GROUNDWATER MODEL**

DATE: ENVIRONMENTAL ENGINEERING DWG NO: 726209-01002

**FIGURE 6-12
 MASS BALANCE
 DISCREPANCY TO
 100 YEARS (SCENARIO 2)**

SCALE: NA DATE: OCTOBER 1995

30 YEARS FROM PRESENT

50 YEARS FROM PRESENT

100 YEARS FROM PRESENT



C:\ACAD\SENECA\ASHMODEL\30LAY1.DWG

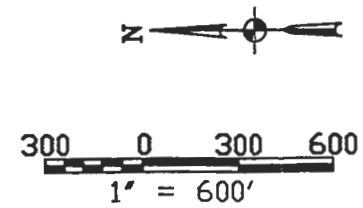
P PARSONS
 PARSONS ENGINEERING SCIENCE, INC.

CLIENT/PROJECT TITLE
 SENECA ARMY DEPOT ACTIVITY
 ASH LANDFILL GROUNDWATER MODEL

DEPT. ENVIRONMENTAL ENGINEERING Dwg No.

FIGURE 6-13
 SIMULATION OF EXISTING VOC PLUME IN LAYER 1
 AFTER SOURCE REMOVAL AT 30,50, AND 100 YEARS
 FROM THE PRESENT (SCENARIO 3)

SCALE 1" = 600' DATE SEPTEMBER 1995 REV. A



30 YEARS FROM PRESENT

50 YEARS FROM PRESENT

100 YEARS FROM PRESENT



C:\ACAD\SENECA\ASHMODEL\SLAY2.DWG

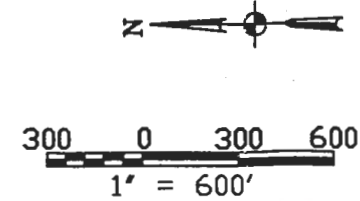
P PARSONS
 PARSONS ENGINEERING SCIENCE, INC.

CLIENT/PROJECT TITLE
 SENECA ARMY DEPOT ACTIVITY
 ASH LANDFILL GROUNDWATER MODEL

DEPT. ENVIRONMENTAL ENGINEERING Dwg. No.

FIGURE 6-14
 SIMULATION OF EXISTING VOC PLUME IN LAYER 2
 AFTER SOURCE REMOVAL AT 30,50, AND 100 YEARS
 FROM THE PRESENT (SCENARIO 3)

SCALE 1" = 600' DATE OCTOBER 1996 REV A



30 YEARS FROM PRESENT

50 YEARS FROM PRESENT

100 YEARS FROM PRESENT



C:\ACAD\SENECA\ASHMODEL\31LAY3.DWG

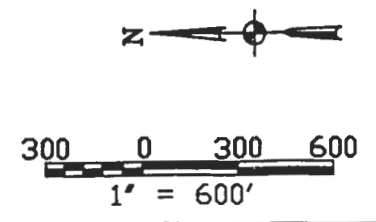
P PARSONS
PARSONS ENGINEERING SCIENCE, INC.

CLIENT/PROJECT TITLE
**SENECA ARMY DEPOT ACTIVITY
 ASH LANDFILL GROUNDWATER MODEL**

DEPT. ENVIRONMENTAL ENGINEERING Dwg. No.

FIGURE 6-15
 SIMULATION OF EXISTING VOC PLUME IN LAYER 3
 AFTER SOURCE REMOVAL AT 30,50, AND 100 YEARS
 FROM THE PRESENT (SCENARIO 3)

SCALE 1" = 600' DATE OCTOBER 1985 REV A



In layers 2 and 3 the model predicts that the plume sizes and concentrations in Scenario 3 will be significantly less than shown under Scenario 2 (Figures 6-14 and 6-15). In layer 2, the plume remains within the SEDA boundary at 30 years and concentrations are less than 1,000 ug/L (Figure 6-14). At 50 years the plume is only slightly larger than at 30 years but the model predicts that it will migrate beyond the SEDA boundary. By 100 years the concentrations are greatly reduced (less than 100 ug/L) and the plume is mostly off of SEDA, with the 10 ug/L contour 500 feet west of the farmhouse. In layer 3, the plume is reduced to a small area with concentrations below 100 ug/L at both 30 and 50 years, and it has not migrated off of SEDA (Figure 6-15). At 100 years the plume is represented by an even smaller area (approximately 100 feet by 200 feet) defined by the 10 ug/L contour (Figure 6-15).

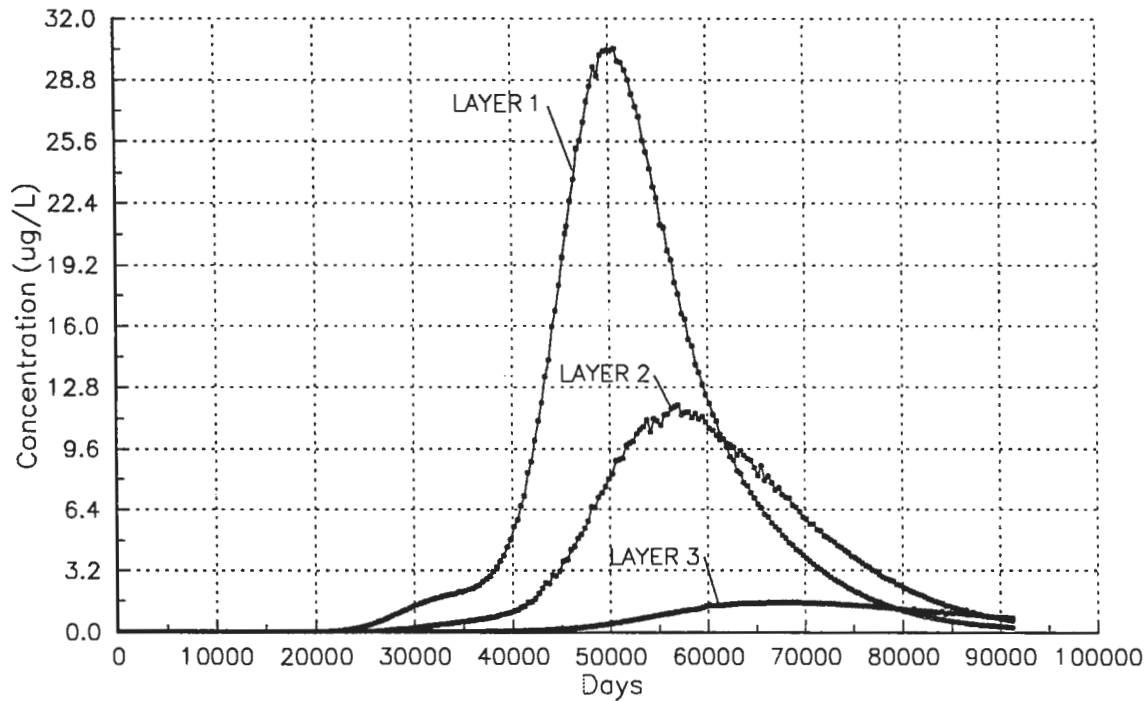
For Scenario 3, an X-Y plot of concentration versus time for the model cells in layers 1, 2, and 3 that corresponds to the location of the farmhouse were made to show the nature of the potential impacts at the farmhouse (Figure 6-16). The model predicts that the groundwater in layer 1 will be impacted by the dispersion front of the plume after approximately 70 years and that a maximum concentration of 30 ug/L will occur at approximately 137 years (Figure 6-16). In layer 2 the groundwater will be impacted after approximately 95 years with a maximum concentration of 11 ug/L at 150 years (Figure 6-16). Lastly, for layer 3, the first impact is at approximately 130 years with a maximum concentration of 1.5 ug/L predicted at 180 years (Figure 6-16).

The mass balance discrepancy for Scenario 3 shows initial instability followed by stabilization at approximately 4 % for the model run to 100 years (Figure 6-17).

6.6 Sensitivity Analysis

A sensitivity analysis was performed after the transport model was calibrated. The purpose of the sensitivity analysis was to determine how sensitive the model is to variations or uncertainty in the degradation constant rate (K) parameter. Thus, during the sensitivity analysis the calibrated value for the degradation constant rate ($K = 0.00005/\text{day}$) was systematically changed within a wide range of values over many model runs that simulated plume migration to 100 years. The sensitivity analysis was performed by changing the value of the calibrated K up to \pm one order of magnitude and the effects on the maximum concentration observed at selected monitoring points (i.e., cells) was evaluated.

VOC CONCENTRATIONS PREDICTED AT THE FARMHOUSE
Scenario 3



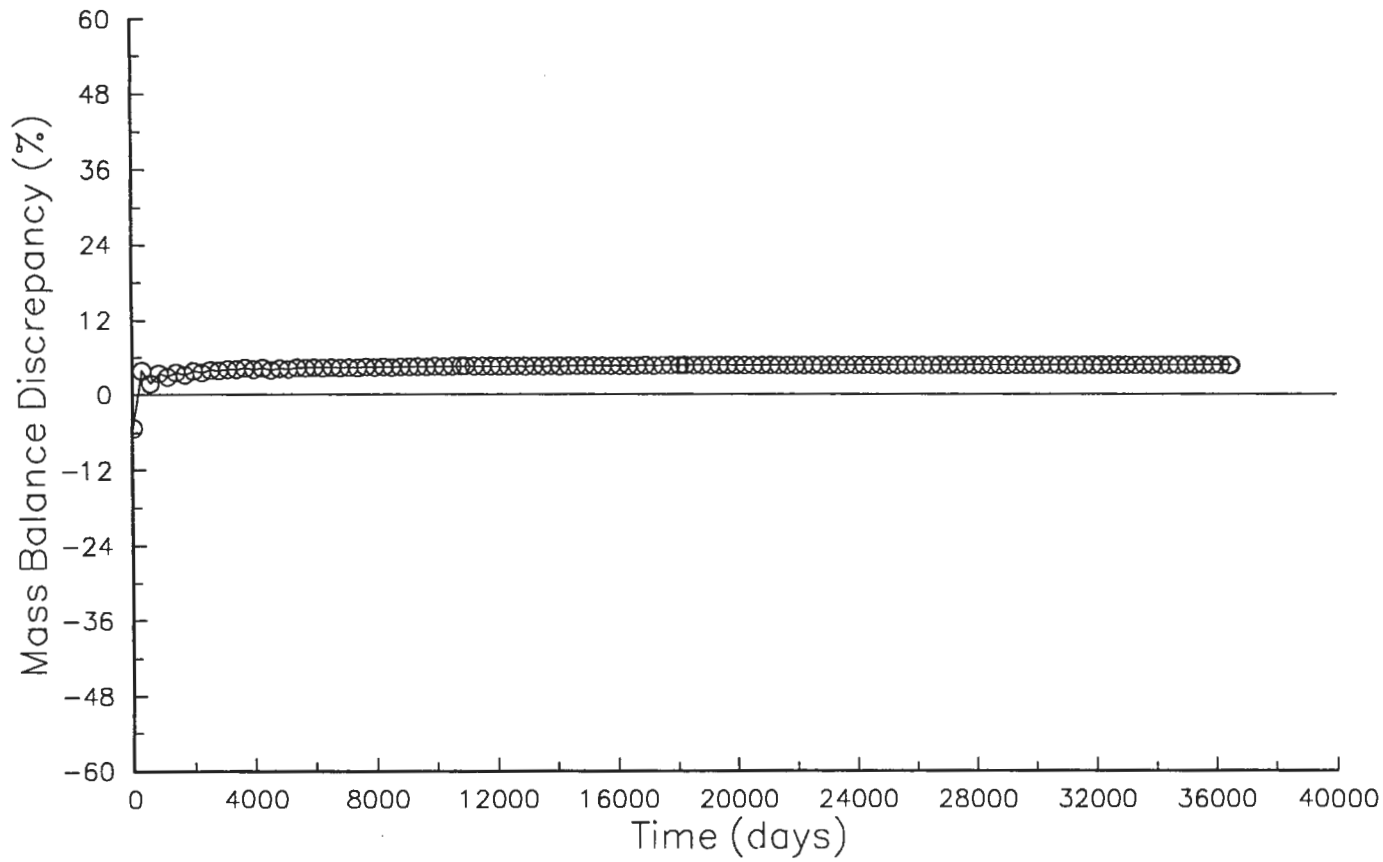
CLIENT/PROJECT TITLE
**SENECA ARMY DEPOT ACTIVITY
ASH LANDFILL GROUNDWATER MODEL**

DEPT. ENVIRONMENTAL ENGINEERING DWG. NO. 726209-01002

**FIGURE 6-16
VOC CONCENTRATIONS PREDICTED
AT THE FARMHOUSE
(SCENARIO 3)**

SCALE NA DATE OCTOBER 1995

Scenario 3



CLIENT/PROJECT TITLE
**SENECA ARMY DEPOT ACTIVITY
ASH LANDFILL GROUNDWATER MODEL**

DEPT. ENVIRONMENTAL ENGINEERING DWG NO. 726209-01002

**FIGURE 6-17
MASS BALANCE
DISCREPANCY TO
100 YEARS (SCENARIO 3)**

Four cells along the longitudinal axis of the plume were selected as points at which the concentration data was saved over time by the model. The cell coordinates of the monitoring points are as follows:

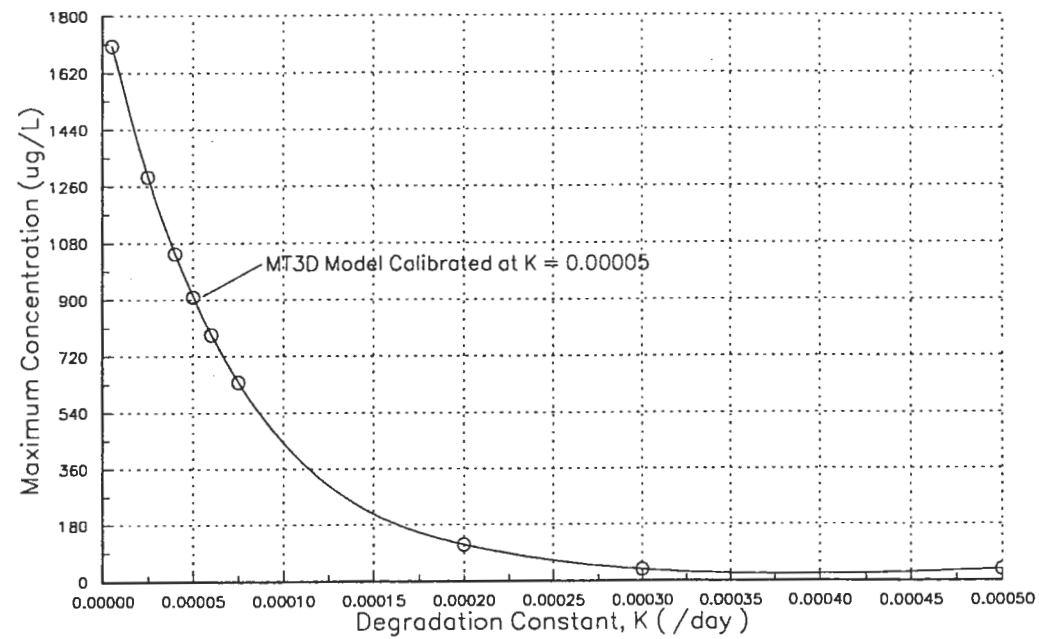
1. Layer 1, row 102, column 38 (within existing plume)
2. Layer 1, row 131, column 40
3. Layer 1, row 155, column 42
4. Layer 1, row 177, column 42 (at farmhouse).

The locations of the cell coordinates within the model grid can be seen on Figure 5-4.

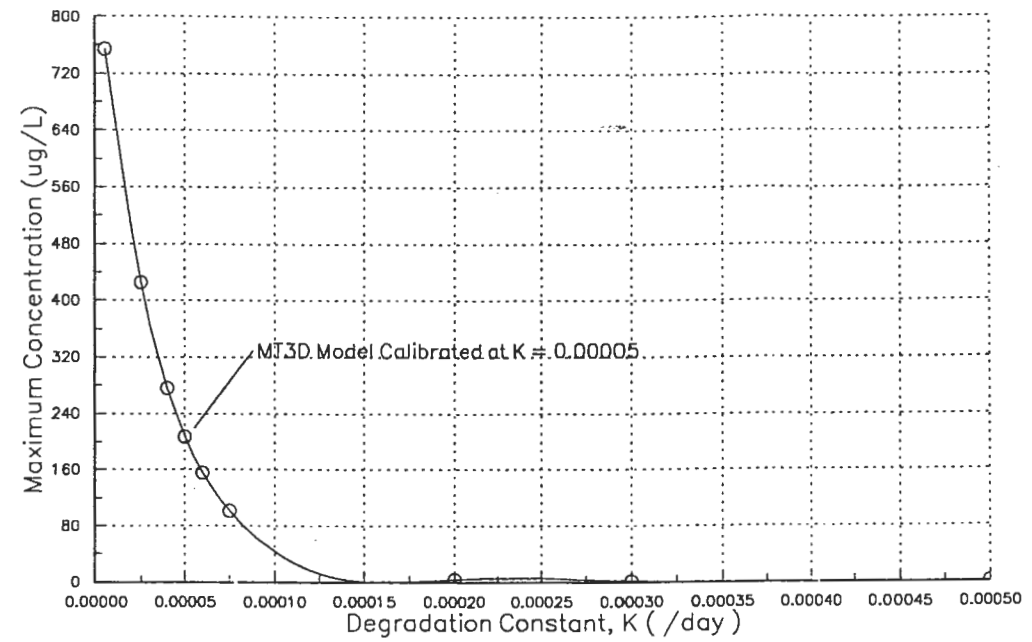
The results of the sensitivity analysis runs are shown of Figure 6-18. These x-y plots show how the maximum concentration predicted at a monitoring point changes with differing K values; the data points were connected using a spline function. Not unexpectedly, all of the plots exhibit a trend where the maximum concentration increases with decreasing K values, and at higher end K values the maximum concentrations are greatly reduced. K values that are several times the calibrated value result in concentrations that are zero or approach zero. Thus, as K values become increasingly small, the maximum concentrations are expected to be more influenced by advective processes.

As a comparison, the K value obtained from the literature for the ODAST model is not believed to be as representative of site conditions as the new value calculated for the more complex MT3D model. A K value of 0.00005/day was calculated for the model using on-site chemical data and the MT3D transport model was calibrated in Scenario 1 using this value. This is different from the literature value of 0.00062/day used in the ODAST one dimensional transport model run. Using a K value one order of magnitude greater than the calibrated value, as was used in the ODAST model, results in significant degradation of VOCs to nearly zero at the monitoring point within the existing plume, and to zero at the monitoring points downgradient of the existing plume after 150 years (Figure 6-18). This would support the preliminary conclusion reached after running the ODAST model that the plume had achieved a steady-state condition. However, the MT3D transport model could not be calibrated using a K value that approached 0.00062/day; lending support to the calculated K value of 0.00005/day used in this study.

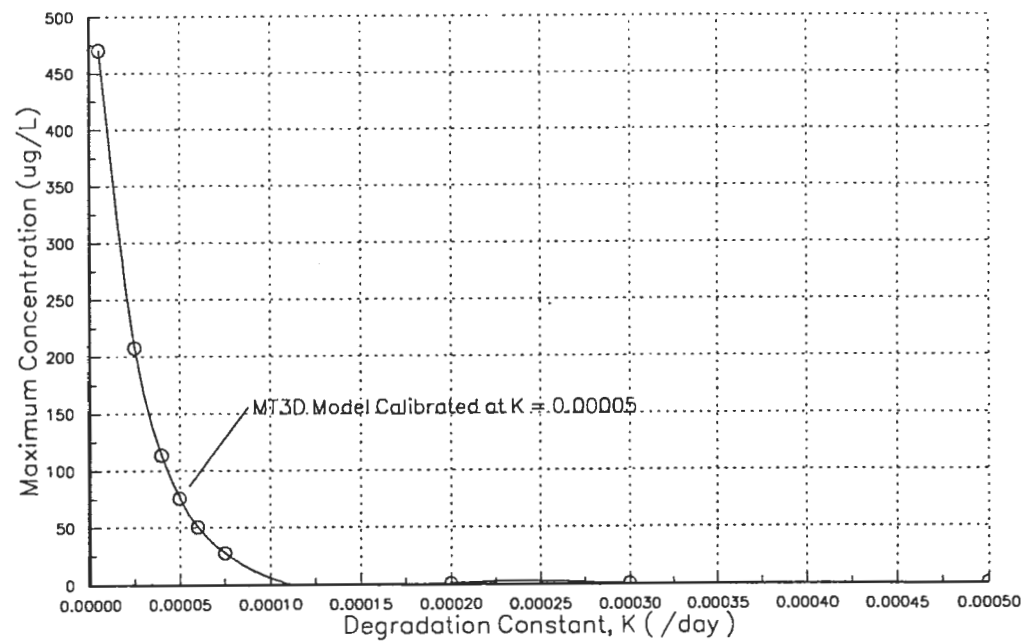
Cell: Layer 1, Row 102, Column 38
Scenario 3



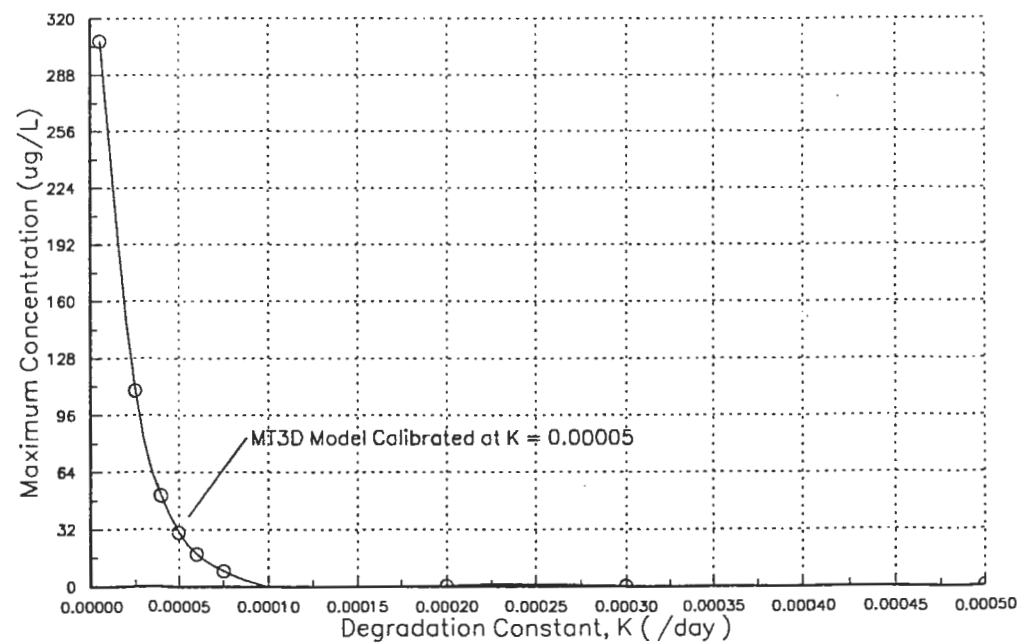
Cell: Layer 1, Row 131, Column 40
Scenario 3



Cell: Layer 1, Row 155, Column 42
Scenario 3



Cell: Layer 1, Row 177, Column 42
Scenario 3



PARSONS
PARSONS ENGINEERING SCIENCE, INC.

CLIENT/PROJECT TITLE
**SENECA ARMY DEPOT ACTIVITY
ASH LANDFILL GROUNDWATER MODEL**

DEPT. ENVIRONMENTAL ENGINEERING DWG NO. 726209-01002

FIGURE 6-18
PLOTS SHOWING THE SENSITIVITY OF
THE TRANSPORT MODEL TO THE
DEGRADATION CONSTANT, K

SCALE: NA DATE: OCTOBER 1995

7.0 SUMMARY AND CONCLUSIONS

Groundwater flow and contaminant transport modeling were combined to simulate the migration of a VOC plume under several scenarios within a steady-state flow system at the Ash Landfill and surrounding area. The primary goal of the modeling was to evaluate the potential for future impacts to off-site farmhouse wells by VOCs migrating from the Ash Landfill under pre- and post-VOC source removal scenarios.

The groundwater flow model consisted of a flow system defined by three model layers, layer 1 for the till/weathered shale and layers 2 and 3 for the competent shale. The MODFLOW model simulated a groundwater flow system defined by a constant head boundary at Seneca Lake, a groundwater divide no flow boundary between Seneca and Cayuga lakes, and streamline no flow boundaries along the northern and southern sides of the model. An important aspect of the groundwater flow system near the Ash Landfill is that much of the water that enters the system via precipitation is returned to the atmosphere through a combination of evapotranspiration and capillary rise in the fine-grained till. Thus, the net recharge rate was a significant factor affecting the head calculated by the MODFLOW model.

Head and flow data from the calibrated flow model were incorporated into the MT3D contaminant transport model to simulate the migration of the VOC plume under three scenarios. Under Scenario 1 the transport model was calibrated using the existing plume as a basis of comparison. The plume was simulated from the time of the release ($t = 0$) to 50 years with two constant sources of VOCs in the Ash Landfill. The results indicate that the simulated concentrations in layer 1 matched the existing plume configuration at approximately 35 years after the time of the release. VOCs concentrations in layers 2 and 3 were found to be higher than those measured in nearby bedrock wells and thus the model is expected to represent an over estimation scenario for these layers.

Scenario 2 is an extension of Scenario 1 in which the model was run for a time frame of 100 years with the same source term as Scenario 1.

Under Scenario 3 the constant source of VOCs was removed from the model to reflect the removal action performed at the Ash Landfill in the Spring of 1995. As expected, this significantly reduced the size (i.e., lengths) and concentration in the plume over time when compared to Scenario 2. Degradation of the existing groundwater plume was likely occurring based upon the measured concentrations of breakdown products in downgradient wells. This degradation rate was quantified for use in the MT3D model to support the hypothesis that, combined with source removal, the indigenous microbial community was capable of eliminating the remaining plume prior to the plume reaching any off-site receptors. Parsons ES was able to provide supporting information that the

conditions at the site are favorable for biotic reductive dechlorination, although the conditions are not strongly favorable. In fact, the degradation rate calculated for use in the model is slow and consistent with the supporting site data. Under this scenario in layer 1, the plume reached the farmhouse in 70 years with a maximum concentration of 30 ug/L at 137 years. In layers 2 and 3 the plume was predicted to reach the farmhouse in 95 and 150 years, respectively.

Therefore, based on the contaminant transport simulations, the removal of VOC source soils at the Ash Landfill reduced the size and VOC concentrations in the plume as it moves west from the Ash Landfill but did not eliminate the plume from reaching the farmhouse.

8.0 REFERENCES

- American Geophysical Union, 1984. *Groundwater Transport: Handbook of Mathematical Models*, pp. 5-22.
- Anderson, M.P., 1979 "Using Models to Simulate the Movement of Contaminants through Groundwater Flow System." *CRC Critical Reviews in Environmental Control V9*, pp 97-156.
- Anderson, M.P. and Woessner, W.W., 1992, *Applied Groundwater Modeling, Simulation of Flow and Advective Transport*, Academic Press, San Diego, CA, 381 pp.
- Bouwer H. and Rice R.C., 1976, A Slug Test for Determining Hydraulic Conductivity of Unconfined Aquifers with Completely or Partially Penetrating Wells, *Water Resources Research*, Vol. 12, No. 3 pp. 423-428.
- Brett, C.E., Dick, V.B, Baird, G.C., 1991, "Comparative Taphonomy and Paleocology of Middle Devonian Dark Gray and Black Shale Facies from Western New York;" in eds., Landing, E.L. and Brett, C.E., *Dynamic Stratigraphy and Depositional Environments of the Hamilton Group (Middle Devonian) in New York State, Part II, New York State Museum Bulletin Number 469*. pp. 5-36.
- Davis, Stanley N, and Roger J.M. DeWiest, 1966. *Hydrogeology*. John Wiley and Sons, Inc., New York.
- de Marsily, Ghislain, 1986. *Quantitative Hydrogeology*, Academic Press, Inc., Austin.
- Demenico, P.A. and Schwartz, F.W., 1990, *Physical and Chemical Hydrogeology*, John Wiley & Sons, New York, NY 824 pp.
- Environmental Progress*, "In Situ Biodegradation of TCE Contaminated Groundwater." Vol. 9, No. 3, August, 1990.
- Fetter, C.W. Jr., 1980. *Applied Hydrogeology*. Charles E. Merrill Publishing Co., Columbus, Ohio
- Freeze, R.A. and Cherry, J.A., 1979. *Groundwater*, Prentice-Hall, Inc. Englewood Cliffs, New Jersey 07632, 604 pp.
- Gray, L.M., 1991, "Paleocology, Origin, and Significance of a Shell-Rich Bed in the Lowermost Part of the Ludlowville Formation (Middle Peronian, Central New York)," in eds. Landing, E.L. and Brett, C.E., *Dynamic Stratigraphy and Depositional Environments of the Hamilton Group (Middle Devonian) in New York State, Part II, New York State Museum Bulletin 469*, p.93-105.

- Groundwater*. "Extraction of TCE-Contaminated Groundwater by Subsurface Drains and a Pumping Well", vol. 28, no. 1, January-February 1990.
- Harte, Philip, T., 1994, Comparison of Vertical Discretization Techniques in Finite Difference Models of Groundwater Flow Example from a Hypothetical New England Setting, U.S. Geological Survey Open-File Report 94-343, 25 pp.
- Hendry, M.J., 1988. "Hydrogeology of Clay Till in a Prairie Region of Canada." *Groundwater*, Vol. 26, No. 5, September-October.
- Houlsby, A.C., 1976. "Routine Interpretation of the Lugeon Water-Test." *Quarterly Journal of Engineering Geology*. Vol. 9, pp. 303-313.
- Jones, LaDon, Tracy Lemar, and Chin-Ta Tsai, 1992. "Results of Two Pumping Tests in Wisconsin Age Weathered Till in Iowa." *Groundwater*, Vol 30, No. 4, July-August.
- Keller, C.K., G. Van Der Kamp, and J.A. Cherry, 1988. "Hydrogeology of Two Saskatchewan Tills, I. Fractures, Bulk Permeability, and Spatial Variability of Downward Flow." *Journal of Hydrology*, 101:97-121.
- LaSala, A.M. Jr., 1968, Groundwater Resources of the Erie-Niagara Basin, New York: Basic Planning Report ENB-3, State of New York Conservation Department with Resources Commission.
- Looney, B.B., Grant, M.W., and King, C.M., 1987, Estimation of Geochemical Parameters for Assessing Subsurface Transport at the Savannah River Plant, United States Department of Defense, Contract DE-AC09-76SR00001, EI du Pont de Nemours & Co., Savannah River Laboratory, Aiken, SC.
- McDonald, M.G. and Harbaugh, A.W., 1988, A Modular Three-Dimensional Finite-Difference Ground-Water Flow Model, Techniques of Water Resources of the U.S.G.S., Book 6, Chapter A1.
- Merin, Ira. S., 1992, "Conceptual Model of Ground Water Flow in Fractured Siltstone Based on Analysis of Rock Cores, Borehole Geophysics, and Thin Sections." *Ground Water Monitoring Review*, Fall, 1992.
- MFI/EM, The USGS Program to Input Data for MODFLOW Extended Memory Version for 80386 and 80486 Computers, Maximal Engineering Software, Inc., November 1994.
- MODFLOW/EM, The USGS Three Dimensional Ground Water Flow Model Extended Memory Version for 80386 and 80486 Computers, Maximal Engineering Software, Inc., August, 1993.

- MODPATH/EM, The USGS Model to Calculate Pathlines Using the Results of MODFLOW Extended Memory Version for 80386 and 80486 Computers, Maximal Engineering Software, Inc., November 1994.
- MODPATH-PLOT/EM, The USGS Program for Displaying Pathlines and Endpoints Calculated by MODPATH Extended Memory Version for 80386 and 80486 Computers, Maximal Engineering Software, Inc., November 1994.
- Mozola, A.J., 1951, The Groundwater Resources of Seneca County, New York, Bulletin GW-26. Water, Power and Control Commission, Department of Conservation, State of New York, Albany, New York.
- MT3D, A Modular Three-Dimensional Transport Model for Simulation of Advection, Dispersion, and Chemical Reactions of Contaminants in Groundwater Systems, Version 1.85, Documentation and User's Guide, S.S. Papadopoulos & Associates, Inc.
- Muller E.H. and Cadwel D.H., 1986, Surficial Geologic Map of New York State Finger Lakes
- National Ground Water Association, Use of Modflow for Simulation of Ground Water Flow and Advective Transport, Short Course, Instructors: Michael McDonald, Arlen Harbaugh, Daniel Morissey, and David Pollock, Nov. 1994.
- Parsons ES, Remedial Investigation Report at the Ash Landfill Site, 1994a.
- Parsons ES, Action Memorandum, Ash Landfill Removal Action, 1994b.
- Parsons ES, Expanded Site Inspection Seven Low Priority AOCs SEADs 60, 62, 63, 64(A, B, C and D), 67, 70, and 71, 1995a.
- Parsons ES, Expanded Site Inspection Eight Moderately Low Priority AOCs SEADs 5, 9, 12(A and B), (43, 56, 69), 44(A and B), 50, 58, and 59, 1995b.
- Parsons ES, Expanded Site Inspection Seven High Priority AOCs SEADs 4, 16, 17, 24, 25, 26 and 45, 1995c.
- Pollock, D.W. 1994, User's Guide for MODPATH/MODPATH-PLOT, Version 3: A particle tracking post-processing package for MODFLOW, the U.S. Geological Survey finite-difference ground-water flow model, U.S. Geological Survey, Open-File Report 94-464.
- Shacklette, H.T. at Boennger, J.G., 1984, "Element Concentrations in Soils at other Surficial Materials of the Contiguous United States" U.S.G.S. Prof Paper 1270, Washington
- Soil Survey of Seneca County, New York, April, 1972.

- Telford, W.M., Geldart, L.P., Sheriff, R.E., Keys, D.A. 1981, *Applied Geophysics*, Cambridge University Press, Cambridge, England, 860 pp.
- Thornthwaite and J.R., Mather, 1957, *Publications in Climatology*, Volume X, Number 3; Instructions and Tables for Computing Potential Evapotranspiration and The Water Balance.
- Todd, David Keith, 1980. *Groundwater Hydrology*. John Wiley & Sons, New York. (2ed.)
- U.S. Department of Agriculture, Soil Conservation Service, April 1972 Soil Survey, Seneca County New York
- U.S. Army Environmental Hygiene Agency, 1979. Army Pollution Abatement Program Study, No. D-1031-W, Landfill Leachate Study Seneca Army Depot, Romulus, New York, 23 July - 3 August 1979.
- U.S. Army Environmental Hygiene Agency, 1984. Phase 4 Evaluation of the Open Burning/Open Detonation Grounds. Investigation of Soil Contamination, Hazardous Waste Study No. 37-26-0479-85.
- U.S. Environmental Protection Agency, Office of Research and Development, 1992, Quality Assurance and Quality Control in the Development and Application of Groundwater Models, EPA/600/R-93/011.
- U.S. Environmental Protection Agency, Office of Research and Development, 1993, Compilation of Groundwater Models, EPA/600/R-93/118.
- U.S. Environmental Protection Agency, Office of Research and Development, 1989, Super Fund Ground Water Issue, Contaminant Transport in Fractured Media: Models for Decision Makers, EPA540/4-89/004.
- U.S. Environmental Protection Agency, 1975. Use of the Water Balance Method for Predicting Leachate Generation from Solid Waste Disposal Sites.
- U.S. Geological Survey Quadrangle Maps, Towns of Ovid and Dresden, New York, 1970.
- U.S. Geological Map of New York State, 1978.
- Van Genuchten, M. Th., and W.J. Alves, 1982. Analytical solutions of the one-dimensional convective-dispersive solute transport equation, *U.S. Dep. of Agric. Tech. Bull.* 1661, 149 pp.
- Water Information Center, "Water Atlas of the United States," 1973.

Wiedemeier, Todd, H., Swanson, M.A., Wilson, J.T., Kampbell, D.H., Miller, R.N., Hanson, J.E.,
1995, Comparison of Two Methods for Determining Biodegradation Rates at the Field
Scale, Submittal to Groundwater Monitoring and Remediation, 1995.

APPENDIX A

**Northeast Regional Climate Center,
Daily Evapotranspiration and Soil Moisture Estimates
for the Northeastern United States - MORECS model**

NORTHEAST
REGIONAL
CLIMATE
CENTER

1123 Bradfield Hall
Cornell University
Ithaca, NY 14853-1901

Phone: (607) 255-1751
Fax: (607) 255-2106

Internet mail: nrcc@cornell.edu



9 May 1995

Mr. Paul Meriney
Parsons Engineering Science Inc.
Prudential Center
Boston, MA 02199-7697

Dear Mr. Meriney:

Enclosed is the climatic data that you ordered. The tabulated values indicate the monthly total evapotranspiration from a grass-covered surface at Ithaca, NY. These values were derived using our evapotranspiration model which is described in the publication which I have included. A bill for this data is also enclosed.

I hope that this information is useful for your application. If you have any further questions, please don't hesitate to contact me.

Sincerely,

Arthur T. DeGaetano, Ph.D.
Research Climatologist

MONTHLY EVAPOTRANSPIRATION FROM GRASS

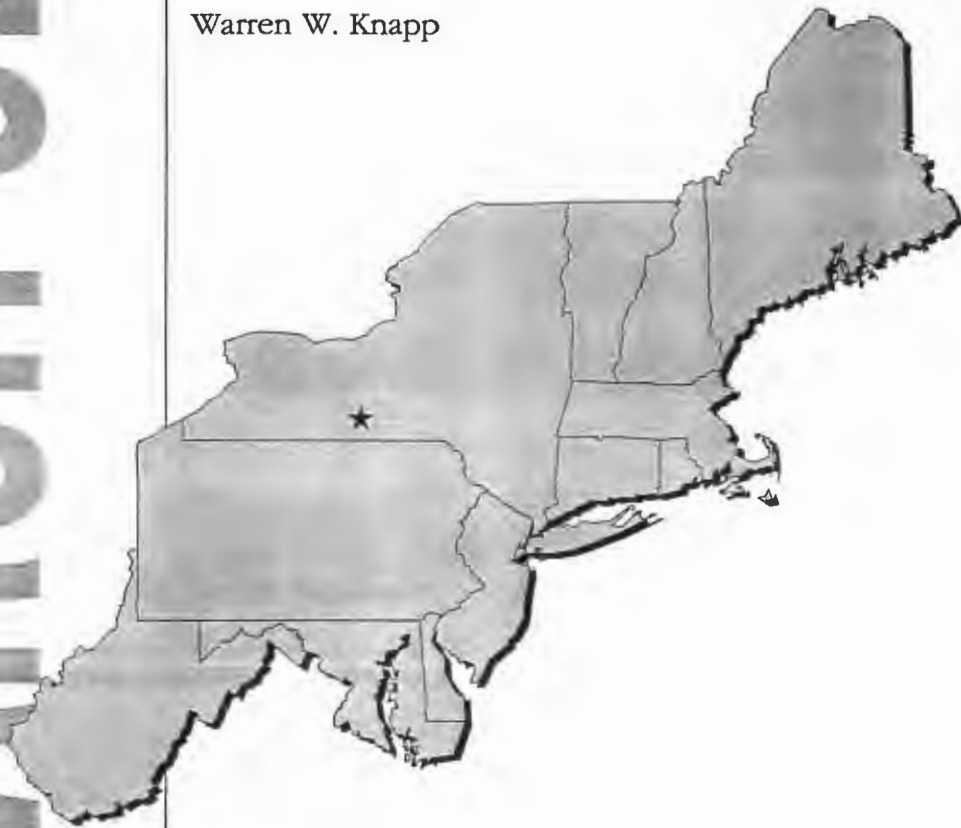
ITHACA, NY

Month	1984	1985	1986	1987	1988	1989	1990	1991	1992	1993	1994
January	0.24	0.22	0.28	0.24	0.27	0.37	0.33	0.30	0.27	0.24	0.17
February	0.53	0.39	0.31	0.55	0.48	0.35	0.53	0.47	0.22	0.43	0.54
March	0.80	1.28	1.20	1.65	1.26	1.19	1.27	1.00	0.67	0.93	0.87
April	1.80	2.00	2.17	1.96	1.73	1.91	1.99	2.08	1.64	1.57	1.93
May	2.12	3.48	3.71	3.46	3.20	2.51	2.52	4.03	2.84	3.43	2.64
June	4.30	3.15	3.38	3.51	4.39	3.02	3.60	3.65	3.51	3.42	4.20
July	4.26	4.10	3.49	4.19	3.43	4.51	3.81	3.38	2.35	4.09	4.05
August	3.39	2.77	3.34	3.08	3.33	3.27	3.10	2.03	2.91	3.00	2.97
September	2.37	2.38	2.00	1.52	2.57	2.04	2.03	1.04	2.21	1.53	2.05
October	1.30	1.27	0.93	1.09	0.94	1.41	1.10	1.44	1.14	1.11	1.45
November	0.52	0.32	0.40	0.51	0.53	0.33	0.69	0.53	0.43	0.42	0.61
December	0.32	0.21	0.27	0.28	0.34	0.25	0.31	0.30	0.28	0.40	0.41

NORTHEAST REGIONAL CLIMATE CENTER

Daily Evapotranspiration and Soil Moisture Estimates for the Northeastern United States

Arthur T. DeGaetano
Keith L. Eggleston
Warren W. Knapp



Cornell University
Ithaca, New York

Publication No. RR 94-1
January 1994

Daily Evapotranspiration and Soil Moisture Estimates for the Northeastern United States

Arthur T. DeGaetano

Keith L. Eggleston

Warren W. Knapp

Cornell University
Ithaca, New York

Publication No. RR 94-1

January 1994

The mission of the Northeast Regional Climate Center (NRCC) is to facilitate and enhance the collection, dissemination and use of climate data as well as to monitor and assess climatic conditions and impacts in the twelve-state, northeastern region of the United States. Implementing this mission involves three programmatic objectives: 1) the development and management of regional climate data bases, 2) the dissemination of information and educational services regarding climate and its impacts, and 3) the performance and support of applied climate research.

Established in 1983, the Northeast Regional Climate Center (NRCC) is one of six regional climate centers now operating throughout the nation. These regional centers serve as sources of climate data and information to public and private institutions and individuals as well as expertise on local and regional climate problems. The Center's staff cooperate with State Climatologists and research scientists in disseminating climate data and information, analyzing environmental and economic impacts of climate variability, and developing new applications of weather and climate data for agriculture, business, industry, and government operations.

The NRCC Research Report series is intended to make available to interested users the full results of climate research that has been supported by the NRCC. This report series supplements the normal reporting of research results in professional journals and provides an outlet for more complete and comprehensive accounts of work performed than is generally possible in journals.

For further information please write or call:

Northeast Regional Climate Center

1123 Bradfield Hall
Cornell University
Ithaca, New York 14853-1901
(607) 255-1751



The Northeast Regional Climate Center is supported by a Grant from the National Oceanic and Atmospheric Administration.

Daily Evapotranspiration and Soil Moisture Estimates for the Northeastern United States

Arthur T. DeGaetano
Keith L. Eggleston
Warren W. Knapp

Northeast Regional Climate Center
Research Series
Publication No. RR 94-1
January 1994

CONTENTS

Introduction	1
Model Description	
Evaporation	3
Precipitation	5
Dew Deposition	6
Runoff	6
Water Budget Calculations	6
Modifications for winter conditions	7
Validation	7
Summary	10
Acknowledgements	10
References	10

INTRODUCTION

A recent survey of climate information users in the northeastern United States indicated a strong interest in current evapotranspiration (ET) and soil moisture values. Such data has a wide variety of applications including the planning of agricultural operations, flood potential forecasting, and the scheduling of urban lawn watering. Unfortunately, routine measurements of evaporation and soil moisture are not widely available in the region. Only about 30 cooperative network stations in the Northeast measure pan evaporation, and soil moisture is observed at a limited number of specialized stations. These measurements are not reported, however, with sufficient frequency to be useful in monitoring real-time ET rates or soil moisture status. In addition, the historical records of such observations show many gaps and inconsistencies.

Because the inventory of evaporation and soil moisture measurements is so limited, numerous methods to estimate ET and soil moisture status have been proposed and implemented. Broadly, such methods can be classified as either climatological or physically-based. Climatological methods are designed to estimate potential ET using routinely measured meteorological data such as air temperature, and do not relate well to actual situations where both crop and soil factors affect the rate of ET. Such methods are useful only for estimating maximum ET values over periods of a month or longer. Formally, potential evapotranspiration is defined as the rate of water loss from an extended surface of short green crop assuming that the crop fully shades the ground, exerts negligible resistance to the flow of water and is continually well supplied with water.

Perhaps the most widely used climatological method for estimating ET is that of Thornthwaite (1948). Based on mean monthly temperature (T_i), in °C, Thornthwaite's method estimates potential ET (ETP) for month i using the formula:

$$ETP_i = 1.6 (10(T_i)/I)^a \quad (1)$$

where ETP has units of centimeters and the exponent a is given by:

$$a = 6.75 \times 10^{-7} (I^3) - 7.71 \times 10^{-5} (I^2) + 1.79 \times 10^{-2} (I) + 0.49. \quad (2)$$

I is a heat index given as:

$$I = \sum_{i=1}^{12} (T_i/5)^{1.514} \quad (3)$$

Application of the Thornthwaite method to estimate ETP over periods shorter than a month leads to significant errors because short-term temperature means are an unsatisfactory surrogate for net radiation, which physically drives evapotranspiration. Other climatological methods have been proposed by Blaney and Criddle (1950), and Jensen and Haise (1963).

Physically-based methods for estimating evaporation allow for more reliable, short-term estimates at the expensive of requiring considerably more meteorological input data. This is exemplified by the commonly used Penman Method (Penman, 1948) given in simplified form as:

$$E = (\Delta H + \gamma E_a) / (m + \gamma) \quad (4)$$

where E is daily evaporation from an open water surface, Δ is the slope of the saturation vapor pressure curve at the mean air temperature, H is an estimate of net radiation and γ is the psychrometric constant. E_a , which relies on the saturation and actual vapor pressures, e_s and e_a , respectively, and the mean wind speed, u, is given as:

$$E_a = 0.35(e_s - e_a)(1 + u \times 10^{-2}). \quad (5)$$

Other physically-based methods for estimating evaporation, include those proposed by Thornthwaite and Holzman (1942), Swinbank (1951), and Suomi and Tanner (1958). A physically-based method for estimating evapotranspiration was developed by Monteith (1963).

Combining the methods of Penman and Monteith provides a physically-based means of estimating ET from surfaces other than open water. The Penman-Monteith equation (Monteith, 1965) calculates ET as:

$$\lambda E = \frac{\Delta(R_n - G) + \rho c_p (e_s - e_a)/r_a}{\Delta + \gamma (1 + r_s/r_a)} \quad (6)$$

where

- E = rate of water loss ($\text{Kg m}^{-2}\text{s}^{-1}$)
- Δ = rate of change of e_s with temperature ($\text{mb } ^\circ\text{C}^{-1}$)
- R_n = net radiation (Wm^{-2})
- G = soil heat flux (Wm^{-2})
- ρ = air density (Kg m^{-3})
- c_p = specific heat of air at constant pressure ($1005 \text{ JKg}^{-1} \text{ } ^\circ\text{C}^{-1}$)
- e_s = saturation vapor pressure (mb)
- e_a = actual vapor pressure (mb)
- λ = latent heat of vaporization ($2.465 \times 10^6 \text{ JKg}^{-1}$)
- γ = psychrometric constant ($0.66 \text{ mb } ^\circ\text{C}^{-1}$)
- r_s = surface resistance (sm^{-1})
- r_a = aerodynamic resistance (sm^{-1})

Due to its physical basis and its ability to provide reliable daily ET estimates, the Penman-Monteith equation is commonly used to estimate ET for a variety of surface types and locations. The Penman-Monteith equation forms the basis for the British Meteorological Office Rainfall and Evaporation Calculation System (MORECS) (Thompson et al., 1981). MORECS is used operationally in Great Britain to obtain weekly and monthly estimates of average evaporation and soil moisture deficits over

40 km x 40 km grid squares. The system relies on routinely observed daily meteorological data as its input. An important feature of MORECS is a scheme designed to determine potential and actual ET over a variety of different surface types. Using MORECS, such estimates can be obtained for open water, bare soil, grass, cereals, potatoes, deciduous trees, conifers, orchards and pastures.

The Penman-Monteith equation is also the primary means by which ET is calculated in the CERES-Maize corn simulation model (Jones and Kiniry, 1986). This model is used operationally by the Midwest Climate Center to estimate soil moisture status under corn crops in the midwestern U.S. (Kunkel, 1990). Although well suited for use in the Midwest, where corn is a widely grown agricultural crop, such a crop-specific model is not a good choice the Northeast due to the wide variety of land uses.

Because of this need for a more general ET model, the British MORECS has been modified and validated for use in the northeastern United States. Presently, historical and real-time estimates of potential ET from grass, evaporation from bare soil and standard evaporation pans, as well as actual ET from grass- and deciduous tree-covered surfaces are available for the region. In addition, soil moisture deficits can be calculated under grass, bare soil and deciduous trees. ET and soil moisture estimates can also be obtained for a variety of other crops, however the unavailability of reliable verification data for other surface covers has precluded validation of the model for other surface cover types.

MODEL DESCRIPTION

a. Evaporation

Calculation of ET values using Equation 6 requires several supplementary physical and empirical relationships with which to compute values for terms that are not routinely measured. Because solar radiation measurements are not widely available in the Northeast, daily estimates of downward shortwave solar radiation are calculated based on hourly cloudiness, dew point and station pressure observations using the methods described in DeGaetano et al., 1993. Net radiation is obtained by decreasing the short wave radiation estimate according to the surface albedo, and summing this estimate and the net long wave radiation given by Linacre (1968) as:

$$R_{LN} = \epsilon \sigma T^4 [1.35(e_s/T)^{0.143} - 1] (0.6) \quad (7)$$

where R_{LN} = net long wave radiation (Wm^{-2})
 ϵ = emissivity (0.95)
 σ = Stefan's constant ($5.67 \times 10^{-8} Wm^{-2} \text{ } ^\circ K^{-4}$)
 e_s = saturation vapor pressure (mb)
 T = shelter temperature ($^\circ K$).

The constant 0.6 accounts for cloudiness assuming a constant cloud cover of five tenths.

During daylight hours, G is defined as the flux density of heat into the soil and is calculated as:

$$G_d = (0.3 - 0.03L)R_{Nd} \quad (8)$$

where L is the leaf area index and R_{Nd} is daytime net radiation. For grass, L varies from 2.0 during winter (December-February) to 5.0 in summer (July-September). However, L is assumed to equal 3.33 when calculating G_d . The leaf area index used to calculate G_d for deciduous trees varies linearly from 0.1 during dormancy to 6.0 at full leaf. A similar linear decrease in leaf area index is assumed during senescence. For bare soil, $L = 0.0$. At night, an estimate of G is given by:

$$G_n = (D(G_d) - P)/(24 - D) \quad (9)$$

where D is the number of daylight hours and P is the average daily heat storage in soil (Whr m^{-2}). Monthly values of P were empirically determined by Wales-Smith and Arnott (1980) and are given in Thompson et al. (1981). It is assumed that the British heat storage values are suitable for use in the northeastern U.S. When estimating pan evaporation, G is set equal to 0.0.

Using the logarithmic wind profile and assuming neutral stability, r_a is given as:

$$r_a = (6.25/u) \ln(10.0/z_o) \ln(6.0/z_o) \quad (10)$$

where u is the wind speed (ms^{-1}) at a height of 10 m above the ground and z_o is the roughness length (m). Fixed roughness lengths of 1.5×10^{-2} , 5.0×10^{-3} and 5.0×10^{-4} m are assigned to grass, bare soil and water, respectively. For deciduous trees, roughness length varies linearly between 0.2 m at leaf emergence to 1.0 m for full leaf. During autumn, roughness length is linearly decreased from the full leaf value to a defoliated value of 1.5×10^{-2} m. Similarly, roughness length is linearly increased during the period of bud break in spring.

In MORECS, water may be extracted from both the soil and the crop. Thus, the surface resistance term incorporates resistances due to both the crop and soil. Daytime values of crop resistance are prescribed for each surface type. These values reflect a crop that is freely supplied with water and thus represent a minimum resistance associated with each crop type. For deciduous trees, the minimum resistance is set equal to 80 sm^{-1} , while for grass this value varies from 50 during winter to 40 sm^{-1} in the summer months. Despite the lack of crop cover, a relatively high crop resistance value of 600 sm^{-1} is used for evaporation from bare soil to ensure that transpiration is negligible.

MORECS assumes two soil moisture reservoirs. Water in the top reservoir (x) is freely available for ET, while water in the second reservoir (y) becomes increasingly more difficult to extract as soil moisture decreases. The contents of each reservoir can be subdivided into water available for evaporation (x_{SOIL} or y_{SOIL}) and water available for transpiration (x_{CROP} or y_{CROP}). In the case of bare soil, water can only be evaporated from x_{SOIL} or y_{SOIL} . Provided water exists in x , the crop resistance remains at the minimum value. Soil resistance, is set to 100 sm^{-1} until x_{SOIL} has been depleted. After this point, soil resistance increases according to the formula:

$$r_{\text{SOIL}} = 100C_{x_{\text{max}}}/(x_{\text{SOIL}} + x_{\text{CROP}} + 0.01C_{x_{\text{max}}}) \quad (11)$$

where r_{SOIL} is the soil resistance, x_{SOIL} and x_{CROP} are the amount of water contained in each reservoir, and $C_{x_{\text{max}}}$ is the maximum amount of water that can be held in x_{CROP} . For potential evapotranspiration, r_{SOIL} remains at 100 sm^{-1} and crop resistance is set at the minimum value for grass.

Once the water in the x reservoir has been exhausted, r_{SOIL} is set to 10^4 sm^{-1} and the crop resistance (r_{CROP}) is increased proportionally to the water deficit of the y reservoir using the formula:

$$r_{CROP} = (r_{CROP})_{min} ((2.5y_{max}/(y_{SOIL} + y_{CROP})) - 1.5) \quad (12)$$

where y_{SOIL} and y_{CROP} are the amount of water contained in each reservoir, y_{max} is the maximum amount of water that can be held in the y reservoir and $(r_{CROP})_{min}$ is the minimum crop resistance value.

Daytime surface resistance, r_s , is related to r_{CROP} and r_{SOIL} by the expression:

$$r_s = r_{CROP} r_{SOIL} / ((r_{SOIL}(1-A)) + (r_{CROP} A)) \quad (13)$$

where $A = 0.7^L$. At night, when stomata are closed, r_s is given by:

$$r_s = 2500(r_{SOIL}) / (r_{SOIL}(L) + 2500). \quad (14)$$

However, when the surface is bare soil and all water in x_{SOIL} has been depleted, regardless of the time of day, r_s is specified as:

$$r_s = 100(3.5(1 - (y_{SOIL}/S_{y_{max}})) + \exp(0.2(S_{y_{max}}/(y_{SOIL} - 1)))) \quad (15)$$

where $S_{y_{max}}$ is the maximum amount of water that can be held in y_{SOIL} . For an open water surface, r_s equals 0.0.

b. Precipitation

Each of the soil reservoirs can be replenished by rainfall and, theoretically, by dew deposition. In cases where the soil surface is covered by vegetation, a certain amount of rainfall is intercepted by the plant canopy and is thus unavailable to the soil. The proportion of rainfall that can be intercepted by grass, P, is:

$$P = (1.0 - 0.5^L). \quad (16)$$

The amount of interception, I, is simply the product of P and the daily rainfall. However, I can not exceed 20% of the leaf area index, L (i.e., $I \leq 0.2L$). Particularly during summer, several individual showers may contribute to the daily rainfall total. In such cases, the interception associated with the first shower may evaporate prior to any subsequent rainfall. Thus, Thompson et al. (1981) suggest the calculated value of I be multiplied by an adjustment factor during the months from March through November. These adjustment factors are given in Table 1. During all months, however, I is limited to the daily rainfall total.

Table 1. Adjustment factors to allow for evaporation of interception resulting from multiple daily rainfall events.

Month	Mar	Apr	May	Jun	Jul	Aug	Sep	Oct	Nov
Factor	1.2	1.4	1.6	2.0	2.0	2.0	1.8	1.4	1.2

Interception by deciduous trees is treated differently. Helvey and Patric (1965) present a regression-based approach for estimating interception of rainfall in eastern

hardwood forests. During dormancy (trees are in a defoliated state), interception is given as:

$$I = 0.086R + 0.015 \quad (17)$$

Interception by trees in full leaf is calculated using:

$$I = 0.099R + 0.031 \quad (18)$$

where R is the daily rainfall and the date of full leaf is obtained using phenological data. During leaf emergence, I is linearly increased from its dormancy value. Conversely, during senescence, I is linearly decreased from its full leaf value.

When interception is present, evaporation of the intercepted moisture occurs prior to any evapotranspiration from the soil. After setting r_s to 0.0, the open water value, evaporation is calculated hourly until the foliage is completely dry (no interception). Subsequent hourly ET estimates are calculated using r_s given by Equations 13 and/ or 14. If intercepted water still exists after 24 hours, the unevaporated interception is assumed to fall to the soil.

c. Dew Deposition

The formation of dew is assumed when nighttime evaporation is negative. In these instances, dew is treated as open water and nighttime evaporation is recalculated after setting r_s to zero. If this calculation again yields negative evaporation, the deposition of dew is assumed with the amount of dew equal to the absolute value of evaporation. Ensuing calculations treat dew deposition in the same manner as rainfall. If recalculation yields positive evaporation, nighttime evaporation is set to zero. In such cases it is assumed that only dew has evaporated.

d. Runoff

For surface types other than deciduous trees, runoff is assumed equal to zero unless both the x and y reservoirs are at capacity. In the case of trees, runoff is also assumed to occur if the daily rainfall exceeds 1.00 inch or regardless of the daily rainfall total, when x_{SOIL} is greater than zero. These criteria are based on the curve number method (USDA, 1972). Using a simplification of this method, the runoff from a tree covered surface is:

$$RO_{tree} = (R - 0.2D)^2 / (R + 0.8D) \quad (19)$$

R is the daily rainfall (cm), and D is given by:

$$D = (x_{max} + y_{max}) - (x_{soil} + x_{crop} + y_{soil} + y_{crop}) \quad (20)$$

where x_{max} and y_{max} are the capacities of the x and y soil water reservoirs.

e. Water Budget Calculations

The maximum total amount of water available for ET from a specific crop (AW) is assumed to fill two soil moisture reservoirs. Water in the x reservoir, 40% of AW, is freely available for ET, while the remaining 60% of AW, which fills the y reservoir, becomes increasingly difficult to transpire or evaporate as the contents of y decrease. The amount of water within each reservoir is further subdivided into water available

for evaporation from bare soil (x_{soil} or y_{soil}) and water available for ET from a crop covered surface (x_{crop} or y_{crop}). For soil with typical water holding capacity, AW is assigned a value of 20 mm for bare soil; 125 mm for grass and 175 mm for trees. Thus, regardless of crop type, x_{soil} and y_{soil} can not exceed 8 and 12 mm, respectively for a soil with average water holding capacity.

Through the process of ET, water is withdrawn from x_{soil} until this sub-reservoir is empty. Subsequent ET draws water from x_{crop} until the entire x reservoir is exhausted. At this point ET draws water from the y reservoir, depleting y_{soil} before tapping the reserve stored in y_{crop} . Soil moisture is replenished in a similar manner. Rainfall must fill the x_{soil} sub-reservoir to capacity before replenishing any moisture deficit in x_{crop} . Once the x reservoir is at capacity, additional rainfall fills y_{soil} and finally y_{crop} . This sequence of ET and recharge qualitatively represents the decreasing availability of soil moisture for evaporation and/or transpiration. Such an assumption simplifies the process of specifying crop and soil resistances as soil moisture becomes increasingly depleted or recharged.

f. Modifications for winter conditions

Because MORECS was developed for a climate in which snowfall is uncommon, several modifications were required to adapt the model for use in the northeastern U.S. where snowfall is possible throughout the cold half of the year. These modifications are designed to assure that soil moisture conditions are correctly initialized at the start of the growing season. Precipitation is assumed to fall in liquid form throughout the year. Therefore, the liquid water contained in snowfall is assumed to immediately replenish the soil moisture reservoirs. Although these assumptions allow soil moisture conditions to be tracked through the winter, individual daily soil moisture values are overestimated when snow cover is present or the soil is frozen.

Two additional modifications are also incorporated when snow cover exists and/or the air temperature falls below 30° F. The surface resistance is set to 0.0 on days with snow cover, because the presence of snow implies that any evaporation will occur from an open, although frozen, water surface. At temperatures below 30° F, the value of λ , used in Eq. 6, is assigned the latent heat of sublimation ($2.799 \times 10^6 \text{ Jkg}^{-1}$).

VALIDATION

To assess the accuracy of the ET and soil moisture values estimated by the model, output values were compared with observations at several sites in the northeastern United States. Unfortunately, sets of high-quality soil moisture observations are extremely scarce, so much of the validation analysis is based on pan evaporation measurements. Daily pan evaporation observations were obtained from 4 sites in the region and compared with the corresponding model estimates of open water evaporation. Mean errors (ME), (model - observed), mean absolute errors (MAE) and root mean square errors (RMSE) were computed at each site. These results appear in Table 2.

The results in Table 2 indicate close agreement between the observed and modeled evaporation values. The model appears to be unbiased as indicated by the overall

Table 2. Mean error (ME), mean absolute error (MAE) and root mean square error (RMSE) associated with modeled pan evaporation at the indicated sites. Errors have units of inches. The daily average observed pan evaporation (PAN), period of record (Years) and number of daily observations (OBS) are also given.

<u>Station</u>	<u>ME</u>	<u>MAE</u>	<u>RMSE</u>	<u>PAN</u>	<u>Years</u>	<u>OBS</u>
Beltsville, MD	0.00	0.04	0.06	0.19	1985 - 1990	1043
Emmaus, PA	0.01	0.05	0.07	0.17	1985 - 1991	1278
Ithaca, NY	0.00	0.03	0.05	0.15	1984 - 1990	1277
New Brunswick, NJ	0.01	0.04	0.05	0.17	1985 - 1990	1003
All Stations	0.00	0.04	0.06	0.17		4601

mean error value of zero. Little bias is apparent at the individual stations as well. On average, individual evaporation estimates deviate from the observed value by approximately ± 0.04 inches. This value is remarkably consistent among the four stations, as are the RMSE values. Errors were also calculated for monthly periods and for days with and without precipitation reported. Generally, these results were similar to those given in Table 2.

Model-derived soil moisture estimates under grass and bare soil were verified using weekly data collected at Rock Springs, PA (McKee, 1983). Figure 1 compares actual and model-derived soil moisture under grass during 1977. This growing season was generally characterized by a dry spring and moist early summer. Dry weather during the late summer and early autumn was followed by wet late-autumn conditions. Despite these frequent and rather abrupt changes in soil moisture conditions, the modeled values follow the observed values quite closely. The largest deviations between the two curves occur in mid-August and mid-September. During these periods, observed soil moisture exceeds the modeled value. Because coincident meteorological and soil moisture observations were unavailable, these deviations most likely result from differences in the amount of precipitation received at Rock Springs and the rain gauge site at State College, PA which is located approximately 10 miles to the northeast. Prior to 8 August, errors (model - observed) averaged -0.06

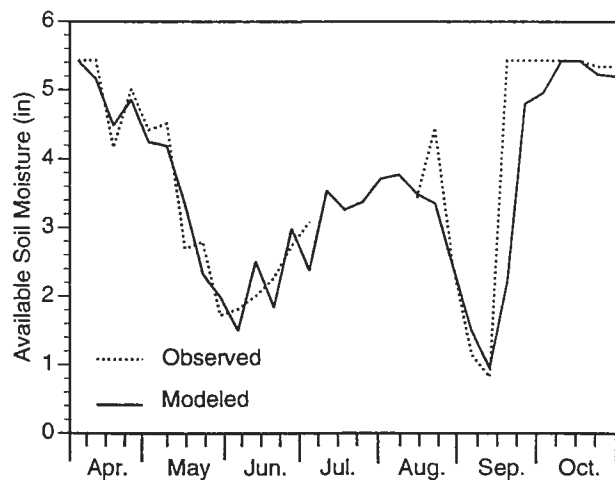


Figure 1. Comparison of modeled and observed soil moisture under grass during 1977 at Rock Springs, PA.

inches, while the mean absolute error and root mean square error were 0.34 and 0.40 inches, respectively. Over this period actual soil moisture averaged 3.40 inches. Similar agreement between observed and model-derived soil moisture values was achieved during other growing seasons and for bare soil.

Soil moisture observations taken within a deciduous forest were available from the Hubbard Brook Experimental Forest in New Hampshire. Figure 2a compares actual and model-derived soil moisture at this site during 1971. During this growing season, dry weather during the spring and early summer was followed by generally wet conditions during late-summer and autumn. As was the case for grass, the modeled values follow the observed values quite closely. However, particularly from July onward, a tendency for the model to overestimate soil moisture is apparent. This bias most likely results from runoff characteristics which are specific to the Hubbard Brook site. For instance, sharp increases in estimated soil moisture follow rainfalls of over

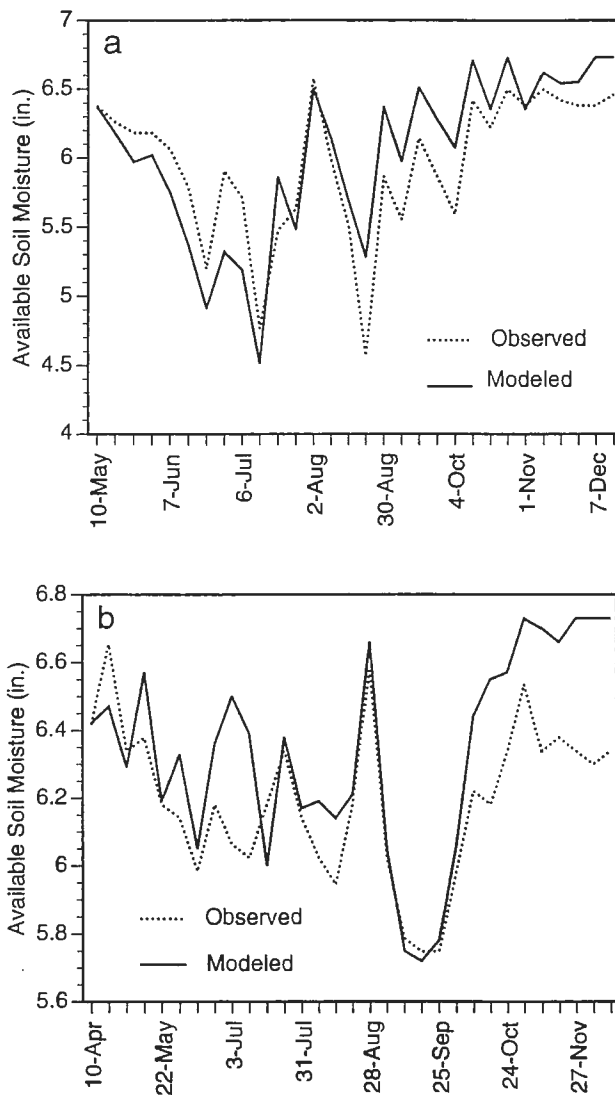


Figure 2. Comparison of modeled and observed soil moisture under a deciduous forest during (a) 1971 and (b) 1972. Growing season observations are at approximately seven day intervals.

1.8 inches on 27-28 August; 1.90 inches over the period from 12 to 14 September and 2.13 inches on October 9. Sharp increases in soil moisture are also associated with frequent rainfall events during 1972, particularly in autumn and the late spring and early summer (Fig. 2b). During 1971, mean errors averaged -0.07 inches, while the mean absolute and root mean square errors were 0.28 and 0.33 inches, respectively.

SUMMARY

Evapotranspiration and soil moisture measurements in the northeastern United States are relatively few in number and have limited periods of record. Since this semi-physical model requires only standard hourly surface observations and daily precipitation as inputs, current ET and soil moisture estimates can be generated at several dozen hourly observing sites within the region. Historical ET and soil moisture estimates dating back to 1948 can also be computed at approximately 30 sites in the Northeast. This data base of estimated ET and soil moisture values will provide essential data for applications ranging from drought and flood monitoring to the scheduling of urban lawn watering.

ACKNOWLEDGMENTS

We would like to thank Dr. Tony Federer for providing the soil moisture observations from the Hubbard Brook Experimental Forest. We are also indebted to Dr. Ed Ciolkosz for the data from Rock Springs, PA. This work was supported by NOAA Grant No. NA16CP-0220-02.

REFERENCES

- Blaney, H.F. and W.D. Criddle, 1950: Determining water requirements in irrigated areas from climatological and irrigation data. *USDA Soil Conservation Service Tech. Paper No. 96*, 48 pp.
- DeGaetano, A.T., K.L. Eggleston and W.W. Knapp, 1993: *Daily solar radiation estimates for the northeastern United States*. Northeast Regional Climate Center Research Publication RR 93-4, 7 pp.
- Helvey, J.D. and J.H. Patric, 1965: Canopy and litter interception of rainfall by hardwoods of eastern United States. *Water Resour. Res.*, **1**, 193-206.
- Jensen, M.E. and H.R. Haise, 1963: Estimating evapotranspiration from solar radiation. *J. Irrigation Drainage Div. Amer. Soc. Civil Eng.*, **89**, 15-41.
- Jones, C.A. and J.R. Kiniry, 1986: *CERES-Maize A Simulation Model of Maize Growth and Development*. Texas A&M University Press, 194 pp.
- Kunkel, K.E., 1990: Operational soil moisture estimation for the midwestern United States. *J. Appl. Meteor.*, **29**, 1158-1166.
- Linacre, E.T., 1968: Estimating the net radiation flux. *Agric. Meteorol.*, **5**, 49-63.

- McKee, G.W., 1983: *Weather Observations 1969-1982 Agronomy Research Farm Rock Springs*. Agronomy Series 75, Department of Agronomy, The Pennsylvania State University, 209 pp.
- Monteith, J.L., 1963: Gas exchange in plant communities. *Environmental Control of Plant Growth*, L.T. Evans, ed., Academic Press, New York, 95-112.
- _____, 1965: Evaporation and environment. *Symp. Soc. Exp. Biol.*, **19**, 205-234.
- Penman, H.L., 1948: Natural evaporation from open water, bare soil and grass. *Proc. Roy. Soc. A.*, **193**, 120-145.
- Suomi, V.E. and C.B. Tanner, 1958: Evapotranspiration estimates from heat budget measurements over a field crop. *Trans. Amer. Geophys. Union*, **39**, 298-304.
- Swinbank, W.C., 1951: The measurement of vertical transfer of heat and water vapor by eddies in the lower atmosphere. *J. Meteorol.*, **8**, 135-145.
- Thompson, N., I.A. Barrie and M. Ayles, 1981: *The Meteorological Office Rainfall and Evaporation Calculation System (MORECS)*. United Kingdom Meteorological Office Hydrological Memorandum No. 45, 72 pp.
- Thornthwaite, C.W., 1948: An approach toward a rational classification of climate. *Geogr. Rev.*, **38**, 55-94.
- _____ and B. Holzman, 1942: *Measurement of evaporation from land and water surfaces*. USDA Tech. Bull. No. 817, 75 pp.
- USDA, 1972: *Soil Conservation Service, National Engineering Handbook, Hydrology*, Section 4, Chapters 4-10.
- Wales-Smith, B.G. and J.A. Arnott, 1980: *The evaporation calculation system used in the United Kingdom*. Unpublished paper available from the National Meteorological Library, Bracknell UK.

NRCC RESEARCH SERIES

- Knapp, W.W. and K.L. Eggleston, *Some Impacts of Recent Climate Variability on the Northeast*, NRCC Research Publication RR 91-1.
- Wilks, D.S., *Gamma Distribution Probability Tables for Use in Climatology*, NRCC Research Publication RR 91-2.
- Samelson, D., *A Simple Method for Predicting Snowpack Water Equivalent in the Northeastern United States*, NRCC Research Publication RR 92-1.
- Wilks, D.S., *Spline Interpolated Parameters for Adjusting Climatological Precipitation Distributions using the 30- and 90-Day Outlooks*, NRCC Research Publication RR 92-2.
- Cember, R.P. and D.S. Wilks, *Climatological Atlas of Snowfall and Snow Depth for the Northeastern United States and Southeastern Canada*, NRCC Research Publication RR 93-1.
- DeGaetano, A.T., K.L. Eggleston, and W.W. Knapp, *A Method to Produce Serially Complete Daily Maximum and Minimum Temperature Data for the Northeast*, NRCC Research Publication RR 93-2.
- DeGaetano, A.T., W.W. Knapp, and K.L. Eggleston, *Standardizing Growing Degree Day Totals for Differences in Temperature Observing Schedules*, NRCC Research Publication RR 93-3.
- DeGaetano, A.T., K.L. Eggleston, and W.W. Knapp, *Daily Solar Radiation Estimates for the Northeastern United States*, NRCC Research Publication RR 93-4.
- Wilks, D.S. and R.P. Cember, *Atlas of Precipitation Extremes for the Northeastern United States and Southeastern Canada*, NRCC Research Publication RR 93-5.
- DeGaetano, A.T., K.L. Eggleston, and W.W. Knapp, *Climatology of Extreme Maximum Temperature Occurrences for the Northeastern United States*, NRCC Research Publication RR 93-6.

NRCC DIGITAL DATA SETS

- Eggleston, K.L. and D.S. Wilks, *Gridded Monthly Precipitation Distribution Parameters for the Continental United States*, NRCC Data Set DS 92-1.
- Cember, R.P., K.L. Eggleston, and D.S. Wilks, *Digital Snowfall and Snow Depth Probabilities for the Northeastern United States and Southeastern Canada*, NRCC Data Set DS 93-1.
- McKay, M., D.S. Wilks, and T.W. Schmidlin, *Quality-Controlled Snow Water Equivalent Data for the Northeastern United States*, NRCC Data Set DS 94-1.

CORNELL
UNIVERSITY

Department of Soil, Crop and Atmospheric Sciences
Ithaca, New York 14853

APPENDIX B

Preliminary Water Budget Calculations
(Q_{in} vs. Q_{out})



PRELIMINARY WATER BALANCE CALCULATIONS

RECHARGE CALCULATION (Qin)

Total Area of Active Model Grid: 150,413,697.20 square feet
Recharge from Precipitation: 0.001622 feet/year
Qin = 243,971.02 cu. feet/day

FLOW OUT OF AQUIFER INTO SENECA LAKE (Qout)

Qout for Layer 1:

Flow through west-facing cells:

Total N-S Length: 6,945.20 feet
Saturated Thickness: 6 feet
Area = 41,671.20 square feet

Flow through south-facing cells:

Total N-S Length: 2,278.08 feet
Saturated Thickness: 6 feet
Area = 13,668.48 square feet

Total area for Layer 1 = 55,339.68 square feet

Qout Layer 1

	K	A	I
	feet/day	square feet	
Qout =	1.03	55,339.68	0.02
Qout =	1,140.00 cu. feet/day		



Qout for Layer 2:

Flow through west-facing cells:

Total N-S Length: 6,945.20 feet
Saturated Thickness: 20 feet
Area = 138,904.00 square feet

Flow through south-facing cells:

Total N-S Length: 2,278.08 feet
Saturated Thickness: 20 feet
Area = 45,561.60 square feet

Total area for Layer 1 = 184,465.60 square feet

Qout Layer 1

	K	A	I
	feet/day	square feet	
Qout =	0.2	184,465.60	0.03
Qout =	922.33	cu. feet/day	

Qout for Layer 3:

Flow through west-facing cells:

Total N-S Length: 6,945.20 feet
Saturated Thickness: 20 feet
Area = 138,904.00 square feet

Flow through south-facing cells:

Total N-S Length: 2,278.08 feet
Saturated Thickness: 20 feet
Area = 45,561.60 square feet

Total area for Layer 1 = 184,465.60 square feet

Qout Layer 1

	K	A	I
	feet/day	square feet	
Qout =	0.04	184,465.60	0.03
Qout =	184.47	cu. feet/day	



Qout for Layer 4:

Flow through west-facing cells:

Total N-S Length: 6,945.20 feet
Saturated Thickness: 20 feet
Area = 138,904.00 square feet

Flow through south-facing cells:

Total N-S Length: 2,278.08 feet
Saturated Thickness: 20 feet
Area = 45,561.60 square feet

Total area for Layer 1 = 184,465.60 square feet

Qout Layer 1

	K	A	I
	feet/day	square feet	
Qout =	0.0023	184,465.60	0.03
Qout =	10.61	cu. feet/day	

Total Qout Flow System

Qout Layer 1 = 1,140.00 cu feet/day
Qout Layer 2 = 922.33 cu feet/day
Qout Layer 3 = 184.47 cu feet/day
Qout Layer 4 = 10.61 cu feet/day
Total = 2,257.40 cu feet/day



APPENDIX C
MODFLOW Output File



0123
0124
0125
0126
0127
0128
0129
0130
0131
0132
0133
0134
0135
0136
0137
0138
0139
0140
0141
0142
0143
0144
0145
0146
0147
0148
0149
0150
0151
0152

1 1 0 1 0
 2 1 0 1 0
 3 1 0 1 0
 * CONSTANT HEAD* BUDGET VALUES WILL BE SAVED ON UNIT 41 AT END OF TIME STEP 1, STRESS PERIOD 1
 FLOW RIGHT FACE BUDGET VALUES WILL BE SAVED ON UNIT 41 AT END OF TIME STEP 1, STRESS PERIOD 1
 FLOW FRONT FACE BUDGET VALUES WILL BE SAVED ON UNIT 41 AT END OF TIME STEP 1, STRESS PERIOD 1
 FLOW LOWER FACE BUDGET VALUES WILL BE SAVED ON UNIT 41 AT END OF TIME STEP 1, STRESS PERIOD 1
 * RECHARGE* BUDGET VALUES WILL BE SAVED ON UNIT 41 AT END OF TIME STEP 1, STRESS PERIOD 1

HEADS AND FLOW TERMS SAVED ON UNIT 60 FOR USE BY MT3D TRANSPORT MODEL
 HEAD IN LAYER 1 AT END OF TIME STEP 1 IN STRESS PERIOD 1

	1	2	3	4	5	6	7	8	9	10
1	11	12	13	14	15	16	17	18	19	20
2	21	22	23	24	25	26	27	28	29	30
3	31	32	33	34	35	36	37	38	39	40
4	41	42	43	44	45	46	47	48	49	50
5	51	52	53	54	55	56	57	58	59	60
6	61	62	63	64	65	66	67	68	69	70
7	71	72	73	74	75	76	77	78	79	80
8	81	82								
0 1	1000.	1000.	1000.	1000.	1000.	1000.	1000.	1000.	1000.	1000.
0 2	738.5	738.5	738.5	1000.	1000.	1000.	1000.	1000.	1000.	1000.
0 3	738.4	738.4	738.3	738.2	738.1	738.0	1000.	1000.	1000.	1000.
0 4	738.2	738.2	738.2	738.1	738.0	737.9	737.7	737.6	737.5	737.4
0 5	737.3	737.2	737.2	737.2	737.2	737.2	737.2	737.2	737.2	737.2
0 6	737.6	737.6	737.6	737.5	737.5	737.4	737.3	737.2	737.1	737.1
0 7	737.2	737.2	737.2	737.1	737.1	737.0	736.9	736.9	736.8	736.8
0 8	736.7	736.7	736.7	736.6	736.6	736.6	736.6	736.6	736.6	736.6
0 9	735.9	735.9	735.9	735.8	735.8	735.8	735.8	735.7	735.7	735.7
0 10	735.2	735.2	735.2	735.2	735.2	735.2	735.2	735.2	735.2	735.2
0 11	734.7	734.7	734.7	734.7	734.7	734.6	734.6	734.5	734.5	734.5

	574.9	574.9	574.9	574.8	574.8	574.8	574.8	574.7	574.7	574.7
	574.7	574.6	574.6	574.6	574.6	574.5	574.5	574.5	574.5	574.4
	574.4	574.4	574.4	574.3	574.3	574.3	574.2	574.2	574.2	574.2
	574.2	574.1	574.1	574.1	574.1	574.0	574.0	574.0	574.0	573.9
	573.9	573.9	573.9	573.8	573.8	573.8	573.8	573.7	573.7	573.7
	573.6	573.6	573.5	573.3	573.1	572.8	572.6	572.4	572.3	572.1
	572.1	572.0								
0198	571.1	571.0	571.0	570.8	570.7	570.5	570.3	570.1	569.9	569.7
	569.6	569.5	569.5	569.5	569.4	569.4	569.4	569.4	569.3	569.3
	569.3	569.3	569.2	569.2	569.2	569.1	569.1	569.1	569.0	569.0
	569.0	569.0	569.0	568.9	568.9	568.9	568.8	568.8	568.8	568.8
	568.7	568.7	568.7	568.6	568.6	568.6	568.5	568.5	568.5	568.5
	568.4	568.4	568.4	568.4	568.3	568.3	568.3	568.2	568.2	568.2
	568.2	568.1	568.1	568.1	568.0	568.0	568.0	568.0	567.9	567.9
	567.8	567.8	567.6	567.5	567.2	566.9	566.7	566.5	566.3	566.1
	566.0	566.0								
0199	565.6	565.5	565.5	565.3	565.2	565.0	564.7	564.5	564.2	564.1
	564.0	563.9	563.8	563.8	563.8	563.7	563.7	563.4	563.3	563.3
	563.6	563.5	563.5	563.5	563.5	563.4	563.4	563.4	563.3	563.3
	563.3	563.2	563.2	563.2	563.2	563.1	563.1	563.0	563.0	563.0
	563.0	562.9	562.9	562.9	562.8	562.8	562.8	562.7	562.7	562.7
	562.6	562.6	562.6	562.5	562.5	562.5	562.4	562.4	562.4	562.3
	562.3	562.3	562.2	562.2	562.2	562.1	562.1	562.1	562.0	562.0
	561.9	561.8	561.7	561.5	561.2	560.9	560.6	560.3	560.1	560.0
	559.8	559.8								
0200	560.0	560.0	559.9	559.8	559.6	559.4	559.1	558.8	558.5	558.3
	558.2	558.1	558.1	558.0	558.0	558.0	557.9	557.9	557.9	557.8
	557.8	557.8	557.7	557.7	557.7	557.6	557.5	557.5	557.5	557.5
	557.4	557.4	557.4	557.3	557.3	557.3	557.2	557.2	557.2	557.1
	557.1	557.0	557.0	557.0	556.9	556.9	556.9	556.8	556.8	556.8
	556.7	556.7	556.6	556.6	556.6	556.5	556.5	556.5	556.4	556.4
	556.3	556.3	556.3	556.2	556.2	556.2	556.1	556.1	556.1	556.0
	555.9	555.8	555.7	555.5	555.1	554.7	554.4	554.1	553.8	553.6
	553.5	553.4								
0201	554.5	554.4	554.3	554.1	553.9	553.7	553.4	553.1	552.8	552.6
	552.4	552.3	552.2	552.2	552.2	552.1	552.1	552.0	552.0	552.0
	551.9	551.9	551.8	551.8	551.8	551.7	551.7	551.7	551.6	551.6
	551.5	551.5	551.5	551.4	551.4	551.3	551.3	551.3	551.2	551.2
	551.1	551.1	551.0	551.0	551.0	550.9	550.9	550.8	550.8	550.8
	550.7	550.7	550.6	550.6	550.5	550.5	550.5	550.4	550.4	550.3
	550.3	550.3	550.2	550.2	550.1	550.1	550.0	550.0	550.0	549.9
	549.8	549.7	549.5	549.3	548.9	548.5	548.1	547.7	547.4	547.2
	547.0	546.9								
0202	548.8	548.8	548.6	548.5	548.2	548.0	547.6	547.3	546.9	546.7
	546.5	546.4	546.3	546.3	546.2	546.2	546.2	546.1	546.1	546.0
	546.0	545.9	545.9	545.9	545.8	545.8	545.7	545.7	545.6	545.6
	545.5	545.5	545.5	545.4	545.4	545.3	545.3	545.2	545.2	545.1
	545.1	545.0	545.0	544.9	544.9	544.9	544.8	544.8	544.7	544.7
	544.6	544.6	544.5	544.5	544.4	544.4	544.3	544.3	544.2	544.2
	544.1	544.1	544.0	544.0	543.9	543.9	543.9	543.8	543.8	543.7
	543.6	543.5	543.3	543.0	542.5	542.0	541.6	541.2	540.8	540.5
	540.3	540.2								
0203	543.1	543.1	542.9	542.8	542.5	542.2	541.8	541.4	541.0	540.8
	540.6	540.5	540.4	540.3	540.3	540.2	540.2	540.1	540.1	540.0
	540.0	539.9	539.9	539.8	539.8	539.7	539.7	539.6	539.6	539.5
	539.5	539.4	539.4	539.3	539.3	539.2	539.2	539.1	539.1	539.0
	539.0	538.9	538.9	538.8	538.8	538.7	538.7	538.6	538.5	538.5
	538.4	538.4	538.3	538.3	538.2	538.2	538.1	538.1	538.0	538.0
	537.9	537.8	537.8	537.7	537.7	537.6	537.6	537.5	537.5	537.4
	537.3	537.1	536.9	536.6	536.1	535.5	534.9	534.4	534.0	533.7
	533.5	533.3								
0204	537.4	537.4	537.2	537.0	536.7	536.4	536.0	535.5	535.1	534.8
	534.6	534.4	534.3	534.3	534.2	534.2	534.1	534.1	534.0	534.0
	533.9	533.8	533.8	533.7	533.7	533.6	533.6	533.5	533.5	533.4
	533.3	533.3	533.2	533.2	533.1	533.1	533.0	532.9	532.9	532.8
	532.8	532.7	532.6	532.6	532.5	532.5	532.4	532.4	532.3	532.2
	532.2	532.1	532.0	532.0	531.9	531.9	531.8	531.7	531.7	531.6
	531.6	531.5	531.4	531.4	531.3	531.2	531.2	531.1	531.1	531.0
	530.9	530.7	530.4	530.0	529.5	528.8	528.1	527.6	527.1	526.7
	526.4	526.2								
0205	531.7	531.6	531.4	531.2	530.9	530.5	530.1	529.6	529.1	528.7
	528.5	528.4	528.2	528.2	528.1	528.1	528.0	527.9	527.9	527.8
	527.8	527.7	527.6	527.6	527.5	527.5	527.4	527.3	527.3	527.2
	527.1	527.1	527.0	527.0	526.9	526.8	526.8	526.7	526.6	526.6
	526.5	526.4	526.4	526.3	526.2	526.2	526.1	526.0	526.0	525.9
	525.8	525.8	525.7	525.6	525.5	525.5	525.4	525.3	525.3	525.2
	525.1	525.1	525.0	524.9	524.9	524.8	524.7	524.6	524.6	524.5
	524.4	524.2	523.9	523.4	522.7	521.9	521.2	520.5	519.9	519.4
	519.1	518.9								
0206	525.9	525.8	525.7	525.4	525.1	524.6	524.1	523.6	523.0	522.7
	522.4	522.2	522.1	522.0	522.0	521.9	521.8	521.8	521.7	521.6
	521.6	521.5	521.4	521.4	521.3	521.2	521.2	521.1	521.0	520.9
	520.9	520.8	520.7	520.7	520.6	520.5	520.4	520.4	520.3	520.2
	520.2	520.1	520.0	519.9	519.9	519.8	519.7	519.6	519.6	519.5
	519.4	519.3	519.3	519.2	519.1	519.0	518.9	518.9	518.8	518.7
	518.6	518.5	518.5	518.4	518.3	518.2	518.2	518.1	518.0	517.9
	517.7	517.5	517.2	516.7	515.9	515.0	514.1	513.3	512.5	511.9
	511.5	511.3								
0207	510.2	510.1	510.0	510.0	510.0	510.0	510.0	510.0	510.0	510.0
	516.3	516.1	515.9	515.8	515.8	515.7	515.6	515.5	515.5	515.4
	515.3	515.2	515.2	515.1	515.0	514.9	514.9	514.8	514.7	514.6
	514.6	514.5	514.4	514.3	514.2	514.2	514.1	514.0	513.9	513.8
	513.8	513.7	513.6	513.5	513.4	513.3	513.3	513.2	513.1	513.0
	512.9	512.8	512.7	512.7	512.6	512.5	512.4	512.3	512.2	512.1
	511.1	511.0	510.9	510.8	510.7	510.6	510.5	510.4	510.3	510.2
	503.6	503.3								
0208	514.4	514.3	514.1	513.7	513.3	512.8	512.2	511.5	510.8	510.4
	510.1	509.8	509.7	509.6	509.5	509.4	509.4	509.3	509.2	509.1
	509.0	508.9	508.9	508.8	508.7	508.6	508.5	508.4	508.3	508.3
	508.2	508.1	508.0	507.9	507.8	507.8	507.7	507.6	507.5	507.4
	507.3	507.2	507.1	507.0	506.9	506.8	506.7	506.6	506.5	506.5
	506.4	506.3	506.2	506.1	506.0	505.9	505.8	505.7	505.6	505.5
	505.4	505.3	505.2	505.1	505.0	504.9	504.8	504.7	504.6	504.5
	504.3	504.0	503.6	502.9	501.9	500.7	499.4	498.2	497.1	496.1
	495.4	495.0								
0209	508.6	508.5	508.3	507.9	507.4	506.8	506.2	505.4	504.7	504.2
	503.8	503.6	503.4	503.3	503.2	503.1	503.1	503.0	502.9	502.8
	502.7	502.6	502.5	502.4	502.3	502.3	502.2	502.1	502.0	501.9
	501.8	501.7	501.6	501.5	501.4	501.3	501.2	501.1	501.0	500.9
	500.8	500.7	500.6	500.5	500.4	500.3	500.2	500.1	500.0	499.9
	499.8	499.7	499.6	499.5	499.4	499.2	499.1	499.0	498.9	498.8
	498.7	498.6	498.5	498.4	498.3	498.2	498.0	497.9	497.8	497.7
	497.5	497.1	496.7	495.9	494.8	493.4	491.9	490.4	489.0	487.7
	486.7	486.1								
0210	502.9	502.8	502.5	502.1	501.6	500.9	500.2	499.3	498.5	498.0
	497.6	497.3	497.2	497.0	496.9	496.8	496.7	496.6	496.5	496.5
	496.4	496.3	496.2	496.1	496.0	495.9	495.8	495.7	495.6	495.5
	495.3	495.2	495.1	495.0	494.9	494.8	494.7	494.6	494.5	494.4
	494.3	494.2	494.0	493.						

	594.6	594.6	594.6	594.6	594.6	594.5	594.5	594.5	594.5	594.5	594.5
	594.4	594.4	594.3	594.2	594.1	594.0	593.8	593.7	593.6	593.6	593.6
	593.5	593.5									
0193	594.3	594.3	594.3	594.2	594.1	594.0	593.9	593.8	593.6	593.5	593.5
	593.5	593.4	593.4	593.4	593.4	593.4	593.3	593.3	593.3	593.3	593.3
	593.3	593.3	593.3	593.2	593.2	593.2	593.2	593.2	593.2	593.2	593.2
	593.1	593.1	593.1	593.1	593.1	593.0	593.0	593.0	593.0	593.0	593.0
	593.0	592.9	592.9	592.9	592.9	592.9	592.9	592.9	592.9	592.9	592.9
	592.8	592.8	592.8	592.8	592.7	592.7	592.7	592.7	592.7	592.7	592.7
	592.6	592.6	592.6	592.6	592.6	592.6	592.5	592.5	592.5	592.5	592.5
	592.5	592.4	592.3	592.3	592.1	592.0	591.8	591.7	591.6	591.5	591.5
	591.5	591.4									
0194	591.5	591.4	591.4	591.3	591.2	591.1	591.0	590.8	590.7	590.6	590.6
	590.5	590.5	590.5	590.5	590.4	590.4	590.4	590.4	590.4	590.4	590.4
	590.3	590.3	590.3	590.3	590.3	590.3	590.2	590.2	590.2	590.2	590.2
	590.2	590.2	590.1	590.1	590.1	590.1	590.1	590.0	590.0	590.0	590.0
	590.0	590.0	590.0	589.9	589.9	589.9	589.9	589.9	589.9	589.9	589.9
	589.8	589.8	589.8	589.8	589.8	589.7	589.7	589.7	589.7	589.7	589.7
	589.6	589.6	589.6	589.6	589.6	589.6	589.5	589.5	589.5	589.5	589.5
	589.5	589.4	589.3	589.2	589.1	588.9	588.8	588.6	588.5	588.4	588.4
	588.4	588.4									
0195	587.1	587.1	587.0	587.0	586.9	586.7	586.6	586.4	586.3	586.2	586.2
	586.1	586.1	586.0	586.0	586.0	586.0	586.0	585.9	585.9	585.9	585.9
	585.9	585.9	585.8	585.8	585.8	585.8	585.8	585.7	585.7	585.7	585.7
	585.7	585.7	585.7	585.6	585.6	585.6	585.6	585.6	585.5	585.5	585.5
	585.5	585.5	585.5	585.4	585.4	585.4	585.4	585.4	585.3	585.3	585.3
	585.3	585.3	585.3	585.2	585.2	585.2	585.2	585.2	585.1	585.1	585.1
	585.1	585.1	585.1	585.0	585.0	585.0	585.0	585.0	585.0	584.9	584.9
	584.9	584.8	584.8	584.6	584.5	584.3	584.1	584.0	583.9	583.8	583.8
	583.7	583.7									
0196	581.8	581.8	581.8	581.7	581.6	581.4	581.2	581.1	580.9	580.8	580.8
	580.7	580.6	580.6	580.6	580.6	580.5	580.5	580.5	580.5	580.5	580.5
	580.4	580.4	580.4	580.4	580.3	580.3	580.3	580.3	580.3	580.3	580.3
	580.2	580.2	580.2	580.2	580.1	580.1	580.1	580.1	580.0	580.0	580.0
	580.0	580.0	580.0	579.9	579.9	579.9	579.9	579.8	579.8	579.8	579.8
	579.8	579.8	579.7	579.7	579.7	579.7	579.6	579.6	579.6	579.6	579.6
	579.6	579.5	579.5	579.5	579.5	579.4	579.4	579.4	579.4	579.4	579.4
	579.3	579.3	579.2	579.0	578.8	578.6	578.4	578.3	578.1	578.0	578.0
	577.9	577.9									
0197	576.5	576.5	576.4	576.3	576.2	576.0	575.8	575.6	575.4	575.3	575.3
	575.2	575.1	575.1	575.1	575.0	575.0	575.0	575.0	574.9	574.9	574.9
	574.9	574.9	574.8	574.8	574.8	574.8	574.8	574.7	574.7	574.7	574.7
	574.7	574.6	574.6	574.6	574.6	574.5	574.5	574.5	574.5	574.4	574.4
	574.4	574.4	574.4	574.3	574.3	574.3	574.3	574.2	574.2	574.2	574.2
	574.2	574.1	574.1	574.1	574.1	574.0	574.0	574.0	574.0	573.9	573.9
	573.9	573.9	573.9	573.8	573.8	573.8	573.8	573.7	573.7	573.7	573.7
	573.6	573.6	573.5	573.3	573.1	572.8	572.6	572.4	572.3	572.1	572.1
	572.1	572.0									
0198	571.1	571.0	571.0	570.8	570.7	570.5	570.3	570.1	569.9	569.7	569.7
	569.6	569.5	569.5	569.5	569.4	569.4	569.4	569.4	569.3	569.3	569.3
	569.3	569.2	569.2	569.2	569.2	569.1	569.1	569.1	569.1	569.0	569.0
	569.0	569.0	569.0	568.9	568.9	568.9	568.8	568.8	568.8	568.8	568.8
	568.7	568.7	568.7	568.6	568.6	568.6	568.5	568.5	568.5	568.5	568.5
	568.4	568.4	568.4	568.4	568.3	568.3	568.3	568.2	568.2	568.2	568.2
	568.2	568.1	568.1	568.1	568.0	568.0	568.0	568.0	567.9	567.9	567.9
	567.8	567.8	567.6	567.5	567.2	566.9	566.7	566.5	566.3	566.1	566.1
	566.0	566.0									
0199	565.6	565.5	565.5	565.3	565.2	565.0	564.7	564.5	564.2	564.1	564.1
	564.0	563.9	563.8	563.8	563.8	563.7	563.7	563.7	563.6	563.6	563.6
	563.6	563.5	563.5	563.5	563.5	563.4	563.4	563.4	563.3	563.3	563.3
	563.3	563.2	563.2	563.2	563.1	563.1	563.1	563.0	563.0	563.0	563.0
	562.9	562.9	562.9	562.9	562.8	562.8	562.8	562.7	562.7	562.7	562.7
	562.6	562.6	562.6	562.5	562.5	562.5	562.4	562.4	562.4	562.3	562.3
	562.3	562.3	562.2	562.2	562.2	562.1	562.1	562.1	562.0	562.0	562.0
	561.9	561.8	561.7	561.5	561.2	560.9	560.6	560.3	560.1	560.0	560.0
	559.8	559.8									
0200	558.0	558.0	559.9	559.8	559.6	559.4	559.1	558.8	558.5	558.3	558.3
	558.2	558.1	558.1	558.0	558.0	558.0	557.9	557.9	557.9	557.8	557.8
	557.8	557.8	557.7	557.7	557.6	557.6	557.6	557.5	557.5	557.5	557.5
	557.4	557.4	557.4	557.3	557.3	557.3	557.2	557.2	557.2	557.1	557.1
	557.1	557.0	557.0	557.0	556.9	556.9	556.9	556.8	556.8	556.8	556.8
	556.7	556.7	556.6	556.6	556.6	556.5	556.5	556.5	556.4	556.4	556.4
	556.3	556.3	556.3	556.2	556.2	556.2	556.1	556.1	556.0	556.0	556.0
	555.9	555.8	555.7	555.4	555.1	554.7	554.4	554.1	553.8	553.6	553.6
	553.5	553.4									
0201	554.4	554.4	554.3	554.1	553.9	553.7	553.4	553.1	552.8	552.6	552.6
	552.4	552.3	552.2	552.2	552.1	552.1	552.1	552.0	552.0	552.0	552.0
	551.9	551.9	551.8	551.8	551.8	551.7	551.7	551.7	551.6	551.6	551.6
	551.5	551.5	551.5	551.4	551.4	551.3	551.3	551.2	551.2	551.2	551.2
	551.1	551.1	551.0	551.0	551.0	550.9	550.9	550.8	550.8	550.8	550.8
	550.7	550.7	550.6	550.6	550.5	550.5	550.4	550.4	550.4	550.3	550.3
	550.3	550.2	550.2	550.2	550.1	550.1	550.0	550.0	550.0	549.9	549.9
	549.8	549.7	549.5	549.3	548.9	548.5	548.1	547.7	547.4	547.2	547.2
	547.0	546.9									
0202	548.8	548.8	548.6	548.5	548.2	548.0	547.6	547.3	546.9	546.7	546.7
	546.5	546.4	546.3	546.3	546.2	546.2	546.2	546.1	546.1	546.0	546.0
	546.0	545.9	545.9	545.9	545.8	545.8	545.7	545.7	545.6	545.6	545.6
	545.5	545.5	545.5	545.4	545.4	545.3	545.3	545.2	545.2	545.1	545.1
	545.1	545.0	545.0	544.9	544.9	544.9	544.8	544.8	544.7	544.7	544.7
	544.6	544.6	544.5	544.5	544.4	544.4	544.3	544.3	544.2	544.2	544.2
	544.1	544.1	544.0	544.0	543.9	543.9	543.9	543.8	543.8	543.7	543.7
	543.6	543.5	543.3	543.0	542.5	542.0	541.6	541.1	540.8	540.5	540.5
	540.3	540.2									
0203	543.1	543.1	542.9	542.7	542.5	542.2	541.8	541.4	541.0	540.8	540.8
	540.6	540.4	540.4	540.3	540.3	540.2	540.2	540.1	540.1	540.0	540.0
	540.0	539.9	539.9	539.8	539.8	539.7	539.7	539.6	539.6	539.5	539.5
	539.5	539.4	539.4	539.3	539.3	539.2	539.2	539.1	539.1	539.0	539.0
	539.0	538.9	538.9	538.8	538.8	538.7	538.6	538.6	538.5	538.5	538.5
	538.4	538.4	538.3	538.3	538.2	538.2	538.1	538.1	538.0	537.9	537.9
	537.9	537.8	537.8	537.7	537.7	537.6	537.6	537.5	537.5	537.4	537.4
	537.3	537.1	536.9	536.6	536.1	535.5	534.9	534.4	534.0	533.7	533.7
	533.5	533.3									
0204	537.4	537.3	537.2	537.0	536.7	536.4	536.0	535.5	535.1	534.8	534.8
	534.6	534.4	534.3	534.3	534.2	534.2	534.1	534.1	534.0	534.0	534.0
	533.9	533.8	533.8	533.7	533.7	533.6	533.6	533.5	533.5	533.4	533.4
	533.3	533.3	533.2	533.2	533.1	533.1	533.0	532.9	532.9	532.8	532.8
	532.8	532.7	532.6	532.6	532.5	532.5	532.4	532.3	532.3	532.2	532.2
	532.2	532.1	532.0	532.0	531.9	531.9	531.8	531.7	531.7	531.6	531.6
	531.6	531.5	531.4	531.4	531.3	531.2	531.2	531			


```

1000. 1000. 1000. 1000. 1000. 1000. 1000. 1000. 1000. 1000.
1000. 1000.
0220 455.0 1000. 1000. 1000. 1000. 1000. 1000. 1000. 1000.
1000. 1000. 1000. 1000. 1000. 1000. 1000. 1000. 1000.
1000. 1000. 1000. 1000. 1000. 1000. 1000. 1000. 1000.
1000. 1000. 1000. 1000. 1000. 1000. 1000. 1000. 1000.
1000. 1000. 1000. 1000. 1000. 1000. 1000. 1000. 1000.
1000. 1000. 1000. 1000. 1000. 1000. 1000. 1000. 1000.
1000. 1000. 1000. 1000. 1000. 1000. 1000. 1000. 1000.
1000. 1000.

```

0 HEAD WILL BE SAVED ON UNIT 42 AT END OF TIME STEP 1, STRESS PERIOD 1

```

0
          VOLUMETRIC BUDGET FOR ENTIRE MODEL AT END OF TIME STEP 1 IN STRESS PERIOD 1
          -----
          CUMULATIVE VOLUMES          L**3          RATES FOR THIS TIME STEP          L**3/T
          -----
          IN:
          ---
          STORAGE = 0.00000
          CONSTANT HEAD = 0.00000
          RECHARGE = 2003.9
          TOTAL IN = 2003.9
          OUT:
          ---
          STORAGE = 0.00000
          CONSTANT HEAD = 2004.0
          RECHARGE = 0.00000
          TOTAL OUT = 2004.0
          IN - OUT = -0.77393E-01
          PERCENT DISCREPANCY = 0.00
          -----
          IN:
          ---
          STORAGE = 0.00000
          CONSTANT HEAD = 0.00000
          RECHARGE = 2003.9
          TOTAL IN = 2003.9
          OUT:
          ---
          STORAGE = 0.00000
          CONSTANT HEAD = 2004.0
          RECHARGE = 0.00000
          TOTAL OUT = 2004.0
          IN - OUT = -0.77393E-01
          PERCENT DISCREPANCY = 0.00

```

0

```

TIME SUMMARY AT END OF TIME STEP 1 IN STRESS PERIOD 1
          TIME STEP LENGTH = 1.00000
          STRESS PERIOD TIME = 1.00000
          TOTAL SIMULATION TIME = 1.00000

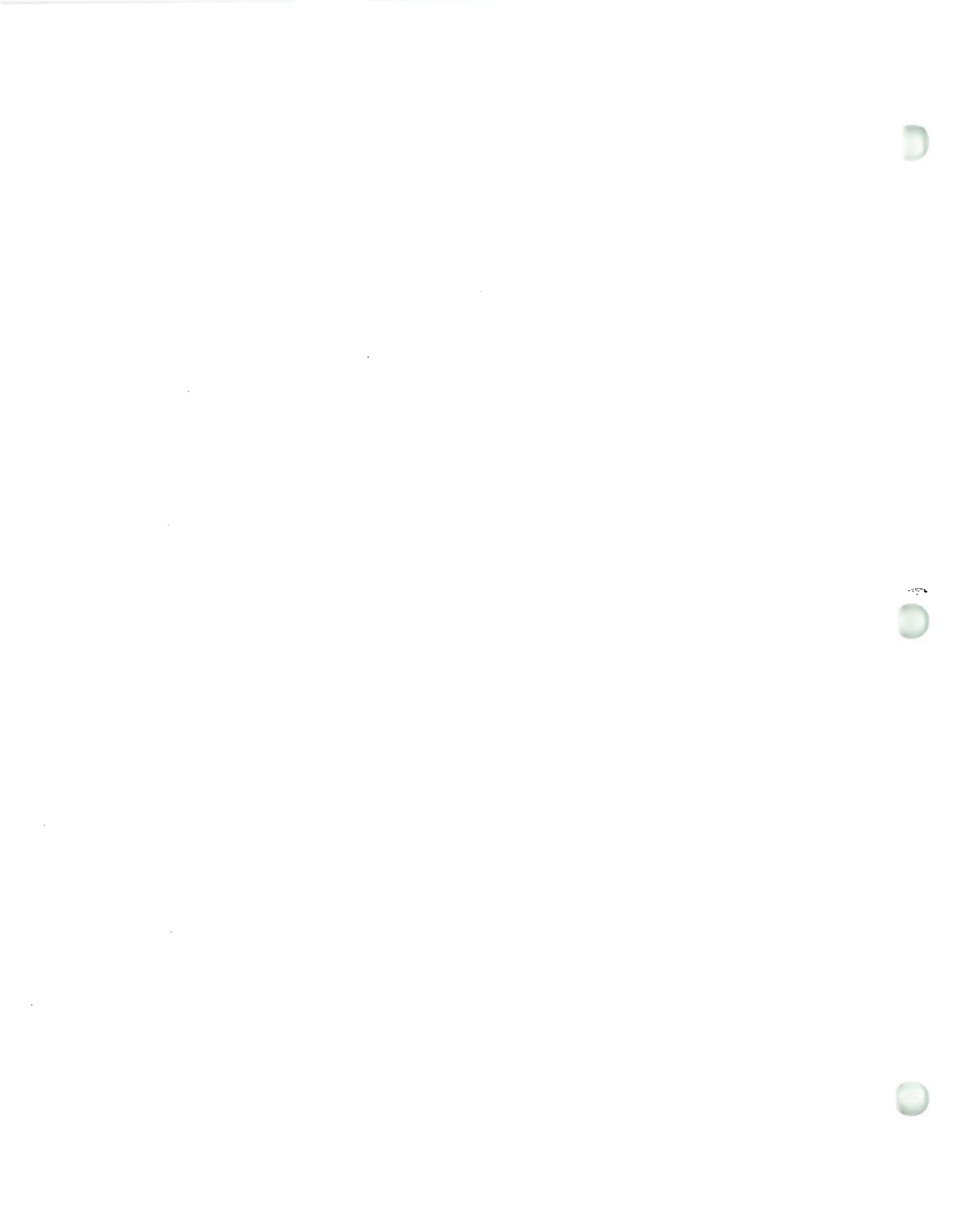
```

1

APPENDIX D

MODFLOW Model Sensitivity Analysis Results

- **Sensitivity of Heads to Net Recharge**
- **Sensitivity of Heads to K_h**
- **Sensitivity of Heads to K_v**



- **Sensitivity of Header to Net Recharge**



Sensitivity of Heads to Net Recharge

WELL	MODEL COLUMN	MODEL ROW	MODEL LAYER	MEAS. HIGH	MEAS. LOW	TARGET MEAN	TARGET HIGH	TARGET LOW	0%		
									Recharge: MODEL HEAD	1.332E-05 Difference (feet)	(ft/day) Absolute Difference
MW25-3	4	9	1	742.41	742.41	740.75	743.75	737.75	736.1	-4.7	4.7
MW64A-1	82	11	1	736.63	736.63	737.87	740.87	734.87	734.0	-3.9	3.9
MW64A-3	82	12	1	734.08	734.08	735.32	738.32	732.32	733.2	-2.1	2.1
MW17-1	4	15	1	733.47	733.47	731.81	734.81	728.81	730.8	-1.0	1.0
MW16-1	2	13	1	732.14	732.14	730.97	733.97	727.97	732.9	1.9	1.9
MW16-2	2	14	1	731.01	731.01	729.84	732.84	726.84	731.9	2.1	2.1
MW17-3	4	16	1	729.77	729.77	728.11	731.11	725.11	729.5	1.4	1.4
GHOST19	42	18	1	NA	NA	715.00	718.00	712.00	726.7	11.7	11.7
GHOST20	42	18	2	NA	NA	714.00	717.00	711.00	726.7	12.7	12.7
GHOST21	42	18	3	NA	NA	713.00	716.00	710.00	726.7	13.7	13.7
GHOST1	77	28	1	NA	NA	695.00	698.00	692.00	707.3	12.3	12.3
GHOST4	9	27	1	NA	NA	695.00	698.00	692.00	709.8	14.8	14.8
GHOST5	9	27	2	NA	NA	694.00	697.00	691.00	709.8	15.8	15.8
GHOST2	77	28	2	NA	NA	694.00	697.00	691.00	707.3	13.3	13.3
GHOST3	77	28	3	NA	NA	693.00	696.00	690.00	707.3	14.3	14.3
GHOST6	9	27	3	NA	NA	693.00	696.00	690.00	709.8	16.8	16.8
MW-41D	11	42	2	687.96	685.74	686.82	687.32	686.32	663.9	-22.9	22.9
MW-42D	70	43	2	680.66	674.94	678.34	678.84	677.84	660.6	-17.7	17.7
PT-10	47	44	2	677.79	670.57	673.51	674.01	673.01	658.5	-15.0	15.0
MW64D-1	77	44	1	665.03	664.36	663.37	663.87	662.87	658.3	-5.1	5.1
MW-39	17	61	1	657.99	656.37	657.12	657.62	656.62	650.4	-6.7	6.7
MW-60	72	62	1	658.13	654.83	656.99	657.49	656.49	649.8	-7.2	7.2
MW64D-4	79	59	1	657.39	655.10	655.73	656.23	655.23	650.7	-5.0	5.0
MW-40	46	65	1	656.40	652.18	654.55	655.05	654.05	648.8	-5.8	5.8
MW-59	71	65	1	654.95	651.61	653.78	654.28	653.28	648.7	-5.1	5.1
MW-43	35	63	1	655.42	652.46	653.76	654.26	653.26	649.6	-4.2	4.2
PT-11	66	66	1	654.02	648.49	651.68	652.18	651.18	648.4	-3.3	3.3
PT-18	46	72	1	651.78	646.72	649.85	650.35	649.35	646.2	-3.7	3.7
MW-44	34	73	1	648.63	646.98	648.59	649.09	648.09	645.9	-2.7	2.7
MW-45	24	82	1	648.47	644.75	646.88	647.38	646.38	642.6	-4.3	4.3
MW-46	34	83	1	647.28	642.61	645.62	646.12	645.12	642.2	-3.4	3.4
MW-49D	34	83	2	647.11	642.74	645.45	645.95	644.95	642.2	-3.3	3.3
MW64D-3	77	72	1	646.91	645.89	645.25	645.75	644.75	646.0	0.7	0.7
PT-12	44	81	1	647.25	641.73	644.90	645.40	644.40	642.9	-2.0	2.0
MW-50D	34	83	3	646.39	642.90	644.73	645.23	644.23	642.2	-2.5	2.5
MW-48	26	89	1	645.47	641.57	643.75	644.25	643.25	639.9	-3.9	3.9
PT-21	43	88	2	647.51	635.37	641.03	641.53	640.53	640.2	-0.8	0.8
PT-22	43	88	1	645.45	637.85	640.95	641.45	640.45	640.2	-0.7	0.7
PT-19	58	85	1	642.35	637.81	640.17	640.67	639.67	641.3	1.1	1.1
PT-20	51	89	1	644.21	636.11	640.02	640.52	639.52	639.8	-0.2	0.2
MW-32	58	96	1	637.84	632.40	635.11	635.61	634.61	637.0	1.9	1.9
PT-23	30	101	1	638.71	632.56	635.05	635.55	634.55	635.2	0.1	0.1
PT-17	53	100	1	636.85	630.12	634.21	634.71	633.71	635.5	1.3	1.3
MW-38D	18	107	2	634.67	632.76	633.97	634.47	633.47	632.9	-1.1	1.1
MW-27	33	103	1	635.62	630.37	633.45	633.95	632.95	634.4	0.9	0.9
PT-16	18	107	1	635.06	630.17	633.43	633.93	632.93	632.9	-0.5	0.5
MW-33	63	98	1	635.95	630.02	633.41	633.91	632.91	636.2	2.8	2.8
MW-30	56	101	1	636.37	629.73	633.13	633.63	632.63	635.1	2.0	2.0
MW64D-2	75	92	1	633.49	630.75	631.83	632.33	631.33	638.4	6.6	6.6
MW-55D	47	103	3	633.37	630.23	631.71	632.21	631.21	634.3	2.6	2.6
MW-31	61	103	1	634.60	627.21	631.64	632.14	631.14	634.3	2.7	2.7
MW-54D	47	103	2	633.29	629.88	631.63	632.13	631.13	634.3	2.7	2.7
MW-28	36	105	1	633.28	628.26	631.58	632.08	631.08	633.6	2.0	2.0
MW-53	47	103	1	632.83	630.13	631.17	631.67	630.67	634.4	3.2	3.2
PT-24	40	109	1	633.19	627.85	631.02	631.52	630.52	632.0	1.0	1.0
PT-25	64	104	1	633.66	625.45	630.56	631.06	630.06	633.9	3.3	3.3
PT-15	71	99	1	634.09	627.40	630.35	630.85	629.85	635.8	5.5	5.5
MW-29	46	107	1	631.82	626.83	630.19	630.69	629.69	632.8	2.6	2.6
MW-37	7	116	1	630.91	626.65	629.14	629.64	628.64	629.6	0.5	0.5
MW-35D	61	114	2	629.66	628.01	629.08	629.58	628.58	629.9	0.8	0.8
MW-36	61	114	1	629.94	626.43	629.02	629.52	628.52	629.9	0.9	0.9
MW-34	75	100	1	630.28	626.39	628.38	628.88	627.88	635.3	6.9	6.9
MW-56	48	119	1	627.78	626.67	627.27	627.77	626.77	627.9	0.6	0.6
MW-57D	48	119	2	628.60	627.11	626.94	627.44	626.44	627.9	1.0	1.0
MW-58D	48	119	3	628.53	625.66	626.87	627.37	626.37	627.9	1.0	1.0

MW-51D	35	128	2	625.68	621.56	624.02	624.52	623.52	624.3	0.3	0.3
MW-47	35	128	1	625.69	621.47	623.96	624.46	623.46	624.3	0.3	0.3
MW-52D	35	128	3	624.20	620.04	622.54	623.04	622.04	624.3	1.8	1.8
PT-26	73	174	1	611.82	603.10	608.28	608.78	607.78	604.0	-4.3	4.3
GHOST22	42	174	1	NA	NA	601.00	604.00	598.00	604.5	3.5	3.5
GHOST23	42	174	2	NA	NA	600.00	603.00	597.00	604.5	4.5	4.5
GHOST24	42	174	3	NA	NA	599.00	602.00	596.00	604.5	5.5	5.5
GHOST10	7	199	1	NA	NA	575.00	578.00	572.00	560.6	-14.4	14.4
GHOST7	77	198	1	NA	NA	575.00	578.00	572.00	566.7	-8.3	8.3
GHOST8	77	198	2	NA	NA	574.00	577.00	571.00	566.7	-7.3	7.3
GHOST11	7	199	2	NA	NA	574.00	577.00	571.00	564.7	-9.3	9.3
GHOST9	77	198	3	NA	NA	573.00	576.00	570.00	566.7	-6.3	6.3
GHOST12	7	199	3	NA	NA	573.00	576.00	570.00	564.7	-8.3	8.3
GHOST16	6	213	1	NA	NA	515.00	518.00	512.00	483.2	-31.8	31.8
GHOST17	6	213	2	NA	NA	514.00	517.00	511.00	483.2	-30.8	30.8
GHOST18	6	213	3	NA	NA	513.00	516.00	510.00	483.2	-29.8	29.8
GHOST13	74	211	1	NA	NA	495.00	498.00	492.00	481.8	-13.2	13.2
GHOST14	74	211	2	NA	NA	494.00	497.00	491.00	481.8	-12.2	12.2
GHOST15	74	211	3	NA	NA	493.00	496.00	490.00	481.8	-11.2	11.2

Statistical Calculations:

Monitoring Wells Only	
ME=	-1.58
MAE=	4.03

Sensitivity of Heads to Net Recharge

WELL	MODEL COLUMN	MODEL ROW	MODEL LAYER	MEAS. HIGH	MEAS. LOW	TARGET MEAN	TARGET HIGH	TARGET LOW	Recharge: -5%		
									MODEL HEAD	1.260E-05 Difference (feet)	(ft/day) Absolute Difference
MW25-3	4	9	1	742.41	742.41	740.75	743.75	737.75	720.9	-19.9	19.9
MW64A-1	82	11	1	736.63	736.63	737.87	740.87	734.87	718.9	-19.0	19.0
MW64A-3	82	12	1	734.08	734.08	735.32	738.32	732.32	718.2	-17.1	17.1
MW17-1	4	15	1	733.47	733.47	731.81	734.81	728.81	715.9	-15.9	15.9
MW16-1	2	13	1	732.14	732.14	730.97	733.97	727.97	717.9	-13.1	13.1
MW16-2	2	14	1	731.01	731.01	729.84	732.84	726.84	716.9	-12.9	12.9
MW17-3	4	16	1	729.77	729.77	728.11	731.11	725.11	714.7	-13.4	13.4
GHOST19	42	18	1	NA	NA	715.00	718.00	712.00	712.0	-3.0	3.0
GHOST20	42	18	2	NA	NA	714.00	717.00	711.00	712.0	-2.0	2.0
GHOST21	42	18	3	NA	NA	713.00	716.00	710.00	712.0	-1.0	1.0
GHOST1	77	28	1	NA	NA	695.00	698.00	692.00	693.7	-1.3	1.3
GHOST4	9	27	1	NA	NA	695.00	698.00	692.00	696.0	1.0	1.0
GHOST5	9	27	2	NA	NA	694.00	697.00	691.00	696.0	2.0	2.0
GHOST2	77	28	2	NA	NA	694.00	697.00	691.00	693.7	-0.3	0.3
GHOST3	77	28	3	NA	NA	693.00	696.00	690.00	693.7	0.7	0.7
GHOST6	9	27	3	NA	NA	693.00	696.00	690.00	696.0	3.0	3.0
MW-41D	11	42	2	687.96	685.74	686.82	687.32	686.32	632.6	-34.2	34.2
MW-42D	70	43	2	680.66	674.94	678.34	678.84	677.84	649.5	-28.8	28.8
PT-10	47	44	2	677.79	670.57	673.51	674.01	673.01	647.5	-26.0	26.0
MW64D-1	77	44	1	665.03	664.36	663.37	663.87	662.87	647.3	-16.1	16.1
MW-39	17	61	1	657.99	656.37	657.12	657.62	656.62	639.8	-17.3	17.3
MW-60	72	62	1	658.13	654.83	656.99	657.49	656.49	639.3	-17.7	17.7
MW64D-4	79	59	1	657.39	655.10	655.73	656.23	655.23	640.2	-15.5	15.5
MW-40	46	65	1	656.40	652.18	654.55	655.05	654.05	638.3	-16.3	16.3
MW-59	71	65	1	654.95	651.61	653.78	654.28	653.28	638.2	-15.6	15.6
MW-43	35	63	1	655.42	652.46	653.76	654.26	653.26	639.1	-14.7	14.7
PT-11	66	66	1	654.02	648.49	651.68	652.18	651.18	637.9	-13.8	13.8
PT-18	46	72	1	651.78	646.72	649.85	650.35	649.35	635.9	-14.0	14.0
MW-44	34	73	1	648.63	646.98	648.59	649.09	648.09	635.6	-13.0	13.0
MW-45	24	82	1	648.47	644.75	646.88	647.38	646.38	632.4	-14.5	14.5
MW-46	34	83	1	647.28	642.61	645.62	646.12	645.12	632.0	-13.6	13.6
MW-49D	34	83	2	647.11	642.74	645.45	645.95	644.95	632.0	-13.5	13.5
MW64D-3	77	72	1	646.91	645.89	645.25	645.75	644.75	635.7	-9.6	9.6
PT-12	44	81	1	647.25	641.73	644.90	645.40	644.40	632.7	-12.2	12.2
MW-50D	34	83	3	646.39	642.90	644.73	645.23	644.23	632.0	-12.7	12.7
MW-48	26	89	1	645.47	641.57	643.75	644.25	643.25	629.9	-13.9	13.9
PT-21	43	88	2	647.51	635.37	641.03	641.53	640.53	630.2	-10.8	10.8
PT-22	43	88	1	645.45	637.85	640.95	641.45	640.45	630.2	-10.7	10.7
PT-19	58	85	1	642.35	637.81	640.17	640.67	639.67	631.2	-9.0	9.0
PT-20	51	89	1	644.21	636.11	640.02	640.52	639.52	629.8	-10.2	10.2
MW-32	58	96	1	637.84	632.40	635.11	635.61	634.61	627.2	-7.9	7.9
PT-23	30	101	1	638.71	632.56	635.05	635.55	634.55	625.5	-9.6	9.6
PT-17	53	100	1	636.85	630.12	634.21	634.71	633.71	627.7	-8.5	8.5
MW-38D	18	107	2	634.67	632.76	633.97	634.47	633.47	623.3	-10.7	10.7
MW-27	33	103	1	635.62	630.37	633.45	633.95	632.95	624.7	-8.8	8.8
PT-16	18	107	1	635.06	630.17	633.43	633.93	632.93	623.3	-10.1	10.1
MW-33	63	98	1	635.95	630.02	633.41	633.91	632.91	626.4	-7.0	7.0
MW-30	56	101	1	636.37	629.73	633.13	633.63	632.63	625.4	-7.7	7.7
MW64D-2	75	92	1	633.49	630.75	631.83	632.33	631.33	628.5	-3.3	3.3
MW-55D	47	103	3	633.37	630.23	631.71	632.21	631.21	624.7	-7.0	7.0
MW-31	61	103	1	634.60	627.21	631.64	632.14	631.14	624.6	-7.0	7.0
MW-54D	47	103	2	633.29	629.88	631.63	632.13	631.13	624.7	-6.9	6.9
MW-28	36	105	1	633.28	628.26	631.58	632.08	631.08	624.0	-7.6	7.6
MW-53	47	103	1	632.83	630.13	631.17	631.67	630.67	624.7	-6.5	6.5
PT-24	40	109	1	633.19	627.85	631.02	631.52	630.52	622.4	-8.6	8.6
PT-25	64	104	1	633.66	625.45	630.56	631.06	630.06	624.2	-6.4	6.4
PT-15	71	99	1	634.09	627.40	630.35	630.85	629.85	626.0	-4.3	4.3
MW-29	46	107	1	631.82	626.83	630.19	630.69	629.69	623.2	-7.0	7.0
MW-37	7	116	1	630.91	626.65	629.14	629.64	628.64	620.1	-9.0	9.0
MW-35D	61	114	2	629.66	628.01	629.08	629.58	628.58	620.4	-8.7	8.7
MW-36	61	114	1	629.94	626.43	629.02	629.52	628.52	620.4	-8.6	8.6
MW-34	75	100	1	630.28	626.39	628.38	628.88	627.88	625.5	-2.9	2.9
MW-56	48	119	1	627.78	626.67	627.27	627.77	626.77	618.6	-8.7	8.7
MW-57D	48	119	2	628.60	627.11	626.94	627.44	626.44	618.6	-8.3	8.3
MW-58D	48	119	3	628.53	625.66	626.87	627.37	626.37	618.6	-8.3	8.3

MW-51D	35	128	2	625.68	621.56	624.02	624.52	623.52	615.2	-8.8	8.8
MW-47	35	128	1	625.69	621.47	623.96	624.46	623.46	615.2	-8.8	8.8
MW-52D	35	128	3	624.20	620.04	622.54	623.04	622.04	615.2	-7.3	7.3
PT-26	73	174	1	611.82	603.10	608.28	608.78	607.78	596.0	-12.3	12.3
GHOST22	42	174	1	NA	NA	601.00	604.00	598.00	596.4	-4.6	4.6
GHOST23	42	174	2	NA	NA	600.00	603.00	597.00	596.4	-3.6	3.6
GHOST24	42	174	3	NA	NA	599.00	602.00	596.00	596.4	-2.6	2.6
GHOST10	7	199	1	NA	NA	575.00	578.00	572.00	558.8	-16.2	16.2
GHOST7	77	198	1	NA	NA	575.00	578.00	572.00	560.6	-14.4	14.4
GHOST8	77	198	2	NA	NA	574.00	577.00	571.00	560.6	-13.4	13.4
GHOST11	7	199	2	NA	NA	574.00	577.00	571.00	558.8	-15.2	15.2
GHOST9	77	198	3	NA	NA	573.00	576.00	570.00	560.6	-12.4	12.4
GHOST12	7	199	3	NA	NA	573.00	576.00	570.00	558.8	-14.2	14.2
GHOST16	6	213	1	NA	NA	515.00	518.00	512.00	481.7	-33.3	33.3
GHOST17	6	213	2	NA	NA	514.00	517.00	511.00	481.7	-32.3	32.3
GHOST18	6	213	3	NA	NA	513.00	516.00	510.00	481.7	-31.3	31.3
GHOST13	74	211	1	NA	NA	495.00	498.00	492.00	480.4	-14.6	14.6
GHOST14	74	211	2	NA	NA	494.00	497.00	491.00	480.4	-13.6	13.6
GHOST15	74	211	3	NA	NA	493.00	496.00	490.00	480.4	-12.6	12.6

Statistical Calculations:

Monitoring Wells Only	
MAE=	-13.95
MAE=	13.95

Sensitivity of Heads to Net Recharge

WELL	MODEL COLUMN	MODEL ROW	MODEL LAYER	MEAS. HIGH	MEAS. LOW	TARGET MEAN	TARGET HIGH	TARGET LOW	-15%		
									Recharge: MODEL HEAD	1.132E-05 Difference (feet)	(ft/day) Absolute Difference
MW25-3	4	9	1	742.41	742.41	740.75	743.75	737.75	693.9	-46.9	46.9
MW64A-1	82	11	1	736.63	736.63	737.87	740.87	734.87	692.1	-45.8	45.8
MW64A-3	82	12	1	734.08	734.08	735.32	738.32	732.32	691.4	-43.9	43.9
MW17-1	4	15	1	733.47	733.47	731.81	734.81	728.81	689.4	-42.4	42.4
MW16-1	2	13	1	732.14	732.14	730.97	733.97	727.97	691.2	-39.8	39.8
MW16-2	2	14	1	731.01	731.01	729.84	732.84	726.84	690.3	-39.5	39.5
MW17-3	4	16	1	729.77	729.77	728.11	731.11	725.11	688.3	-39.8	39.8
GHOST19	42	18	1	NA	NA	715.00	718.00	712.00	685.9	-29.1	29.1
GHOST20	42	18	2	NA	NA	714.00	717.00	711.00	685.9	-28.1	28.1
GHOST21	42	18	3	NA	NA	713.00	716.00	710.00	685.9	-27.1	27.1
GHOST1	77	28	1	NA	NA	695.00	698.00	692.00	669.4	-25.6	25.6
GHOST4	9	27	1	NA	NA	695.00	698.00	692.00	671.5	-23.5	23.5
GHOST5	9	27	2	NA	NA	694.00	697.00	691.00	671.5	-22.5	22.5
GHOST2	77	28	2	NA	NA	694.00	697.00	691.00	669.4	-24.6	24.6
GHOST3	77	28	3	NA	NA	693.00	696.00	690.00	669.4	-23.6	23.6
GHOST6	9	27	3	NA	NA	693.00	696.00	690.00	671.5	-21.5	21.5
MW-41D	11	42	2	687.96	685.74	686.82	687.32	686.32	632.6	-54.2	54.2
MW-42D	70	43	2	680.66	674.94	678.34	678.84	677.84	629.7	-48.6	48.6
PT-10	47	44	2	677.79	670.57	673.51	674.01	673.01	627.9	-45.6	45.6
MW64D-1	77	44	1	665.03	664.36	663.37	663.87	662.87	627.8	-35.6	35.6
MW-39	17	61	1	657.99	656.37	657.12	657.62	656.62	621.0	-36.1	36.1
MW-60	72	62	1	658.13	654.83	656.99	657.49	656.49	620.6	-36.4	36.4
MW64D-4	79	59	1	657.39	655.10	655.73	656.23	655.23	621.3	-34.4	34.4
MW-40	46	65	1	656.40	652.18	654.55	655.05	654.05	619.7	-34.9	34.9
MW-59	71	65	1	654.95	651.61	653.78	654.28	653.28	619.6	-34.2	34.2
MW-43	35	63	1	655.42	652.46	653.76	654.26	653.26	620.4	-33.4	33.4
PT-11	66	66	1	654.02	648.49	651.68	652.18	651.18	619.3	-32.4	32.4
PT-18	46	72	1	651.78	646.72	649.85	650.35	649.35	617.5	-32.4	32.4
MW-44	34	73	1	648.63	646.98	648.59	649.09	648.09	617.2	-31.4	31.4
MW-45	24	82	1	648.47	644.75	646.88	647.38	646.38	614.4	-32.5	32.5
MW-46	34	83	1	647.28	642.61	645.62	646.12	645.12	614.1	-31.5	31.5
MW-49D	34	83	2	647.11	642.74	645.45	645.95	644.95	614.1	-31.4	31.4
MW64D-3	77	72	1	646.91	645.89	645.25	645.75	644.75	617.3	-28.0	28.0
PT-12	44	81	1	647.25	641.73	644.90	645.40	644.40	614.7	-30.2	30.2
MW-50D	34	83	3	646.39	642.90	644.73	645.23	644.23	614.1	-30.6	30.6
MW-48	26	89	1	645.47	641.57	643.75	644.25	643.25	612.1	-31.7	31.7
PT-21	43	88	2	647.51	635.37	641.03	641.53	640.53	612.4	-28.6	28.6
PT-22	43	88	1	645.45	637.85	640.95	641.45	640.45	612.4	-28.5	28.5
PT-19	58	85	1	642.35	637.81	640.17	640.67	639.67	613.3	-26.9	26.9
PT-20	51	89	1	644.21	636.11	640.02	640.52	639.52	612.0	-28.0	28.0
MW-32	58	96	1	637.84	632.40	635.11	635.61	634.61	609.7	-25.4	25.4
PT-23	30	101	1	638.71	632.56	635.05	635.55	634.55	608.2	-26.9	26.9
PT-17	53	100	1	636.85	630.12	634.21	634.71	633.71	608.4	-25.8	25.8
MW-38D	18	107	2	634.67	632.76	633.97	634.47	633.47	606.2	-27.8	27.8
MW-27	33	103	1	635.62	630.37	633.45	633.95	632.95	607.5	-26.0	26.0
PT-16	18	107	1	635.06	630.17	633.43	633.93	632.93	606.2	-27.2	27.2
MW-33	63	98	1	635.95	630.02	633.41	633.91	632.91	609.0	-24.4	24.4
MW-30	56	101	1	636.37	629.73	633.13	633.63	632.63	608.1	-25.0	25.0
MW64D-2	75	92	1	633.49	630.75	631.83	632.33	631.33	610.9	-20.9	20.9
MW-55D	47	103	3	633.37	630.23	631.71	632.21	631.21	607.4	-24.3	24.3
MW-31	61	103	1	634.60	627.21	631.64	632.14	631.14	607.4	-24.2	24.2
MW-54D	47	103	2	633.29	629.88	631.63	632.13	631.13	607.4	-24.2	24.2
MW-28	36	105	1	633.28	628.26	631.58	632.08	631.08	606.8	-24.8	24.8
MW-53	47	103	1	632.83	630.13	631.17	631.67	630.67	607.4	-23.8	23.8
PT-24	40	109	1	633.19	627.85	631.02	631.52	630.52	605.4	-25.6	25.6
PT-25	64	104	1	633.66	625.45	630.56	631.06	630.06	607.0	-23.6	23.6
PT-15	71	99	1	634.09	627.40	630.35	630.85	629.85	608.6	-21.7	21.7
MW-29	46	107	1	631.82	626.83	630.19	630.69	629.69	606.1	-24.1	24.1
MW-37	7	116	1	630.91	626.65	629.14	629.64	628.64	603.4	-25.7	25.7
MW-35D	61	114	2	629.66	628.01	629.08	629.58	628.58	603.6	-25.5	25.5
MW-36	61	114	1	629.94	626.43	629.02	629.52	628.52	603.6	-25.4	25.4
MW-34	75	100	1	630.28	626.39	628.38	628.88	627.88	608.2	-20.2	20.2
MW-56	48	119	1	627.78	626.67	627.27	627.77	626.77	602.0	-25.3	25.3
MW-57D	48	119	2	628.60	627.11	626.94	627.44	626.44	602.0	-24.9	24.9
MW-58D	48	119	3	628.53	625.66	626.87	627.37	626.37	602.0	-24.9	24.9

MW-51D	35	128	2	625.68	621.56	624.02	624.52	623.52	598.9	-25.1	25.1
MW-47	35	128	1	625.69	621.47	623.96	624.46	623.46	598.9	-25.1	25.1
MW-52D	35	128	3	624.20	620.04	622.54	623.04	622.04	598.9	-23.6	23.6
PT-26	73	174	1	611.82	603.10	608.28	608.78	607.78	581.6	-26.7	26.7
GHOST22	42	174	1	NA	NA	601.00	604.00	598.00	582.0	-19.0	19.0
GHOST23	42	174	2	NA	NA	600.00	603.00	597.00	582.0	-18.0	18.0
GHOST24	42	174	3	NA	NA	599.00	602.00	596.00	582.0	-17.0	17.0
GHOST10	7	199	1	NA	NA	575.00	578.00	572.00	548.3	-26.7	26.7
GHOST7	77	198	1	NA	NA	575.00	578.00	572.00	549.9	-25.1	25.1
GHOST8	77	198	2	NA	NA	574.00	577.00	571.00	549.9	-24.1	24.1
GHOST11	7	199	2	NA	NA	574.00	577.00	571.00	548.3	-25.7	25.7
GHOST9	77	198	3	NA	NA	573.00	576.00	570.00	549.9	-23.1	23.1
GHOST12	7	199	3	NA	NA	573.00	576.00	570.00	548.3	-24.7	24.7
GHOST16	6	213	1	NA	NA	515.00	518.00	512.00	479.0	-36.0	36.0
GHOST17	6	213	2	NA	NA	514.00	517.00	511.00	478.9	-35.1	35.1
GHOST18	6	213	3	NA	NA	513.00	516.00	510.00	478.9	-34.1	34.1
GHOST13	74	211	1	NA	NA	495.00	498.00	492.00	477.8	-17.2	17.2
GHOST14	74	211	2	NA	NA	494.00	497.00	491.00	477.8	-16.2	16.2
GHOST15	74	211	3	NA	NA	493.00	496.00	490.00	477.8	-15.2	15.2

Statistical Calculations:

Monitoring Wells Only	
ME=	-35.95
MAE=	35.95

Sensitivity of Heads to Net Recharge

WELL	MODEL COLUMN	MODEL ROW	MODEL LAYER	MEAS. HIGH	MEAS. LOW	TARGET MEAN	TARGET HIGH	TARGET LOW	Recharge: -25%		
									MODEL HEAD	1.001E-05 Difference (feet)	(ft/day) Absolute Difference
MW25-3	4	9	1	742.41	742.41	740.75	743.75	737.75	666.2	-74.6	74.6
MW64A-1	82	11	1	736.63	736.63	737.87	740.87	734.87	664.6	-73.3	73.3
MW64A-3	82	12	1	734.08	734.08	735.32	738.32	732.32	664.1	-71.2	71.2
MW17-1	4	15	1	733.47	733.47	731.81	734.81	728.81	662.2	-69.6	69.6
MW16-1	2	13	1	732.14	732.14	730.97	733.97	727.97	663.9	-67.1	67.1
MW16-2	2	14	1	731.01	731.01	729.84	732.84	726.84	663.1	-66.7	66.7
MW17-3	4	16	1	729.77	729.77	728.11	731.11	725.11	661.3	-66.8	66.8
GHOST19	42	18	1	NA	NA	715.00	718.00	712.00	659.2	-55.8	55.8
GHOST20	42	18	2	NA	NA	714.00	717.00	711.00	659.2	-54.8	54.8
GHOST21	42	18	3	NA	NA	713.00	716.00	710.00	659.2	-53.8	53.8
GHOST1	77	28	1	NA	NA	695.00	698.00	692.00	644.6	-50.4	50.4
GHOST4	9	27	1	NA	NA	695.00	698.00	692.00	646.5	-48.5	48.5
GHOST5	9	27	2	NA	NA	694.00	697.00	691.00	646.5	-47.5	47.5
GHOST2	77	28	2	NA	NA	694.00	697.00	691.00	644.6	-49.4	49.4
GHOST3	77	28	3	NA	NA	693.00	696.00	690.00	644.6	-48.4	48.4
GHOST6	9	27	3	NA	NA	693.00	696.00	690.00	646.5	-46.5	46.5
MW-41D	11	42	2	687.96	685.74	686.82	687.32	686.32	612.0	-74.8	74.8
MW-42D	70	43	2	680.66	674.94	678.34	678.84	677.84	609.5	-68.8	68.8
PT-10	47	44	2	677.79	670.57	673.51	674.01	673.01	607.9	-65.6	65.6
MW64D-1	77	44	1	665.03	664.36	663.37	663.87	662.87	607.8	-55.6	55.6
MW-39	17	61	1	657.99	656.37	657.12	657.62	656.62	601.8	-55.3	55.3
MW-60	72	62	1	658.13	654.83	656.99	657.49	656.49	601.4	-55.6	55.6
MW64D-4	79	59	1	657.39	655.10	655.73	656.23	655.23	602.1	-53.6	53.6
MW-40	46	65	1	656.40	652.18	654.55	655.05	654.05	600.7	-53.9	53.9
MW-59	71	65	1	654.95	651.61	653.78	654.28	653.28	600.6	-53.2	53.2
MW-43	35	63	1	655.42	652.46	653.76	654.26	653.26	601.2	-52.6	52.6
PT-11	66	66	1	654.02	648.49	651.68	652.18	651.18	600.3	-51.4	51.4
PT-18	46	72	1	651.78	646.72	649.85	650.35	649.35	598.7	-51.2	51.2
MW-44	34	73	1	648.63	646.98	648.59	649.09	648.09	598.5	-50.1	50.1
MW-45	24	82	1	648.47	644.75	646.88	647.38	646.38	596.0	-50.9	50.9
MW-46	34	83	1	647.28	642.61	645.62	646.12	645.12	595.6	-50.0	50.0
MW-49D	34	83	2	647.11	642.74	645.45	645.95	644.95	595.6	-49.9	49.9
MW64D-3	77	72	1	646.91	645.89	645.25	645.75	644.75	598.5	-46.8	46.8
PT-12	44	81	1	647.25	641.73	644.90	645.40	644.40	596.2	-48.7	48.7
MW-50D	34	83	3	646.39	642.90	644.73	645.23	644.23	595.6	-49.1	49.1
MW-48	26	89	1	645.47	641.57	643.75	644.25	643.25	594.0	-49.8	49.8
PT-21	43	88	2	647.51	635.37	641.03	641.53	640.53	594.2	-46.8	46.8
PT-22	43	88	1	645.45	637.85	640.95	641.45	640.45	594.2	-46.7	46.7
PT-19	58	85	1	642.35	637.81	640.17	640.67	639.67	595.0	-45.2	45.2
PT-20	51	89	1	644.21	636.11	640.02	640.52	639.52	593.9	-46.1	46.1
MW-32	58	96	1	637.84	632.40	635.11	635.61	634.61	591.8	-43.3	43.3
PT-23	30	101	1	638.71	632.56	635.05	635.55	634.55	590.4	-44.7	44.7
PT-17	53	100	1	636.85	630.12	634.21	634.71	633.71	590.6	-43.6	43.6
MW-38D	18	107	2	634.67	632.76	633.97	634.47	633.47	588.7	-45.3	45.3
MW-27	33	103	1	635.62	630.37	633.45	633.95	632.95	589.8	-43.7	43.7
PT-16	18	107	1	635.06	630.17	633.43	633.93	632.93	588.7	-44.7	44.7
MW-33	63	98	1	635.95	630.02	633.41	633.91	632.91	591.2	-42.2	42.2
MW-30	56	101	1	636.37	629.73	633.13	633.63	632.63	590.3	-42.8	42.8
MW64D-2	75	92	1	633.49	630.75	631.83	632.33	631.33	592.8	-39.0	39.0
MW-55D	47	103	3	633.37	630.23	631.71	632.21	631.21	589.8	-41.9	41.9
MW-31	61	103	1	634.60	627.21	631.64	632.14	631.14	589.7	-41.9	41.9
MW-54D	47	103	2	633.29	629.88	631.63	632.13	631.13	589.8	-41.8	41.8
MW-28	36	105	1	633.28	628.26	631.58	632.08	631.08	589.2	-42.4	42.4
MW-53	47	103	1	632.83	630.13	631.17	631.67	630.67	589.8	-41.4	41.4
PT-24	40	109	1	633.19	627.85	631.02	631.52	630.52	588.0	-43.0	43.0
PT-25	64	104	1	633.66	625.45	630.56	631.06	630.06	589.4	-41.2	41.2
PT-15	71	99	1	634.09	627.40	630.35	630.85	629.85	590.9	-39.4	39.4
MW-29	46	107	1	631.82	626.83	630.19	630.69	629.69	588.6	-41.6	41.6
MW-37	7	116	1	630.91	626.65	629.14	629.64	628.64	586.2	-42.9	42.9
MW-35D	61	114	2	629.66	628.01	629.08	629.58	628.58	586.4	-42.7	42.7
MW-36	61	114	1	629.94	626.43	629.02	629.52	628.52	586.4	-42.6	42.6
MW-34	75	100	1	630.28	626.39	628.38	628.88	627.88	590.5	-37.9	37.9
MW-56	48	119	1	627.78	626.67	627.27	627.77	626.77	585.0	-42.3	42.3
MW-57D	48	119	2	628.60	627.11	626.94	627.44	626.44	585.0	-41.9	41.9
MW-58D	48	119	3	628.53	625.66	626.87	627.37	626.37	585.0	-41.9	41.9

MW-51D	35	128	2	625.68	621.56	624.02	624.52	623.52	582.2	-41.8	41.8
MW-47	35	128	1	625.69	621.47	623.96	624.46	623.46	582.3	-41.7	41.7
MW-52D	35	128	3	624.20	620.04	622.54	623.04	622.04	582.2	-40.3	40.3
PT-26	73	174	1	611.82	603.10	608.28	608.78	607.78	566.9	-41.4	41.4
GHOST22	42	174	1	NA	NA	601.00	604.00	598.00	567.3	-33.7	33.7
GHOST23	42	174	2	NA	NA	600.00	603.00	597.00	567.3	-32.7	32.7
GHOST24	42	174	3	NA	NA	599.00	602.00	596.00	567.3	-31.7	31.7
GHOST10	7	199	1	NA	NA	575.00	578.00	572.00	537.5	-37.5	37.5
GHOST7	77	198	1	NA	NA	575.00	578.00	572.00	538.9	-36.1	36.1
GHOST8	77	198	2	NA	NA	574.00	577.00	571.00	538.9	-35.1	35.1
GHOST11	7	199	2	NA	NA	574.00	577.00	571.00	537.5	-36.5	36.5
GHOST9	77	198	3	NA	NA	573.00	576.00	570.00	538.9	-34.1	34.1
GHOST12	7	199	3	NA	NA	573.00	576.00	570.00	537.5	-35.5	35.5
GHOST16	6	213	1	NA	NA	515.00	518.00	512.00	476.2	-38.8	38.8
GHOST17	6	213	2	NA	NA	514.00	517.00	511.00	476.2	-37.8	37.8
GHOST18	6	213	3	NA	NA	513.00	516.00	510.00	476.2	-36.8	36.8
GHOST13	74	211	1	NA	NA	495.00	498.00	492.00	475.1	-19.9	19.9
GHOST14	74	211	2	NA	NA	494.00	497.00	491.00	475.1	-18.9	18.9
GHOST15	74	211	3	NA	NA	493.00	496.00	490.00	475.1	-17.9	17.9

Statistical Calculations:

Monitoring Wells Only	
ME=	-58.47
MAE=	58.47

Sensitivity of Heads to Net Recharge

WELL	MODEL COLUMN	MODEL ROW	MODEL LAYER	MEAS. HIGH	MEAS. LOW	TARGET MEAN	TARGET HIGH	TARGET LOW	+5%		
									Recharge: MODEL HEAD	1.399E-05 Difference (feet)	(ft/day) Absolute Difference
MW25-3	4	9	1	742.41	742.41	740.75	743.75	737.75	750.2	9.4	9.4
MW64A-1	82	11	1	736.63	736.63	737.87	740.87	734.87	748.0	10.1	10.1
MW64A-3	82	12	1	734.08	734.08	735.32	738.32	732.32	747.2	11.9	11.9
MW17-1	4	15	1	733.47	733.47	731.81	734.81	728.81	744.6	12.8	12.8
MW16-1	2	13	1	732.14	732.14	730.97	733.97	727.97	746.9	15.9	15.9
MW16-2	2	14	1	731.01	731.01	729.84	732.84	726.84	745.8	16.0	16.0
MW17-3	4	16	1	729.77	729.77	728.11	731.11	725.11	743.4	15.3	15.3
GHOST19	42	18	1	NA	NA	715.00	718.00	712.00	740.3	25.3	25.3
GHOST20	42	18	2	NA	NA	714.00	717.00	711.00	740.3	26.3	26.3
GHOST21	42	18	3	NA	NA	713.00	716.00	710.00	740.3	27.3	27.3
GHOST1	77	28	1	NA	NA	695.00	698.00	692.00	720.0	25.0	25.0
GHOST4	9	27	1	NA	NA	695.00	698.00	692.00	722.6	27.6	27.6
GHOST5	9	27	2	NA	NA	694.00	697.00	691.00	722.6	28.6	28.6
GHOST2	77	28	2	NA	NA	694.00	697.00	691.00	720.0	26.0	26.0
GHOST3	77	28	3	NA	NA	693.00	696.00	690.00	720.0	27.0	27.0
GHOST6	9	27	3	NA	NA	693.00	696.00	690.00	722.6	29.6	29.6
MW-41D	11	42	2	687.96	685.74	686.82	686.82	686.32	674.5	-12.3	12.3
MW-42D	70	43	2	680.66	674.94	678.34	678.84	677.84	670.9	-7.4	7.4
PT-10	47	44	2	677.79	670.57	673.51	674.01	673.01	668.7	-4.8	4.8
MW64D-1	77	44	1	665.03	664.36	663.37	663.87	662.87	668.5	5.1	5.1
MW-39	17	61	1	657.99	656.37	657.12	657.62	656.62	660.2	3.1	3.1
MW-60	72	62	1	658.13	654.83	656.99	657.49	656.49	659.6	2.6	2.6
MW64D-4	79	59	1	657.39	655.10	655.73	656.23	655.23	660.6	4.9	4.9
MW-40	46	65	1	656.40	652.18	654.55	655.05	654.05	658.6	4.0	4.0
MW-59	71	65	1	654.95	651.61	653.78	654.28	653.28	658.5	4.7	4.7
MW-43	35	63	1	655.42	652.46	653.76	654.26	653.26	659.4	5.6	5.6
PT-11	66	66	1	654.02	648.49	651.68	652.18	651.18	658.1	6.4	6.4
PT-18	46	72	1	651.78	646.72	649.85	650.35	649.35	655.9	6.0	6.0
MW-44	34	73	1	648.63	646.98	648.59	649.09	648.09	655.5	6.9	6.9
MW-45	24	82	1	648.47	644.75	646.88	647.38	646.38	652.0	5.1	5.1
MW-46	34	83	1	647.28	642.61	645.62	646.12	645.12	651.6	6.0	6.0
MW-49D	34	83	2	647.11	642.74	645.45	645.95	644.95	651.6	6.1	6.1
MW64D-3	77	72	1	646.91	645.89	645.25	645.75	644.75	655.6	10.3	10.3
PT-12	44	81	1	647.25	641.73	644.90	645.40	644.40	652.3	7.4	7.4
MW-50D	34	83	3	646.39	642.90	644.73	645.23	644.23	651.6	6.9	6.9
MW-48	26	89	1	645.47	641.57	643.75	644.25	643.25	649.2	5.4	5.4
PT-21	43	88	2	647.51	635.37	641.03	641.53	640.53	649.5	8.5	8.5
PT-22	43	88	1	645.45	637.85	640.95	641.45	640.45	649.5	8.6	8.6
PT-19	58	85	1	642.35	637.81	640.17	640.67	639.67	650.7	10.5	10.5
PT-20	51	89	1	644.21	636.11	640.02	640.52	639.52	649.1	9.1	9.1
MW-32	58	96	1	637.84	632.40	635.11	635.61	634.61	645.0	9.9	9.9
PT-23	30	101	1	638.71	632.56	635.05	635.55	634.55	644.3	9.2	9.2
PT-17	53	100	1	636.85	630.12	634.21	634.71	633.71	644.6	10.4	10.4
MW-38D	18	107	2	634.67	632.76	633.97	634.47	633.47	641.9	7.9	7.9
MW-27	33	103	1	635.62	630.37	633.45	633.95	632.95	643.5	10.0	10.0
PT-16	18	107	1	635.06	630.17	633.43	633.93	632.93	641.9	8.5	8.5
MW-33	63	98	1	635.95	630.02	633.41	633.91	632.91	645.3	11.9	11.9
MW-30	56	101	1	636.37	629.73	633.13	633.63	632.63	644.2	11.1	11.1
MW64D-2	75	92	1	633.49	630.75	631.83	632.33	631.33	647.7	15.9	15.9
MW-55D	47	103	3	633.37	630.23	631.71	632.21	631.21	643.4	11.7	11.7
MW-31	61	103	1	634.60	627.21	631.64	632.14	631.14	643.3	11.7	11.7
MW-54D	47	103	2	633.29	629.88	631.63	632.13	631.13	643.4	11.8	11.8
MW-28	36	105	1	633.28	628.26	631.58	632.08	631.08	642.6	11.0	11.0
MW-53	47	103	1	632.83	630.13	631.17	631.67	630.67	643.4	12.2	12.2
PT-24	40	109	1	633.19	627.85	631.02	631.52	630.52	640.9	9.9	9.9
PT-25	64	104	1	633.66	625.45	630.56	631.06	630.06	642.9	12.3	12.3
PT-15	71	99	1	634.09	627.40	630.35	630.85	629.85	644.9	14.6	14.6
MW-29	46	107	1	631.82	626.83	630.19	630.69	629.69	641.7	11.5	11.5
MW-37	7	116	1	630.91	626.65	629.14	629.64	628.64	638.3	9.2	9.2
MW-35D	61	114	2	629.66	628.01	629.08	629.58	628.58	638.7	9.6	9.6
MW-36	61	114	1	629.94	626.43	629.02	629.52	628.52	638.7	9.7	9.7
MW-34	75	100	1	630.28	626.39	628.38	628.88	627.88	644.4	16.0	16.0
MW-56	48	119	1	627.78	626.67	627.27	627.77	626.77	636.6	9.3	9.3
MW-57D	48	119	2	628.60	627.11	626.94	627.44	626.44	636.6	9.7	9.7
MW-58D	48	119	3	628.53	625.66	626.87	627.37	626.37	636.6	9.7	9.7

MW-51D	35	128	2	625.68	621.56	624.02	624.52	623.52	632.8	8.8	8.8
MW-47	35	128	1	625.69	621.47	623.96	624.46	623.46	632.8	8.8	8.8
MW-52D	35	128	3	624.20	620.04	622.54	623.04	622.04	632.8	10.3	10.3
PT-26	73	174	1	611.82	603.10	608.28	608.78	607.78	611.5	3.2	3.2
GHOST22	42	174	1	NA	NA	601.00	604.00	598.00	612.0	11.0	11.0
GHOST23	42	174	2	NA	NA	600.00	603.00	597.00	612.0	12.0	12.0
GHOST24	42	174	3	NA	NA	599.00	602.00	596.00	612.0	13.0	13.0
GHOST10	7	199	1	NA	NA	575.00	578.00	572.00	570.3	-4.7	4.7
GHOST7	77	198	1	NA	NA	575.00	578.00	572.00	572.3	-2.7	2.7
GHOST8	77	198	2	NA	NA	574.00	577.00	571.00	572.3	-1.7	1.7
GHOST11	7	199	2	NA	NA	574.00	577.00	571.00	570.3	-3.7	3.7
GHOST9	77	198	3	NA	NA	573.00	576.00	570.00	572.3	-0.7	0.7
GHOST12	7	199	3	NA	NA	573.00	576.00	570.00	570.3	-2.7	2.7
GHOST16	6	213	1	NA	NA	515.00	518.00	512.00	484.6	-30.4	30.4
GHOST17	6	213	2	NA	NA	514.00	517.00	511.00	484.6	-29.4	29.4
GHOST18	6	213	3	NA	NA	513.00	516.00	510.00	484.6	-28.4	28.4
GHOST13	74	211	1	NA	NA	495.00	498.00	492.00	483.2	-11.8	11.8
GHOST14	74	211	2	NA	NA	494.00	497.00	491.00	483.2	-10.8	10.8
GHOST15	74	211	3	NA	NA	493.00	496.00	490.00	483.1	-9.9	9.9

Statistical Calculations:

Monitoring Wells Only	
ME=	9.92
MAE=	10.88

Sensitivity of Heads to Net Recharge

WELL	MODEL COLUMN	MODEL ROW	MODEL LAYER	MEAS. HIGH	MEAS. LOW	TARGET MEAN	TARGET HIGH	TARGET LOW	Recharge: +15%		
									MODEL HEAD	1.532E-05 Difference (feet)	(ft/day) Absolute Difference
MW25-3	4	9	1	742.41	742.41	740.75	743.75	737.75	778.3	37.5	37.5
MW64A-1	82	11	1	736.63	736.63	737.87	740.87	734.87	775.8	37.9	37.9
MW64A-3	82	12	1	734.08	734.08	735.32	738.32	732.32	775.0	39.7	39.7
MW17-1	4	15	1	733.47	733.47	731.81	734.81	728.81	772.2	40.4	40.4
MW16-1	2	13	1	732.14	732.14	730.97	733.97	727.97	774.7	43.7	43.7
MW16-2	2	14	1	731.01	731.01	729.84	732.84	726.84	773.5	43.7	43.7
MW17-3	4	16	1	729.77	729.77	728.11	731.11	725.11	770.8	42.7	42.7
GHOST19	42	18	1	NA	NA	715.00	718.00	712.00	767.5	52.5	52.5
GHOST20	42	18	2	NA	NA	714.00	717.00	711.00	767.5	53.5	53.5
GHOST21	42	18	3	NA	NA	713.00	716.00	710.00	767.5	54.5	54.5
GHOST1	77	28	1	NA	NA	695.00	698.00	692.00	745.2	50.2	50.2
GHOST4	9	27	1	NA	NA	695.00	698.00	692.00	748.1	53.1	53.1
GHOST5	9	27	2	NA	NA	694.00	697.00	691.00	748.1	54.1	54.1
GHOST2	77	28	2	NA	NA	694.00	697.00	691.00	745.2	51.2	51.2
GHOST3	77	28	3	NA	NA	693.00	696.00	690.00	745.2	52.2	52.2
GHOST6	9	27	3	NA	NA	693.00	696.00	690.00	748.0	55.0	55.0
MW-41D	11	42	2	687.96	685.74	686.82	687.32	686.32	695.3	8.5	8.5
MW-42D	70	43	2	680.66	674.94	678.34	678.84	677.84	691.5	13.2	13.2
PT-10	47	44	2	677.79	670.57	673.51	674.01	673.01	689.0	15.5	15.5
MW64D-1	77	44	1	665.03	664.36	663.37	663.87	662.87	688.8	25.4	25.4
MW-39	17	61	1	657.99	656.37	657.12	657.62	656.62	697.7	40.6	40.6
MW-60	72	62	1	658.13	654.83	656.99	657.49	656.49	679.1	22.1	22.1
MW64D-4	79	59	1	657.39	655.10	655.73	656.23	655.23	680.1	24.4	24.4
MW-40	46	65	1	656.40	652.18	654.55	655.05	654.05	677.9	23.3	23.3
MW-59	71	65	1	654.95	651.61	653.78	654.28	653.28	677.8	24.0	24.0
MW-43	35	63	1	655.42	652.46	653.76	654.26	653.26	678.8	25.0	25.0
PT-11	66	66	1	654.02	648.49	651.68	652.18	651.18	677.4	25.7	25.7
PT-18	46	72	1	651.78	646.72	649.85	650.35	649.35	674.9	25.0	25.0
MW-44	34	73	1	648.63	646.98	648.59	649.09	648.09	674.6	26.0	26.0
MW-45	24	82	1	648.47	644.75	646.88	647.38	646.38	670.7	23.8	23.8
MW-46	34	83	1	647.28	642.61	645.62	646.12	645.12	670.3	24.7	24.7
MW-49D	34	83	2	647.11	642.74	645.45	645.95	644.95	670.3	24.8	24.8
MW64D-3	77	72	1	646.91	645.89	645.25	645.75	644.75	674.7	29.4	29.4
PT-12	44	81	1	647.25	641.73	644.90	645.40	644.40	671.1	26.2	26.2
MW-50D	34	83	3	646.39	642.90	644.73	645.23	644.23	670.3	25.6	25.6
MW-48	26	89	1	645.47	641.57	643.75	644.25	643.25	667.7	23.9	23.9
PT-21	43	88	2	647.51	635.37	641.03	641.53	640.53	668.0	27.0	27.0
PT-22	43	88	1	645.45	637.85	640.95	641.45	640.45	668.0	27.1	27.1
PT-19	58	85	1	642.35	637.81	640.17	640.67	639.67	669.3	29.1	29.1
PT-20	51	89	1	644.21	636.11	640.02	640.52	639.52	667.5	27.5	27.5
MW-32	58	96	1	637.84	632.40	635.11	635.61	634.61	664.4	29.3	29.3
PT-23	30	101	1	638.71	632.56	635.05	635.55	634.55	662.3	27.2	27.2
PT-17	53	100	1	636.85	630.12	634.21	634.71	633.71	662.6	28.4	28.4
MW-38D	18	107	2	634.67	632.76	633.97	634.47	633.47	659.6	25.6	25.6
MW-27	33	103	1	635.62	630.37	633.45	633.95	632.95	661.4	27.9	27.9
PT-16	18	107	1	635.06	630.17	633.43	633.93	632.93	659.6	26.2	26.2
MW-33	63	98	1	635.95	630.02	633.41	633.91	632.91	663.4	30.0	30.0
MW-30	56	101	1	636.37	629.73	633.13	633.63	632.63	662.1	29.0	29.0
MW64D-2	75	92	1	633.49	630.75	631.83	632.33	631.33	666.0	34.2	34.2
MW-55D	47	103	3	633.37	630.23	631.71	632.21	631.21	661.3	29.6	29.6
MW-31	61	103	1	634.60	627.21	631.64	632.14	631.14	661.2	29.6	29.6
MW-54D	47	103	2	633.29	629.88	631.63	632.13	631.13	661.3	29.7	29.7
MW-28	36	105	1	633.28	628.26	631.58	632.08	631.08	660.4	28.8	28.8
MW-53	47	103	1	632.83	630.13	631.17	631.67	630.67	661.3	30.1	30.1
PT-24	40	109	1	633.19	627.85	631.02	631.52	630.52	658.6	27.6	27.6
PT-25	64	104	1	633.66	625.45	630.56	631.06	630.06	660.7	30.1	30.1
PT-15	71	99	1	634.09	627.40	630.35	630.85	629.85	662.9	32.6	32.6
MW-29	46	107	1	631.82	626.83	630.19	630.69	629.69	659.5	29.3	29.3
MW-37	7	116	1	630.91	626.65	629.14	629.64	628.64	655.8	26.7	26.7
MW-35D	61	114	2	629.66	628.01	629.08	629.58	628.58	656.1	27.0	27.0
MW-36	61	114	1	629.94	626.43	629.02	629.52	628.52	656.1	27.1	27.1
MW-34	75	100	1	630.28	626.39	628.38	628.88	627.88	662.4	34.0	34.0
MW-56	48	119	1	627.78	626.67	627.27	627.77	626.77	653.9	26.6	26.6
MW-57D	48	119	2	628.60	627.11	626.94	627.44	626.44	653.9	27.0	27.0
MW-58D	48	119	3	628.53	625.66	626.87	627.37	626.37	653.9	27.0	27.0

MW-51D	35	128	2	625.68	621.56	624.02	624.52	623.52	649.7	25.7	25.7
MW-47	35	128	1	625.69	621.47	623.96	624.46	623.46	649.8	25.8	25.8
MW-52D	35	128	3	624.20	620.04	622.54	623.04	622.04	649.7	27.2	27.2
PT-26	73	174	1	611.82	603.10	608.28	608.78	607.78	626.4	18.1	18.1
GHOST22	42	174	1	NA	NA	601.00	604.00	598.00	626.9	25.0	25.0
GHOST23	42	174	2	NA	NA	600.00	603.00	597.00	626.9	26.9	26.9
GHOST24	42	174	3	NA	NA	599.00	602.00	596.00	626.9	27.9	27.9
GHOST10	7	199	1	NA	NA	575.00	578.00	572.00	581.2	6.2	6.2
GHOST7	77	198	1	NA	NA	575.00	578.00	572.00	583.5	8.5	8.5
GHOST8	77	198	2	NA	NA	574.00	577.00	571.00	583.4	9.4	9.4
GHOST11	7	199	2	NA	NA	574.00	577.00	571.00	581.2	7.2	7.2
GHOST9	77	198	3	NA	NA	573.00	576.00	570.00	583.4	10.4	10.4
GHOST12	7	199	3	NA	NA	573.00	576.00	570.00	581.2	8.2	8.2
GHOST16	6	213	1	NA	NA	515.00	518.00	512.00	487.4	-27.6	27.6
GHOST17	6	213	2	NA	NA	514.00	517.00	511.00	487.4	-26.6	26.6
GHOST18	6	213	3	NA	NA	513.00	516.00	510.00	487.4	-25.6	25.6
GHOST13	74	211	1	NA	NA	495.00	498.00	492.00	485.8	-9.2	9.2
GHOST14	74	211	2	NA	NA	494.00	497.00	491.00	485.8	-8.2	8.2
GHOST15	74	211	3	NA	NA	493.00	496.00	490.00	485.8	-7.2	7.2

Statistical Calculations:

Monitoring Wells Only	
ME=	33.15
MAE=	33.15

Sensitivity of Heads to Net Recharge

WELL	MODEL COLUMN	MODEL ROW	MODEL LAYER	MEAS. HIGH	MEAS. LOW	TARGET MEAN	TARGET HIGH	TARGET LOW	+25%		
									Recharge: MODEL HEAD	1.665E-05 Difference (feet)	(ft/day) Absolute Difference
MW25-3	4	9	1	742.41	742.41	740.75	743.75	737.75	806.4	65.6	65.6
MW64A-1	82	11	1	736.63	736.63	737.87	740.87	734.87	803.7	65.8	65.8
MW64A-3	82	12	1	734.08	734.08	735.32	738.32	732.32	802.8	67.5	67.5
MW17-1	4	15	1	733.47	733.47	731.81	734.81	728.81	799.7	67.9	67.9
MW16-1	2	13	1	732.14	732.14	730.97	733.97	727.97	802.4	71.4	71.4
MW16-2	2	14	1	731.01	731.01	729.84	732.84	726.84	801.1	71.3	71.3
MW17-3	4	16	1	729.77	729.77	728.11	731.11	725.11	798.2	70.1	70.1
GHOST19	42	18	1	NA	NA	715.00	718.00	712.00	794.6	79.6	79.6
GHOST20	42	18	2	NA	NA	714.00	717.00	711.00	794.6	80.6	80.6
GHOST21	42	18	3	NA	NA	713.00	716.00	710.00	794.6	81.6	81.6
GHOST1	77	28	1	NA	NA	695.00	698.00	692.00	770.4	75.4	75.4
GHOST4	9	27	1	NA	NA	695.00	698.00	692.00	773.5	78.5	78.5
GHOST5	9	27	2	NA	NA	694.00	697.00	691.00	773.5	79.5	79.5
GHOST2	77	28	2	NA	NA	694.00	697.00	691.00	770.4	76.4	76.4
GHOST3	77	28	3	NA	NA	693.00	696.00	690.00	770.4	77.4	77.4
GHOST6	9	27	3	NA	NA	693.00	696.00	690.00	773.5	80.5	80.5
MW-41D	11	42	2	687.96	685.74	686.82	687.32	686.32	716.2	29.4	29.4
MW-42D	70	43	2	680.66	674.94	678.34	678.84	677.84	725.3	47.0	47.0
PT-10	47	44	2	677.79	670.57	673.51	674.01	673.01	709.3	35.8	35.8
MW64D-1	77	44	1	665.03	664.36	663.37	663.87	662.87	709.1	45.7	45.7
MW-39	17	61	1	657.99	656.37	657.12	657.62	656.62	699.2	42.1	42.1
MW-60	72	62	1	658.13	654.83	656.99	657.49	656.49	698.5	41.5	41.5
MW64D-4	79	59	1	657.39	655.10	655.73	656.23	655.23	699.7	44.0	44.0
MW-40	46	65	1	656.40	652.18	654.55	655.05	654.05	697.3	42.7	42.7
MW-59	71	65	1	654.95	651.61	653.78	654.28	653.28	697.1	43.3	43.3
MW-43	35	63	1	655.42	652.46	653.76	654.26	653.26	698.2	44.4	44.4
PT-11	66	66	1	654.02	648.49	651.68	652.18	651.18	696.7	45.0	45.0
PT-18	46	72	1	651.78	646.72	649.85	650.35	649.35	694.0	44.1	44.1
MW-44	34	73	1	648.63	646.98	648.59	649.09	648.09	693.6	45.0	45.0
MW-45	24	82	1	648.47	644.75	646.88	647.38	646.38	689.5	42.6	42.6
MW-46	34	83	1	647.28	642.61	645.62	646.12	645.12	688.9	43.3	43.3
MW-49D	34	83	2	647.11	642.74	645.45	645.95	644.95	688.9	43.4	43.4
MW64D-3	77	72	1	646.91	645.89	645.25	645.75	644.75	693.7	48.4	48.4
PT-12	44	81	1	647.25	641.73	644.90	645.40	644.40	689.8	44.9	44.9
MW-50D	34	83	3	646.39	642.90	644.73	645.23	644.23	688.9	44.2	44.2
MW-48	26	89	1	645.47	641.57	643.75	644.25	643.25	686.1	42.3	42.3
PT-21	43	88	2	647.51	635.37	641.03	641.53	640.53	686.5	45.5	45.5
PT-22	43	88	1	645.45	637.85	640.95	641.45	640.45	686.5	45.6	45.6
PT-19	58	85	1	642.35	637.81	640.17	640.67	639.67	687.9	47.7	47.7
PT-20	51	89	1	644.21	636.11	640.02	640.52	639.52	686.0	46.0	46.0
MW-32	58	96	1	637.84	632.40	635.11	635.61	634.61	682.6	47.5	47.5
PT-23	30	101	1	638.71	632.56	635.05	635.55	634.55	680.3	45.2	45.2
PT-17	53	100	1	636.85	630.12	634.21	634.71	633.71	680.6	46.4	46.4
MW-38D	18	107	2	634.67	632.76	633.97	634.47	633.47	677.4	43.4	43.4
MW-27	33	103	1	635.62	630.37	633.45	633.95	632.95	697.3	63.8	63.8
PT-16	18	107	1	635.06	630.17	633.43	633.93	632.93	677.4	44.0	44.0
MW-33	63	98	1	635.95	630.02	633.41	633.91	632.91	681.5	48.1	48.1
MW-30	56	101	1	636.37	629.73	633.13	633.63	632.63	680.1	47.0	47.0
MW64D-2	75	92	1	633.49	630.75	631.83	632.33	631.33	684.3	52.5	52.5
MW-55D	47	103	3	633.37	630.23	631.71	632.21	631.21	679.2	47.5	47.5
MW-31	61	103	1	634.60	627.21	631.64	632.14	631.14	679.1	47.5	47.5
MW-54D	47	103	2	633.29	629.88	631.63	632.13	631.13	679.2	47.6	47.6
MW-28	36	105	1	633.28	628.26	631.58	632.08	631.08	678.3	46.7	46.7
MW-53	47	103	1	632.83	630.13	631.17	631.67	630.67	679.2	48.0	48.0
PT-24	40	109	1	633.19	627.85	631.02	631.52	630.52	676.3	45.3	45.3
PT-25	64	104	1	633.66	625.45	630.56	631.06	630.06	678.6	48.0	48.0
PT-15	71	99	1	634.09	627.40	630.35	630.85	629.85	681.0	50.7	50.7
MW-29	46	107	1	631.82	626.83	630.19	630.69	629.69	677.2	47.0	47.0
MW-37	7	116	1	630.91	626.65	629.14	629.64	628.64	673.2	44.1	44.1
MW-35D	61	114	2	629.66	628.01	629.08	629.58	628.58	673.6	44.5	44.5
MW-36	61	114	1	629.94	626.43	629.02	629.52	628.52	673.6	44.6	44.6
MW-34	75	100	1	630.28	626.39	628.38	628.88	627.88	680.4	52.0	52.0
MW-56	48	119	1	627.78	626.67	627.27	627.77	626.77	671.2	43.9	43.9
MW-57D	48	119	2	628.60	627.11	626.94	627.44	626.44	671.2	44.3	44.3
MW-58D	48	119	3	628.53	625.66	626.87	627.37	626.37	671.2	44.3	44.3

MW-51D	35	128	2	625.68	621.56	624.02	624.52	623.52	666.7	42.7	42.7
MW-47	35	128	1	625.69	621.47	623.96	624.46	623.46	666.7	42.7	42.7
MW-52D	35	128	3	624.20	620.04	622.54	623.04	622.04	666.7	44.2	44.2
PT-26	73	174	1	611.82	603.10	608.28	608.78	607.78	641.3	33.0	33.0
GHOST22	42	174	1	NA	NA	601.00	604.00	598.00	641.8	40.8	40.8
GHOST23	42	174	2	NA	NA	600.00	603.00	597.00	641.8	41.8	41.8
GHOST24	42	174	3	NA	NA	599.00	602.00	596.00	641.8	42.8	42.8
GHOST10	7	199	1	NA	NA	575.00	578.00	572.00	592.2	17.2	17.2
GHOST7	77	198	1	NA	NA	575.00	578.00	572.00	594.6	19.6	19.6
GHOST8	77	198	2	NA	NA	574.00	577.00	571.00	594.6	20.6	20.6
GHOST11	7	199	2	NA	NA	574.00	577.00	571.00	592.2	18.2	18.2
GHOST9	77	198	3	NA	NA	573.00	576.00	570.00	594.6	21.6	21.6
GHOST12	7	199	3	NA	NA	573.00	576.00	570.00	592.2	19.2	19.2
GHOST16	6	213	1	NA	NA	515.00	518.00	512.00	490.2	-24.8	24.8
GHOST17	6	213	2	NA	NA	514.00	517.00	511.00	490.2	-23.8	23.8
GHOST18	6	213	3	NA	NA	513.00	516.00	510.00	490.2	-22.8	22.8
GHOST13	74	211	1	NA	NA	495.00	498.00	492.00	488.5	-6.5	6.5
GHOST14	74	211	2	NA	NA	494.00	497.00	491.00	488.5	-5.5	5.5
GHOST15	74	211	3	NA	NA	493.00	496.00	490.00	488.5	-4.5	4.5

Statistical Calculations:

Monitoring Wells Only	
ME=	56.28
MAE=	56.28

- **Sensitivity of Heads to K_h**



Sensitivity of Heads to Kh

WELL	MODEL COLUMN	MODEL ROW	MODEL LAYER	MEAS. HIGH	MEAS. LOW	TARGET MEAN	TARGET HIGH	TARGET LOW	Kh:	0%	(ft/day)
									MODEL HEAD	Difference (feet)	Absolute Difference
MW25-3	4	9	1	742.41	742.41	740.75	743.75	737.75	756.1	-4.7	4.7
MW64A-1	82	11	1	736.63	736.63	737.87	740.87	734.87	734.0	-3.9	3.9
MW64A-3	82	12	1	734.08	734.08	735.32	738.32	732.32	733.2	-2.1	2.1
MW17-1	4	15	1	733.47	733.47	731.81	734.81	728.81	730.8	-1.0	1.0
MW16-1	2	13	1	732.14	732.14	730.97	733.97	727.97	732.9	1.9	1.9
MW16-2	2	14	1	731.01	731.01	729.84	732.84	726.84	731.9	2.1	2.1
MW17-3	4	16	1	729.77	729.77	728.11	731.11	725.11	729.5	1.4	1.4
GHOST19	42	18	1	NA	NA	715.00	718.00	712.00	726.7	11.7	11.7
GHOST20	42	18	2	NA	NA	714.00	717.00	711.00	726.7	12.7	12.7
GHOST21	42	18	3	NA	NA	713.00	716.00	710.00	726.7	13.7	13.7
GHOST1	77	28	1	NA	NA	695.00	698.00	692.00	707.3	12.3	12.3
GHOST4	9	27	1	NA	NA	695.00	698.00	692.00	709.8	14.8	14.8
GHOST5	9	27	2	NA	NA	694.00	697.00	691.00	709.8	15.8	15.8
GHOST2	77	28	2	NA	NA	694.00	697.00	691.00	707.3	13.3	13.3
GHOST3	77	28	3	NA	NA	693.00	696.00	690.00	707.3	14.3	14.3
GHOST6	9	27	3	NA	NA	693.00	696.00	690.00	709.8	16.8	16.8
MW-41D	11	42	2	687.96	685.74	686.82	687.32	686.32	663.9	-22.9	22.9
MW-42D	70	43	2	680.66	674.94	678.34	678.84	677.84	660.6	-17.7	17.7
PT-10	47	44	2	677.79	670.57	673.51	674.01	673.01	658.5	-15.0	15.0
MW64D-1	77	44	1	665.03	664.36	663.37	663.87	662.87	658.3	-5.1	5.1
MW-39	17	61	1	657.99	656.37	657.12	657.62	656.62	650.4	-6.7	6.7
MW-60	72	62	1	658.13	654.83	656.99	657.49	656.49	649.8	-7.2	7.2
MW64D-4	79	59	1	657.39	655.10	655.73	656.23	655.23	650.7	-5.0	5.0
MW-40	46	65	1	656.40	652.18	654.55	655.05	654.05	648.8	-5.8	5.8
MW-59	71	65	1	654.95	651.61	653.78	654.28	653.28	648.7	-5.1	5.1
MW-43	35	63	1	655.42	652.46	653.76	654.26	653.26	649.6	-4.2	4.2
PT-11	66	66	1	654.02	648.49	651.68	652.18	651.18	648.4	-3.3	3.3
PT-18	46	72	1	651.78	646.72	649.85	650.35	649.35	646.2	-3.7	3.7
MW-44	34	73	1	648.63	646.98	648.59	649.09	648.09	645.9	-2.7	2.7
MW-45	24	82	1	648.47	644.75	646.88	647.38	646.38	642.6	-4.3	4.3
MW-46	34	83	1	647.28	642.61	645.62	646.12	645.12	642.2	-3.4	3.4
MW-49D	34	83	2	647.11	642.74	645.45	645.95	644.95	642.2	-3.3	3.3
MW64D-3	77	72	1	646.91	645.89	645.25	645.75	644.75	646.0	0.7	0.7
PT-12	44	81	1	647.25	641.73	644.90	645.40	644.40	642.9	-2.0	2.0
MW-50D	34	83	3	646.39	642.90	644.73	645.23	644.23	642.2	-2.5	2.5
MW-48	26	89	1	645.47	641.57	643.75	644.25	643.25	639.9	-3.9	3.9
PT-21	43	88	2	647.51	635.37	641.03	641.53	640.53	640.2	-0.8	0.8
PT-22	43	88	1	645.45	637.85	640.95	641.45	640.45	640.2	-0.7	0.7
PT-19	58	85	1	642.35	637.81	640.17	640.67	639.67	641.3	1.1	1.1
PT-20	51	89	1	644.21	636.11	640.02	640.52	639.52	639.8	-0.2	0.2
MW-32	58	96	1	637.84	632.40	635.11	635.61	634.61	637.0	1.9	1.9
PT-23	30	101	1	638.71	632.56	635.05	635.55	634.55	635.2	0.1	0.1
PT-17	53	100	1	636.85	630.12	634.21	634.71	633.71	635.5	1.3	1.3
MW-38D	18	107	2	634.67	632.76	633.97	634.47	633.47	632.9	-1.1	1.1
MW-27	33	103	1	635.62	630.37	633.45	633.95	632.95	634.4	0.9	0.9
PT-16	18	107	1	635.06	630.17	633.43	633.93	632.93	632.9	-0.5	0.5
MW-33	63	98	1	635.95	630.02	633.41	633.91	632.91	636.2	2.8	2.8
MW-30	56	101	1	636.37	629.73	633.13	633.63	632.63	635.1	2.0	2.0
MW64D-2	75	92	1	633.49	630.75	631.83	632.33	631.33	638.4	6.6	6.6
MW-55D	47	103	3	633.37	630.23	631.71	632.21	631.21	634.3	2.6	2.6
MW-31	61	103	1	634.60	627.21	631.64	632.14	631.14	634.3	2.7	2.7
MW-54D	47	103	2	633.29	629.88	631.63	632.13	631.13	634.3	2.7	2.7
MW-28	36	105	1	633.28	628.26	631.58	632.08	631.08	633.6	2.0	2.0
MW-53	47	103	1	632.83	630.13	631.17	631.67	630.67	634.4	3.2	3.2
PT-24	40	109	1	633.19	627.85	631.02	631.52	630.52	632.0	1.0	1.0
PT-25	64	104	1	633.66	625.45	630.56	631.06	630.06	633.9	3.3	3.3
PT-15	71	99	1	634.09	627.40	630.35	630.85	629.85	635.8	5.5	5.5
MW-29	46	107	1	631.82	626.83	630.19	630.69	629.69	632.8	2.6	2.6
MW-37	7	116	1	630.91	626.65	629.14	629.64	628.64	629.6	0.5	0.5
MW-35D	61	114	2	629.66	628.01	629.08	629.58	628.58	629.9	0.8	0.8
MW-36	61	114	1	629.94	626.43	629.02	629.52	628.52	629.9	0.9	0.9
MW-34	75	100	1	630.28	626.39	628.38	628.88	627.88	635.3	6.9	6.9
MW-56	48	119	1	627.78	626.67	627.27	627.77	626.77	627.9	0.6	0.6
MW-57D	48	119	2	628.60	627.11	626.94	627.44	626.44	627.9	1.0	1.0
MW-58D	48	119	3	628.53	625.66	626.87	627.37	626.37	627.9	1.0	1.0

MW-51D	35	128	2	625.68	621.56	624.02	624.52	623.52	624.3	0.3	0.3
MW-47	35	128	1	625.69	621.47	623.96	624.46	623.46	624.3	0.3	0.3
MW-52D	35	128	3	624.20	620.04	622.54	623.04	622.04	624.3	1.8	1.8
PT-26	73	174	1	611.82	603.10	608.28	608.78	607.78	604.0	-4.3	4.3
GHOST22	42	174	1	NA	NA	601.00	604.00	598.00	604.5	3.5	3.5
GHOST23	42	174	2	NA	NA	600.00	603.00	597.00	604.5	4.5	4.5
GHOST24	42	174	3	NA	NA	599.00	602.00	596.00	604.5	5.5	5.5
GHOST10	7	199	1	NA	NA	575.00	578.00	572.00	560.6	-14.4	14.4
GHOST7	77	198	1	NA	NA	575.00	578.00	572.00	566.7	-8.3	8.3
GHOST8	77	198	2	NA	NA	574.00	577.00	571.00	566.7	-7.3	7.3
GHOST11	7	199	2	NA	NA	574.00	577.00	571.00	564.7	-9.3	9.3
GHOST9	77	198	3	NA	NA	573.00	576.00	570.00	566.7	-6.3	6.3
GHOST12	7	199	3	NA	NA	573.00	576.00	570.00	564.7	-8.3	8.3
GHOST16	6	213	1	NA	NA	515.00	518.00	512.00	483.2	-31.8	31.8
GHOST17	6	213	2	NA	NA	514.00	517.00	511.00	483.2	-30.8	30.8
GHOST18	6	213	3	NA	NA	513.00	516.00	510.00	483.2	-29.8	29.8
GHOST13	74	211	1	NA	NA	495.00	498.00	492.00	481.8	-13.2	13.2
GHOST14	74	211	2	NA	NA	494.00	497.00	491.00	481.8	-12.2	12.2
GHOST15	74	211	3	NA	NA	493.00	496.00	490.00	481.8	-11.2	11.2

Statistical Calculations:

Monitoring Wells Only	
ME=	-1.58
MAE=	4.03

Sensitivity of Heads to Kh

WELL	MODEL COLUMN	MODEL ROW	MODEL LAYER	MEAS. HIGH	MEAS. LOW	TARGET MEAN	TARGET HIGH	TARGET LOW	Kh:		
									MODEL HEAD	-5% Difference (feet)	(ft/day) Absolute Difference
MW25-3	4	9	1	742.41	742.41	740.75	743.75	737.75	744.2	3.4	3.4
MW64A-1	82	11	1	736.63	736.63	737.87	740.87	734.87	742.0	4.1	4.1
MW64A-3	82	12	1	734.08	734.08	735.32	738.32	732.32	741.3	6.0	6.0
MW17-1	4	15	1	733.47	733.47	731.81	734.81	728.81	738.7	6.9	6.9
MW16-1	2	13	1	732.14	732.14	730.97	733.97	727.97	741.0	10.0	10.0
MW16-2	2	14	1	731.01	731.01	729.84	732.84	726.84	739.9	10.1	10.1
MW17-3	4	16	1	729.77	729.77	728.11	731.11	725.11	737.5	9.4	9.4
GHOST19	42	18	1	NA	NA	715.00	718.00	712.00	734.5	19.5	19.5
GHOST20	42	18	2	NA	NA	714.00	717.00	711.00	734.5	20.5	20.5
GHOST21	42	18	3	NA	NA	713.00	716.00	710.00	734.5	21.5	21.5
GHOST1	77	28	1	NA	NA	695.00	698.00	692.00	714.6	19.6	19.6
GHOST4	9	27	1	NA	NA	695.00	698.00	692.00	717.2	22.2	22.2
GHOST5	9	27	2	NA	NA	694.00	697.00	691.00	717.2	23.2	23.2
GHOST2	77	28	2	NA	NA	694.00	697.00	691.00	714.6	20.6	20.6
GHOST3	77	28	3	NA	NA	693.00	696.00	690.00	714.6	21.6	21.6
GHOST6	9	27	3	NA	NA	693.00	696.00	690.00	717.2	24.2	24.2
MW-41D	11	42	2	687.96	685.74	686.82	687.32	686.32	670.0	-16.8	16.8
MW-42D	70	43	2	680.66	674.94	678.34	678.84	677.84	666.5	-11.8	11.8
PT-10	47	44	2	677.79	670.57	673.51	674.01	673.01	664.4	-9.1	9.1
MW64D-1	77	44	1	665.03	664.36	663.37	663.87	662.87	664.2	0.8	0.8
MW-39	17	61	1	657.99	656.37	657.12	657.62	656.62	656.0	-1.1	1.1
MW-60	72	62	1	658.13	654.83	656.99	657.49	656.49	655.0	-2.0	2.0
MW64D-4	79	59	1	657.39	655.10	655.73	656.23	655.23	656.4	0.7	0.7
MW-40	46	65	1	656.40	652.18	654.55	655.05	654.05	654.4	-0.2	0.2
MW-59	71	65	1	654.95	651.61	653.78	654.28	653.28	654.3	0.5	0.5
MW-43	35	63	1	655.42	652.46	653.76	654.26	653.26	655.2	1.4	1.4
PT-11	66	66	1	654.02	648.49	651.68	652.18	651.18	654.0	2.3	2.3
PT-18	46	72	1	651.78	646.72	649.85	650.35	649.35	651.8	1.9	1.9
MW-44	34	73	1	648.63	646.98	648.59	649.09	648.09	651.4	2.8	2.8
MW-45	24	82	1	648.47	644.75	646.88	647.38	646.38	648.0	1.1	1.1
MW-46	34	83	1	647.28	642.61	645.62	646.12	645.12	647.6	2.0	2.0
MW-49D	34	83	2	647.11	642.74	645.45	645.95	644.95	647.6	2.1	2.1
MW64D-3	77	72	1	646.91	645.89	645.25	645.75	644.75	651.5	6.2	6.2
PT-12	44	81	1	647.25	641.73	644.90	645.40	644.40	648.3	3.4	3.4
MW-50D	34	83	3	646.39	642.90	644.73	645.23	644.23	647.6	2.9	2.9
MW-48	26	89	1	645.47	641.57	643.75	644.25	643.25	645.3	1.5	1.5
PT-21	43	88	2	647.51	635.37	641.03	641.53	640.53	645.6	4.6	4.6
PT-22	43	88	1	645.45	637.85	640.95	641.45	640.45	645.6	4.7	4.7
PT-19	58	85	1	642.35	637.81	640.17	640.67	639.67	646.7	6.5	6.5
PT-20	51	89	1	644.21	636.11	640.02	640.52	639.52	645.1	5.1	5.1
MW-32	58	96	1	637.84	632.40	635.11	635.61	634.61	642.3	7.2	7.2
PT-23	30	101	1	638.71	632.56	635.05	635.55	634.55	640.4	5.3	5.3
PT-17	53	100	1	636.85	630.12	634.21	634.71	633.71	640.7	6.5	6.5
MW-38D	18	107	2	634.67	632.76	633.97	634.47	633.47	638.1	4.1	4.1
MW-27	33	103	1	635.62	630.37	633.45	633.95	632.95	639.6	6.1	6.1
PT-16	18	107	1	635.06	630.17	633.43	633.93	632.93	638.1	4.7	4.7
MW-33	63	98	1	635.95	630.02	633.41	633.91	632.91	641.5	8.1	8.1
MW-30	56	101	1	636.37	629.73	633.13	633.63	632.63	640.3	7.2	7.2
MW64D-2	75	92	1	633.49	630.75	631.83	632.33	631.33	643.7	11.9	11.9
MW-55D	47	103	3	633.37	630.23	631.71	632.21	631.21	639.5	7.8	7.8
MW-31	61	103	1	634.60	627.21	631.64	632.14	631.14	639.5	7.9	7.9
MW-54D	47	103	2	633.29	629.88	631.63	632.13	631.13	639.5	7.9	7.9
MW-28	36	105	1	633.28	628.26	631.58	632.08	631.08	638.8	7.2	7.2
MW-53	47	103	1	632.83	630.13	631.17	631.67	630.67	639.5	8.3	8.3
PT-24	40	109	1	633.19	627.85	631.02	631.52	630.52	637.1	6.1	6.1
PT-25	64	104	1	633.66	625.45	630.56	631.06	630.06	639.0	8.4	8.4
PT-15	71	99	1	634.09	627.40	630.35	630.85	629.85	641.0	10.7	10.7
MW-29	46	107	1	631.82	626.83	630.19	630.69	629.69	637.9	7.7	7.7
MW-37	7	116	1	630.91	626.65	629.14	629.64	628.64	634.6	5.5	5.5
MW-35D	61	114	2	629.66	628.01	629.08	629.58	628.58	634.9	5.8	5.8
MW-36	61	114	1	629.94	626.43	629.02	629.52	628.52	634.9	5.9	5.9
MW-34	75	100	1	630.28	626.39	628.38	628.88	627.88	640.5	12.1	12.1
MW-56	48	119	1	627.78	626.67	627.27	627.77	626.77	632.9	5.6	5.6
MW-57D	48	119	2	628.60	627.11	626.94	627.44	626.44	632.9	6.0	6.0
MW-58D	48	119	3	628.53	625.66	626.87	627.37	626.37	632.9	6.0	6.0

MW-51D	35	128	2	625.68	621.56	624.02	624.52	623.52	629.2	5.2	5.2
MW-47	35	128	1	625.69	621.47	623.96	624.46	623.46	629.2	5.2	5.2
MW-52D	35	128	3	624.20	620.04	622.54	623.04	622.04	629.2	6.7	6.7
PT-26	73	174	1	611.82	603.10	608.28	608.78	607.78	608.3	0.0	0.0
GHOST22	42	174	1	NA	NA	601.00	604.00	598.00	608.8	7.8	7.8
GHOST23	42	174	2	NA	NA	600.00	603.00	597.00	608.8	8.8	8.8
GHOST24	42	174	3	NA	NA	599.00	602.00	596.00	608.8	9.8	9.8
GHOST10	7	199	1	NA	NA	575.00	578.00	572.00	567.9	-7.1	7.1
GHOST7	77	198	1	NA	NA	575.00	578.00	572.00	569.9	-5.1	5.1
GHOST8	77	198	2	NA	NA	574.00	577.00	571.00	569.9	-4.1	4.1
GHOST11	7	199	2	NA	NA	574.00	577.00	571.00	567.9	-6.1	6.1
GHOST9	77	198	3	NA	NA	573.00	576.00	570.00	569.9	-3.1	3.1
GHOST12	7	199	3	NA	NA	573.00	576.00	570.00	567.9	-5.1	5.1
GHOST16	6	213	1	NA	NA	515.00	518.00	512.00	484.0	-31.0	31.0
GHOST17	6	213	2	NA	NA	514.00	517.00	511.00	484.0	-30.0	30.0
GHOST18	6	213	3	NA	NA	513.00	516.00	510.00	484.0	-29.0	29.0
GHOST13	74	211	1	NA	NA	495.00	498.00	492.00	482.6	-12.4	12.4
GHOST14	74	211	2	NA	NA	494.00	497.00	491.00	482.6	-11.4	11.4
GHOST15	74	211	3	NA	NA	493.00	496.00	490.00	482.6	-10.4	10.4

Statistical Calculations:

Monitoring Wells Only	
ME=	5.03
MAE=	6.64

Sensitivity of Heads to Kh

WELL	MODEL COLUMN	MODEL ROW	MODEL LAYER	MEAS. HIGH	MEAS. LOW	TARGET MEAN	TARGET HIGH	TARGET LOW	Kh:	-15%	(ft/day)
									MODEL HEAD	Difference (feet)	Absolute Difference
MW25-3	4	9	1	742.41	742.41	740.75	743.75	737.75	762.0	21.2	21.2
MW64A-1	82	11	1	736.63	736.63	737.87	740.87	734.87	759.7	21.8	21.8
MW64A-3	82	12	1	734.08	734.08	735.32	738.32	732.32	758.8	23.5	23.5
MW17-1	4	15	1	733.47	733.47	731.81	734.81	728.81	756.2	24.4	24.4
MW16-1	2	13	1	732.14	732.14	730.97	733.97	727.97	758.5	27.5	27.5
MW16-2	2	14	1	731.01	731.01	729.84	732.84	726.84	757.4	27.6	27.6
MW17-3	4	16	1	729.77	729.77	728.11	731.11	725.11	754.8	26.7	26.7
GHOST19	42	18	1	NA	NA	715.00	718.00	712.00	751.7	36.7	36.7
GHOST20	42	18	2	NA	NA	714.00	717.00	711.00	751.7	37.7	37.7
GHOST21	42	18	3	NA	NA	713.00	716.00	710.00	751.7	38.7	38.7
GHOST1	77	28	1	NA	NA	695.00	698.00	692.00	730.6	35.6	35.6
GHOST4	9	27	1	NA	NA	695.00	698.00	692.00	733.3	38.3	38.3
GHOST5	9	27	2	NA	NA	694.00	697.00	691.00	733.3	39.3	39.3
GHOST2	77	28	2	NA	NA	694.00	697.00	691.00	730.6	36.6	36.6
GHOST3	77	28	3	NA	NA	693.00	696.00	690.00	730.6	37.6	37.6
GHOST6	9	27	3	NA	NA	693.00	696.00	690.00	733.3	40.3	40.3
MW-41D	11	42	2	687.96	685.74	686.82	687.32	686.32	683.2	-3.6	3.6
MW-42D	70	43	2	680.66	674.94	678.34	678.84	677.84	679.5	1.2	1.2
PT-10	47	44	2	677.79	670.57	673.51	674.01	673.01	677.2	3.7	3.7
MW64D-1	77	44	1	665.03	664.36	663.37	663.87	662.87	677.0	13.6	13.6
MW-39	17	61	1	657.99	656.37	657.12	657.62	656.62	668.4	11.3	11.3
MW-60	72	62	1	658.13	654.83	656.99	657.49	656.49	667.8	10.8	10.8
MW64D-4	79	59	1	657.39	655.10	655.73	656.23	655.23	668.8	13.1	13.1
MW-40	46	65	1	656.40	652.18	654.55	655.05	654.05	666.7	12.1	12.1
MW-59	71	65	1	654.95	651.61	653.78	654.28	653.28	666.6	12.8	12.8
MW-43	35	63	1	655.42	652.46	653.76	654.26	653.26	667.5	13.7	13.7
PT-11	66	66	1	654.02	648.49	651.68	652.18	651.18	666.2	14.5	14.5
PT-18	46	72	1	651.78	646.72	649.85	650.35	649.35	663.9	14.0	14.0
MW-44	34	73	1	648.63	646.98	648.59	649.09	648.09	663.5	14.9	14.9
MW-45	24	82	1	648.47	644.75	646.88	647.38	646.38	659.9	13.0	13.0
MW-46	34	83	1	647.28	642.61	645.62	646.12	645.12	659.4	13.8	13.8
MW-49D	34	83	2	647.11	642.74	645.45	645.95	644.95	659.4	13.9	13.9
MW64D-3	77	72	1	646.91	645.89	645.25	645.75	644.75	663.6	18.3	18.3
PT-12	44	81	1	647.25	641.73	644.90	645.40	644.40	660.2	15.3	15.3
MW-50D	34	83	3	646.39	642.90	644.73	645.23	644.23	659.4	14.7	14.7
MW-48	26	89	1	645.47	641.57	643.75	644.25	643.25	656.9	13.1	13.1
PT-21	43	88	2	647.51	635.37	641.03	641.53	640.53	657.3	16.3	16.3
PT-22	43	88	1	645.45	637.85	640.95	641.45	640.45	657.3	16.4	16.4
PT-19	58	85	1	642.35	637.81	640.17	640.67	639.67	658.4	18.2	18.2
PT-20	51	89	1	644.21	636.11	640.02	640.52	639.52	656.8	16.8	16.8
MW-32	58	96	1	637.84	632.40	635.11	635.61	634.61	653.8	18.7	18.7
PT-23	30	101	1	638.71	632.56	635.05	635.55	634.55	651.8	16.7	16.7
PT-17	53	100	1	636.85	630.12	634.21	634.71	633.71	652.1	17.9	17.9
MW-38D	18	107	2	634.67	632.76	633.97	634.47	633.47	649.3	15.3	15.3
MW-27	33	103	1	635.62	630.37	633.45	633.95	632.95	651.0	17.5	17.5
PT-16	18	107	1	635.06	630.17	633.43	633.93	632.93	649.3	15.9	15.9
MW-33	63	98	1	635.95	630.02	633.41	633.91	632.91	652.9	19.5	19.5
MW-30	56	101	1	636.37	629.73	633.13	633.63	632.63	651.7	18.6	18.6
MW64D-2	75	92	1	633.49	630.75	631.83	632.33	631.33	655.3	23.5	23.5
MW-55D	47	103	3	633.37	630.23	631.71	632.21	631.21	650.9	19.2	19.2
MW-31	61	103	1	634.60	627.21	631.64	632.14	631.14	650.8	19.2	19.2
MW-54D	47	103	2	633.29	629.88	631.63	632.13	631.13	650.9	19.3	19.3
MW-28	36	105	1	633.28	628.26	631.58	632.08	631.08	650.1	18.5	18.5
MW-53	47	103	1	632.83	630.13	631.17	631.67	630.67	650.9	19.7	19.7
PT-24	40	109	1	633.19	627.85	631.02	631.52	630.52	648.3	17.3	17.3
PT-25	64	104	1	633.66	625.45	630.56	631.06	630.06	650.3	19.7	19.7
PT-15	71	99	1	634.09	627.40	630.35	630.85	629.85	652.4	22.1	22.1
MW-29	46	107	1	631.82	626.83	630.19	630.69	629.69	649.1	18.9	18.9
MW-37	7	116	1	630.91	626.65	629.14	629.64	628.64	645.6	16.5	16.5
MW-35D	61	114	2	629.66	628.01	629.08	629.58	628.58	646.0	16.9	16.9
MW-36	61	114	1	629.94	626.43	629.02	629.52	628.52	646.0	17.0	17.0
MW-34	75	100	1	630.28	626.39	628.38	628.88	627.88	651.9	23.5	23.5
MW-56	48	119	1	627.78	626.67	627.27	627.77	626.77	643.9	16.6	16.6
MW-57D	48	119	2	628.60	627.11	627.94	627.44	626.44	643.9	17.0	17.0
MW-58D	48	119	3	628.53	625.66	626.87	627.37	626.37	643.9	17.0	17.0

MW-51D	35	128	2	625.68	621.56	624.02	624.52	623.52	639.9	15.9	15.9
MW-47	35	128	1	625.69	621.47	623.96	624.46	623.46	639.9	15.9	15.9
MW-52D	35	128	3	624.20	620.04	622.54	623.04	622.04	639.9	17.4	17.4
PT-26	73	174	1	611.82	603.10	608.28	608.78	607.78	617.7	9.4	9.4
GHOST22	42	174	1	NA	NA	601.00	604.00	598.00	618.2	17.2	17.2
GHOST23	42	174	2	NA	NA	600.00	603.00	597.00	618.2	18.2	18.2
GHOST24	42	174	3	NA	NA	599.00	602.00	596.00	618.2	19.2	19.2
GHOST10	7	199	1	NA	NA	575.00	578.00	572.00	574.9	-0.1	0.1
GHOST7	77	198	1	NA	NA	575.00	578.00	572.00	577.0	2.0	2.0
GHOST8	77	198	2	NA	NA	574.00	577.00	571.00	577.0	3.0	3.0
GHOST11	7	199	2	NA	NA	574.00	577.00	571.00	574.9	0.9	0.9
GHOST9	77	198	3	NA	NA	573.00	576.00	570.00	577.0	4.0	4.0
GHOST12	7	199	3	NA	NA	573.00	576.00	570.00	574.9	1.9	1.9
GHOST16	6	213	1	NA	NA	515.00	518.00	512.00	485.8	-29.2	29.2
GHOST17	6	213	2	NA	NA	514.00	517.00	511.00	485.8	-28.2	28.2
GHOST18	6	213	3	NA	NA	513.00	516.00	510.00	485.8	-27.2	27.2
GHOST13	74	211	1	NA	NA	495.00	498.00	492.00	484.3	-10.7	10.7
GHOST14	74	211	2	NA	NA	494.00	497.00	491.00	484.3	-9.7	9.7
GHOST15	74	211	3	NA	NA	493.00	496.00	490.00	484.3	-8.7	8.7

Statistical Calculations:

Monitoring Wells Only	
ME=	19.52
MAE=	19.66

Sensitivity of Heads to Kh

WELL	MODEL COLUMN	MODEL ROW	MODEL LAYER	MEAS. HIGH	MEAS. LOW	TARGET MEAN	TARGET HIGH	TARGET LOW	Kh:		
									MODEL HEAD	0.7725 Difference (feet)	(ft/day) Absolute Difference
MW25-3	4	9	1	742.41	742.41	740.75	743.75	737.75	782.1	41.3	41.3
MW64A-1	82	11	1	736.63	736.63	737.87	740.87	734.87	779.6	41.7	41.7
MW64A-3	82	12	1	734.08	734.08	735.32	738.32	732.32	778.7	43.4	43.4
MW17-1	4	15	1	733.47	733.47	731.81	734.81	728.81	775.9	44.1	44.1
MW16-1	2	13	1	732.14	732.14	730.97	733.97	727.97	778.4	47.4	47.4
MW16-2	2	14	1	731.01	731.01	729.84	732.84	726.84	777.2	47.4	47.4
MW17-3	4	16	1	729.77	729.77	728.11	731.11	725.11	774.5	46.4	46.4
GHOST19	42	18	1	NA	NA	715.00	718.00	712.00	771.1	56.1	56.1
GHOST20	42	18	2	NA	NA	714.00	717.00	711.00	771.1	57.1	57.1
GHOST21	42	18	3	NA	NA	713.00	716.00	710.00	771.1	58.1	58.1
GHOST1	77	28	1	NA	NA	695.00	698.00	692.00	748.6	53.6	53.6
GHOST4	9	27	1	NA	NA	695.00	698.00	692.00	751.5	56.5	56.5
GHOST5	9	27	2	NA	NA	694.00	697.00	691.00	751.5	57.5	57.5
GHOST2	77	28	2	NA	NA	694.00	697.00	691.00	748.6	54.6	54.6
GHOST3	77	28	3	NA	NA	693.00	696.00	690.00	748.6	55.6	55.6
GHOST6	9	27	3	NA	NA	693.00	696.00	690.00	751.5	58.5	58.5
MW-41D	11	42	2	687.96	685.74	686.82	687.32	686.32	698.1	11.3	11.3
MW-42D	70	43	2	680.66	674.94	678.34	678.84	677.84	694.2	15.9	15.9
PT-10	47	44	2	677.79	670.57	673.51	674.01	673.01	691.8	18.3	18.3
MW64D-1	77	44	1	665.03	664.36	663.37	663.87	662.87	691.6	28.2	28.2
MW-39	17	61	1	657.99	656.37	657.12	657.62	656.62	682.3	25.2	25.2
MW-60	72	62	1	658.13	654.83	656.99	657.49	656.49	681.7	24.7	24.7
MW64D-4	79	59	1	657.39	655.10	655.73	656.23	655.23	682.8	27.1	27.1
MW-40	46	65	1	656.40	652.18	654.55	655.05	654.05	680.5	25.9	25.9
MW-59	71	65	1	654.95	651.61	653.78	654.28	653.28	680.4	26.6	26.6
MW-43	35	63	1	655.42	652.46	653.76	654.26	653.26	681.4	27.6	27.6
PT-11	66	66	1	654.02	648.49	651.68	652.18	651.18	680.0	28.3	28.3
PT-18	46	72	1	651.78	646.72	649.85	650.35	649.35	677.5	27.6	27.6
MW-44	34	73	1	648.63	646.98	648.59	649.09	648.09	677.1	28.5	28.5
MW-45	24	82	1	648.47	644.75	646.88	647.38	646.38	673.3	26.4	26.4
MW-46	34	83	1	647.28	642.61	645.62	646.12	645.12	672.8	27.2	27.2
MW-49D	34	83	2	647.11	642.74	645.45	645.95	644.95	672.8	27.3	27.3
MW64D-3	77	72	1	646.91	645.89	645.25	645.75	644.75	677.2	31.9	31.9
PT-12	44	81	1	647.25	641.73	644.90	645.40	644.40	673.6	28.7	28.7
MW-50D	34	83	3	646.39	642.90	644.73	645.23	644.23	672.8	28.1	28.1
MW-48	26	89	1	645.47	641.57	643.75	644.25	643.25	670.2	26.4	26.4
PT-21	43	88	2	647.51	635.37	641.03	641.53	640.53	670.5	29.5	29.5
PT-22	43	88	1	645.45	637.85	640.95	641.45	640.45	670.5	29.6	29.6
PT-19	58	85	1	642.35	637.81	640.17	640.67	639.67	671.8	31.6	31.6
PT-20	51	89	1	644.21	636.11	640.02	640.52	639.52	670.0	30.0	30.0
MW-32	58	96	1	637.84	632.40	635.11	635.61	634.61	666.8	31.7	31.7
PT-23	30	101	1	638.71	632.56	635.05	635.55	634.55	664.7	29.6	29.6
PT-17	53	100	1	636.85	630.12	634.21	634.71	633.71	665.0	30.8	30.8
MW-38D	18	107	2	634.67	632.76	633.97	634.47	633.47	662.0	28.0	28.0
MW-27	33	103	1	635.62	630.37	633.45	633.95	632.95	663.8	30.3	30.3
PT-16	18	107	1	635.06	630.17	633.43	633.93	632.93	662.0	28.6	28.6
MW-33	63	98	1	635.95	630.02	633.41	633.91	632.91	665.9	32.5	32.5
MW-30	56	101	1	636.37	629.73	633.13	633.63	632.63	664.5	31.4	31.4
MW64D-2	75	92	1	633.49	630.75	631.83	632.33	631.33	668.4	36.6	36.6
MW-55D	47	103	3	633.37	630.23	631.71	632.21	631.21	656.2	24.5	24.5
MW-31	61	103	1	634.60	627.21	631.64	632.14	631.14	663.6	32.0	32.0
MW-54D	47	103	2	633.29	629.88	631.63	632.13	631.13	663.7	32.1	32.1
MW-28	36	105	1	633.28	628.26	631.58	632.08	631.08	662.8	31.2	31.2
MW-53	47	103	1	632.83	630.13	631.17	631.67	630.67	663.7	32.5	32.5
PT-24	40	109	1	633.19	627.85	631.02	631.52	630.52	661.0	30.0	30.0
PT-25	64	104	1	633.66	625.45	630.56	631.06	630.06	663.1	32.5	32.5
PT-15	71	99	1	634.09	627.40	630.35	630.85	629.85	665.4	35.1	35.1
MW-29	46	107	1	631.82	626.83	630.19	630.69	629.69	661.9	31.7	31.7
MW-37	7	116	1	630.91	626.65	629.14	629.64	628.64	658.1	29.0	29.0
MW-35D	61	114	2	629.66	628.01	629.08	629.58	628.58	658.5	29.4	29.4
MW-36	61	114	1	629.94	626.43	629.02	629.52	628.52	658.5	29.5	29.5
MW-34	75	100	1	630.28	626.39	628.38	628.88	627.88	664.8	36.4	36.4
MW-56	48	119	1	627.78	626.67	627.27	627.77	626.77	656.2	28.9	28.9
MW-57D	48	119	2	628.60	627.11	626.94	627.44	626.44	656.2	29.3	29.3
MW-58D	48	119	3	628.53	625.66	626.87	627.37	626.37	656.2	29.3	29.3

MW-51D	35	128	2	625.68	621.56	624.02	624.52	623.52	652.0	28.0	28.0
MW-47	35	128	1	625.69	621.47	623.96	624.46	623.46	652.0	28.0	28.0
MW-52D	35	128	3	624.20	620.04	622.54	623.04	622.04	652.0	29.5	29.5
PT-26	73	174	1	611.82	603.10	608.28	608.78	607.78	628.4	20.1	20.1
GHOST22	42	174	1	NA	NA	601.00	604.00	598.00	628.9	27.9	27.9
GHOST23	42	174	2	NA	NA	600.00	603.00	597.00	628.9	28.9	28.9
GHOST24	42	174	3	NA	NA	599.00	602.00	596.00	628.9	29.9	29.9
GHOST10	7	199	1	NA	NA	575.00	578.00	572.00	582.7	7.7	7.7
GHOST7	77	198	1	NA	NA	575.00	578.00	572.00	584.9	9.9	9.9
GHOST8	77	198	2	NA	NA	574.00	577.00	571.00	584.9	10.9	10.9
GHOST11	7	199	2	NA	NA	574.00	577.00	571.00	582.7	8.7	8.7
GHOST9	77	198	3	NA	NA	573.00	576.00	570.00	584.9	11.9	11.9
GHOST12	7	199	3	NA	NA	573.00	576.00	570.00	582.7	9.7	9.7
GHOST16	6	213	1	NA	NA	515.00	518.00	512.00	487.8	-27.2	27.2
GHOST17	6	213	2	NA	NA	514.00	517.00	511.00	487.8	-26.2	26.2
GHOST18	6	213	3	NA	NA	513.00	516.00	510.00	487.8	-25.2	25.2
GHOST13	74	211	1	NA	NA	495.00	498.00	492.00	486.2	-8.8	8.8
GHOST14	74	211	2	NA	NA	494.00	497.00	491.00	486.2	-7.8	7.8
GHOST15	74	211	3	NA	NA	493.00	496.00	490.00	486.2	-6.8	6.8

Statistical Calculations:

Monitoring Wells Only	
ME=	35.73
MAE=	35.73

Sensitivity of Heads to Kh

WELL	MODEL COLUMN	MODEL ROW	MODEL LAYER	MEAS. HIGH	MEAS. LOW	TARGET MEAN	TARGET HIGH	TARGET LOW	+5%		
									Kh: MODEL HEAD	1.0800 Difference (feet)	(ft/day) Absolute Difference
MW25-3	4	9	1	742.41	742.41	740.75	743.75	737.75	728.6	-12.2	12.2
MW64A-1	82	11	1	736.63	736.63	737.87	740.87	734.87	726.5	-11.4	11.4
MW64A-3	82	12	1	734.08	734.08	735.32	738.32	732.32	725.8	-9.5	9.5
MW17-1	4	15	1	733.47	733.47	731.81	734.81	728.81	723.4	-8.4	8.4
MW16-1	2	13	1	732.14	732.14	730.97	733.97	727.97	725.6	-5.4	5.4
MW16-2	2	14	1	731.01	731.01	729.84	732.84	726.84	724.6	-5.2	5.2
MW17-3	4	16	1	729.77	729.77	728.11	731.11	725.11	722.3	-5.8	5.8
GHOST19	42	18	1	NA	NA	715.00	718.00	712.00	719.5	4.5	4.5
GHOST20	42	18	2	NA	NA	714.00	717.00	711.00	719.5	5.5	5.5
GHOST21	42	18	3	NA	NA	713.00	716.00	710.00	719.5	6.5	6.5
GHOST1	77	28	1	NA	NA	695.00	698.00	692.00	700.6	5.6	5.6
GHOST4	9	27	1	NA	NA	695.00	698.00	692.00	703.0	8.0	8.0
GHOST5	9	27	2	NA	NA	694.00	697.00	691.00	703.0	9.0	9.0
GHOST2	77	28	2	NA	NA	694.00	697.00	691.00	700.8	6.8	6.8
GHOST3	77	28	3	NA	NA	693.00	696.00	690.00	700.6	7.6	7.6
GHOST6	9	27	3	NA	NA	693.00	696.00	690.00	703.0	10.0	10.0
MW-41D	11	42	2	687.96	685.74	686.82	687.32	686.32	658.4	-28.4	28.4
MW-42D	70	43	2	680.66	674.94	678.34	678.84	677.84	655.1	-23.2	23.2
PT-10	47	44	2	677.79	670.57	673.51	674.01	673.01	653.1	-20.4	20.4
MW64D-1	77	44	1	665.03	664.36	663.37	663.87	662.87	652.9	-10.5	10.5
MW-39	17	61	1	657.99	656.37	657.12	657.62	656.62	645.2	-11.9	11.9
MW-60	72	62	1	658.13	654.83	656.99	657.49	656.49	644.6	-12.4	12.4
MW64D-4	79	59	1	657.39	655.10	655.73	656.23	655.23	645.5	-10.2	10.2
MW-40	46	65	1	656.40	652.18	654.55	655.05	654.05	643.7	-10.9	10.9
MW-59	71	65	1	654.95	651.61	653.78	654.28	653.28	643.6	-10.2	10.2
MW-43	35	63	1	655.42	652.46	653.76	654.26	653.26	644.4	-9.4	9.4
PT-11	66	66	1	654.02	648.49	651.68	652.18	651.18	643.2	-8.5	8.5
PT-18	46	72	1	651.78	646.72	649.85	650.35	649.35	641.2	-8.7	8.7
MW-44	34	73	1	648.63	646.98	648.59	649.09	648.09	640.8	-7.8	7.8
MW-45	24	82	1	648.47	644.75	646.88	647.38	646.38	637.6	-9.3	9.3
MW-46	34	83	1	647.28	642.61	645.62	646.12	645.12	637.2	-8.4	8.4
MW-49D	34	83	2	647.11	642.74	645.45	645.95	644.95	637.2	-8.3	8.3
MW64D-3	77	72	1	646.91	645.89	645.25	645.75	644.75	640.9	-4.4	4.4
PT-12	44	81	1	647.25	641.73	644.90	645.40	644.40	637.9	-7.0	7.0
MW-50D	34	83	3	646.39	642.90	644.73	645.23	644.23	637.2	-7.5	7.5
MW-48	26	89	1	645.47	641.57	643.75	644.25	643.25	635.0	-8.8	8.8
PT-21	43	88	2	647.51	635.37	641.03	641.53	640.53	635.3	-5.7	5.7
PT-22	43	88	1	645.45	637.85	640.95	641.45	640.45	635.3	-5.6	5.6
PT-19	58	85	1	642.35	637.81	640.17	640.67	639.67	636.3	-3.9	3.9
PT-20	51	89	1	644.21	636.11	640.02	640.52	639.52	634.9	-5.1	5.1
MW-32	58	96	1	637.84	632.40	635.11	635.61	634.61	632.2	-2.9	2.9
PT-23	30	101	1	638.71	632.56	635.05	635.55	634.55	630.4	-4.7	4.7
PT-17	53	100	1	636.85	630.12	634.21	634.71	633.71	630.7	-3.5	3.5
MW-38D	18	107	2	634.67	632.76	633.97	634.47	633.47	628.2	-5.8	5.8
MW-27	33	103	1	635.62	630.37	633.45	633.95	632.95	629.7	-3.8	3.8
PT-16	18	107	1	635.06	630.17	633.43	633.93	632.93	628.2	-5.2	5.2
MW-33	63	98	1	635.95	630.02	633.41	633.91	632.91	631.4	-2.0	2.0
MW-30	56	101	1	636.37	629.73	633.13	633.63	632.63	630.3	-2.8	2.8
MW64D-2	75	92	1	633.49	630.75	631.83	632.33	631.33	633.6	1.8	1.8
MW-55D	47	103	3	633.37	630.23	631.71	632.21	631.21	629.6	-2.1	2.1
MW-31	61	103	1	634.60	627.21	631.64	632.14	631.14	629.5	-2.1	2.1
MW-54D	47	103	2	633.29	629.88	631.63	632.13	631.13	629.6	-2.0	2.0
MW-28	36	105	1	633.28	628.26	631.58	632.08	631.08	628.9	-2.7	2.7
MW-53	47	103	1	632.83	630.13	631.17	631.67	630.67	629.6	-1.6	1.6
PT-24	40	109	1	633.19	627.85	631.02	631.52	630.52	627.3	-3.7	3.7
PT-25	64	104	1	633.66	625.45	630.56	631.06	630.06	629.1	-1.5	1.5
PT-15	71	99	1	634.09	627.40	630.35	630.85	629.85	631.0	0.7	0.7
MW-29	46	107	1	631.82	626.83	630.19	630.69	629.69	628.0	-2.2	2.2
MW-37	7	116	1	630.91	626.65	629.14	629.64	628.64	624.9	-4.2	4.2
MW-35D	61	114	2	629.66	628.01	629.08	629.58	628.58	625.2	-3.9	3.9
MW-36	61	114	1	629.94	626.43	629.02	629.52	628.52	625.2	-3.8	3.8
MW-34	75	100	1	630.28	626.39	628.38	628.88	627.88	630.5	2.1	2.1
MW-56	48	119	1	627.78	626.67	627.27	627.77	626.77	623.3	-4.0	4.0
MW-57D	48	119	2	628.60	627.11	626.94	627.44	626.44	623.3	-3.6	3.6
MW-58D	48	119	3	628.53	625.66	626.87	627.37	626.37	623.3	-3.6	3.6

MW-51D	35	128	2	625.68	621.56	624.02	624.52	623.52	619.8	-4.2	4.2
MW-47	35	128	1	625.69	621.47	623.96	624.46	623.46	619.8	-4.2	4.2
MW-52D	35	128	3	624.20	620.04	622.54	623.04	622.04	619.8	-2.7	2.7
PT-26	73	174	1	611.82	603.10	608.28	608.78	607.78	600.1	-8.2	8.2
GHOST22	42	174	1	NA	NA	601.00	604.00	598.00	600.5	-0.5	0.5
GHOST23	42	174	2	NA	NA	600.00	603.00	597.00	600.5	0.5	0.5
GHOST24	42	174	3	NA	NA	599.00	602.00	596.00	600.5	1.5	1.5
GHOST10	7	199	1	NA	NA	575.00	578.00	572.00	561.8	-13.2	13.2
GHOST7	77	198	1	NA	NA	575.00	578.00	572.00	563.7	-11.3	11.3
GHOST8	77	198	2	NA	NA	574.00	577.00	571.00	563.7	-10.3	10.3
GHOST11	7	199	2	NA	NA	574.00	577.00	571.00	561.8	-12.2	12.2
GHOST9	77	198	3	NA	NA	573.00	576.00	570.00	563.7	-9.3	9.3
GHOST12	7	199	3	NA	NA	573.00	576.00	570.00	561.8	-11.2	11.2
GHOST16	6	213	1	NA	NA	515.00	518.00	512.00	482.4	-32.6	32.6
GHOST17	6	213	2	NA	NA	514.00	517.00	511.00	482.4	-31.6	31.6
GHOST18	6	213	3	NA	NA	513.00	516.00	510.00	482.4	-30.6	30.6
GHOST13	74	211	1	NA	NA	495.00	498.00	492.00	481.1	-13.9	13.9
GHOST14	74	211	2	NA	NA	494.00	497.00	491.00	481.1	-12.9	12.9
GHOST15	74	211	3	NA	NA	493.00	496.00	490.00	481.1	-11.9	11.9

Statistical Calculations:

Monitoring Wells Only	
ME=	-7.66
MAE=	7.84

Sensitivity of Heads to Kh

WELL	MODEL COLUMN	MODEL ROW	MODEL LAYER	MEAS. HIGH	MEAS. LOW	TARGET MEAN	TARGET HIGH	TARGET LOW	Kh:	+15%	(ft/day)
									MODEL HEAD	Difference (feet)	Absolute Difference
MW25-3	4	9	1	742.41	742.41	740.75	743.75	737.75	714.2	-26.6	26.6
MW64A-1	82	11	1	736.63	736.63	737.87	740.87	734.87	712.3	-25.6	25.6
MW64A-3	82	12	1	734.08	734.08	735.32	738.32	732.32	711.6	-23.7	23.7
MW17-1	4	15	1	733.47	733.47	731.81	734.81	728.81	709.3	-22.5	22.5
MW16-1	2	13	1	732.14	732.14	730.97	733.97	727.97	711.3	-19.7	19.7
MW16-2	2	14	1	731.01	731.01	729.84	732.84	726.84	710.4	-19.4	19.4
MW17-3	4	16	1	729.77	729.77	728.11	731.11	725.11	708.2	-19.9	19.9
GHOST19	42	18	1	NA	NA	715.00	718.00	712.00	705.5	-9.5	9.5
GHOST20	42	18	2	NA	NA	714.00	717.00	711.00	705.5	-8.5	8.5
GHOST21	42	18	3	NA	NA	713.00	716.00	710.00	705.5	-7.5	7.5
GHOST1	77	28	1	NA	NA	695.00	698.00	692.00	687.7	-7.3	7.3
GHOST4	9	27	1	NA	NA	695.00	698.00	692.00	690.0	-5.0	5.0
GHOST5	9	27	2	NA	NA	694.00	697.00	691.00	690.0	-4.0	4.0
GHOST2	77	28	2	NA	NA	694.00	697.00	691.00	687.7	-6.3	6.3
GHOST3	77	28	3	NA	NA	693.00	696.00	690.00	687.7	-5.3	5.3
GHOST6	9	27	3	NA	NA	693.00	696.00	690.00	690.9	-2.1	2.1
MW-41D	11	42	2	687.96	685.74	686.82	687.32	686.32	647.7	-39.1	39.1
MW-42D	70	43	2	680.66	674.94	678.34	678.84	677.84	644.6	-33.7	33.7
PT-10	47	44	2	677.79	670.57	673.51	674.01	673.01	642.6	-30.9	30.9
MW64D-1	77	44	1	665.03	664.36	663.37	663.87	662.87	642.6	-20.8	20.8
MW-39	17	61	1	657.99	656.37	657.12	657.62	656.62	635.2	-21.9	21.9
MW-60	72	62	1	658.13	654.83	656.99	657.49	656.49	634.7	-22.3	22.3
MW64D-4	79	59	1	657.39	655.10	655.73	656.23	655.23	635.5	-20.2	20.2
MW-40	46	65	1	656.40	652.18	654.55	655.05	654.05	633.7	-20.9	20.9
MW-59	71	65	1	654.95	651.61	653.78	654.28	653.28	633.7	-20.1	20.1
MW-43	35	63	1	655.42	652.46	653.76	654.26	653.26	634.4	-19.4	19.4
PT-11	66	66	1	654.02	648.49	651.68	652.18	651.18	633.3	-18.4	18.4
PT-18	46	72	1	651.78	646.72	649.85	650.35	649.35	631.4	-18.5	18.5
MW-44	34	73	1	648.63	646.98	648.59	649.09	648.09	631.1	-17.5	17.5
MW-45	24	82	1	648.47	644.75	646.88	647.38	646.38	628.0	-18.9	18.9
MW-46	34	83	1	647.28	642.61	645.62	646.12	645.12	627.6	-18.0	18.0
MW-49D	34	83	2	647.11	642.74	645.45	645.95	644.95	627.6	-17.9	17.9
MW64D-3	77	72	1	646.91	645.89	645.25	645.75	644.75	631.1	-14.2	14.2
PT-12	44	81	1	647.25	641.73	644.90	645.40	644.40	628.3	-16.6	16.6
MW-50D	34	83	3	646.39	642.90	644.73	645.23	644.23	627.6	-17.1	17.1
MW-48	26	89	1	645.47	641.57	643.75	644.25	643.25	625.5	-18.3	18.3
PT-21	43	88	2	647.51	635.37	641.03	641.53	640.53	625.8	-15.2	15.2
PT-22	43	88	1	645.45	637.85	640.95	641.45	640.45	625.8	-15.1	15.1
PT-19	58	85	1	642.35	637.81	640.17	640.67	639.67	626.8	-13.4	13.4
PT-20	51	89	1	644.21	636.11	640.02	640.52	639.52	625.4	-14.6	14.6
MW-32	58	96	1	637.84	632.40	635.11	635.61	634.61	622.9	-12.2	12.2
PT-23	30	101	1	638.71	632.56	635.05	635.55	634.55	621.2	-13.9	13.9
PT-17	53	100	1	636.85	630.12	634.21	634.71	633.71	621.5	-12.7	12.7
MW-38D	18	107	2	634.67	632.76	633.97	634.47	633.47	619.1	-14.9	14.9
MW-27	33	103	1	635.62	630.37	633.45	633.95	632.95	620.5	-13.0	13.0
PT-16	18	107	1	635.06	630.17	633.43	633.93	632.93	619.1	-14.3	14.3
MW-33	63	98	1	635.95	630.02	633.41	633.91	632.91	622.1	-11.3	11.3
MW-30	56	101	1	636.37	629.73	633.13	633.63	632.63	621.1	-12.0	12.0
MW64D-2	75	92	1	633.49	630.75	631.83	632.33	631.33	624.2	-7.6	7.6
MW-55D	47	103	3	633.37	630.23	631.71	632.21	631.21	620.4	-11.3	11.3
MW-31	61	103	1	634.60	627.21	631.64	632.14	631.14	620.3	-11.3	11.3
MW-54D	47	103	2	633.29	629.88	631.63	632.13	631.13	620.4	-11.2	11.2
MW-28	36	105	1	633.28	628.26	631.58	632.08	631.08	619.7	-11.9	11.9
MW-53	47	103	1	632.83	630.13	631.17	631.67	630.67	620.4	-10.8	10.8
PT-24	40	109	1	633.19	627.85	631.02	631.52	630.52	618.2	-12.8	12.8
PT-25	64	104	1	633.66	625.45	630.56	631.06	630.06	619.9	-10.7	10.7
PT-15	71	99	1	634.09	627.40	630.35	630.85	629.85	621.7	-8.6	8.6
MW-29	46	107	1	631.82	626.83	630.19	630.69	629.69	618.9	-11.3	11.3
MW-37	7	116	1	630.91	626.65	629.14	629.64	628.64	616.0	-13.1	13.1
MW-35D	61	114	2	629.66	628.01	629.08	629.58	628.58	616.3	-12.8	12.8
MW-36	61	114	1	629.94	626.43	629.02	629.52	628.52	616.3	-12.7	12.7
MW-34	75	100	1	630.28	626.39	628.38	628.88	627.88	621.3	-7.1	7.1
MW-56	48	119	1	627.78	626.67	627.27	627.77	626.77	614.5	-12.8	12.8
MW-57D	48	119	2	628.60	627.11	626.94	627.44	626.44	614.5	-12.4	12.4
MW-58D	48	119	3	628.53	625.66	626.87	627.37	626.37	614.5	-12.4	12.4

MW-51D	35	128	2	625.68	621.56	624.02	624.52	623.52	611.2	-12.8	12.8
MW-47	35	128	1	625.69	621.47	623.96	624.46	623.46	611.2	-12.8	12.8
MW-52D	35	128	3	624.20	620.04	622.54	623.04	622.04	611.2	-11.3	11.3
PT-26	73	174	1	611.82	603.10	608.28	608.78	607.78	592.4	-15.9	15.9
GHOST22	42	174	1	NA	NA	601.00	604.00	598.00	592.8	-8.2	8.2
GHOST23	42	174	2	NA	NA	600.00	603.00	597.00	592.8	-7.2	7.2
GHOST24	42	174	3	NA	NA	599.00	602.00	596.00	592.8	-6.2	6.2
GHOST10	7	199	1	NA	NA	575.00	578.00	572.00	556.2	-18.8	18.8
GHOST7	77	198	1	NA	NA	575.00	578.00	572.00	558.0	-17.0	17.0
GHOST8	77	198	2	NA	NA	574.00	577.00	571.00	558.0	-16.0	16.0
GHOST11	7	199	2	NA	NA	574.00	577.00	571.00	556.2	-17.8	17.8
GHOST9	77	198	3	NA	NA	573.00	576.00	570.00	558.0	-15.0	15.0
GHOST12	7	199	3	NA	NA	573.00	576.00	570.00	556.2	-16.8	16.8
GHOST16	6	213	1	NA	NA	515.00	518.00	512.00	481.0	-34.0	34.0
GHOST17	6	213	2	NA	NA	514.00	517.00	511.00	481.0	-33.0	33.0
GHOST18	6	213	3	NA	NA	513.00	516.00	510.00	481.0	-32.0	32.0
GHOST13	74	211	1	NA	NA	495.00	498.00	492.00	479.7	-15.3	15.3
GHOST14	74	211	2	NA	NA	494.00	497.00	491.00	479.7	-14.3	14.3
GHOST15	74	211	3	NA	NA	493.00	496.00	490.00	479.7	-13.3	13.3

Statistical Calculations:

Monitoring Wells Only	
ME=	-19.38
MAE=	19.38

Sensitivity of Heads to Kh

WELL	MODEL COLUMN	MODEL ROW	MODEL LAYER	MEAS. HIGH	MEAS. LOW	TARGET MEAN	TARGET HIGH	TARGET LOW	Kh:		
									MODEL HEAD	+25% 1.2875 Difference (feet)	(ft/day) Absolute Difference
MW25-3	4	9	1	742.41	742.41	740.75	743.75	737.75	701.4	-39.4	39.4
MW64A-1	82	11	1	736.63	736.63	737.87	740.87	734.87	699.6	-38.3	38.3
MW64A-3	82	12	1	734.08	734.08	735.32	738.32	732.32	698.9	-36.4	36.4
MW17-1	4	15	1	733.47	733.47	731.81	734.81	728.81	696.8	-35.0	35.0
MW16-1	2	13	1	732.14	732.14	730.97	733.97	727.97	698.7	-32.3	32.3
MW16-2	2	14	1	731.01	731.01	729.84	732.84	726.84	697.8	-32.0	32.0
MW17-3	4	16	1	729.77	729.77	728.11	731.11	725.11	695.7	-32.4	32.4
GHOST19	42	18	1	NA	NA	715.00	718.00	712.00	693.2	-21.8	21.8
GHOST20	42	18	2	NA	NA	714.00	717.00	711.00	693.2	-20.8	20.8
GHOST21	42	18	3	NA	NA	713.00	716.00	710.00	693.2	-19.8	19.8
GHOST1	77	28	1	NA	NA	695.00	698.00	692.00	676.2	-18.8	18.8
GHOST4	9	27	1	NA	NA	695.00	698.00	692.00	678.4	-16.6	16.6
GHOST5	9	27	2	NA	NA	694.00	697.00	691.00	678.4	-15.6	15.6
GHOST2	77	28	2	NA	NA	694.00	697.00	691.00	676.2	-17.8	17.8
GHOST3	77	28	3	NA	NA	693.00	696.00	690.00	676.2	-16.8	16.8
GHOST6	9	27	3	NA	NA	693.00	696.00	690.00	678.4	-14.6	14.6
MW-41D	11	42	2	687.96	685.74	686.82	687.32	686.32	638.2	-48.6	48.6
MW-42D	70	43	2	680.66	674.94	678.34	678.84	677.84	635.2	-43.1	43.1
PT-10	47	44	2	677.79	670.57	673.51	674.01	673.01	633.4	-40.1	40.1
MW64D-1	77	44	1	665.03	664.36	663.37	663.87	662.87	633.2	-30.2	30.2
MW-39	17	61	1	657.99	656.37	657.12	657.62	656.62	626.3	-30.8	30.8
MW-60	72	62	1	658.13	654.83	656.99	657.49	656.49	625.8	-31.2	31.2
MW64D-4	79	59	1	657.39	655.10	655.73	656.23	655.23	626.6	-29.1	29.1
MW-40	46	65	1	656.40	652.18	654.55	655.05	654.05	624.9	-29.7	29.7
MW-59	71	65	1	654.95	651.61	653.78	654.28	653.28	624.8	-29.0	29.0
MW-43	35	63	1	655.42	652.46	653.76	654.26	653.26	625.6	-28.2	28.2
PT-11	66	66	1	654.02	648.49	651.68	652.18	651.18	624.5	-27.2	27.2
PT-18	46	72	1	651.78	646.72	649.85	650.35	649.35	622.7	-27.2	27.2
MW-44	34	73	1	648.63	646.98	648.59	649.09	648.09	622.4	-26.2	26.2
MW-45	24	82	1	648.47	644.75	646.88	647.38	646.38	619.5	-27.4	27.4
MW-46	34	83	1	647.28	642.61	645.62	646.12	645.12	619.1	-26.5	26.5
MW-49D	34	83	2	647.11	642.74	645.45	645.95	644.95	619.1	-26.4	26.4
MW64D-3	77	72	1	646.91	645.89	645.25	645.75	644.75	622.4	-22.9	22.9
PT-12	44	81	1	647.25	641.73	644.90	645.40	644.40	619.7	-25.2	25.2
MW-50D	34	83	3	646.39	642.90	644.73	645.23	644.23	619.1	-25.6	25.6
MW-48	26	89	1	645.47	641.57	643.75	644.25	643.25	617.1	-26.7	26.7
PT-21	43	88	2	647.51	635.37	641.03	641.53	640.53	617.4	-23.6	23.6
PT-22	43	88	1	645.45	637.85	640.95	641.45	640.45	617.4	-23.5	23.5
PT-19	58	85	1	642.35	637.81	640.17	640.67	639.67	618.3	-21.9	21.9
PT-20	51	89	1	644.21	636.11	640.02	640.52	639.52	617.0	-23.0	23.0
MW-32	58	96	1	637.84	632.40	635.11	635.61	634.61	614.6	-20.5	20.5
PT-23	30	101	1	638.71	632.56	635.05	635.55	634.55	613.0	-22.1	22.1
PT-17	53	100	1	636.85	630.12	634.21	634.71	633.71	613.3	-20.9	20.9
MW-38D	18	107	2	634.67	632.76	633.97	634.47	633.47	611.0	-23.0	23.0
MW-27	33	103	1	635.62	630.37	633.45	633.95	632.95	612.3	-21.2	21.2
PT-16	18	107	1	635.06	630.17	633.43	633.93	632.93	611.0	-22.4	22.4
MW-33	63	98	1	635.95	630.02	633.41	633.91	632.91	613.9	-19.5	19.5
MW-30	56	101	1	636.37	629.73	633.13	633.63	632.63	612.9	-20.2	20.2
MW64D-2	75	92	1	633.49	630.75	631.83	632.33	631.33	615.8	-16.0	16.0
MW-55D	47	103	3	633.37	630.23	631.71	632.21	631.21	612.2	-19.5	19.5
MW-31	61	103	1	634.60	627.21	631.64	632.14	631.14	612.2	-19.4	19.4
MW-54D	47	103	2	633.29	629.88	631.63	632.13	631.13	612.2	-19.4	19.4
MW-28	36	105	1	633.28	628.26	631.58	632.08	631.08	611.6	-20.0	20.0
MW-53	47	103	1	632.83	630.13	631.17	631.67	630.67	612.2	-19.0	19.0
PT-24	40	109	1	633.19	627.85	631.02	631.52	630.52	610.2	-20.8	20.8
PT-25	64	104	1	633.66	625.45	630.56	631.06	630.06	611.8	-18.8	18.8
PT-15	71	99	1	634.09	627.40	630.35	630.85	629.85	613.5	-16.8	16.8
MW-29	46	107	1	631.82	626.83	630.19	630.69	629.69	610.9	-19.3	19.3
MW-37	7	116	1	630.91	626.65	629.14	629.64	628.64	608.1	-21.0	21.0
MW-35D	61	114	2	629.66	628.01	629.08	629.58	628.58	608.3	-20.8	20.8
MW-36	61	114	1	629.94	626.43	629.02	629.52	628.52	608.3	-20.7	20.7
MW-34	75	100	1	630.28	626.39	628.38	628.88	627.88	613.1	-15.3	15.3
MW-56	48	119	1	627.78	626.67	627.27	627.77	626.77	606.6	-20.7	20.7
MW-57D	48	119	2	628.60	627.11	626.94	627.44	626.44	606.6	-20.3	20.3
MW-58D	48	119	3	628.53	625.66	626.87	627.37	626.37	606.6	-20.3	20.3

MW-51D	35	128	2	625.68	621.56	624.02	624.52	623.52	603.5	-20.5	20.5
MW-47	35	128	1	625.69	621.47	623.96	624.46	623.46	603.5	-20.5	20.5
MW-52D	35	128	3	624.20	620.04	622.54	623.04	622.04	603.5	-19.0	19.0
PT-26	73	174	1	611.82	603.10	608.28	608.78	607.78	585.6	-22.7	22.7
GHOST22	42	174	1	NA	NA	601.00	604.00	598.00	586.0	-15.0	15.0
GHOST23	42	174	2	NA	NA	600.00	603.00	597.00	586.0	-14.0	14.0
GHOST24	42	174	3	NA	NA	599.00	602.00	596.00	586.0	-13.0	13.0
GHOST10	7	199	1	NA	NA	575.00	578.00	572.00	551.2	-23.8	23.8
GHOST7	77	198	1	NA	NA	575.00	578.00	572.00	552.9	-22.1	22.1
GHOST8	77	198	2	NA	NA	574.00	577.00	571.00	552.9	-21.1	21.1
GHOST11	7	199	2	NA	NA	574.00	577.00	571.00	551.2	-22.8	22.8
GHOST9	77	198	3	NA	NA	573.00	576.00	570.00	552.9	-20.1	20.1
GHOST12	7	199	3	NA	NA	573.00	576.00	570.00	551.2	-21.8	21.8
GHOST16	6	213	1	NA	NA	515.00	518.00	512.00	479.7	-35.3	35.3
GHOST17	6	213	2	NA	NA	514.00	517.00	511.00	479.7	-34.3	34.3
GHOST18	6	213	3	NA	NA	513.00	516.00	510.00	479.7	-33.3	33.3
GHOST13	74	211	1	NA	NA	495.00	498.00	492.00	478.5	-16.5	16.5
GHOST14	74	211	2	NA	NA	494.00	497.00	491.00	478.5	-15.5	15.5
GHOST15	74	211	3	NA	NA	493.00	496.00	490.00	478.5	-14.5	14.5

Statistical Calculations:

Monitoring Wells Only	
ME=	-29.80
MAE=	29.80

- **Sensitivity of Heads to K_v**



Sensitivity of Heads to Kv

WELL	MODEL COLUMN	MODEL ROW	MODEL LAYER	MEAS. HIGH	MEAS. LOW	TARGET MEAN	TARGET HIGH	TARGET LOW	Kv:		
									MODEL HEAD	0% Difference (feet)	(ft/day) Absolute Difference
MW25-3	4	9	1	742.41	742.41	740.75	743.75	737.75	736.1	-4.7	4.7
MW64A-1	82	11	1	736.63	736.63	737.87	740.87	734.87	734.0	-3.9	3.9
MW64A-3	82	12	1	734.08	734.08	735.32	738.32	732.32	733.2	-2.1	2.1
MW17-1	4	15	1	733.47	733.47	731.81	734.81	728.81	730.8	-1.0	1.0
MW16-1	2	13	1	732.14	732.14	730.97	733.97	727.97	732.9	1.9	1.9
MW16-2	2	14	1	731.01	731.01	729.84	732.84	726.84	731.9	2.1	2.1
MW17-3	4	16	1	729.77	729.77	728.11	731.11	725.11	729.5	1.4	1.4
GHOST19	42	18	1	NA	NA	715.00	718.00	712.00	726.7	11.7	11.7
GHOST20	42	18	2	NA	NA	714.00	717.00	711.00	726.7	12.7	12.7
GHOST21	42	18	3	NA	NA	713.00	716.00	710.00	726.7	13.7	13.7
GHOST1	77	28	1	NA	NA	695.00	698.00	692.00	707.3	12.3	12.3
GHOST4	9	27	1	NA	NA	695.00	698.00	692.00	709.8	14.8	14.8
GHOST5	9	27	2	NA	NA	694.00	697.00	691.00	709.8	15.8	15.8
GHOST2	77	28	2	NA	NA	694.00	697.00	691.00	707.3	13.3	13.3
GHOST3	77	28	3	NA	NA	693.00	696.00	690.00	707.3	14.3	14.3
GHOST6	9	27	3	NA	NA	693.00	696.00	690.00	709.8	16.8	16.8
MW-41D	11	42	2	687.96	685.74	686.82	687.32	686.32	663.9	-22.9	22.9
MW-42D	70	43	2	680.66	674.94	678.34	678.84	677.84	660.6	-17.7	17.7
PT-10	47	44	2	677.79	670.57	673.51	674.01	673.01	658.5	-15.0	15.0
MW64D-1	77	44	1	665.03	664.36	663.37	663.87	662.87	658.3	-5.1	5.1
MW-39	17	61	1	657.99	656.37	657.12	657.62	656.62	650.4	-6.7	6.7
MW-60	72	62	1	658.13	654.83	656.99	657.49	656.49	649.8	-7.2	7.2
MW64D-4	79	59	1	657.39	655.10	655.73	656.23	655.23	650.7	-5.0	5.0
MW-40	46	65	1	656.40	652.18	654.55	655.05	654.05	648.8	-5.8	5.8
MW-59	71	65	1	654.95	651.61	653.78	654.28	653.28	648.7	-5.1	5.1
MW-43	35	63	1	655.42	652.46	653.76	654.26	653.26	649.6	-4.2	4.2
PT-11	66	66	1	654.02	648.49	651.68	652.18	651.18	648.4	-3.3	3.3
PT-18	46	72	1	651.78	646.72	649.85	650.35	649.35	646.2	-3.7	3.7
MW-44	34	73	1	648.63	646.98	648.59	649.09	648.09	645.9	-2.7	2.7
MW-45	24	82	1	648.47	644.75	646.88	647.38	646.38	642.6	-4.3	4.3
MW-46	34	83	1	647.28	642.61	645.62	646.12	645.12	642.2	-3.4	3.4
MW-49D	34	83	2	647.11	642.74	645.45	645.95	644.95	642.2	-3.3	3.3
MW64D-3	77	72	1	646.91	645.89	645.25	645.75	644.75	646.0	0.7	0.7
PT-12	44	81	1	647.25	641.73	644.90	645.40	644.40	642.9	-2.0	2.0
MW-50D	34	83	3	646.39	642.90	644.73	645.23	644.23	642.2	-2.5	2.5
MW-48	26	89	1	645.47	641.57	643.75	644.25	643.25	639.9	-3.9	3.9
PT-21	43	88	2	647.51	635.37	641.03	641.53	640.53	640.2	-0.8	0.8
PT-22	43	88	1	645.45	637.85	640.95	641.45	640.45	640.2	-0.7	0.7
PT-19	58	85	1	642.35	637.81	640.17	640.67	639.67	641.3	1.1	1.1
PT-20	51	89	1	644.21	636.11	640.02	640.52	639.52	639.8	-0.2	0.2
MW-32	58	96	1	637.84	632.40	635.11	635.61	634.61	637.0	1.9	1.9
PT-23	30	101	1	638.71	632.56	635.05	635.55	634.55	635.2	0.1	0.1
PT-17	53	100	1	636.85	630.12	634.21	634.71	633.71	635.5	1.3	1.3
MW-38D	18	107	2	634.67	632.76	633.97	634.47	633.47	632.9	-1.1	1.1
MW-27	33	103	1	635.62	630.37	633.45	633.95	632.95	634.4	0.9	0.9
PT-16	18	107	1	635.06	630.17	633.43	633.93	632.93	632.9	-0.5	0.5
MW-33	63	98	1	635.95	630.02	633.41	633.91	632.91	636.2	2.8	2.8
MW-30	56	101	1	636.37	629.73	633.13	633.63	632.63	635.1	2.0	2.0
MW64D-2	75	92	1	633.49	630.75	631.83	632.33	631.33	638.4	6.6	6.6
MW-55D	47	103	3	633.37	630.23	631.71	632.21	631.21	634.3	2.6	2.6
MW-31	61	103	1	634.60	627.21	631.64	632.14	631.14	634.3	2.7	2.7
MW-54D	47	103	2	633.29	629.88	631.63	632.13	631.13	634.3	2.7	2.7
MW-28	36	105	1	633.28	628.26	631.58	632.08	631.08	633.6	2.0	2.0
MW-53	47	103	1	632.83	630.13	631.17	631.67	630.67	634.4	3.2	3.2
PT-24	40	109	1	633.19	627.85	631.02	631.52	630.52	632.0	1.0	1.0
PT-25	64	104	1	633.66	625.45	630.56	631.06	630.06	633.9	3.3	3.3
PT-15	71	99	1	634.09	627.40	630.35	630.85	629.85	635.8	5.5	5.5
MW-29	46	107	1	631.82	626.83	630.19	630.69	629.69	632.8	2.6	2.6
MW-37	7	116	1	630.91	626.65	629.14	629.64	628.64	629.6	0.5	0.5
MW-35D	61	114	2	629.66	628.01	629.08	629.58	628.58	629.9	0.8	0.8
MW-36	61	114	1	629.94	626.43	629.02	629.52	628.52	629.9	0.9	0.9
MW-34	75	100	1	630.28	626.39	628.38	628.88	627.88	635.3	6.9	6.9
MW-56	48	119	1	627.78	626.67	627.27	627.77	626.77	627.9	0.6	0.6
MW-57D	48	119	2	628.60	627.11	626.94	627.44	626.44	627.9	1.0	1.0
MW-58D	48	119	3	628.53	625.66	626.87	627.37	626.37	627.9	1.0	1.0

MW-51D	35	128	2	625.68	621.56	624.02	624.52	623.52	624.3	0.3	0.3
MW-47	35	128	1	625.69	621.47	623.96	624.46	623.46	624.3	0.3	0.3
MW-52D	35	128	3	624.20	620.04	622.54	623.04	622.04	624.3	1.8	1.8
PT-26	73	174	1	611.82	603.10	608.28	608.78	607.78	604.0	-4.3	4.3
GHOST22	42	174	1	NA	NA	601.00	604.00	598.00	604.5	3.5	3.5
GHOST23	42	174	2	NA	NA	600.00	603.00	597.00	604.5	4.5	4.5
GHOST24	42	174	3	NA	NA	599.00	602.00	596.00	604.5	5.5	5.5
GHOST10	7	199	1	NA	NA	575.00	578.00	572.00	560.6	-14.4	14.4
GHOST7	77	198	1	NA	NA	575.00	578.00	572.00	566.7	-8.3	8.3
GHOST8	77	198	2	NA	NA	574.00	577.00	571.00	566.7	-7.3	7.3
GHOST11	7	199	2	NA	NA	574.00	577.00	571.00	564.7	-9.3	9.3
GHOST9	77	198	3	NA	NA	573.00	576.00	570.00	566.7	-6.3	6.3
GHOST12	7	199	3	NA	NA	573.00	576.00	570.00	564.7	-8.3	8.3
GHOST16	6	213	1	NA	NA	515.00	518.00	512.00	483.2	-31.8	31.8
GHOST17	6	213	2	NA	NA	514.00	517.00	511.00	483.2	-30.8	30.8
GHOST18	6	213	3	NA	NA	513.00	516.00	510.00	483.2	-29.8	29.8
GHOST13	74	211	1	NA	NA	495.00	498.00	492.00	481.8	-13.2	13.2
GHOST14	74	211	2	NA	NA	494.00	497.00	491.00	481.8	-12.2	12.2
GHOST15	74	211	3	NA	NA	493.00	496.00	490.00	481.8	-11.2	11.2

Statistical Calculations:

Monitoring Wells Only	
ME=	-1.58
MAE=	4.03

Sensitivity of Heads to Kv

WELL	MODEL COLUMN	MODEL ROW	MODEL LAYER	MEAS. HIGH	MEAS. LOW	TARGET MEAN	TARGET HIGH	TARGET LOW	Kv:	-5%	(ft/day)
									MODEL HEAD	Difference (feet)	Absolute Difference
MW25-3	4	9	1	742.41	742.41	740.75	743.75	737.75	736.1	-4.7	4.7
MW64A-1	82	11	1	736.63	736.63	737.87	740.87	734.87	734.0	-3.9	3.9
MW64A-3	82	12	1	734.08	734.08	735.32	738.32	732.32	733.2	-2.1	2.1
MW17-1	4	15	1	733.47	733.47	731.81	734.81	728.81	730.8	-1.0	1.0
MW16-1	2	13	1	732.14	732.14	730.97	733.97	727.97	732.9	1.9	1.9
MW16-2	2	14	1	731.01	731.01	729.84	732.84	726.84	731.9	2.1	2.1
MW17-3	4	16	1	729.77	729.77	728.11	731.11	725.11	729.5	1.4	1.4
GHOST19	42	18	1	NA	NA	715.00	718.00	712.00	726.7	11.7	11.7
GHOST20	42	18	2	NA	NA	714.00	717.00	711.00	726.7	12.7	12.7
GHOST21	42	18	3	NA	NA	713.00	716.00	710.00	726.7	13.7	13.7
GHOST1	77	28	1	NA	NA	695.00	698.00	692.00	707.3	12.3	12.3
GHOST4	9	27	1	NA	NA	695.00	698.00	692.00	709.8	14.8	14.8
GHOST5	9	27	2	NA	NA	694.00	697.00	691.00	709.8	15.8	15.8
GHOST2	77	28	2	NA	NA	694.00	697.00	691.00	707.3	13.3	13.3
GHOST3	77	28	3	NA	NA	693.00	696.00	690.00	707.3	14.3	14.3
GHOST6	9	27	3	NA	NA	693.00	696.00	690.00	709.8	16.8	16.8
MW-41D	11	42	2	687.96	685.74	686.82	687.32	686.32	663.9	-22.9	22.9
MW-42D	70	43	2	680.66	674.94	678.34	678.84	677.84	660.6	-17.7	17.7
PT-10	47	44	2	677.79	670.57	673.51	674.01	673.01	658.5	-15.0	15.0
MW64D-1	77	44	1	665.03	664.36	663.37	663.87	662.87	658.3	-5.1	5.1
MW-39	17	61	1	657.99	656.37	657.12	657.62	656.62	650.4	-6.7	6.7
MW-60	72	62	1	658.13	654.83	656.99	657.49	656.49	649.8	-7.2	7.2
MW64D-4	79	59	1	657.39	655.10	655.73	656.23	655.23	650.7	-5.0	5.0
MW-40	46	65	1	656.40	652.18	654.55	655.05	654.05	648.8	-5.8	5.8
MW-59	71	65	1	654.95	651.61	653.78	654.28	653.28	648.7	-5.1	5.1
MW-43	35	63	1	655.42	652.46	653.76	654.26	653.26	649.6	-4.2	4.2
PT-11	66	66	1	654.02	648.49	651.68	652.18	651.18	648.4	-3.3	3.3
PT-18	46	72	1	651.78	646.72	649.85	650.35	649.35	646.2	-3.7	3.7
MW-44	34	73	1	648.63	646.98	648.59	649.09	648.09	645.9	-2.7	2.7
MW-45	24	82	1	648.47	644.75	646.88	647.38	646.38	642.6	-4.3	4.3
MW-46	34	83	1	647.28	642.61	645.62	646.12	645.12	642.2	-3.4	3.4
MW-49D	34	83	2	647.11	642.74	645.45	645.95	644.95	642.2	-3.3	3.3
MW64D-3	77	72	1	646.91	645.89	645.25	645.75	644.75	646.0	0.7	0.7
PT-12	44	81	1	647.25	641.73	644.90	645.40	644.40	642.9	-2.0	2.0
MW-50D	34	83	3	646.39	642.90	644.73	645.23	644.23	642.2	-2.5	2.5
MW-48	26	89	1	645.47	641.57	643.75	644.25	643.25	639.9	-3.9	3.9
PT-21	43	88	2	647.51	635.37	641.03	641.53	640.53	640.2	-0.8	0.8
PT-22	43	88	1	645.45	637.85	640.95	641.45	640.45	640.2	-0.7	0.7
PT-19	58	85	1	642.35	637.81	640.17	640.67	639.67	641.3	1.1	1.1
PT-20	51	89	1	644.21	636.11	640.02	640.52	639.52	639.8	-0.2	0.2
MW-32	58	96	1	637.84	632.40	635.11	635.61	634.61	637.0	1.9	1.9
PT-23	30	101	1	638.71	632.56	635.05	635.55	634.55	635.2	0.1	0.1
PT-17	53	100	1	636.85	630.12	634.21	634.71	633.71	635.5	1.3	1.3
MW-38D	18	107	2	634.67	632.76	633.97	634.47	633.47	632.9	-1.1	1.1
MW-27	33	103	1	635.62	630.37	633.45	633.95	632.95	634.4	0.9	0.9
PT-16	18	107	1	635.06	630.17	633.43	633.93	632.93	632.9	-0.5	0.5
MW-33	63	98	1	635.95	630.02	633.41	633.91	632.91	636.2	2.8	2.8
MW-30	56	101	1	636.37	629.73	633.13	633.63	632.63	635.1	2.0	2.0
MW64D-2	75	92	1	633.49	630.75	631.83	632.33	631.33	638.4	6.6	6.6
MW-55D	47	103	3	633.37	630.23	631.71	632.21	631.21	634.3	2.6	2.6
MW-31	61	103	1	634.60	627.21	631.64	632.14	631.14	634.3	2.7	2.7
MW-54D	47	103	2	633.29	629.88	631.63	632.13	631.13	634.3	2.7	2.7
MW-28	36	105	1	633.28	628.26	631.58	632.08	631.08	633.6	2.0	2.0
MW-53	47	103	1	632.83	630.13	631.17	631.67	630.67	634.4	3.2	3.2
PT-24	40	109	1	633.19	627.85	631.02	631.52	630.52	632.0	1.0	1.0
PT-25	64	104	1	633.66	625.45	630.56	631.06	630.06	633.9	3.3	3.3
PT-15	71	99	1	634.09	627.40	630.35	630.85	629.85	635.8	5.5	5.5
MW-29	46	107	1	631.82	626.83	630.19	630.69	629.69	632.8	2.6	2.6
MW-37	7	116	1	630.91	626.65	629.14	629.64	628.64	629.6	0.5	0.5
MW-35D	61	114	2	629.66	628.01	629.08	629.58	628.58	629.9	0.8	0.8
MW-36	61	114	1	629.94	626.43	629.02	629.52	628.52	629.9	0.9	0.9
MW-34	75	100	1	630.28	626.39	628.38	628.88	627.88	635.3	6.9	6.9
MW-56	48	119	1	627.78	626.67	627.27	627.77	626.77	627.9	0.6	0.6
MW-57D	48	119	2	628.60	627.11	626.94	627.44	626.44	627.9	1.0	1.0
MW-58D	48	119	3	628.53	625.66	626.87	627.37	626.37	627.9	1.0	1.0

MW-51D	35	128	2	625.68	621.56	624.02	624.52	623.52	624.3	0.3	0.3
MW-47	35	128	1	625.69	621.47	623.96	624.46	623.46	624.3	0.3	0.3
MW-52D	35	128	3	624.20	620.04	622.54	623.04	622.04	624.3	1.8	1.8
PT-26	73	174	1	611.82	603.10	608.28	608.78	607.78	604.0	-4.3	4.3
GHOST22	42	174	1	NA	NA	601.00	604.00	598.00	604.5	3.5	3.5
GHOST23	42	174	2	NA	NA	600.00	603.00	597.00	604.5	4.5	4.5
GHOST24	42	174	3	NA	NA	599.00	602.00	596.00	604.5	5.5	5.5
GHOST10	7	199	1	NA	NA	575.00	578.00	572.00	560.6	-14.4	14.4
GHOST7	77	198	1	NA	NA	575.00	578.00	572.00	566.7	-8.3	8.3
GHOST8	77	198	2	NA	NA	574.00	577.00	571.00	566.7	-7.3	7.3
GHOST11	7	199	2	NA	NA	574.00	577.00	571.00	564.7	-9.3	9.3
GHOST9	77	198	3	NA	NA	573.00	576.00	570.00	566.7	-6.3	6.3
GHOST12	7	199	3	NA	NA	573.00	576.00	570.00	564.7	-8.3	8.3
GHOST16	6	213	1	NA	NA	515.00	518.00	512.00	483.2	-31.8	31.8
GHOST17	6	213	2	NA	NA	514.00	517.00	511.00	483.2	-30.8	30.8
GHOST18	6	213	3	NA	NA	513.00	516.00	510.00	483.2	-29.8	29.8
GHOST13	74	211	1	NA	NA	495.00	498.00	492.00	481.8	-13.2	13.2
GHOST14	74	211	2	NA	NA	494.00	497.00	491.00	481.8	-12.2	12.2
GHOST15	74	211	3	NA	NA	493.00	496.00	490.00	481.8	-11.2	11.2

Statistical Calculations:

Monitoring Wells Only	
ME=	-1.58
MAE=	4.03

Sensitivity of Heads to Kv

WELL	MODEL COLUMN	MODEL ROW	MODEL LAYER	MEAS. HIGH	MEAS. LOW	TARGET MEAN	TARGET HIGH	TARGET LOW	Kv: -15%		
									MODEL HEAD	Difference (feet)	(ft/day) Absolute Difference
MW25-3	4	9	1	742.41	742.41	740.75	743.75	737.75	736.1	-4.7	4.7
MW64A-1	82	11	1	736.63	736.63	737.87	740.87	734.87	734.0	-3.9	3.9
MW64A-3	82	12	1	734.08	734.08	735.32	738.32	732.32	733.2	-2.1	2.1
MW17-1	4	15	1	733.47	733.47	731.81	734.81	728.81	730.8	-1.0	1.0
MW16-1	2	13	1	732.14	732.14	730.97	733.97	727.97	732.9	1.9	1.9
MW16-2	2	14	1	731.01	731.01	729.84	732.84	726.84	731.9	2.1	2.1
MW17-3	4	16	1	729.77	729.77	728.11	731.11	725.11	729.5	1.4	1.4
GHOST19	42	18	1	NA	NA	715.00	718.00	712.00	726.7	11.7	11.7
GHOST20	42	18	2	NA	NA	714.00	717.00	711.00	726.7	12.7	12.7
GHOST21	42	18	3	NA	NA	713.00	716.00	710.00	726.7	13.7	13.7
GHOST1	77	28	1	NA	NA	695.00	698.00	692.00	707.3	12.3	12.3
GHOST4	9	27	1	NA	NA	695.00	698.00	692.00	709.8	14.8	14.8
GHOST5	9	27	2	NA	NA	694.00	697.00	691.00	709.8	15.8	15.8
GHOST2	77	28	2	NA	NA	694.00	697.00	691.00	707.3	13.3	13.3
GHOST3	77	28	3	NA	NA	693.00	696.00	690.00	707.3	14.3	14.3
GHOST6	9	27	3	NA	NA	693.00	696.00	690.00	709.8	16.8	16.8
MW-41D	11	42	2	687.96	685.74	686.82	687.32	686.32	663.9	-22.9	22.9
MW-42D	70	43	2	680.66	674.94	678.34	678.84	677.84	660.6	-17.7	17.7
PT-10	47	44	2	677.79	670.57	673.51	674.01	673.01	658.5	-15.0	15.0
MW64D-1	77	44	1	665.03	664.36	663.37	663.87	662.87	658.3	-5.1	5.1
MW-39	17	61	1	657.99	656.37	657.12	657.62	656.62	650.4	-6.7	6.7
MW-60	72	62	1	658.13	654.83	656.99	657.49	656.49	649.8	-7.2	7.2
MW64D-4	79	59	1	657.39	655.10	655.73	656.23	655.23	650.7	-5.0	5.0
MW-40	46	65	1	656.40	652.18	654.55	655.05	654.05	648.8	-5.8	5.8
MW-59	71	65	1	654.95	651.61	653.78	654.28	653.28	648.7	-5.1	5.1
MW-43	35	63	1	655.42	652.46	653.76	654.26	653.26	649.6	-4.2	4.2
PT-11	66	66	1	654.02	648.49	651.68	652.18	651.18	648.4	-3.3	3.3
PT-18	46	72	1	651.78	646.72	649.85	650.35	649.35	646.2	-3.7	3.7
MW-44	34	73	1	648.63	646.98	648.59	649.09	648.09	645.9	-2.7	2.7
MW-45	24	82	1	648.47	644.75	646.88	647.38	646.38	642.6	-4.3	4.3
MW-46	34	83	1	647.28	642.61	645.62	646.12	645.12	642.2	-3.4	3.4
MW-49D	34	83	2	647.11	642.74	645.45	645.95	644.95	642.2	-3.3	3.3
MW64D-3	77	72	1	646.91	645.89	645.25	645.75	644.75	646.0	0.7	0.7
PT-12	44	81	1	647.25	641.73	644.90	645.40	644.40	642.9	-2.0	2.0
MW-50D	34	83	3	646.39	642.90	644.73	645.23	644.23	642.2	-2.5	2.5
MW-48	26	89	1	645.47	641.57	643.75	644.25	643.25	639.9	-3.9	3.9
PT-21	43	88	2	647.51	635.37	641.03	641.53	640.53	640.2	-0.8	0.8
PT-22	43	88	1	645.45	637.85	640.95	641.45	640.45	640.2	-0.7	0.7
PT-19	58	85	1	642.35	637.81	640.17	640.67	639.67	641.3	1.1	1.1
PT-20	51	89	1	644.21	636.11	640.02	640.52	639.52	639.8	-0.2	0.2
MW-32	58	96	1	637.84	632.40	635.11	635.61	634.61	637.0	1.9	1.9
PT-23	30	101	1	638.71	632.56	635.05	635.55	634.55	635.2	0.1	0.1
PT-17	53	100	1	636.85	630.12	634.21	634.71	633.71	635.5	1.3	1.3
MW-38D	18	107	2	634.67	632.76	633.97	634.47	633.47	632.9	-1.1	1.1
MW-27	33	103	1	635.62	630.37	633.45	633.95	632.95	634.4	0.9	0.9
PT-16	18	107	1	635.06	630.17	633.43	633.93	632.93	632.9	-0.5	0.5
MW-33	63	98	1	635.95	630.02	633.41	633.91	632.91	636.2	2.8	2.8
MW-30	56	101	1	636.37	629.73	633.13	633.63	632.63	635.1	2.0	2.0
MW64D-2	75	92	1	633.49	630.75	631.83	632.33	631.33	638.4	6.6	6.6
MW-55D	47	103	3	633.37	630.23	631.71	632.21	631.21	634.3	2.6	2.6
MW-31	61	103	1	634.60	627.21	631.64	632.14	631.14	634.3	2.7	2.7
MW-54D	47	103	2	633.29	629.88	631.63	632.13	631.13	634.3	2.7	2.7
MW-28	36	105	1	633.28	628.26	631.58	632.08	631.08	633.6	2.0	2.0
MW-53	47	103	1	632.83	630.13	631.17	631.67	630.67	634.4	3.2	3.2
PT-24	40	109	1	633.19	627.85	631.02	631.52	630.52	632.0	1.0	1.0
PT-25	64	104	1	633.66	625.45	630.56	631.06	630.06	633.9	3.3	3.3
PT-15	71	99	1	634.09	627.40	630.35	630.85	629.85	635.8	5.5	5.5
MW-29	46	107	1	631.82	626.83	630.19	630.69	629.69	632.8	2.6	2.6
MW-37	7	116	1	630.91	626.65	629.14	629.64	628.64	629.6	0.5	0.5
MW-35D	61	114	2	629.66	628.01	629.08	629.58	628.58	629.9	0.8	0.8
MW-36	61	114	1	629.94	626.43	629.02	629.52	628.52	629.9	0.9	0.9
MW-34	75	100	1	630.28	626.39	628.38	628.88	627.88	635.3	6.9	6.9
MW-56	48	119	1	627.78	626.67	627.27	627.77	626.77	627.9	0.6	0.6
MW-57D	48	119	2	628.60	627.11	626.94	627.44	626.44	627.9	1.0	1.0
MW-58D	48	119	3	628.53	625.66	626.87	627.37	626.37	627.9	1.0	1.0

MW-51D	35	128	2	625.68	621.56	624.02	624.52	623.52	624.3	0.3	0.3
MW-47	35	128	1	625.69	621.47	623.96	624.46	623.46	624.3	0.3	0.3
MW-52D	35	128	3	624.20	620.04	622.54	623.04	622.04	624.3	1.8	1.8
PT-26	73	174	1	611.82	603.10	608.28	608.78	607.78	604.0	-4.3	4.3
GHOST22	42	174	1	NA	NA	601.00	604.00	598.00	604.5	3.5	3.5
GHOST23	42	174	2	NA	NA	600.00	603.00	597.00	604.5	4.5	4.5
GHOST24	42	174	3	NA	NA	599.00	602.00	596.00	604.5	5.5	5.5
GHOST10	7	199	1	NA	NA	575.00	578.00	572.00	560.6	-14.4	14.4
GHOST7	77	198	1	NA	NA	575.00	578.00	572.00	566.7	-8.3	8.3
GHOST8	77	198	2	NA	NA	574.00	577.00	571.00	566.7	-7.3	7.3
GHOST11	7	199	2	NA	NA	574.00	577.00	571.00	564.7	-9.3	9.3
GHOST9	77	198	3	NA	NA	573.00	576.00	570.00	566.7	-6.3	6.3
GHOST12	7	199	3	NA	NA	573.00	576.00	570.00	564.7	-8.3	8.3
GHOST16	6	213	1	NA	NA	515.00	518.00	512.00	483.2	-31.8	31.8
GHOST17	6	213	2	NA	NA	514.00	517.00	511.00	483.2	-30.8	30.8
GHOST18	6	213	3	NA	NA	513.00	516.00	510.00	483.2	-29.8	29.8
GHOST13	74	211	1	NA	NA	495.00	498.00	492.00	481.8	-13.2	13.2
GHOST14	74	211	2	NA	NA	494.00	497.00	491.00	481.8	-12.2	12.2
GHOST15	74	211	3	NA	NA	493.00	496.00	490.00	481.8	-11.2	11.2

Statistical Calculations:

Monitoring Wells Only	
ME=	-1.58
MAE=	4.03

Sensitivity of Heads to Kv

WELL	MODEL COLUMN	MODEL ROW	MODEL LAYER	MEAS. HIGH	MEAS. LOW	TARGET MEAN	TARGET HIGH	TARGET LOW	Kv: -25% 0.0014 (ft/day)		
									MODEL HEAD	Difference (feet)	Absolute Difference
MW25-3	4	9	1	742.41	742.41	740.75	743.75	737.75	736.1	-4.7	4.7
MW64A-1	82	11	1	736.63	736.63	737.87	740.87	734.87	734.0	-3.9	3.9
MW64A-3	82	12	1	734.08	734.08	735.32	738.32	732.32	733.2	-2.1	2.1
MW17-1	4	15	1	733.47	733.47	731.81	734.81	728.81	730.8	-1.0	1.0
MW16-1	2	13	1	732.14	732.14	730.97	733.97	727.97	732.9	1.9	1.9
MW16-2	2	14	1	731.01	731.01	729.84	732.84	726.84	731.9	2.1	2.1
MW17-3	4	16	1	729.77	729.77	728.11	731.11	725.11	729.5	1.4	1.4
GHOST19	42	18	1	NA	NA	715.00	718.00	712.00	726.7	11.7	11.7
GHOST20	42	18	2	NA	NA	714.00	717.00	711.00	726.7	12.7	12.7
GHOST21	42	18	3	NA	NA	713.00	716.00	710.00	726.7	13.7	13.7
GHOST1	77	28	1	NA	NA	695.00	698.00	692.00	707.3	12.3	12.3
GHOST4	9	27	1	NA	NA	695.00	698.00	692.00	709.8	14.8	14.8
GHOST5	9	27	2	NA	NA	694.00	697.00	691.00	709.8	15.8	15.8
GHOST2	77	28	2	NA	NA	694.00	697.00	691.00	707.3	13.3	13.3
GHOST3	77	28	3	NA	NA	693.00	696.00	690.00	707.3	14.3	14.3
GHOST6	9	27	3	NA	NA	693.00	696.00	690.00	709.8	16.8	16.8
MW-41D	11	42	2	687.96	685.74	686.82	687.32	686.32	663.9	-22.9	22.9
MW-42D	70	43	2	680.66	674.94	678.34	678.84	677.84	660.6	-17.7	17.7
PT-10	47	44	2	677.79	670.57	673.51	674.01	673.01	658.5	-15.0	15.0
MW64D-1	77	44	1	665.03	664.36	663.37	663.87	662.87	658.3	-5.1	5.1
MW-39	17	61	1	657.99	656.37	657.12	657.62	656.62	650.4	-6.7	6.7
MW-60	72	62	1	658.13	654.83	656.99	657.49	656.49	649.8	-7.2	7.2
MW64D-4	79	59	1	657.39	655.10	655.73	656.23	655.23	650.7	-5.0	5.0
MW-40	46	65	1	656.40	652.18	654.55	655.05	654.05	648.8	-5.8	5.8
MW-59	71	65	1	654.95	651.61	653.78	654.28	653.28	648.7	-5.1	5.1
MW-43	35	63	1	655.42	652.46	653.76	654.26	653.26	649.6	-4.2	4.2
PT-11	66	66	1	654.02	648.49	651.68	652.18	651.18	648.4	-3.3	3.3
PT-18	46	72	1	651.78	646.72	649.85	650.35	649.35	646.2	-3.7	3.7
MW-44	34	73	1	648.63	646.98	648.59	649.09	648.09	645.9	-2.7	2.7
MW-45	24	82	1	648.47	644.75	646.88	647.38	646.38	642.6	-4.3	4.3
MW-46	34	83	1	647.28	642.61	645.62	646.12	645.12	642.2	-3.4	3.4
MW-49D	34	83	2	647.11	642.74	645.45	645.95	644.95	642.2	-3.3	3.3
MW64D-3	77	72	1	646.91	645.89	645.25	645.75	644.75	646.0	0.7	0.7
PT-12	44	81	1	647.25	641.73	644.90	645.40	644.40	642.9	-2.0	2.0
MW-50D	34	83	3	646.39	642.90	644.73	645.23	644.23	642.2	-2.5	2.5
MW-48	26	89	1	645.47	641.57	643.75	644.25	643.25	639.9	-3.9	3.9
PT-21	43	88	2	647.51	635.37	641.03	641.53	640.53	640.2	-0.8	0.8
PT-22	43	88	1	645.45	637.85	640.95	641.45	640.45	640.2	-0.7	0.7
PT-19	58	85	1	642.35	637.81	640.17	640.67	639.67	641.3	1.1	1.1
PT-20	51	89	1	644.21	636.11	640.02	640.52	639.52	639.8	-0.2	0.2
MW-32	58	96	1	637.84	632.40	635.11	635.61	634.61	637.0	1.9	1.9
PT-23	30	101	1	638.71	632.56	635.05	635.55	634.55	635.2	0.1	0.1
PT-17	53	100	1	636.85	630.12	634.21	634.71	633.71	635.5	1.3	1.3
MW-38D	18	107	2	634.67	632.76	633.97	634.47	633.47	632.9	-1.1	1.1
MW-27	33	103	1	635.62	630.37	633.45	633.95	632.95	634.4	0.9	0.9
PT-16	18	107	1	635.06	630.17	633.43	633.93	632.93	632.9	-0.5	0.5
MW-33	63	98	1	635.95	630.02	633.41	633.91	632.91	636.2	2.8	2.8
MW-30	56	101	1	636.37	629.73	633.13	633.63	632.63	635.1	2.0	2.0
MW64D-2	75	92	1	633.49	630.75	631.83	632.33	631.33	638.4	6.6	6.6
MW-55D	47	103	3	633.37	630.23	631.71	632.21	631.21	634.3	2.6	2.6
MW-31	61	103	1	634.60	627.21	631.64	632.14	631.14	634.3	2.7	2.7
MW-54D	47	103	2	633.29	629.88	631.63	632.13	631.13	634.3	2.7	2.7
MW-28	36	105	1	633.28	628.26	631.58	632.08	631.08	633.6	2.0	2.0
MW-53	47	103	1	632.83	630.13	631.17	631.67	630.67	634.4	3.2	3.2
PT-24	40	109	1	633.19	627.85	631.02	631.52	630.52	632.0	1.0	1.0
PT-25	64	104	1	633.66	625.45	630.56	631.06	630.06	633.9	3.3	3.3
PT-15	71	99	1	634.09	627.40	630.35	630.85	629.85	635.8	5.5	5.5
MW-29	46	107	1	631.82	626.83	630.19	630.69	629.69	632.8	2.6	2.6
MW-37	7	116	1	630.91	626.65	629.14	629.64	628.64	629.6	0.5	0.5
MW-35D	61	114	2	629.66	628.01	629.08	629.58	628.58	629.9	0.8	0.8
MW-36	61	114	1	629.94	626.43	629.02	629.52	628.52	629.9	0.9	0.9
MW-34	75	100	1	630.28	626.39	628.38	628.88	627.88	635.3	6.9	6.9
MW-56	48	119	1	627.78	626.67	627.27	627.77	626.77	627.9	0.6	0.6
MW-57D	48	119	2	628.60	627.11	626.94	627.44	626.44	627.9	1.0	1.0
MW-58D	48	119	3	628.53	625.66	626.87	627.37	626.37	627.9	1.0	1.0

MW-51D	35	128	2	625.68	621.56	624.02	624.52	623.52	624.3	0.3	0.3
MW-47	35	128	1	625.69	621.47	623.96	624.46	623.46	624.3	0.3	0.3
MW-52D	35	128	3	624.20	620.04	622.54	623.04	622.04	624.3	1.8	1.8
PT-26	73	174	1	611.82	603.10	608.28	608.78	607.78	604.0	-4.3	4.3
GHOST22	42	174	1	NA	NA	601.00	604.00	598.00	604.5	3.5	3.5
GHOST23	42	174	2	NA	NA	600.00	603.00	597.00	604.5	4.5	4.5
GHOST24	42	174	3	NA	NA	599.00	602.00	596.00	604.5	5.5	5.5
GHOST10	7	199	1	NA	NA	575.00	578.00	572.00	560.6	-14.4	14.4
GHOST7	77	198	1	NA	NA	575.00	578.00	572.00	566.7	-8.3	8.3
GHOST8	77	198	2	NA	NA	574.00	577.00	571.00	566.7	-7.3	7.3
GHOST11	7	199	2	NA	NA	574.00	577.00	571.00	564.7	-9.3	9.3
GHOST9	77	198	3	NA	NA	573.00	576.00	570.00	566.7	-6.3	6.3
GHOST12	7	199	3	NA	NA	573.00	576.00	570.00	564.7	-8.3	8.3
GHOST16	6	213	1	NA	NA	515.00	518.00	512.00	483.2	-31.8	31.8
GHOST17	6	213	2	NA	NA	514.00	517.00	511.00	483.2	-30.8	30.8
GHOST18	6	213	3	NA	NA	513.00	516.00	510.00	483.2	-29.8	29.8
GHOST13	74	211	1	NA	NA	495.00	498.00	492.00	481.8	-13.2	13.2
GHOST14	74	211	2	NA	NA	494.00	497.00	491.00	481.8	-12.2	12.2
GHOST15	74	211	3	NA	NA	493.00	496.00	490.00	481.8	-11.2	11.2

Statistical Calculations:

Monitoring Wells Only	
ME=	-1.58
MAE=	4.03

Sensitivity of Heads to Kv

WELL	MODEL COLUMN	MODEL ROW	MODEL LAYER	MEAS. HIGH	MEAS. LOW	TARGET MEAN	TARGET HIGH	TARGET LOW	Kv: +5% 0.0019 (ft/day)		
									MODEL HEAD	Difference (feet)	Absolute Difference
MW25-3	4	9	1	742.41	742.41	740.75	743.75	737.75	736.1	-4.7	4.7
MW64A-1	82	11	1	736.63	736.63	737.87	740.87	734.87	734.0	-3.9	3.9
MW64A-3	82	12	1	734.08	734.08	735.32	738.32	732.32	733.2	-2.1	2.1
MW17-1	4	15	1	733.47	733.47	731.81	734.81	728.81	730.8	-1.0	1.0
MW16-1	2	13	1	732.14	732.14	730.97	733.97	727.97	732.9	1.9	1.9
MW16-2	2	14	1	731.01	731.01	729.84	732.84	726.84	731.9	2.1	2.1
MW17-3	4	16	1	729.77	729.77	728.11	731.11	725.11	729.5	1.4	1.4
GHOST19	42	18	1	NA	NA	715.00	718.00	712.00	726.7	11.7	11.7
GHOST20	42	18	2	NA	NA	714.00	717.00	711.00	726.7	12.7	12.7
GHOST21	42	18	3	NA	NA	713.00	716.00	710.00	726.7	13.7	13.7
GHOST1	77	28	1	NA	NA	695.00	698.00	692.00	707.3	12.3	12.3
GHOST4	9	27	1	NA	NA	695.00	698.00	692.00	709.8	14.8	14.8
GHOST5	9	27	2	NA	NA	694.00	697.00	691.00	709.8	15.8	15.8
GHOST2	77	28	2	NA	NA	694.00	697.00	691.00	707.3	13.3	13.3
GHOST3	77	28	3	NA	NA	693.00	696.00	690.00	707.3	14.3	14.3
GHOST6	9	27	3	NA	NA	693.00	696.00	690.00	709.8	16.8	16.8
MW-41D	11	42	2	687.96	685.74	686.82	687.32	686.32	663.9	-22.9	22.9
MW-42D	70	43	2	680.66	674.94	678.34	678.84	677.84	660.6	-17.7	17.7
PT-10	47	44	2	677.79	670.57	673.51	674.01	673.01	658.5	-15.0	15.0
MW64D-1	77	44	1	665.03	664.36	663.37	663.87	662.87	658.3	-5.1	5.1
MW-39	17	61	1	657.99	656.37	657.12	657.62	656.62	650.4	-6.7	6.7
MW-60	72	62	1	658.13	654.83	656.99	657.49	656.49	649.8	-7.2	7.2
MW64D-4	79	59	1	657.39	655.10	655.73	656.23	655.23	650.7	-5.0	5.0
MW-40	46	65	1	656.40	652.18	654.55	655.05	654.05	648.8	-5.8	5.8
MW-59	71	65	1	654.95	651.61	653.78	654.28	653.28	648.7	-5.1	5.1
MW-43	35	63	1	655.42	652.46	653.76	654.26	653.26	649.6	-4.2	4.2
PT-11	66	66	1	654.02	648.49	651.68	652.18	651.18	648.4	-3.3	3.3
PT-18	46	72	1	651.78	646.72	649.85	650.35	649.35	646.2	-3.7	3.7
MW-44	34	73	1	648.63	646.98	648.59	649.09	648.09	645.9	-2.7	2.7
MW-45	24	82	1	648.47	644.75	646.88	647.38	646.38	642.6	-4.3	4.3
MW-46	34	83	1	647.28	642.61	645.62	646.12	645.12	642.2	-3.4	3.4
MW-49D	34	83	2	647.11	642.74	645.45	645.95	644.95	642.2	-3.3	3.3
MW64D-3	77	72	1	646.91	645.89	645.25	645.75	644.75	646.0	0.7	0.7
PT-12	44	81	1	647.25	641.73	644.90	645.40	644.40	642.9	-2.0	2.0
MW-50D	34	83	3	646.39	642.90	644.73	645.23	644.23	642.2	-2.5	2.5
MW-48	26	89	1	645.47	641.57	643.75	644.25	643.25	639.9	-3.9	3.9
PT-21	43	88	2	647.51	635.37	641.03	641.53	640.53	640.2	-0.8	0.8
PT-22	43	88	1	645.45	637.85	640.95	641.45	640.45	640.2	-0.7	0.7
PT-19	58	85	1	642.35	637.81	640.17	640.67	639.67	641.3	1.1	1.1
PT-20	51	89	1	644.21	636.11	640.02	640.52	639.52	639.8	-0.2	0.2
MW-32	58	96	1	637.84	632.40	635.11	635.61	634.61	637.0	1.9	1.9
PT-23	30	101	1	638.71	632.56	635.05	635.55	634.55	635.2	0.1	0.1
PT-17	53	100	1	636.85	630.12	634.21	634.71	633.71	635.5	1.3	1.3
MW-38D	18	107	2	634.67	632.76	633.97	634.47	633.47	632.9	-1.1	1.1
MW-27	33	103	1	635.62	630.37	633.45	633.95	632.95	634.4	0.9	0.9
PT-16	18	107	1	635.06	630.17	633.43	633.93	632.93	632.9	-0.5	0.5
MW-33	63	98	1	635.95	630.02	633.41	633.91	632.91	636.2	2.8	2.8
MW-30	56	101	1	636.37	629.73	633.13	633.63	632.63	635.1	2.0	2.0
MW64D-2	75	92	1	633.49	630.75	631.83	632.33	631.33	638.4	6.6	6.6
MW-55D	47	103	3	633.37	630.23	631.71	632.21	631.21	634.3	2.6	2.6
MW-31	61	103	1	634.60	627.21	631.64	632.14	631.14	634.3	2.7	2.7
MW-54D	47	103	2	633.29	629.88	631.63	632.13	631.13	634.3	2.7	2.7
MW-28	36	105	1	633.28	628.26	631.58	632.08	631.08	633.6	2.0	2.0
MW-53	47	103	1	632.83	630.13	631.17	631.67	630.67	634.4	3.2	3.2
PT-24	40	109	1	633.19	627.85	631.02	631.52	630.52	632.0	1.0	1.0
PT-25	64	104	1	633.66	625.45	630.56	631.06	630.06	633.9	3.3	3.3
PT-15	71	99	1	634.09	627.40	630.35	630.85	629.85	635.8	5.5	5.5
MW-29	46	107	1	631.82	626.83	630.19	630.69	629.69	632.8	2.6	2.6
MW-37	7	116	1	630.91	626.65	629.14	629.64	628.64	629.6	0.5	0.5
MW-35D	61	114	2	629.66	628.01	629.08	629.58	628.58	629.9	0.8	0.8
MW-36	61	114	1	629.94	626.43	629.02	629.52	628.52	629.9	0.9	0.9
MW-34	75	100	1	630.28	626.39	628.38	628.88	627.88	635.3	6.9	6.9
MW-56	48	119	1	627.78	626.67	627.27	627.77	626.77	627.9	0.6	0.6
MW-57D	48	119	2	628.60	627.11	626.94	627.44	626.44	627.9	1.0	1.0
MW-58D	48	119	3	628.53	625.66	626.87	627.37	626.37	627.9	1.0	1.0

MW-51D	35	128	2	625.68	621.56	624.02	624.52	623.52	624.3	0.3	0.3
MW-47	35	128	1	625.69	621.47	623.96	624.46	623.46	624.3	0.3	0.3
MW-52D	35	128	3	624.20	620.04	622.54	623.04	622.04	624.3	1.8	1.8
PT-26	73	174	1	611.82	603.10	608.28	608.78	607.78	604.0	-4.3	4.3
GHOST22	42	174	1	NA	NA	601.00	604.00	598.00	604.5	3.5	3.5
GHOST23	42	174	2	NA	NA	600.00	603.00	597.00	604.5	4.5	4.5
GHOST24	42	174	3	NA	NA	599.00	602.00	596.00	604.5	5.5	5.5
GHOST10	7	199	1	NA	NA	575.00	578.00	572.00	560.6	-14.4	14.4
GHOST7	77	198	1	NA	NA	575.00	578.00	572.00	566.7	-8.3	8.3
GHOST8	77	198	2	NA	NA	574.00	577.00	571.00	566.7	-7.3	7.3
GHOST11	7	199	2	NA	NA	574.00	577.00	571.00	564.7	-9.3	9.3
GHOST9	77	198	3	NA	NA	573.00	576.00	570.00	566.7	-6.3	6.3
GHOST12	7	199	3	NA	NA	573.00	576.00	570.00	564.7	-8.3	8.3
GHOST16	6	213	1	NA	NA	515.00	518.00	512.00	483.2	-31.8	31.8
GHOST17	6	213	2	NA	NA	514.00	517.00	511.00	483.2	-30.8	30.8
GHOST18	6	213	3	NA	NA	513.00	516.00	510.00	483.2	-29.8	29.8
GHOST13	74	211	1	NA	NA	495.00	498.00	492.00	481.8	-13.2	13.2
GHOST14	74	211	2	NA	NA	494.00	497.00	491.00	481.8	-12.2	12.2
GHOST15	74	211	3	NA	NA	493.00	496.00	490.00	481.8	-11.2	11.2

Statistical Calculations:

Monitoring Wells Only	
ME=	-1.58
MAE=	4.03

Sensitivity of Heads to Kv

WELL	MODEL COLUMN	MODEL ROW	MODEL LAYER	MEAS. HIGH	MEAS. LOW	TARGET MEAN	TARGET HIGH	TARGET LOW	Kv:	+15%	(ft/day)
									MODEL HEAD	0.0021 Difference (feet)	Absolute Difference
MW25-3	4	9	1	742.41	742.41	740.75	743.75	737.75	736.1	-4.7	4.7
MW64A-1	82	11	1	736.63	736.63	737.87	740.87	734.87	734.0	-3.9	3.9
MW64A-3	82	12	1	734.08	734.08	735.32	738.32	732.32	733.2	-2.1	2.1
MW17-1	4	15	1	733.47	733.47	731.81	734.81	728.81	730.8	-1.0	1.0
MW16-1	2	13	1	732.14	732.14	730.97	733.97	727.97	732.9	1.9	1.9
MW16-2	2	14	1	731.01	731.01	729.84	732.84	726.84	731.9	2.1	2.1
MW17-3	4	16	1	729.77	729.77	728.11	731.11	725.11	729.5	1.4	1.4
GHOST19	42	18	1	NA	NA	715.00	718.00	712.00	726.7	11.7	11.7
GHOST20	42	18	2	NA	NA	714.00	717.00	711.00	726.7	12.7	12.7
GHOST21	42	18	3	NA	NA	713.00	716.00	710.00	726.7	13.7	13.7
GHOST1	77	28	1	NA	NA	695.00	698.00	692.00	707.3	12.3	12.3
GHOST4	9	27	1	NA	NA	695.00	698.00	692.00	709.8	14.8	14.8
GHOST5	9	27	2	NA	NA	694.00	697.00	691.00	709.8	15.8	15.8
GHOST2	77	28	2	NA	NA	694.00	697.00	691.00	707.3	13.3	13.3
GHOST3	77	28	3	NA	NA	693.00	696.00	690.00	707.3	14.3	14.3
GHOST6	9	27	3	NA	NA	693.00	696.00	690.00	709.8	16.8	16.8
MW-41D	11	42	2	687.96	685.74	686.82	687.32	686.32	663.9	-22.9	22.9
MW-42D	70	43	2	680.66	674.94	678.34	678.84	677.84	660.6	-17.7	17.7
PT-10	47	44	2	677.79	670.57	673.51	674.01	673.01	658.5	-15.0	15.0
MW64D-1	77	44	1	665.03	664.36	663.37	663.87	662.87	658.3	-5.1	5.1
MW-39	17	61	1	657.99	656.37	657.12	657.62	656.62	650.4	-6.7	6.7
MW-60	72	62	1	658.13	654.83	656.99	657.49	656.49	649.8	-7.2	7.2
MW64D-4	79	59	1	657.39	655.10	655.73	656.23	655.23	650.7	-5.0	5.0
MW-40	46	65	1	656.40	652.18	654.55	655.05	654.05	648.8	-5.8	5.8
MW-59	71	65	1	654.95	651.61	653.78	654.28	653.28	648.7	-5.1	5.1
MW-43	35	63	1	655.42	652.46	653.76	654.26	653.26	649.6	-4.2	4.2
PT-11	66	66	1	654.02	648.49	651.68	652.18	651.18	648.4	-3.3	3.3
PT-18	46	72	1	651.78	646.72	649.85	650.35	649.35	646.2	-3.7	3.7
MW-44	34	73	1	648.63	646.98	648.59	649.09	648.09	645.9	-2.7	2.7
MW-45	24	82	1	648.47	644.75	646.88	647.38	646.38	642.6	-4.3	4.3
MW-46	34	83	1	647.28	642.61	645.62	646.12	645.12	642.2	-3.4	3.4
MW-49D	34	83	2	647.11	642.74	645.45	645.95	644.95	642.2	-3.3	3.3
MW64D-3	77	72	1	646.91	645.89	645.25	645.75	644.75	646.0	0.7	0.7
PT-12	44	81	1	647.25	641.73	644.90	645.40	644.40	642.9	-2.0	2.0
MW-50D	34	83	3	646.39	642.90	644.73	645.23	644.23	642.2	-2.5	2.5
MW-48	26	89	1	645.47	641.57	643.75	644.25	643.25	639.9	-3.9	3.9
PT-21	43	88	2	647.51	635.37	641.03	641.53	640.53	640.2	-0.8	0.8
PT-22	43	88	1	645.45	637.85	640.95	641.45	640.45	640.2	-0.7	0.7
PT-19	58	85	1	642.35	637.81	640.17	640.67	639.67	641.3	1.1	1.1
PT-20	51	89	1	644.21	636.11	640.02	640.52	639.52	639.8	-0.2	0.2
MW-32	58	96	1	637.84	632.40	635.11	635.61	634.61	637.0	1.9	1.9
PT-23	30	101	1	638.71	632.56	635.05	635.55	634.55	635.2	0.1	0.1
PT-17	53	100	1	636.85	630.12	634.21	634.71	633.71	635.5	1.3	1.3
MW-38D	18	107	2	634.67	632.76	633.97	634.47	633.47	632.9	-1.1	1.1
MW-27	33	103	1	635.62	630.37	633.45	633.95	632.95	634.4	0.9	0.9
PT-16	18	107	1	635.06	630.17	633.43	633.93	632.93	632.9	-0.5	0.5
MW-33	63	98	1	635.95	630.02	633.41	633.91	632.91	636.2	2.8	2.8
MW-30	56	101	1	636.37	629.73	633.13	633.63	632.63	635.1	2.0	2.0
MW64D-2	75	92	1	633.49	630.75	631.83	632.33	631.33	638.4	6.6	6.6
MW-55D	47	103	3	633.37	630.23	631.71	632.21	631.21	634.3	2.6	2.6
MW-31	61	103	1	634.60	627.21	631.64	632.14	631.14	634.3	2.7	2.7
MW-54D	47	103	2	633.29	629.88	631.63	632.13	631.13	634.3	2.7	2.7
MW-28	36	105	1	633.28	628.26	631.58	632.08	631.08	633.6	2.0	2.0
MW-53	47	103	1	632.83	630.13	631.17	631.67	630.67	634.4	3.2	3.2
PT-24	40	109	1	633.19	627.85	631.02	631.52	630.52	632.0	1.0	1.0
PT-25	64	104	1	633.66	625.45	630.56	631.06	630.06	633.9	3.3	3.3
PT-15	71	99	1	634.09	627.40	630.35	630.85	629.85	635.8	5.5	5.5
MW-29	46	107	1	631.82	626.83	630.19	630.69	629.69	632.8	2.6	2.6
MW-37	7	116	1	630.91	626.65	629.14	629.64	628.64	629.6	0.5	0.5
MW-35D	61	114	2	629.66	628.01	629.08	629.58	628.58	629.9	0.8	0.8
MW-36	61	114	1	629.94	626.43	629.02	629.52	628.52	629.9	0.9	0.9
MW-34	75	100	1	630.28	626.39	628.38	628.88	627.88	635.3	6.9	6.9
MW-56	48	119	1	627.78	626.67	627.27	627.77	626.77	627.9	0.6	0.6
MW-57D	48	119	2	628.60	627.11	626.94	627.44	626.44	627.9	1.0	1.0
MW-58D	48	119	3	628.53	625.66	626.87	627.37	626.37	627.9	1.0	1.0

MW-51D	35	128	2	625.68	621.56	624.02	624.52	623.52	624.3	0.3	0.3
MW-47	35	128	1	625.69	621.47	623.96	624.46	623.46	624.3	0.3	0.3
MW-52D	35	128	3	624.20	620.04	622.54	623.04	622.04	624.3	1.8	1.8
PT-26	73	174	1	611.82	603.10	608.28	608.78	607.78	604.0	-4.3	4.3
GHOST22	42	174	1	NA	NA	601.00	604.00	598.00	604.5	3.5	3.5
GHOST23	42	174	2	NA	NA	600.00	603.00	597.00	604.5	4.5	4.5
GHOST24	42	174	3	NA	NA	599.00	602.00	596.00	604.5	5.5	5.5
GHOST10	7	199	1	NA	NA	575.00	578.00	572.00	560.6	-14.4	14.4
GHOST7	77	198	1	NA	NA	575.00	578.00	572.00	566.7	-8.3	8.3
GHOST8	77	198	2	NA	NA	574.00	577.00	571.00	566.7	-7.3	7.3
GHOST11	7	199	2	NA	NA	574.00	577.00	571.00	564.7	-9.3	9.3
GHOST9	77	198	3	NA	NA	573.00	576.00	570.00	566.7	-6.3	6.3
GHOST12	7	199	3	NA	NA	573.00	576.00	570.00	564.7	-8.3	8.3
GHOST16	6	213	1	NA	NA	515.00	518.00	512.00	483.2	-31.8	31.8
GHOST17	6	213	2	NA	NA	514.00	517.00	511.00	483.2	-30.8	30.8
GHOST18	6	213	3	NA	NA	513.00	516.00	510.00	483.2	-29.8	29.8
GHOST13	74	211	1	NA	NA	495.00	498.00	492.00	481.8	-13.2	13.2
GHOST14	74	211	2	NA	NA	494.00	497.00	491.00	481.8	-12.2	12.2
GHOST15	74	211	3	NA	NA	493.00	496.00	490.00	481.8	-11.2	11.2

Statistical Calculations:

Monitoring Wells Only	
ME=	-1.58
MAE=	4.03

Sensitivity of Heads to Kv

WELL	MODEL COLUMN	MODEL ROW	MODEL LAYER	MEAS. HIGH	MEAS. LOW	TARGET MEAN	TARGET HIGH	TARGET LOW	Kv: +25% 0.0023 (ft/day)		
									MODEL HEAD	Difference (feet)	Absolute Difference
MW25-3	4	9	1	742.41	742.41	740.75	743.75	737.75	736.1	-4.7	4.7
MW64A-1	82	11	1	736.63	736.63	737.87	740.87	734.87	734.0	-3.9	3.9
MW64A-3	82	12	1	734.08	734.08	735.32	738.32	732.32	733.2	-2.1	2.1
MW17-1	4	15	1	733.47	733.47	731.81	734.81	728.81	730.8	-1.0	1.0
MW16-1	2	13	1	732.14	732.14	730.97	733.97	727.97	732.9	1.9	1.9
MW16-2	2	14	1	731.01	731.01	729.84	732.84	726.84	731.9	2.1	2.1
MW17-3	4	16	1	729.77	729.77	728.11	731.11	725.11	729.5	1.4	1.4
GHOST19	42	18	1	NA	NA	715.00	718.00	712.00	726.7	11.7	11.7
GHOST20	42	18	2	NA	NA	714.00	717.00	711.00	726.7	12.7	12.7
GHOST21	42	18	3	NA	NA	713.00	716.00	710.00	726.7	13.7	13.7
GHOST1	77	28	1	NA	NA	695.00	698.00	692.00	707.3	12.3	12.3
GHOST4	9	27	1	NA	NA	695.00	698.00	692.00	709.8	14.8	14.8
GHOST5	9	27	2	NA	NA	694.00	697.00	691.00	709.8	15.8	15.8
GHOST2	77	28	2	NA	NA	694.00	697.00	691.00	707.3	13.3	13.3
GHOST3	77	28	3	NA	NA	693.00	696.00	690.00	707.3	14.3	14.3
GHOST6	9	27	3	NA	NA	693.00	696.00	690.00	709.8	16.8	16.8
MW-41D	11	42	2	687.96	685.74	686.82	687.32	686.32	663.9	-22.9	22.9
MW-42D	70	43	2	680.66	674.94	678.34	678.84	677.84	660.6	-17.7	17.7
PT-10	47	44	2	677.79	670.57	673.51	674.01	673.01	658.5	-15.0	15.0
MW64D-1	77	44	1	665.03	664.36	663.37	663.87	662.87	658.3	-5.1	5.1
MW-39	17	61	1	657.99	656.37	657.12	657.62	656.62	650.4	-6.7	6.7
MW-60	72	62	1	658.13	654.83	656.99	657.49	656.49	649.8	-7.2	7.2
MW64D-4	79	59	1	657.39	655.10	655.73	656.23	655.23	650.7	-5.0	5.0
MW-40	46	65	1	656.40	652.18	654.55	655.05	654.05	648.8	-5.8	5.8
MW-59	71	65	1	654.95	651.61	653.78	654.28	653.28	648.7	-5.1	5.1
MW-43	35	63	1	655.42	652.46	653.76	654.26	653.26	649.6	-4.2	4.2
PT-11	66	66	1	654.02	648.49	651.68	652.18	651.18	648.4	-3.3	3.3
PT-18	46	72	1	651.78	646.72	649.85	650.35	649.35	646.2	-3.7	3.7
MW-44	34	73	1	648.63	646.98	648.59	649.09	648.09	645.9	-2.7	2.7
MW-45	24	82	1	648.47	644.75	646.88	647.38	646.38	642.6	-4.3	4.3
MW-46	34	83	1	647.28	642.61	645.62	646.12	645.12	642.2	-3.4	3.4
MW-49D	34	83	2	647.11	642.74	645.45	645.95	644.95	642.2	-3.3	3.3
MW64D-3	77	72	1	646.91	645.89	645.25	645.75	644.75	646.0	0.7	0.7
PT-12	44	81	1	647.25	641.73	644.90	645.40	644.40	642.9	-2.0	2.0
MW-50D	34	83	3	646.39	642.90	644.73	645.23	644.23	642.2	-2.5	2.5
MW-48	26	89	1	645.47	641.57	643.75	644.25	643.25	639.9	-3.9	3.9
PT-21	43	88	2	647.51	635.37	641.03	641.53	640.53	640.2	-0.8	0.8
PT-22	43	88	1	645.45	637.85	640.95	641.45	640.45	640.2	-0.7	0.7
PT-19	58	85	1	642.35	637.81	640.17	640.67	639.67	641.3	1.1	1.1
PT-20	51	89	1	644.21	636.11	640.02	640.52	639.52	639.8	-0.2	0.2
MW-32	58	96	1	637.84	632.40	635.11	635.61	634.61	637.0	1.9	1.9
PT-23	30	101	1	638.71	632.56	635.05	635.55	634.55	635.2	0.1	0.1
PT-17	53	100	1	636.85	630.12	634.21	634.71	633.71	635.5	1.3	1.3
MW-38D	18	107	2	634.67	632.76	633.97	634.47	633.47	632.9	-1.1	1.1
MW-27	33	103	1	635.62	630.37	633.45	633.95	632.95	634.4	0.9	0.9
PT-16	18	107	1	635.06	630.17	633.43	633.93	632.93	632.9	-0.5	0.5
MW-33	63	98	1	635.95	630.02	633.41	633.91	632.91	636.2	2.8	2.8
MW-30	56	101	1	636.37	629.73	633.13	633.63	632.63	635.1	2.0	2.0
MW64D-2	75	92	1	633.49	630.75	631.83	632.33	631.33	638.4	6.6	6.6
MW-55D	47	103	3	633.37	630.23	631.71	632.21	631.21	634.3	2.6	2.6
MW-31	61	103	1	634.60	627.21	631.64	632.14	631.14	634.3	2.7	2.7
MW-54D	47	103	2	633.29	629.88	631.63	632.13	631.13	634.3	2.7	2.7
MW-28	36	105	1	633.28	628.26	631.58	632.08	631.08	633.6	2.0	2.0
MW-53	47	103	1	632.83	630.13	631.17	631.67	630.67	634.4	3.2	3.2
PT-24	40	109	1	633.19	627.85	631.02	631.52	630.52	632.0	1.0	1.0
PT-25	64	104	1	633.66	625.45	630.56	631.06	630.06	633.9	3.3	3.3
PT-15	71	99	1	634.09	627.40	630.35	630.85	629.85	635.8	5.5	5.5
MW-29	46	107	1	631.82	626.83	630.19	630.69	629.69	632.8	2.6	2.6
MW-37	7	116	1	630.91	626.65	629.14	629.64	628.64	629.6	0.5	0.5
MW-35D	61	114	2	629.66	628.01	629.08	629.58	628.58	629.9	0.8	0.8
MW-36	61	114	1	629.94	626.43	629.02	629.52	628.52	629.9	0.9	0.9
MW-34	75	100	1	630.28	626.39	628.38	628.88	627.88	635.3	6.9	6.9
MW-56	48	119	1	627.78	626.67	627.27	627.77	626.77	627.9	0.6	0.6
MW-57D	48	119	2	628.60	627.11	626.94	627.44	626.44	627.9	1.0	1.0
MW-58D	48	119	3	628.53	625.66	626.87	627.37	626.37	627.9	1.0	1.0

MW-51D	35	128	2	625.68	621.56	624.02	624.52	623.52	624.3	0.3	0.3
MW-47	35	128	1	625.69	621.47	623.96	624.46	623.46	624.3	0.3	0.3
MW-52D	35	128	3	624.20	620.04	622.54	623.04	622.04	624.3	1.8	1.8
PT-26	73	174	1	611.82	603.10	608.28	608.78	607.78	604.0	-4.3	4.3
GHOST22	42	174	1	NA	NA	601.00	604.00	598.00	604.5	3.5	3.5
GHOST23	42	174	2	NA	NA	600.00	603.00	597.00	604.5	4.5	4.5
GHOST24	42	174	3	NA	NA	599.00	602.00	596.00	604.5	5.5	5.5
GHOST10	7	199	1	NA	NA	575.00	578.00	572.00	560.6	-14.4	14.4
GHOST7	77	198	1	NA	NA	575.00	578.00	572.00	566.7	-8.3	8.3
GHOST8	77	198	2	NA	NA	574.00	577.00	571.00	566.7	-7.3	7.3
GHOST11	7	199	2	NA	NA	574.00	577.00	571.00	564.7	-9.3	9.3
GHOST9	77	198	3	NA	NA	573.00	576.00	570.00	566.7	-6.3	6.3
GHOST12	7	199	3	NA	NA	573.00	576.00	570.00	564.7	-8.3	8.3
GHOST16	6	213	1	NA	NA	515.00	518.00	512.00	483.2	-31.8	31.8
GHOST17	6	213	2	NA	NA	514.00	517.00	511.00	483.2	-30.8	30.8
GHOST18	6	213	3	NA	NA	513.00	516.00	510.00	483.2	-29.8	29.8
GHOST13	74	211	1	NA	NA	495.00	498.00	492.00	481.8	-13.2	13.2
GHOST14	74	211	2	NA	NA	494.00	497.00	491.00	481.8	-12.2	12.2
GHOST15	74	211	3	NA	NA	493.00	496.00	490.00	481.8	-11.2	11.2

Statistical Calculations:

Monitoring Wells Only	
ME=	-1.58
MAE=	4.03

APPENDIX E
MODPATH Output File



2	3	1	-1.8678	-0.26445E-01
3	1	1	-1.6787	-0.29498E-01
3	2	1	-1.3247	-0.27356E-01
3	3	1	-1.1328	-0.27546E-01
3	4	1	-1.4237	-0.27483E-01
3	5	1	-1.6417	-0.28150E-01
3	6	1	-1.7526	-0.26775E-01
4	1	1	-1.3420	-0.30015E-01
4	2	1	-1.0962	-0.26502E-01
4	3	1	-1.0337	-0.26399E-01
4	4	1	-1.0932	-0.26979E-01
4	5	1	-1.0675	-0.26466E-01
4	7	1	-1.3663	-0.29847E-01
4	8	1	-1.6325	-0.31139E-01
4	9	1	-1.5569	-0.21768E-01
4	10	1	-1.3729	-0.14998E-01
4	11	1	-1.0695	-0.96084E-02
4	74	1	-1.0723	-0.11826E-01
4	75	1	-1.5892	-0.22201E-01
5	1	1	-1.0157	-0.27313E-01
5	7	1	-1.0626	-0.28863E-01
5	8	1	-1.1552	-0.29197E-01
5	9	1	-1.1087	-0.20022E-01
5	76	1	-1.2047	-0.23787E-01
5	77	1	-1.3692	-0.23293E-01
5	78	1	-1.6370	-0.25153E-01
5	79	1	-1.7793	-0.25254E-01
5	80	1	-1.9513	-0.25854E-01
5	81	1	-2.1178	-0.26319E-01
5	82	1	-2.2844	-0.26664E-01
6	18	1	1.1152	0.75489E-02
6	77	1	-1.0284	-0.24309E-01
6	78	1	-1.0838	-0.24010E-01
6	79	1	-1.1835	-0.24839E-01
6	80	1	-1.2101	-0.24231E-01
6	81	1	-1.3141	-0.25222E-01
6	82	1	-1.3580	-0.25051E-01
7	23	1	1.1327	0.77884E-02
7	82	1	-1.0091	-0.25400E-01
8	14	1	1.1904	0.85092E-02
8	68	1	1.2200	0.82695E-02
10	14	1	1.0077	0.74989E-02
10	17	1	-3.4377	-0.25654E-01
10	20	1	1.2946	0.95977E-02
11	17	1	-1.5691	-0.12079E-01
11	18	1	1.3408	0.10299E-01
12	18	1	1.0134	0.79321E-02
12	67	1	1.0683	0.81515E-02
13	15	1	1.0870	0.87765E-02
13	20	1	1.0169	0.82086E-02
13	56	1	1.0459	0.83513E-02
14	14	1	1.0922	0.91148E-02
14	19	1	1.0285	0.85899E-02
14	53	1	1.0704	0.88887E-02
16	58	1	1.0489	0.93681E-02
17	16	1	-1.7424	-0.16293E-01
17	17	1	-1.1590	-0.10978E-01
17	18	1	1.4442	0.13620E-01
17	60	1	-1.4800	-0.13769E-01
18	16	1	-2.2075	-0.21716E-01
18	17	1	1.4083	0.13867E-01
18	60	1	-2.6237	-0.25525E-01
18	62	1	1.3667	0.13271E-01
19	18	1	1.0218	0.10358E-01
19	60	1	-1.9720	-0.20122E-01
19	61	1	1.4955	0.15254E-01
20	16	1	-1.0309	-0.10944E-01
20	17	1	1.1967	0.12671E-01
27	68	1	-1.1816	-0.16366E-01
28	68	1	-1.5395	-0.22246E-01
1	2	2	4.5729	0.22399E-01
2	1	2	4.4312	0.23274E-01
2	2	2	2.8309	0.25168E-01
2	3	2	3.3515	0.23449E-01
3	1	2	2.6113	0.24127E-01
3	2	2	2.1864	0.24604E-01
3	3	2	1.5155	0.20687E-01
3	4	2	2.1267	0.22051E-01
3	5	2	2.4330	0.21788E-01
3	6	2	2.9381	0.22715E-01
4	1	2	1.8119	0.22422E-01
4	2	2	1.7139	0.23242E-01
4	3	2	1.5224	0.22003E-01
4	4	2	1.6002	0.22227E-01
4	5	2	1.5644	0.21847E-01
4	6	2	1.3638	0.22059E-01
4	7	2	1.9086	0.22981E-01
4	8	2	2.2551	0.23059E-01
4	9	2	2.0304	0.15526E-01
4	10	2	1.6580	0.10191E-01

4	11	2	1.2881	0.67070E-02
4	74	2	1.7084	0.97200E-02
4	75	2	2.9083	0.19939E-01
5	1	2	1.4723	0.22586E-01
5	2	2	1.3266	0.21438E-01
5	3	2	1.3424	0.22437E-01
5	4	2	1.3026	0.21845E-01
5	5	2	1.2912	0.21752E-01
5	6	2	1.3379	0.22751E-01
5	7	2	1.4940	0.23193E-01
5	8	2	1.6785	0.23981E-01
5	9	2	1.5191	0.15671E-01
5	10	2	1.3272	0.10449E-01
5	11	2	1.0000	0.63097E-02
5	12	2	1.2291	0.64940E-02
5	74	2	1.1093	0.10472E-01
5	75	2	1.1572	0.16643E-01
5	76	2	1.6063	0.17088E-01
5	77	2	2.3283	0.20624E-01
5	78	2	2.4718	0.19224E-01
5	79	2	2.8883	0.20252E-01
5	80	2	3.2213	0.20598E-01
5	81	2	3.5537	0.20818E-01
5	82	2	4.1691	0.22371E-01
6	1	2	1.1336	0.20858E-01
6	2	2	1.1394	0.21694E-01
6	3	2	1.1722	0.22820E-01
6	4	2	1.1496	0.22572E-01
6	5	2	1.1649	0.22893E-01
6	6	2	1.1601	0.22590E-01
6	7	2	1.2626	0.23684E-01
6	8	2	1.2816	0.23031E-01
6	9	2	1.2181	0.15534E-01
6	75	2	1.0004	0.15888E-01
6	76	2	1.3218	0.19117E-01
6	77	2	1.4161	0.18687E-01
6	78	2	1.6774	0.20509E-01
6	79	2	1.8176	0.20835E-01
6	80	2	1.9723	0.21369E-01
6	81	2	2.0044	0.20627E-01
6	82	2	2.3355	0.22900E-01
7	2	2	1.0517	0.23271E-01
7	7	2	1.0469	0.23090E-01
7	8	2	1.0771	0.23204E-01
7	76	2	1.0771	0.19521E-01
7	77	2	1.0853	0.18715E-01
7	78	2	1.2089	0.19892E-01
7	79	2	1.2847	0.20261E-01
7	80	2	1.3051	0.19815E-01
7	81	2	1.4622	0.21455E-01
7	82	2	1.6425	0.23340E-01
8	80	2	1.0618	0.20669E-01
8	81	2	1.0899	0.20701E-01
8	82	2	1.2054	0.22380E-01
10	16	2	-1.8659	-0.87105E-02
10	18	2	2.0817	0.98221E-02
11	17	2	1.1508	0.55648E-02
11	18	2	1.7154	0.81966E-02
17	15	2	-1.1477	-0.67852E-02
17	17	2	1.4871	0.89126E-02
18	17	2	1.8912	0.11697E-01
18	59	2	-1.5450	-0.95068E-02
18	61	2	1.9457	0.12038E-01
19	17	2	1.1983	0.77314E-02
19	61	2	1.7157	0.11011E-01
21	16	2	1.1090	0.77702E-02
1	2	3	6.8706	0.53189E-02
2	1	3	5.3275	0.44583E-02
2	2	3	2.7465	0.41676E-02
2	3	3	3.9682	0.46244E-02
3	1	3	3.1029	0.49215E-02
3	2	3	2.4659	0.48423E-02
3	3	3	1.6036	0.38705E-02
3	4	3	2.4849	0.44697E-02
3	5	3	2.8445	0.43614E-02
3	6	3	3.6245	0.47269E-02
4	1	3	1.8051	0.39224E-02
4	2	3	1.9494	0.46739E-02
4	3	3	1.6654	0.42715E-02
4	4	3	1.7862	0.43927E-02
4	5	3	1.8407	0.45542E-02
4	6	3	1.5855	0.45801E-02
4	7	3	2.3609	0.49889E-02
4	8	3	2.7871	0.49388E-02
4	9	3	2.4257	0.32415E-02
4	10	3	1.7317	0.18808E-02
4	74	3	1.5545	0.15077E-02
4	75	3	2.3750	0.26986E-02
5	1	3	1.6859	0.46056E-02
5	2	3	1.5101	0.43575E-02

5	3	3	1.5574	0.46565E-02
5	4	3	1.4751	0.44253E-02
5	5	3	1.4168	0.42703E-02
5	6	3	1.6689	0.50828E-02
5	7	3	1.7841	0.49356E-02
5	8	3	1.9720	0.49967E-02
5	9	3	1.7262	0.31711E-02
5	10	3	1.3245	0.18679E-02
5	11	3	1.0060	0.11440E-02
5	74	3	1.0625	0.17790E-02
5	75	3	1.1369	0.29017E-02
5	76	3	1.1341	0.20943E-02
5	77	3	2.5744	0.39002E-02
5	78	3	2.6162	0.34316E-02
5	79	3	3.1952	0.37322E-02
5	80	3	3.6081	0.37965E-02
5	81	3	4.2724	0.40680E-02
5	82	3	5.0924	0.43767E-02
6	1	3	1.3743	0.45443E-02
6	2	3	1.2074	0.41353E-02
6	3	3	1.2993	0.45553E-02
6	4	3	1.2605	0.44586E-02
6	5	3	1.2794	0.45298E-02
6	6	3	1.3413	0.47043E-02
6	7	3	1.4627	0.49339E-02
6	8	3	1.4347	0.46263E-02
6	9	3	1.1794	0.27044E-02
6	10	3	1.0508	0.17898E-02
6	76	3	1.3155	0.33770E-02
6	77	3	1.3808	0.32148E-02
6	78	3	1.6408	0.35209E-02
6	79	3	1.7019	0.34072E-02
6	80	3	2.1982	0.41461E-02
6	81	3	2.2711	0.40521E-02
6	82	3	2.6050	0.44086E-02
7	2	3	1.1402	0.45662E-02
7	3	3	1.0402	0.42331E-02
7	4	3	1.0005	0.41035E-02
7	5	3	1.1528	0.47316E-02
7	6	3	1.1050	0.44974E-02
7	7	3	1.1481	0.45823E-02
7	8	3	1.2116	0.47193E-02
7	76	3	1.1387	0.37051E-02
7	78	3	1.0818	0.31793E-02
7	79	3	1.3782	0.38761E-02
7	80	3	1.3012	0.35149E-02
7	81	3	1.5274	0.39798E-02
7	82	3	1.7047	0.42928E-02
8	80	3	1.0456	0.36647E-02
8	81	3	1.1213	0.38308E-02
8	82	3	1.1662	0.38895E-02
10	15	3	-1.5818	-0.13634E-02
10	18	3	2.2029	0.19048E-02
11	19	3	-1.3141	-0.11525E-02
17	17	3	1.3329	0.14723E-02
18	17	3	1.2581	0.14336E-02
18	18	3	-1.1949	-0.13582E-02
18	58	3	-1.2475	-0.14215E-02
18	61	3	1.3610	0.15519E-02
19	62	3	-1.4187	-0.16739E-02

***** PARTICLE TERMINATION INFORMATION

PARTICLE 1 WAS STOPPED IN ROW 210, COL 62, LAY 2 TIME= 1.1876E+05

TRAVEL TIME SUMMARY FOR ALL PARTICLES:

MINIMUM TRAVEL TIME = 1.18759E+05

MAXIMUM TRAVEL TIME = 1.18759E+05

AVERAGE TRAVEL TIME = 1.18759E+05

100.0% OF THE PARTICLES HAD TRAVEL TIMES LESS THAN THE AVERAGE TRAVEL TIME

0 PARTICLES REMAIN ACTIVE

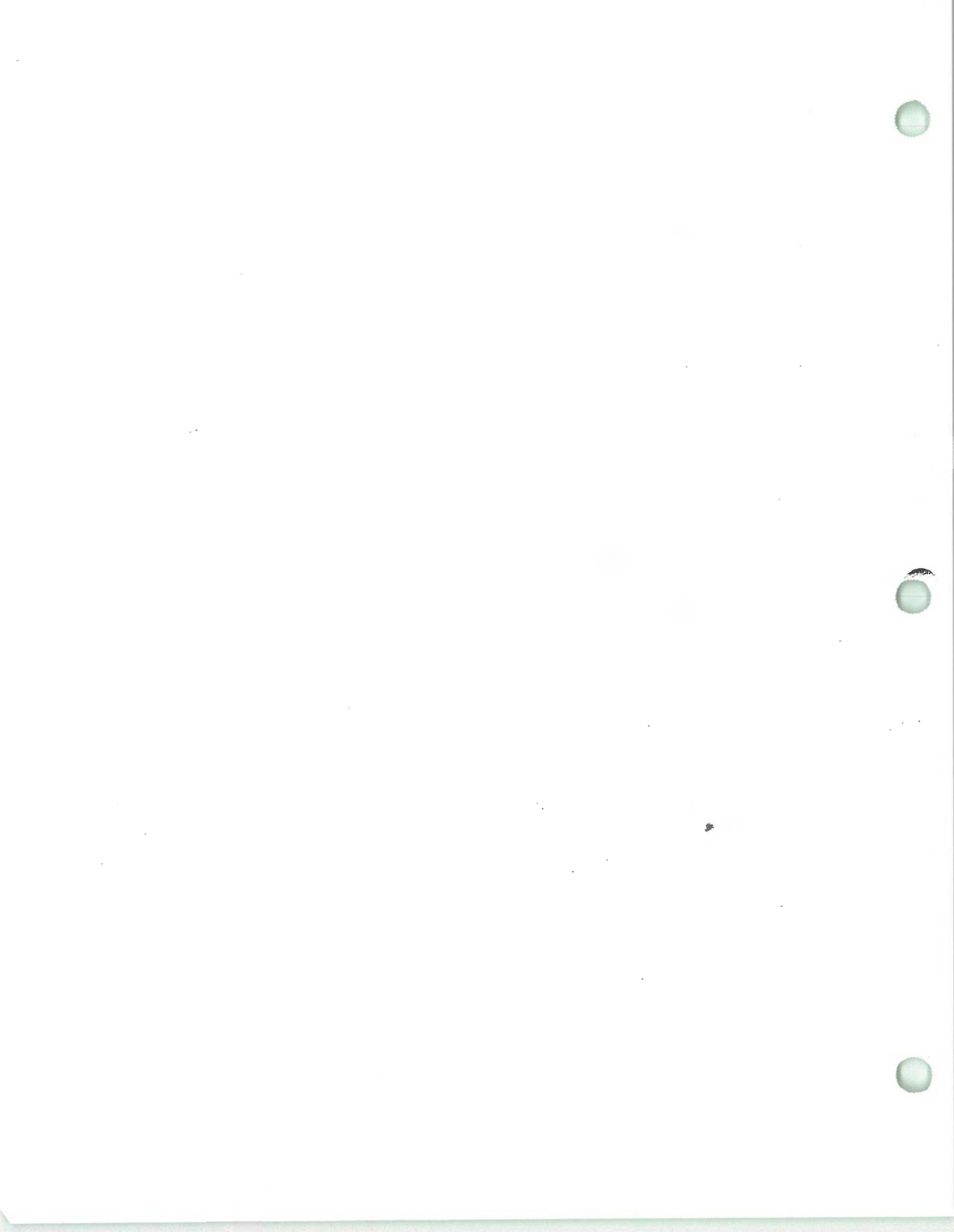
0 PARTICLES STOPPED AT INTERNAL SINKS/SOURCES OR BOUNDARIES

1 PARTICLES STOPPED IN AN AUTOMATIC TERMINATION ZONE

0 PARTICLES WERE STRANDED IN INACTIVE CELLS

0 PARTICLES WERE NOT RELEASED

1 PARTICLES ACCOUNTED FOR OUT OF A TOTAL OF 1



APPENDIX F

MT3D Output File

Scenario 3



Scenario 3



Available Upon Request

